RAFT memorabilia

❄ living ❄ radical polymerization in homogeneous and heterogeneous media

Hans de Brouwer

RAFT memorabilia

❇ living ❇ radical polymerization

in homogeneous and heterogeneous media

Hans de Brouwer

CIP-DATA LIBRARY TECHNISCHE UNIVERSITEIT EINDHOVEN

Brouwer, Hans de

RAFT memorabilia : living radical polymerization in homogeneous and heterogeneous media / by Hans de Brouwer. - Eindhoven : Technische Universiteit Eindhoven, 2001. -
Proefschrift. - ISBN 90-386-2802-1
NUGI 813
Trefwoorden: polymerisatie ; radikaalreacties / emulsiepolymerisatie / reactiekinetiek / ketenoverdracht ; RAFT
Subject headings: polymerization ; radical reactions / emulsion polymerisation / reaction kinetics / chain transfer ; RAFT

Druk: Universiteitsdrukkerij, Technische Universiteit Eindhoven
Omslagontwerp: Hans de Brouwer

RAFT memorabilia

living radical polymerization
in homogeneous and heterogeneous media

PROEFSCHRIFT

ter verkrijging van de graad van doctor
aan de Technische Universiteit Eindhoven,
op gezag van
de Rector Magnificus, prof.dr. M. Rem,
voor een commissie
aangewezen door het College voor Promoties
in het openbaar te verdedigen
op woensdag 30 mei 2001 om 16.00 uur

door

Johannes A. M. de Brouwer

geboren te Goirle

Dit proefschrift is goedgekeurd door de promotoren:

prof.dr.ir. A. L. German
en
prof.dr. J. F. Schork

Copromotor:
dr. M. J. Monteiro

Het werk in dit proefschrift is financieel ondersteund door de Stichting Emulsiepolymerisatie (SEP) / The work in this thesis was financially supported by the Foundation Emulsion polymerization (SEP)

look around, wonder why

we can live a life that's never satisfied

lonely hearts, troubled minds

looking for a way that we can never find

many roads are ahead of us

with choices to be made

but life's just one of the games we play

there is no special way

from *Winter in July* on the album *Unknown Territory* by Bomb the Bass

Table of Contents

» you're gonna take control of the chemistry
and you're gonna manifest the mystery
you got a magic wheel in your memory
I'm wasted in time and I'm looking everywhere «[1]

1. Introduction

1.1. The Ways of Science

The beaker on the cover of this thesis is more than the obvious indicator of the experimental and chemical content of this work. Hopefully, you – as the reader of this booklet – will find that the technical quality of the scientific content gathered between the two covers matches that of this image, but its meaning goes deeper than this superficial reference. More subtly, it attempts to expose the problem of observation.

How can a piece of colorless transparent glass leave such a clear and detailed picture on one's retina, other than by the elucidating action of projection, shadow and reflection? Where direct perception is impossible, the underlying reality is reconstructed from these secondary observations.

In this way this simple beaker, or rather the image of the beaker, or even more accurately: the image of the projections of this beaker, symbolize the scientists' dilemma: how to gain knowledge on reality? How to unravel the truth when it goes under-cover among mirages, illusions and delusions and only manifests itself indirectly?

The problem was already described allegorically by Plato in his *Politeia*.[2] The Greek philosopher composed a parable about a group of captives that were forced to look at the dead end of a cave. On this wall they observed shadows. Projections of objects and people moving behind there backs, their shadows cast on the blind wall by a fire lit in the caves' entrance. These people had never seen anything else than their own shadows and those of the objects that were carried around behind them. They were chained such that they could not look around. How were they to know that a reality existed other than that of the shadows they observed? In the eye of the beholder these captives possess only a very limited view on reality while they are unaware of this restraint. Plato acknowledged the difficulty of this problem but

did not consider it impossible to know reality. For Plato it was enough to realize this situation and to attempt to gain deeper knowledge; somehow finding enlightenment, rising above the world of observation, realizing the existence of reality.

Nietzsche was one of the first to explicitly classify this pursuit as a vial attempt to do the impossible.[3] Science is unable to truly comprehend things but only allows the description of phenomena. All progress in science can be designated as improvements and refinements in this describing capability, devoid of any advance in understanding things, as he describes on several occasions in *the gay science*. Paragraph 112 in the third book, for instance, starts with the following:

> ***»Erklärung« nennen wir's: aber »Beschreibung« ist es, was uns vor älteren Stufen der Erkenntnis und Wissenschaft auszeichnet. Wir beschreiben besser – wir erklären ebensowenig wie alle Früheren...***

According to Nietzsche, truth and reality are no longer universal and objectivity is non-existent.

In our post-modern era, even the existence of something more real than the original shadows is disputed.[4,5] Surely something would cause this shadow, but why would this object be more representative of reality than the projection it produces? Why would it be something else than a mere reflection itself? Why would there be something deeper, or more meaningful than this chaotic ensemble of mirror images, projections and reflections?

This may not be the most optimistic way to start a thesis; declining thorough understanding of matters. It pinpoints, however, what science is really aimed at: describing observations, recording measurements in the hope to be able to generalize and extrapolate, to model and predict, resulting in simulations and calculations being able to replace experimental procedures, rendering a comprehensive picture. In this respect, this thesis is aimed at the addition of yet another small fragment to this immense jigsaw. Though only of small size, the author sincerely hopes that it will be one of those valuable pieces that allow a whole new corner of this puzzle, representing this mouldable flexible shapable, and above all, *plastic* reality, to be actively explored.

1.2. Polymers

Plastic, derived from the Greek '*plassein*' meaning '*to mold*' or '*to shape*', is often used as a *pars pro toto* for the class of polymer materials as a whole. Polymers or plastics have been wrestling with the image of pollution, environmental-unfriendliness and non-biodegradability like, for instance, in Coupland's *Generation X*,[6] acclaimed for its strong portrayal of the *Zeitgeist*:[7]

> ***DUMPSTER CLOCKING: The tendency when looking at objects to guesstimate the amount of time they will take to eventually decompose: "Ski boots are the worst. Solid plastic. They'll be around till the sun goes supernova."***

Nothing could be further from the truth, however. Most polymers can be recycled and even when they are not, they form a most useful intermediate between fossil organic fuel and the power station's incinerator, not adding much to the environmental burdening intrinsic to the generation of energy. In fact, a full cradle-to-grave analysis depicts plastic packaging products as the preferred alternative to paper or wood.[8,9] Recycling is the key factor in this case and not so much the biodegradability. The fact that most polymers disintegrate slowly does not mean that polymers are unnatural. Polymers belong to nature's most sophisticated molecules. Life itself stores its variables, parameters and other software components in this genetic polymer database called DNA. Completely biocompatible by nature. Proteins, copolymers of amino acids, are deployed as enzymes; nanobots regulating all of the fine organic chemistry taking place in our body, maintaining delicate equilibria.

While these may be appealing examples to show the high-tech aspects of polymers, it must be said that DNA and proteins are exceptional and specialized polymers. Right now, we can only marvel at their functional complexity although the application of polymers in high-tech man-made systems like electronic components is coming on. Display panels, memory chips and other semiconductor technologies based entirely on polymers are on the verge of replacing the old metal & sand based units.[11] Polymeric drug delivery systems are able to generate a long lasting supply of medication at 'just the right dose'.[12] Smart clothing is being developed with properties that adapt to the temperature and humidity of both the body and environment.[13]

Also when it comes to mere mechanical properties, polymers are among nature's topflight picks. Trees for instance owe their strength to the stretched cellulose fibres that are aligned with their trunk and embedded in lignine. The effectiveness of this reinforced composite architecture can regularly be witnessed in news reports. When tornados rage over picturesque little tropical islands, more often than not the houses and other artificial constructions, build from isotropic materials like stone, are restored to their state of highest entropy while trees, relying on the flexibility and toughness of their polymeric cellulose skeleton, are still erect if the ground has held them.

While in nature polymers appear to be the material of choice for a wide variety of applications, to us human beings, polymers for a long time have been the poor man's cheap replacement for natural fibres like silk and wool, an easily applicable material for the production of bulk commodity goods and a convenient source for packaging materials.[14,15] Only during the last few decades of the past millennium we have passed a turning point when it was recognized that polymers can form truly unique and intelligent substances possessing properties beyond the scope of traditional materials like metals and ceramics. In some fields this knowledge has lead to superior products, while for many other areas we still lack the appropriate techniques to translate ideas into materials with sufficient precision. For advances in this field first rely on more precise construction methods of these polymer chains and not as much on the use of more exotic starting materials. Just 'making long molecules' no longer suffices and the design aspect is gaining importance. Starting from the same type and amount of monomer(s) one can create polymer architectures with highly different macroscopic properties by tailoring the chain length distribution, monomer sequence distribution, tacticity, functionality type distribution and the degree of branching, for instance.

1.3. Free–Radical Polymerization

Free-radical polymerization is one of the most convenient ways to prepare polymers on a large industrial scale. In fact, more than 70% of vinyl polymers – more than 50% of all plastics – is produced in this way.[16] The versatility of the technique stems from its tolerance towards all kinds of impurities like stabilizers, trace amounts of oxygen and water.[17] The facile polymerization in an aqueous medium is truly unique and offers many benefits as evidenced by the large proportion (40–50%) of free-radical polymerizations that are conducted in this way, in the

form of emulsion polymerizations.[18] Moreover, the range of monomers that can be polymerized by radical means is considerably larger than those compatible with other techniques.[19] Unfortunately, however, control over the polymer architecture is difficult to attain in free radical polymerization. Molar mass distributions are generally broad and can only be influenced to some extent by the use of chain transfer agents and variations in the initiator concentration. Continuous or semi-batch processes may reduce the variations in macroscopic conditions that typically occur during a batch reaction, but on a microscopic scale, statistical variations in the environment of the growing chains will give a polymer product with a large variation in *e.g.* chain length, composition, composition distribution and degree of branching. This lack of control confines the versatility of the free radical process, because of the intimate relationship that exists between the polymer chain architecture and the macroscopic behavior of the polymer material. The absence of control over the incorporation of monomer into the polymeric chain implies that many macroscopic properties cannot be influenced sufficiently.

Block copolymers with amphiphilic properties, star-shaped specimens and hyperbranched structures have become more important in recent years. To comply with these ever growing demands, polymer chemistry has resorted to the application of living polymerization techniques, such as anionic polymerization, group-transfer polymerization, and several others. Despite the structural control that these techniques offer, major drawbacks exist. For instance, their requirement of ultra-pure reagents and, more importantly, the fact that tey allow only a small fraction of the commercially interesting monomers to be polymerized. This renders these living polymerization techniques less interesting from a commercial point of view. Clearly, techniques are desired that combine structural control with the robustness and versatility of radical polymerization.

1.4. Objective and Outline of this Thesis

This thesis is meant to present a sturdy polymerization technique, which allows the construction of some types of polymer with a much higher level of microstructural ‘user-input’ than was possible before, while retaining the advantages of free-radical techniques. This is the realm of controlled or *living* radical polymerizations, a more sophisticated variety of conventional free-radical polymerization. More specifically, this thesis aims to investigate Reversible Addition–Fragmentation chain Transfer (RAFT) polymerization thereby focussing on its application in dispersed

media. The prospects of RAFT are appealing, for the addition of RAFT agent to a system should in principle not influence the radical concentration and polymerization rate. Therefore, existing recipes and technology can be used to which RAFT agent can be added as the *magic* ingredient, much in the same way in which appropriate spices transform a mishmash of nutriments into a delicious dish. The fact that only a handful of publications have appeared after its invention, however, might serve as an indicator that the application of RAFT is more complicated than is to be expected at first sight. The investigations in this thesis are aimed at gaining a more thorough understanding of the RAFT system and the prevailing mechanisms, espesially those that are important in heterogeneous media.

Chapter 2, presents a short overview of living radical techniques, highlighting differences and similarities with other established approaches like ATRP and nitroxide-mediated polymerizations. Several characteristic kinetic and mechanistic aspects of RAFT polymerizations are indicated and investigated using simulations and experiments in homogeneous media.

Chapter 3 is dedicated to the preparation of the type of RAFT agents applied in this thesis, namely dithioesters. The first part of this chapter presents a range of different synthetic pathways leading to these compounds, while the second part gives the experimental details of the syntheses of the dithiobenzoate derivatives that are used as RAFT agents for this research.

Chapter 4 is concerned with the controlled copolymerization of styrene and maleic anhydride. Whereas other living radical polymerizations have produced a very large gamut of controlled architectures of various monomers over the years, a particular class of vinylic monomers was found to cause problems, namely those with a carboxylic acid or anhydride group. The versatility of RAFT polymerizations is exemplified by copolymerizing maleic anhydride and styrene and illustrated further in a particular application in which the controlled polymerization of maleic anhydride can yield unique materials, namely functionalized polyolefin block copolymers.

Chapter 5 describes the application of RAFT in emulsion polymerization. The effect of the presence of RAFT agent on the rate is investigated by elimination of the complex nucleation stage through the use of seed latices. Seeded experiments are performed both in the presence and in the absence of monomer droplets. Fur-

thermore, the effect of RAFT on the nucleation process is studied in *ab initio* reactions. Stability issues are partly eliminated by the application of nonionic surfactants.

Chapter 6 continues with the study of miniemulsion polymerizations in the presence of RAFT. The stability of the miniemulsion polymerizations is shown to be affected by RAFT, much in the same way as in the macroemulsions in Chapter 5, when ionic surfactants are used. Nonionic surfactants give stable systems and consequently allow living radical polymerizations to be conducted in a dispersed medium in a straightforward fashion. This is demonstrated by the preparation of low polydispersity homopolymer and block copolymer dispersions.

1.5. References

1. Sonic Youth, fragment from *Cotton Crown* on the album *Sister* © Cesstone Music, **1987**
2. Plato, *Politeia* (Dutch translation: Gerard Koolschijn, Impressum Amsterdam Athenaeum-Polak & Van Gennep, 3th revised edition, **1991**)
3. Friedrich Nietzsche, *Die fröhliche Wissenschaft*, 2nd edition, **1887**, Insel Verlag Frankfurt am Main, **1982**
4. Jean Baudrillard, *La Guerre du Golfe n'a pas en lieu*, Éditions Galilée, **1991** (English translation by Paul Patton, Indiana University Press, Bloomington & Indianapolis, **1995**)
5. Jean Baudrillard, *Simulacres et simulation*, Éditions Galilée, **1981** (English translation by Sheila Faria Glaser, The University of Michigan Press **1994**)
6. Douglas Coupland, *Generation X*, St. Martin's Press, **1991**
7. *e.g.* Jay McInerney's book review in The New York Times (June 11, **1995**)
8. www.plasticsresources.com
9. Hocking, M. B. *Science* **1991**, *251*, 504
10. Fukuda,Y.; Watanabe, T.; Wakimoto, T.; Miyaguchi, S.; Tsugida, M. *Synthetic Metals* **2000**, *111–112*, 1
11. '*Polymer Electronics*', Philips Research, www.research.philips.com, **1998**
12. *e.g.* Heller J.; Pangburn S. H.; and Penhale D. W. H.; in *Controlled-Release Technology, Pharmaceutical Applications*, Lee P. I.; and Good W. R. (Eds.), Washington DC, ACS Symposium Series, pp 172—187, **1987**
13. Handley, S, *Nylon; The Manmade Fashion Revolution*, **1999**, Bloomsburry publishing, London, p.175–176
14. *Early Plastics, Perspectives 1850–1950*, Mossman, S. (Ed.), **1997**, Leicester University Press, London
15. Meikle, J. L., *American Plastic, a cultural history* **1995**, Rutgers University Press, New Brunswick, New Jersey
16. Otsu, T. *J. Polym. Sci., Part A Polym. Chem.* **2000**, *38*, 2121
17. Moad, G.; Solomon, D. H. *The Chemistry of Free Radical Polymerization*, 1st ed.; Elsevier Science Ltd.: Oxford, **1995**
18. Gilbert, R. G. *Emulsion Polymerization: A Mechanistic Approach*; Academic: London, **1995**
19. Stevens, M. P. *Polymer Chemistry, an introduction* **1990**, 2nd ed., Oxford University Press, New York, p.189

» — Think of all the bad things in the world.
Then think about shopping... that's why I love shopping. «[1]

2. RAFT Perspectives

Synopsis: This chapter presents different perspectives on RAFT polymerization and its peculiarities. The mechanism of RAFT polymerizations is explained and compared with ordinary free-radical polymerization and other living radical polymerization techniques. The effect of the transfer rate on the polymerization characteristics is demonstrated via simulations and elucidated with results from polymerizations in homogeneous media. Furthermore, simulations are used to gain insight in possible mechanisms causing retardation in RAFT polymerizations.

2.1. Living Radical Polymerization

Living polymerizations were first discovered and described by Szwarc,[2,3] who stated that for a polymerization to be considered 'living' it should meet the following requirements:

I. the polymerization proceeds to full conversion. Further addition of monomer leads to continued polymerization.

II. the number average molar mass is linearly dependent on conversion.

III. the number of polymer chains is constant during polymerization.

IV. the molar mass can be controlled by the reaction stoichiometry

V. the polydispersity of the polymer molar mass distribution is low.

VI. chain-end functionalized polymers can be obtained quantitatively.

VII. in radical polymerization, the number of active end groups should be two; one for each chain end.

Therefore, by definition, living polymerizations allow the preparation of complex macromolecular architectures in a controlled manner. The degree of polymerization can be set by choosing appropriate concentration levels for the various reactants and polydispersity will be very low. Traditionally these processes were

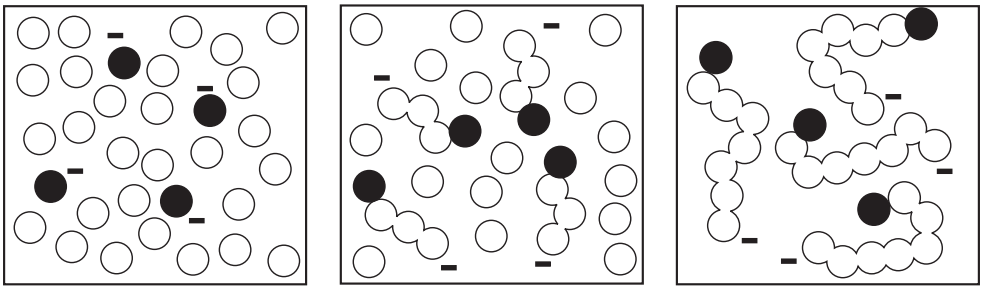

Scheme 2.1. Schematic representation of a living anionic polymerization. The initiator dissociates quantitatively, producing a number of anions (● –). These add to monomer (○), forming growing polymer chains. The number of growing chains is constant throughout the polymerization and equal to the number of initiator derived anions. At full conversion, the polymer chains are of approximately equal length because each of them has grown for the same period of time and at the same rate. The chain length is given by the ratio of monomer to initiator.

restricted to anionic polymerizations and although excellent living character can be obtained, the limited choice of monomers and the stringent reaction conditions form a serious drawback, preventing widespread commercial application. A simplified visualization shows the mechanism of a living anionic polymerization, see Scheme 2.1. The initiator dissociates quantitatively at the start of the reaction. Each of the produced anions adds to monomer and starts growing. As every chain starts growing at the same moment and grows at an equal rate, all chains will have the same degree of polymerization which is dependent on conversion. At complete conversion the monomer is divided over all polymer chains allowing the final degree of polymerization to be set by the ratio of monomer to initiator. Bimolecular termination is absent because the polymer chains carry an equal charge.

During the last few decades of the past millennium, living polymerizations underwent a revival by the application of radical chemistry. Living would usually be surrounded by quotation marks as these polymerizations were considered less animate than anionic polymerizations.[4] The onset of this revival can be traced back to the early 80s, when Otsu, recapitulating on some of his older work and literature reports from others, discovered that the addition of certain compounds (*e.g.* dithiocarbamates, disulfides) to a radical polymerization resulted in a system that exhibited some living characteristics.[5] Otsu introduced the term *iniferter* for this technique because the dithiocarbamates acted as initiators as well as transfer and termination agents (reaction **a**–**d**, Scheme 2.2).[6] Although this system was prone to side reactions and unable to produce low polydispersity material, some interesting results were obtained and, more importantly, insight was gained in the requirements for living radical polymerizations. This resulted in a general model which would

Scheme 2.2. General scheme of living radical polymerization with iniferters. Iniferter **AB** dissociates thermally or photochemically, forming a reactive radical **A** and a stable radical **B** (**a**). **A** initiates polymerization (**b**) and can be deactivated by coupling with **B** (**c**). This is a reversible process. Transfer to iniferter (**d**) and transfer to dormant polymer (**e**) are other possible reactions that may occur depending on the structure of the iniferter. Besides, as in any free radical process, bimolecular termination takes place (**f**) by combination or disproportionation.

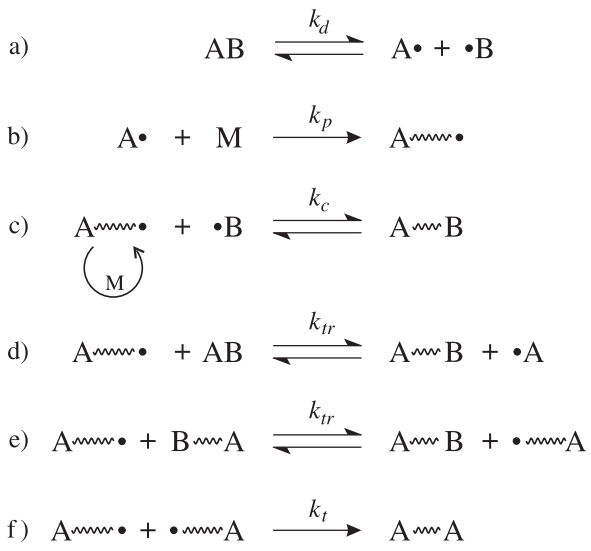

form the basis for living radical polymerizations based on reversible termination, which will be elucidated further in paragraph 2.1.1. Although transfer to the iniferter was mentioned as an alternative chain-stoppage mechanism (reaction **d**), transfer rates to the dormant polymer species (reaction **e**) would generally be low[6] and this was not recognized as a second possible mechanism for living radical polymerization. Several polymerization mechanisms would later be developed based on such a reversible transfer process, among which reversible addition–fragmentation polymerization (RAFT), the subject of this thesis. The essential feature of living radical polymerizations is the mechanism of reversible deactivation, which ensures that all chains grow during the entire polymerization process, mimicking the behaviour of anionic polymerization. Although the chains do not actively grow at every discrete instant of time, an equilibrium between the active and the dormant states garantees that macroscopic variations in the reaction conditions throughout the conversion trajectory are translated into intramolecular variations rather than large differences *between* the individual chains, resulting in a homogeneous and well-defined product.

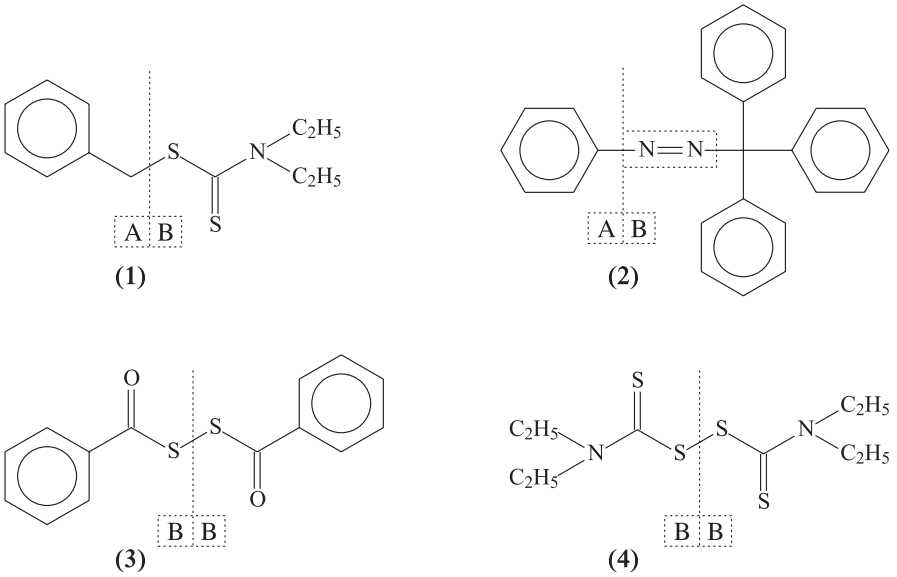

Scheme 2.3. Iniferter structures: *N*,*N*-diethyldithiocarbamate (**1**) Triphenylphenylazomethane (**2**) Dibenzoyl disulfide (**3**) Tetraethylthiuram disulfide (**4**). The dotted lines indicate where the iniferter molecules are ideally cleaved by either chemical, thermal or photochemical procedures. The **A** and **B** signs indicate the dominant function of the formed radical in the reactions depicted in Scheme 2.2. The system suffers from a variety of side reactions as some of the formed radicals are of a mixed **A**/**B** character and alternative fragmentation routes exist.

2.1.1. Reversible Termination

Iniferters

Otsu realized that the position of the equilibrium in reaction **c** (Scheme 2.2) is of paramount importance. A polymer that is required to grow during the entire polymerization reaction is allowed to spend only a minute fraction of its reaction time in the actual radical-state. This means that the equilibrium should be strongly shifted towards the dormant, right hand side. Furthermore, the deactivation reaction itself should be fast as compared with propagation. Ideally, the number of monomer units inserted during each activation–deactivation cycle is small compared with the degree of polymerization that is aimed at. Scheme 2.3 depicts several iniferter structures with their locus of fragmentation and the type of radicals that are produced (**A** or **B** according to Scheme 2.2). The number of monomer units taken up during each cycle in the iniferter process was estimated to be around 30,[7] resulting in high polydispersities. This was caused by the relative low activity of **B**

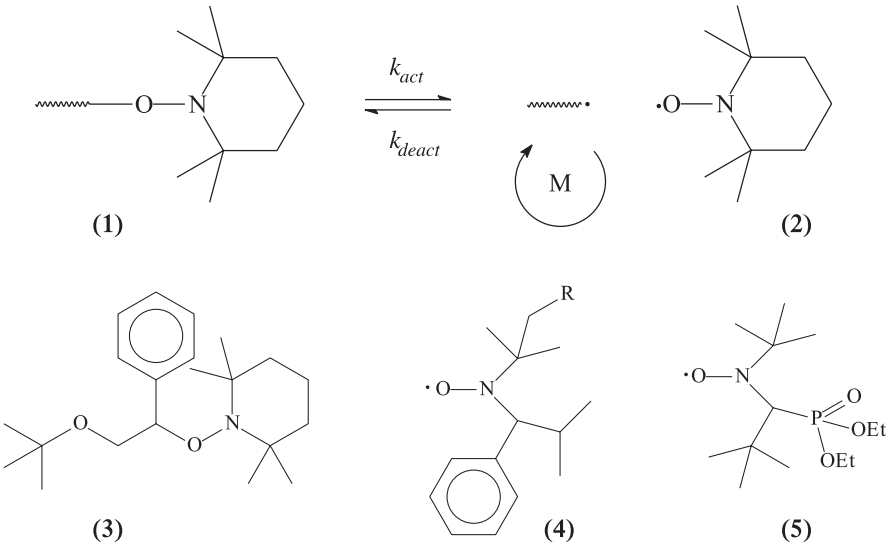

Scheme 2.4. a) The activation–deactivation equilibrium in nitroxide mediated polymerization (reaction **c**, Scheme 2.2). An alkoxyamine (**1**) dissociates reversibly to produce a radical, which can add monomer, and the persistent 2,2,6,6-tetramethylpiperidinine-*N*-oxyl (**2**, TEMPO) radical. A typical example of an initial alkoxyamine structure (**3**) that is applied as initiator for *e.g.* the polymerization of styrene. 2,2,5-Trimethyl-3-(1'-phenylethoxy)-4-phenyl-3-azahexane (**4**)[8,9] and *N*-tert-butyl-*N*-[1-diethylphosphono-(2,2-dimethylpropyl) nitroxide (**5**)[10,11] are two examples of more versatile nitroxides applicable to *e.g.* acrylates and conjugated dienes as well.

as a deactivator. Furthermore, side reactions occurred that caused the dormant polymer chain to split up in an alternative way, thereby irreversibly destructing the counterradical.

The iniferter dissociates into two different radical species (reaction **a**). One of these species is able to add to monomer and form a growing polymer chain (reaction **b**). The other radical should be inactive in this respect and serves only to terminate the growing polymer chain (reaction **c**). The species generated in this process is a dormant polymer chain, which can be reactivated photochemically or by thermal energy, allowing gradual growth throughout the polymerization.

Nitroxides

In 1984, living radical polymerization was reported by Rizzardo *et al.*[12,13] These authors reported the application of stable nitroxide radicals as deactivators. The activation and deactivation rate constants (reaction **c**, Scheme 2.2 and reaction **a**, Scheme 2.4) had more favorable values than those in the iniferter system, resulting in rapid deactivation of propagating radicals and an equilibrium which

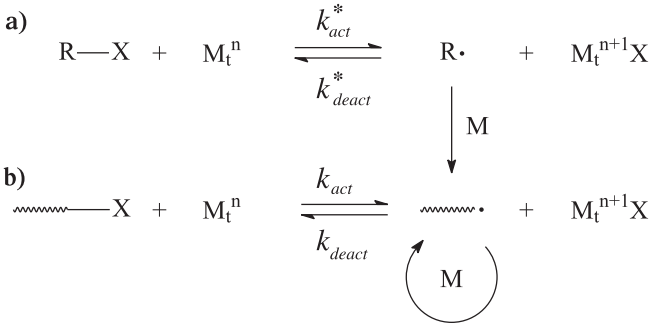

Scheme 2.5. General scheme of reversible deactivation in Atom Transfer Radical Polymerization. **a**) A halide atom (X, *e.g.* Br, Cl) is transferred from the alkyl halide initiator to a transition metal complex (M, *e.g.* Cu, Fe) upon which a radical is formed that initiates polymerization. (reaction **a**, Scheme 2.2) **b**) The same type of equilibrium is established between propagating radicals and dormant, halogen end-capped polymer chains (reaction **c**, Scheme 2.2).

was shifted strongly to the dormant side. This allowed the preparation of very low polydispersity polystyrenes by radical reactions for the first time in history. Initially, this chemistry seemed applicable exclusively to styrene polymerizations at high temperatures,[14,15] but recent literature reports more versatile nitroxides that can also be used in combination with acrylates and at lower temperatures.[8,9,10,11,16] Refering to Scheme 2.2, reactions **d** and **e** do not take place in nitroxide mediated polymerization, and the system relies exclusively on reversible termination.[17] The kinetics are governed by the so-called persistent radical effect, described by Fischer.[18,19] Once the initiator has been converted to dormant species through reactions **a** and **b**, an equilibrium is established between active chains and dormant species. Propagating species and deactivating persistent radicals (*i.e.* nitroxides) are generated in equimolar amounts. Propagating species are slowly taken out of this equilibrium via bimolecular termination (reaction **f**) resulting in an excess of nitroxide that shifts the equilibrium (**c**) to the left, increasing the level of control over the reaction, but also decelerating polymerization.

Atom Transfer Radical Polymerization

Another living radical polymerization technique based on reversible deactivation is atom transfer radical polymerization (ATRP).[20,21,22] This system utilizes a transition metal complex to deactivate a propagating radical by transfer of a halogen atom to the polymer chain-end, thereby reducing the oxidation state of the metal ion complex (Scheme 2.5). A widely investigated system is based on copper (with a transition of Cu(II) into Cu(I)), but also nickel, palladium, ruthenium and

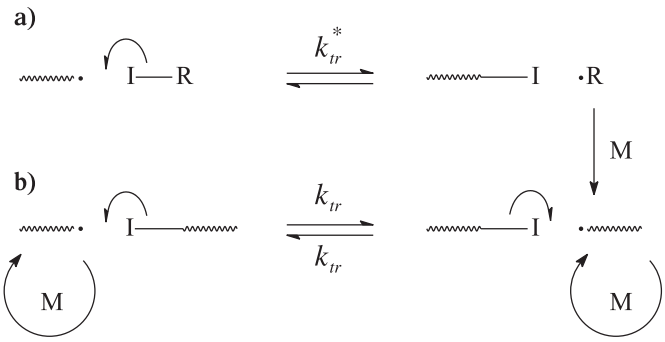

Scheme 2.6. General scheme of degenerative transfer. In contrast to Schemes 2.4 and 2.5, radicals are generated by a conventional initiator. **a**) Transfer takes place to an alkyl iodide (*e.g.* 1-phenylethyl iodide), end-capping the propagating chain with an iodine atom (reaction **d**, Scheme 2.2). **b**) An equilibrium is established between propagating chains and dormant iodine-ended chains (reaction **e**, Scheme 2.2). Note the similarity between these reactions and those in Scheme 2.5. The use of bromide and cloride chains requires the metal complex; direct transfer is only possible when iodine is used.

iron qualify as suitable candidates. The halogen is usually bromine or chloride. The process can be applied to a wide range of monomers and at mild reaction conditions, though it must be said that trace amounts of oxygen can have a much more dramatic effect on the reaction rate than in a conventional radical polymerization.[23] Notable examples of monomers that cause problems are those with anhydride groups or protonated acids (maleic anhydride, acrylic acid, methacrylic acid). A further drawback, restricting industrial application, is the presence of considerable amounts of metal in the product. Nonetheless, numerous well-defined complex polymer architectures have been prepared with ATRP.[24,25]

2.1.2. Reversible Transfer

Alkyl Iodides

Much more dynamic by nature are living radical polymerizations based on degenerative transfer reaction schemes. The number of radicals in such a process is determined by the addition of a initiator that produces radicals, similar to conventional free-radical polymerization. Alkyl iodides fall in this category where a direct equilibrium is established between growing and dormant polymer chains (Scheme 2.6). The radical is exchanged with a iodine atom to stop the growth of the propagating radical and (re)activate the alkyl iodide. Suitable starting materials are 1-phenylethyl iodide[17] and 1-iodotridecafluorohexane.[26] The transfer rate coefficient is

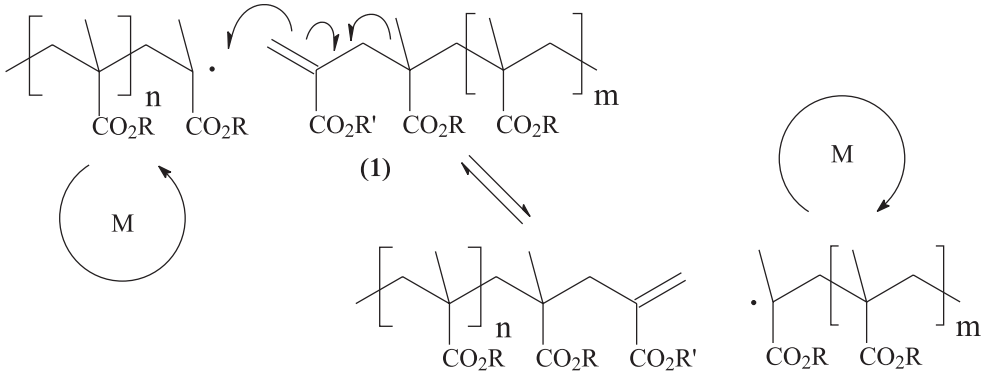

Scheme 2.7. Reversible addition–fragmentation chain transfer using methacrylic macromonomers. One single methacrylic unit is exchanged in the process. This can be either the same or a different R-group. The transfer constant of the process is generally low. In order for the process to exhibit living characteristics the polymerization should be conducted under starved conditions.

relatively low (*e.g.* for 1-phenylethyl iodide $k_{tr} = 2400\,\mathrm{dm^3 \cdot mol^{-1} \cdot s^{-1}}$ for styrene at 80 °C),[17] such that starved conditions have to be used in order to obtain low polydispersities.

Reversible Addition–Fragmentation Chain Transfer (RAFT)

Methacrylate monomers were the first species used as RAFT agents. The discovery of cobalt complexes that acted as catalytic chain transfer agents[27] allowed the facile preparation of short methacrylate oligomers with a terminal carbon–carbon double bond (**1**, Scheme 2.7).[28] It was found that these macromonomers could be applied as chain transfer agents, operating via a so-called addition–fragmentation process.[29,30] When applied in the polymerization of the same or another methacrylate monomer, the process would be reversible (Scheme 2.7). Due to the low reactivity of these macromonomers[31] a high monomer concentration would lead to the transfer reaction being unable to compete with propagation. Moad *et al.*[31] showed, however, that such polymerizations could lead to living radical characteristics when conducted under starved conditions with respect to the monomer. The reversible character would disappear if monomers other than methacrylates were present. Polystyryl and -acryl chains form poor leaving groups, resulting in a loss of living character. Obviously, for such a process to be generally applicable in batch reactions, more reactive transfer agents would be required. These were found in the form of dithioesters,[32,33] selected dithiocarbamates,[34,35] xanthates[34] and trithiocarbonates.[34,36] These molecular structures were remarkably similar to the original iniferters, but were optimized for more efficient transfer reac-

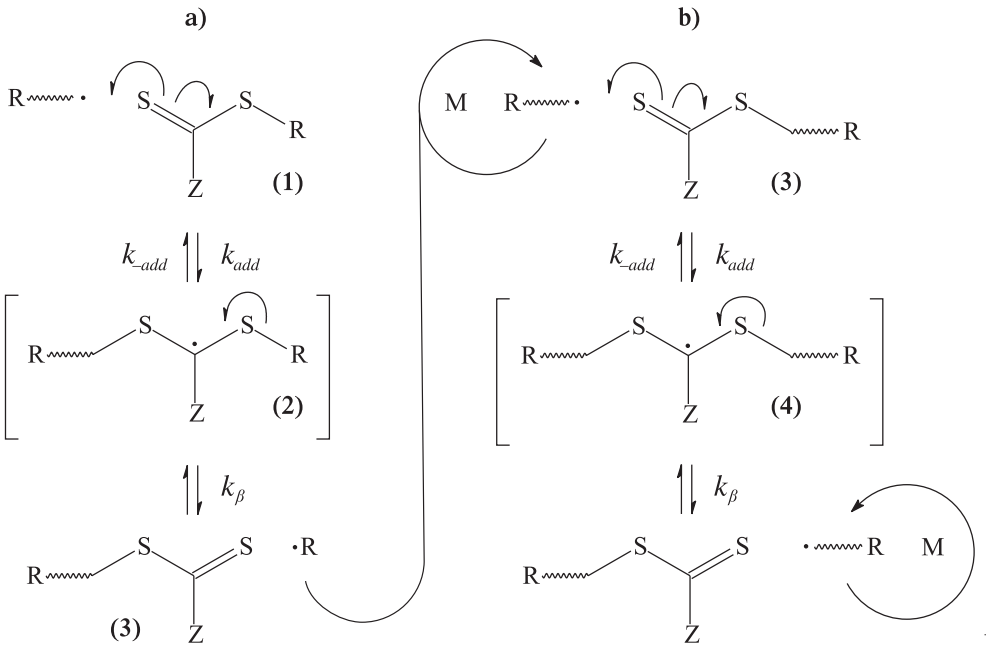

Scheme 2.8. Schematic representation of reversible addition–fragmentation chain transfer using a dithioester (**1**). **a**) reaction of the initial transfer agent with a propagating radical, forming a dormant species (**3**) and releasing radical R. The expelled radical initiates polymerization and forms a propagating chain. **b**) equilibrium between active propagating chains and dormant chains with a dithioester moiety. Note that all reactions are equilibria, but that the *k* values refer to the downward direction of the reaction. Also note that these equilibria are not restricted to specific pairs of chains, but that *any* radical can react with *any* dormant species / RAFT agent.

tions. The patent detailing the invention[32] shows their application in both homogeneous and heterogeneous systems in combination with many different monomers and being compatible with many kinds of functional groups. The reaction paths of these species are similar to those of the macromonomers. In the remainder of this thesis, RAFT will be used to describe the polymerization system using these specific compounds. The reaction scheme is depicted in Scheme 2.8.

Propagating radicals, generated by initiator decomposition and addition of initiator derived radicals to monomer, add to the carbon–sulfur double bond of the RAFT agent (**1**, reaction **a**). The labile intermediate radical (**2**) that is formed fragments to regenerate the starting materials or to form a temporarily deactivated dormant polymer species (**3**) together with a radical (**R**) derived from the RAFT agent. This radical should add to monomer, thereby reinitiating polymerization. An essential featrure in the RAFT mechanism is the fact that the dithiocarbonate moiety (**Z-C(S)S-**), present in the initial RAFT agent (**1**) is retained in the polymer

product (**3**). Because of this, the dormant polymer chains can act as transfer agents themselves. This is shown in reaction **b**. Like in reaction **a**, a propagating radical reacts with the polymeric RAFT agent (**3**). Through this reaction, the propagating radical is transformed into a dormant polymer, while the polymer chain from the polymeric RAFT agent is released as a radical which is capable of further growth. Similar to reaction **a**, the dithiocarbonate moiety is retained and again, the newly formed dormant species can be reactivated.

It is important to realize that Scheme 2.8 offers a *schematic* representation of the process. The equilibria that are shown take place between the whole population of propagating radicals and the whole population of dormant chains rather than the the pair-wise reaction between a specific radical and a specific dormant chain, which might be infered from Scheme 2.8. The latter construct would require the concentration of active radicals to match that of the dormant species which is obviously not the case. The concentration of radicals is in principle unaffected by transfer reactions in general, of which the reactions in Scheme 2.8 are an example.* This means that the (pseudo steady-state) radical concentration is determined in the same manner as in an uncontrolled radical polymerization, *viz.* by the equilibrium between initiation and termination. The radical concentration in a typical polymerization is of the order of magintude of $10^{-9}-10^{-8}$ mol·dm^{-3}. The concentration of RAFT agent (the sum of the polymeric RAFT and the initial agent) is constant as the dithiocarbonate moiety is not destroyed in the transfer reactions.* Its concentration is therefore equal to the initial RAFT concentration at the beginning of the reaction, which in a typical polymerization amounts to $10^{-4}-10^{-2}$ mol·dm^{-3}. This indicates that a small number of radicals are exchanged amongst a large number of polymer chains at any given moment in time. The concentration of the intermediate species will be discussed in more detail in section 2.3 on page 43. Its concentration, and its existence are unimportant to the understanding of the manner in which control is obtained in RAFT polymerization.

* This is only true in a first approximation. As transfer agents influence the radical chain length distribution, the termination rate coefficient will be affected and with it the equilibrium between initiation and termination. Furthermore, section 2.3 describes a side reaction in the RAFT scheme that seriously decreases the concentration of propagating radicals and also destroys a small fraction of the RAFT moieties. In order to understand how control is achieved in RAFT polymerizations, however, this side reaction is unimportant.

For RAFT polymerizations to obey the rules of living polymerizations a few aspects in the reaction scheme are of importance:

I. A rapid exchange reaction.

II. Good homolytically leaving R group, capable of reinitiation.

III. Constant number of chains during the polymerization.

I. The exchange reaction during the polymerization (**b**) should be rapid compared with propagation. As can be deduced from the symmetrical structure of intermediate species (**4**), there is no preference for the direction of fragmentation. In other words, the equilibrium constant for the reaction as a whole is unity. The transfer rate R_{tr}, the unidirectional rate of the reaction is given in Eq. 2-1, where the transfer rate coefficient k_{tr} can be split up in contributions from addition and fragmentation, shown in Eq. 2-2:

$$R_{tr} = k_{tr} \cdot [radical] \cdot [RAFT] \qquad \textbf{(2-1)}$$

$$k_{tr} = k_{add} \cdot \frac{k_{\beta}}{k_{\beta} + k_{-add}} \qquad \textbf{(2-2)}$$

Obviously, there is no preference for the direction of the fragmentation process as in both cases a polymer chain with a similar structure leaves the molecule, a negligible difference being its chain length. Therefore, k_{-add} and k_{β} (reaction **b**, Scheme 2.8) are identical and the equation simplifies to Eq. 2-3, which implies that the fragmentation rate coefficient is unimportant in this respect.

$$k_{tr} = 0.5 \cdot k_{add} \qquad \textbf{(2-3)}$$

Assuming that transfer is fast compared to propagation, the radical is exchanged rapidly among the chains. All chains have an equal chance to add monomer and all will grow at the same rate.

II. For the final molar mass distribution to have a low polydispersity it is also important that all chains have started growing at the same time, namely the onset of the reaction. Therefore the initial transformation from RAFT agent to dormant polymer species (reaction **a**, Scheme 2.8) needs to be rapid. In this reaction, the intermediate species (**2**) is not symmetrical and the R group will need to be chosen in such a way that it is a better homolytic leaving group than the (oligomeric)

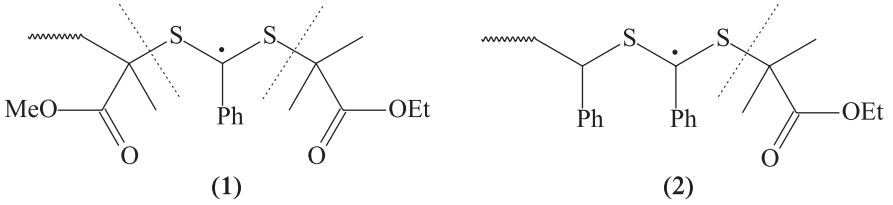

Scheme 2.9. Intermediate radicals formed in the polymerizations of methyl methacrylate (**1**) and styrene (**2**) in the presence of 2-(ethoxycarbonyl)prop-2-yl dithiobenzoate (EMA-RAFT). Dotted lines indicate the preferred fragmentation routes.

polymer chain. In general, the leaving-group character is better for more substituted alkyls and can be increased further by substitution with groups that stabilize the expelled radical through resonance.

An example to illustrate this can be found in the application of 2-(ethoxycarbonyl)prop-2-yl dithiobenzoate (EMA-RAFT). Despite the fact that the 2-(ethoxycarbonyl)prop-2-yl radical is a relatively good leaving group, it will give rise to higher polydispersities (>1.5) in the polymerization of methyl methacrylate (MMA).[32,37] Analysis of the structure of the intermediate species that is formed upon addition of a propagating PMMA radical to the transfer agent (**1**, Scheme 2.9) reveals that the groups attached to the sulfur atoms are almost identical but for their chain length. Therefore, there is no preference for the transfer agent to be converted to a dormant polymer species. Work with the aforementioned MMA macromonomers has revealed that in a comparable case, larger chains have a greater tendency to break,[38] which suggests that the equilibrium in this case is even shifted towards the starting materials. When the same transfer agent is applied in the polymerization of styrene, the 2-(ethoxycarbonyl)prop-2-yl radical is more readily expelled from the intermediate radical (**2**, Scheme 2.9) than the polystyryl radical and low polydispersities (<1.2)[37] are obtained.

Another example can be found in the preparation of poly(styrene–*block*–methyl methacrylate) which can be approached from two directions. One of the monomers is first polymerized in the presence of RAFT, creating polymeric dormant species. These chains are then added to the polymerization of the second monomer, thereby forming block copolymers through the addition to the second monomer. The polymer formed in the first reaction acts as the R-group and must be the better leaving group. Irrespective of the route that is followed (*i.e.* starting with STY or with MMA) the intermediate radical that is formed in the second polymerization has the structure shown in Scheme 2.10. As PMMA is the

Scheme 2.10. The intermediate structure formed during the preparation of poly(styrene–*block*–methyl methacrylate. The preferred fragmentation is indicated by the right arrow resulting in an activated methacrylate chain. The preferred approach therefore is to start with a polymerization of methyl methacrylate and to use these dormant chains as a RAFT agent in the polymerization of styrene.

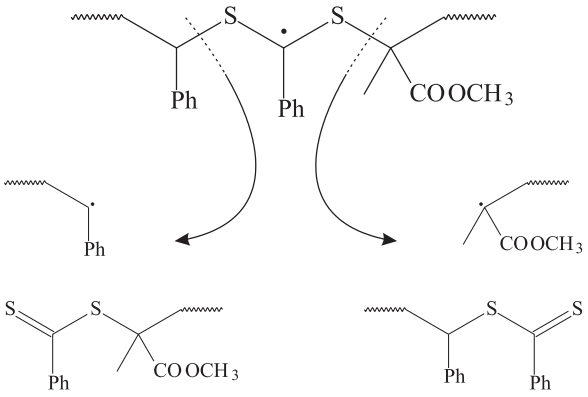

better leaving group, fragmentation preferentially occurs in the position of the right arrow, leading to the products on the right side. If one attempts to make block copolymers by first polymerizing styrene, and using those chains in the MMA polymerization, then the starting materials are regenerated. In terms of Eq. 2-2, k_{-add} is much larger than k_{β}, resulting in a low transfer constant. The molar mass distributions of such a polymerization are depicted in Figure 2.1. The GPC analyses took place after the dithiobenzoate group had been removed by treatment of a polymer solution with triethyl amine and passing the solution through a short silica column. This end-group was removed so that it would not disturb the UV signal. The multidetector setup was used to yield information on the approximate distribution of the individual monomers. The UV detector ($\lambda = 254\,nm$) indicates the styrene units, whereas the refractive index (RI) detector is sensitive to both polymers, though at different levels. With knowledge on the average composition (obtained with ^1H NMR) and the sensitivity of the RI detector towards different polymers,[39] the molar mass distributions were scaled and subtracted to yield information on the composition of the polymer product. Figure 2.1 should be interpreted as follows. The continuous line is the normalized distribution of the starting PS material. The dotted line is the weight distribution calculated from the UV signal of the polymer product, normalized to the same area as that of the starting material. As the amount of styrene units the distribution is based upon remains the same, the areas are chosen to be identical. The areas of the distributions were scaled with mass, or the amount of material. The dashed line represents the entire polymer product and its distribution is a linear combination of those derived from the UV signal and the RI signal. For a given length (*i.e.* a position on the *x*-axis) the ratio of the dotted and the dashed line yields the fraction of styrene within the chain. Obviously, there are considerable experimental errors introduced by this analysis, but an illustrative

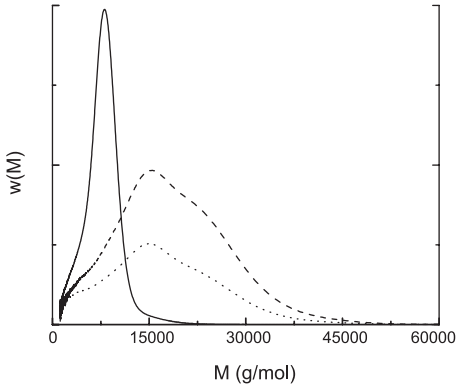

Figure 2.1. Molar mass distributions of the solution polymerization of methyl methacrylate in the presence of polystyryl dithiobenzoate (—). The dormant chain is a poor transfer agent, resulting in a broad block copolymer product (---). The polystyryl chain is however distributed evenly within the product, as can be observed by looking at the UV signal (····).

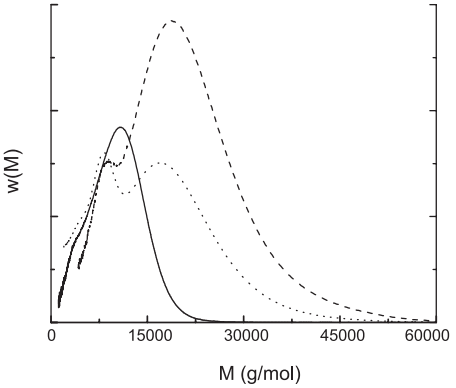

Figure 2.2. Molar mass distributions of the solution polymerization of styrene in the presence of polymethyl methacrylate dithiobenzoate (—). The dormant chain is a good transfer agent, resulting in a narrow block copolymer product (---), with polystyryl chains distributed evenly within the product, as can be observed by the UV signal (····). The product peak at ≈10,000 g/mol consists of PS homopolymer derived from the initiator rather than from the transfer agent.

picture is obtained that indicates that, despite the broad distribution, the creation of block copolymers was successful. When the synthesis is approached from the other direction, referring again to Scheme 2.10, one starts with the ingredients on the left (*i.e.* dormant PMMA chains in a styrene polymerization), and the preferred fragmentation direction yields the desired reaction products. In this case k_{β} exceeds k_{-add} and k_{tr} is high (Eq. 2-2). The molar mass distributions, obtained in the same way as those of Figure 2.1, are given in Figure 2.2. The most important observation is that the polydispersity of the product is much lower for this polymerization, due to the quick and efficient transformation of the dormant PMMA into block copolymers.

These two examples already demonstrate that the demands on the R group of the dithioester RAFT agents are dependent on the monomer that is being polymerized and decrease in the order:

methacrylates > styrenes > acrylates

Examples of versatile transfer agents that work well with the majority of monomers are 2-phenylprop-2-yl dithiobenzoate and 2-cyanoprop-2-yl dithiobenzoate, because of the excellent leaving group character of their respective R groups.

Another important aspect concerning the R-group is its ability to reinitiate polymerization. If the expelled radical R has difficulty adding to monomer, then inhibition and retardation may occur, most notably during the early stages of the polymerization. It results in a slow conversion of the transfer agent and a broadened molar mass distribution. The effect of the reinitiation rate on the polymerization is discussed in more detail in the section 2.3 when retardation is investigated (specifically figures 2.19 to 2.21 on page 52).

III. Finally, a constant number of chains throughout the reaction is of great importance as both chains that cease to grow as well as chains that start growing later during the polymerization would have chain lengths significantly different from that of the bulk of material. The concentration of polymer chains at the beginning of the reaction is equal to the initial concentration of RAFT agent ($[RAFT]_0$), assuming rapid transformation of the RAFT agent into dormant polymer chains. The concentration at the end of the polymerization is given by Eq. 2-4, assuming termination by disproportionation:

$$[chains] = [RAFT] + 2 \cdot f \cdot ([I] - [I]_0) \qquad \textbf{(2-4)}$$

in which $[RAFT]$ represents the concentration of dormant chains, being equal to $[RAFT]_0$, while the second term describes the number of chains that are derived from the decomposed initiator. f is an efficiency factor. For the number of chains to be constant throughout the reaction the term that describes the contribution from the initiator should be neglible compared to the concentration of RAFT agent. This shows that not only the instantanious concentration of radicals is small compared to that of the RAFT agent / dormant species (as discussed on page 28), but that also the cumulative concentration of radicals produced during the polymerization must be small.

Figure 2.3 shows the simulated weight fraction of dead material, originating from termination as a function of conversion for different initiator levels. Clearly, the amount of initiator needs to be considerably smaller than the amount of RAFT agent in order to obtain 'living' material at full conversion. Increased termination is also broadening the molar mass distributions as can be observed in Figure 2.4, which shows the polydispersity as a function of conversion. Under some circumstances, the desire to use a small amount of initiator compared to RAFT agent

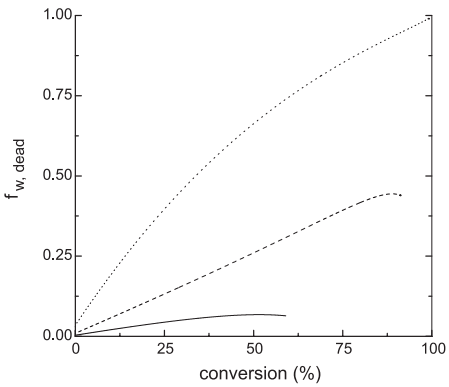

Figure 2.3. Simulation of the weight fraction of dead material ($f_{w,dead}$) as a function of conversion in the solution polymerization of styrene. [styrene]=3 mol·dm^{-3}; [RAFT]=0.04 mol·dm^{-3}; C_T=100; [ini]=0.004 (—); 0.04 (---); 0.4 (····) mol·dm^{-3}. Typical values are used for the remaining parameters. (table 2.2, page 46).

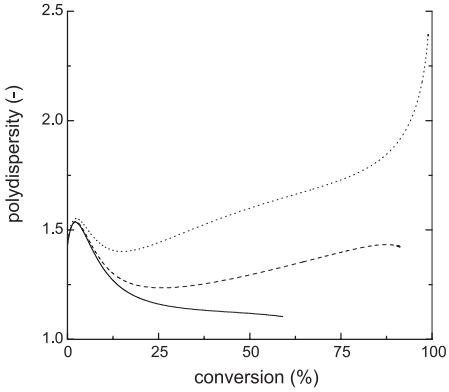

Figure 2.4. Simulation of the polydispersity index as a function of conversion in the solution polymerization of styrene. [styrene]=3 mol·dm^{-3}; [RAFT]=0.04 mol·dm^{-3}; C_T=100; [ini]=0.004 (—); 0.04 (---); 0.4 (····) mol·dm^{-3}. Typical values are used for the remaining parameters. (table 2.2, page 46).

results in exceptionally long polymerization times. This is the case if the amount of RAFT itself is already small, for instance because one aims to achieve high molar masses. The target number average molar mass is given by Eq. 2-5:

$$\overline{M}_n = \frac{[M]_0 \cdot FW_{mon}}{[RAFT]_0} \qquad \textbf{(2-5)}$$

which devides the total mass of polymer at full conversion over the number of chains. The total polymer mass per unit volume is found by multiplying the initial monomer concentration ($[M]_0$) with the molar mass of the monomer (FW_{mon}). The number of chains is equal to that of the (initial) concentration of RAFT agent. For a styrene (FW_{mon} = 104.15 g·mol^{-1}) bulk polymerization starting at a monomer concentration of 8.7 mol·dm^{-3}, aimed at producing polymer with a number average molar mass of 10^5 g·mol^{-1}, a concentration of RAFT agent of $9 \cdot 10^{-3}$ mol·dm^{-3} should be used. This restricts the use of initiator to concentrations much lower than that. When the production of a low polydispersity polystyrene chain is the exclusive goal, the use of initiator concentrations a factor of 4 to 6 lower than that of the RAFT agent yields polymers with a polydispersity index below approximately 1.15. However when an even lower polydispersity is desired or when the polystyrene is only an intermediate for further reaction steps (*e.g.* block copolymer preparation) a considerably lower initiator concentration will need to be used, leading to

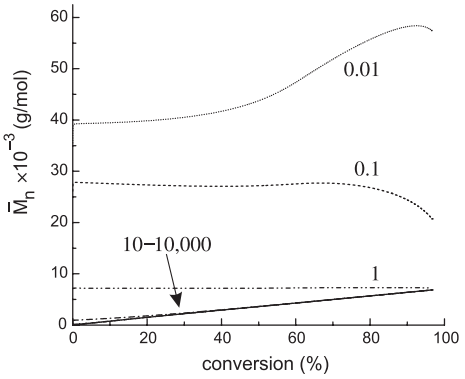

Figure 2.5. The effect of the transfer constant C_T on the development of the number average molar mass with conversion. Labels next to the curves indicate the transfer constant. Four coinciding unlabeled lines correspond with C_T 10/100/1000/10000.

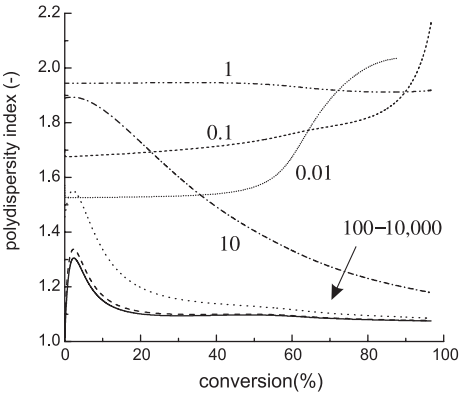

Figure 2.6. The effect of the transfer constant C_T on the development of the polydispersity with conversion. Labels next to the curves indicate the transfer constant.

impractable recipes. This situation is less of a problem when one aimes at lower molar masses, uses monomers with a high propagation rate constant relative to their termination rate constant or when one polymerizes in a system that otherwise increases the ratio of propagation over termination, like for instance in many emulsion polymerizations.

2.2. The Transfer Rate in RAFT Polymerization

2.2.1. The Influence of the Transfer Constant

The transfer constant C_T, defined as the ratio of the transfer and propagation rate coefficients (Eq. 2-6), is of paramount importance in RAFT polymerizations.

$$C_T = k_{tr}/k_p \qquad \textbf{(2-6)}$$

The growing radical center needs to be transferred quickly so that the propagating chain will not grow too rapidly to too long a chain length, and such that the dormant species will have a chance to be reactivated as well. Exactly how large the transfer constant has to be, depends on the goal of the experiment, but Figure 2.5 demonstrates that 10 is the minimum order of magnitude for the number-average molar mass to evolve linearly with conversion. This figure is the result of simulations that were carried out for a batch styrene solution polymerization at 80°C

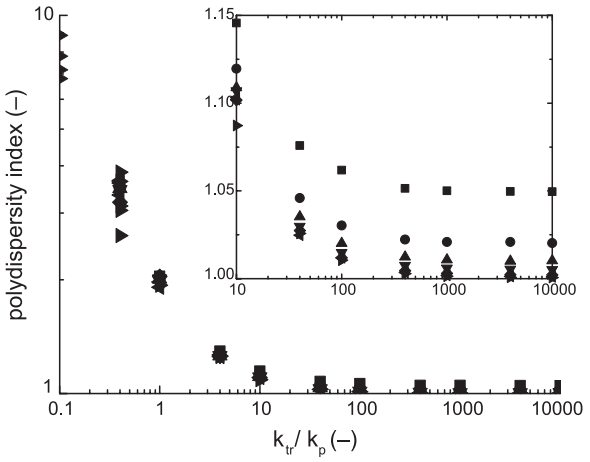

Figure 2.7. Monte Carlo simulations of polydispersity at full conversion for different values for C_T and different target molar masses. Termination is neglected. For low transfer constants, the polydispersity rises rapidly. For values above 10 to 100, the exact size of the transfer constant is no longer important. A small effect of the target molar mass can be observed. Target degrees of polymerization range from 20 (■), 50 (●), 100 (▲) up to 2000. Lower masses correspond to higher polydispersities, however higher molar masses will suffer more if termination is accounted for, corresponding with the practical situation.

using the same concentrations and parameters that will be used in section 2.3, see Table 2.2, on page 46. The simulations make use of the 'Method of Moments' to gain information on the molar mass averages and the polydispersity index and take into account termination and initiation both by initiator decomposition and styrene autoinitiation. The molar mass and polydispersity index are based on the terminated and the dormant material. The technical details of this method are discussed in the appendix on page 191. When a low polydispersity product is important, an even higher transfer constant is desired, although a value of 10 reaches a fairly low polydispersity at full conversion as well. This is demonstrated in Figure 2.6. The upswing in polydispersity at 60% conversion, when a very low activity transfer agent is used, is explained by depletion of initiator after which a considerably lower radical production rate remains, originating from styrene thermal autoinitiation. Müller *et al.*[40] have derived analytical relationships wich enable polydispersity to be estimated for RAFT polymerizations, provided that termination can be neglected. According to these authors, Eq. 2-7 approximates the value of polydispersity that will be reached at full conversion in a batch polymerization, neglecting contributions from termination derived materials:

$$\overline{M}_w/\overline{M}_n = 1 + 1/C_T \qquad \textbf{(2-7)}$$

Similar to the simulations, Eq. 2-7 points out that 10 is a required order of magnitude for the transfer constant to yield low polydispersity material. Additionally, Monte Carlo simulations confirm that for a batch process a minimum transfer

constant of approximately 10 is required to obtain low polydispersities (Figure 2.7). The simulations are carried out using different targets for the degree of polymerization, set by the ratio of monomer to RAFT agent (Eq. 2-5), and for different transfer constants. Details of the simulation can be found in the appendix on page 199. At lower transfer constants, the polydispersity increases steeply with conversion. This increase of polydispersity can be counteracted by semi-batch procedures. At higher transfer constants, the effect of the degree of polymerization can be observed. Shorter chains will be subject to statistical variations. Still, polydispersities can be considered essentially identical and in practice, the deviation from unity will be determined by the level of termination that occurs during the reaction, which is neglected in these Monte Carlo simulations. In this sense, low polydispersities will be more easily attained in reactions designed to yield shorter chains (see the remarks on page 35).

2.2.2. Determination of the Transfer Constant

Conventional Procedures

Determination of the transfer constant (Eq. 2-6) for a certain compound, is typically achieved by the construction of a Mayo plot, based on the average molar mass,[41] or alternatively by the logarithmic chain length distribution method (*ln* CLD method), using the entire molar mass distribution.[42,43] These two methods are fairly similar as both of them ultimately rely on the principle that for a given concentration of monomer and transfer agent, the transfer constant can be derived from the polymer molar mass, provided that other reactions, most notably termination, are unimportant. Basically, a chain with degree of polymerization n is known to have experienced $(n-1)$ propagation steps and a single transfer event. Experimental data are obtained from low conversion bulk or solution polymerizations, such that the concentrations of monomer and transfer agent are known and can be considered constant. A small amount of initiator is used so that termination has a negligible influence. The application of these methods to the RAFT agents that are used in this thesis, is complicated by two factors, *viz.* the very high reactivity and the reversibility of the transfer event. The high reactivity makes that even in low conversion experiments, a large change in the concentration of transfer agent is to be expected. Using RAFT agents, the transfer agent is not consumed, but rather transformed, leaving the total concentration constant. Nonetheless, the transformed transfer agent is a chemically different species. This reversible character of the transfer event is particularly deleterious to these methods. A chain with degree of

polymerization n is still known to be formed by $(n-1)$ propagation steps, but the number of transfer events remains undefined. It is at least one but can also be much higher, even exceeding than the number of propagation steps. Blind application of either the Mayo method[41] or the construction of a *ln* CLD plot[43] will yield an apparent, concentration dependent, transfer constant that is an underestimation of the real value as the calculation assumes a single transfer event to have occured for all chains.[44]

As an alternative, the consumption rate of the transfer agent may be monitored as a function of monomer conversion by an appropiate analytical technique. Goto *et al.* used gel permeation chromatography (GPC) to determine the transfer activity of polymeric dithioester adducts.[45,46] This requires the polymeric radical that is formed upon activation of such a dormant species, to grow to a length that can be distinguished from the starting material in the GPC trace. For polystyryl dithioacetate a transfer constant of 180 was found in a styrene polymerization at 60 °C, considerably higher than the value of 10 obtained by the *ln* CLD method for the compable benzyl dithioacetate RAFT agent.[44] Likewise, the value of 26, found as the transfer constant of benzyl dithiobenzoate,[47] is also expected to be a severe underestimation. With the same GPC technique, the transfer constant of a similar polymeric transfer agent, polystyryl dithiobenzoate could not be accurately determined, but was estimated to be 6000±2000 at 40 °C in a styrene polymerization. For such high transfer rates, experimental conditions that result in the addition of sufficient monomer units upon activation, require an extremely low concentration of RAFT agent which in turn results in other experimental or analytical complications. This is shown by Eq. 2-8:

$$\bar{\nu} = \frac{R_p}{R_{tr}} = \frac{1}{C_T} \cdot \frac{[M]}{[RAFT]} \qquad \textbf{(2-8)}$$

in which $\bar{\nu}$ is the kinetic chain length under the assumption that transfer is the predominant chain stoppage event and R_p and R_{tr} are the rates of propagation and transfer, respectively. This kinetic chain length indicates the number of monomer units that is added to a chain after activation. When, for instance, 50 units are required for a well-separated peak in the GPC trace, a transfer constant of 6000 dictates that the concentration of RAFT agent be $3 \cdot 10^{-6}$ times the monomer concentration, quite possibly leading to analytical errors.

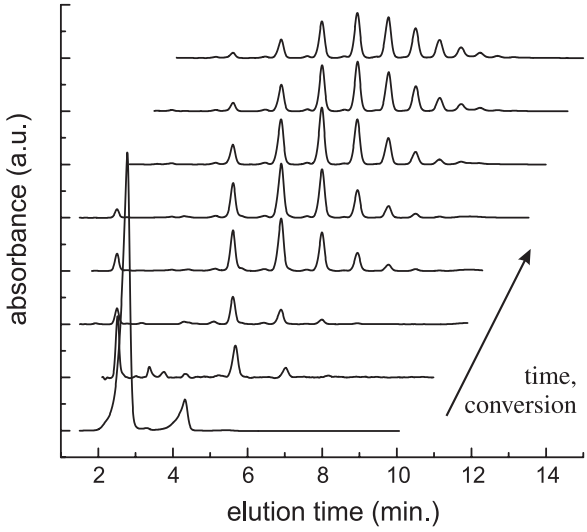

Figure 2.8. HPLC traces of samples taken during a styrene solution polymerization in the presence of EMA-RAFT. The figure shows the UV signal recorded at a wavelength of 320nm, which selectively detects the dithiobenzoate moiety in the dormant oligomers. The transfer agent elutes at 2.5min. and disappears rapidly during the polymerization. A distribution of oligomers is formed that grows in a gradual manner.

A Model Experiment

In order to obtain an estimate of the transfer constant of the RAFT agent and that of short dormant oligomers, a solution polymerization of styrene was undertaken in the presence of 2-(ethoxycarbonyl)prop-2-yl dithiobenzoate. The consumption rate of the RAFT agent and the evolution of the concentrations of oligomeric dormant chains were monitored throughout the polymerization with the aim to compare these concentrations with the results of simulations. Experimental details can be found in Table 2.1. Samples taken during the reaction were analyzed using High Performance Liquid Chromatography (HPLC). Using this technique, individual oligomers could be detected up to a degree of polymerization of approximately 30, of which the first 15–20 were baseline separated. Figure 2.8 shows HPLC traces of samples taken during the reaction. These traces are based on the signal of the UV detector at a wavelength of 320nm, which records the absorption of the dithiobenzoate moiety. The signals at a lower wavelength (254nm, not shown) indicate the presence of a second distribution of oligomers in small quantities at longer polymerization times, caused by termination reactions. The plot allows the construction of conversion–time profiles for each individual dormant chain. For this reason, this reaction was simulated using the 'Exact Model', which simulates the concentrations of all individual dormant, terminated and radical chains. Details on this simulation can be found in the appendix on pages 177 and 185. The experiment is designed to produce chains with a degree of polymerization of 50. The model is capable of simulating systems with chains as long as 100 monomer units on average desktop computers and automatically stops the integration when the

Table 2.1: Recipe for the Solution Polymerization of Styrene Used to Determine the Transfer Constant at 80 °C.

		Quantity (g)	Concentration (mol·dm^{-3})
monomer	styrene	40.0	3.80
initiator	dimethyl 2,2'-azobisisobutyrate	$7.0 \cdot 10^{-2}$	$3.0 \cdot 10^{-3}$
RAFT agent	EMA-RAFT	2.0	$7.5 \cdot 10^{-2}$
solvent	methyl isobutyrate	≈48.5[a)]	

a) solvent was added volumetrically to bring the total volume to 100.00 ml at ambient temperature.

fraction of chains exceeding this length becomes larger than a given limit, which was set to be 1 % of the total of chains. The reaction was simulated using different values for C_T and accepted values for the other parameters. Concentrations are listed in Table 2.1. Rate constants were taken from the literature. The dissociation rate constant was found to be $1.1 \cdot 10^{-4}\,s^{-1}$,[48] and the propagation rate constant for styrene was $660\,dm^{-3} \cdot mol^{-1} \cdot s^{-1}$.[49] Furthermore, a chain-length dependent termination rate coefficient was used, which is explained in more detail in the next section on page 46.[50,51]

The results of the simulation are shown in Figure 2.9, together with the experimental data. For low C_T, dormant species are formed only slowely; this process takes place at the same rate as the consumption of transfer agent. When C_T increases, the dormant species are formed more quickly (compare the *y*-axes) and also dissappear as the reversibility of the reaction becomes important and dormant species are reactivated again. However, the sensitivity of the profiles to the magnitude of C_T is lost above approximately 1,000. The experimental profiles qualitatively correspond to a value for C_T in between 1,000 and 10,000, but the time axis is contracted by a factor of around 3. This can be explained by the fact that retardation occurs in RAFT polymerizations by a mechanism explained in the next section on page 43. The 'Exact Model' which is used here would become computationally too demanding, if retardation was to be accounted for. Experimental data used in the next section, however, show that a decreased polymerization rate by a factor of three is quite plausible for such a system (*e.g.* Figure 2.11). The insensitivity towards C_T for such high values prevents a precise determination of its value, but at least, this method confirms that the value of 6000±2000 that was found for longer polystyryl dithiobenzoate chains also holds for the oligomeric analogues and for 2-(ethoxycarbonyl)prop-2-yl dithiobenzoate. The poor sensitivity of the method can be understood from Figure 2.7, which demonstrates that for a target degree of polymerization of 50, the polydispersity no longer decreases for $C_T \geq 100-500$.

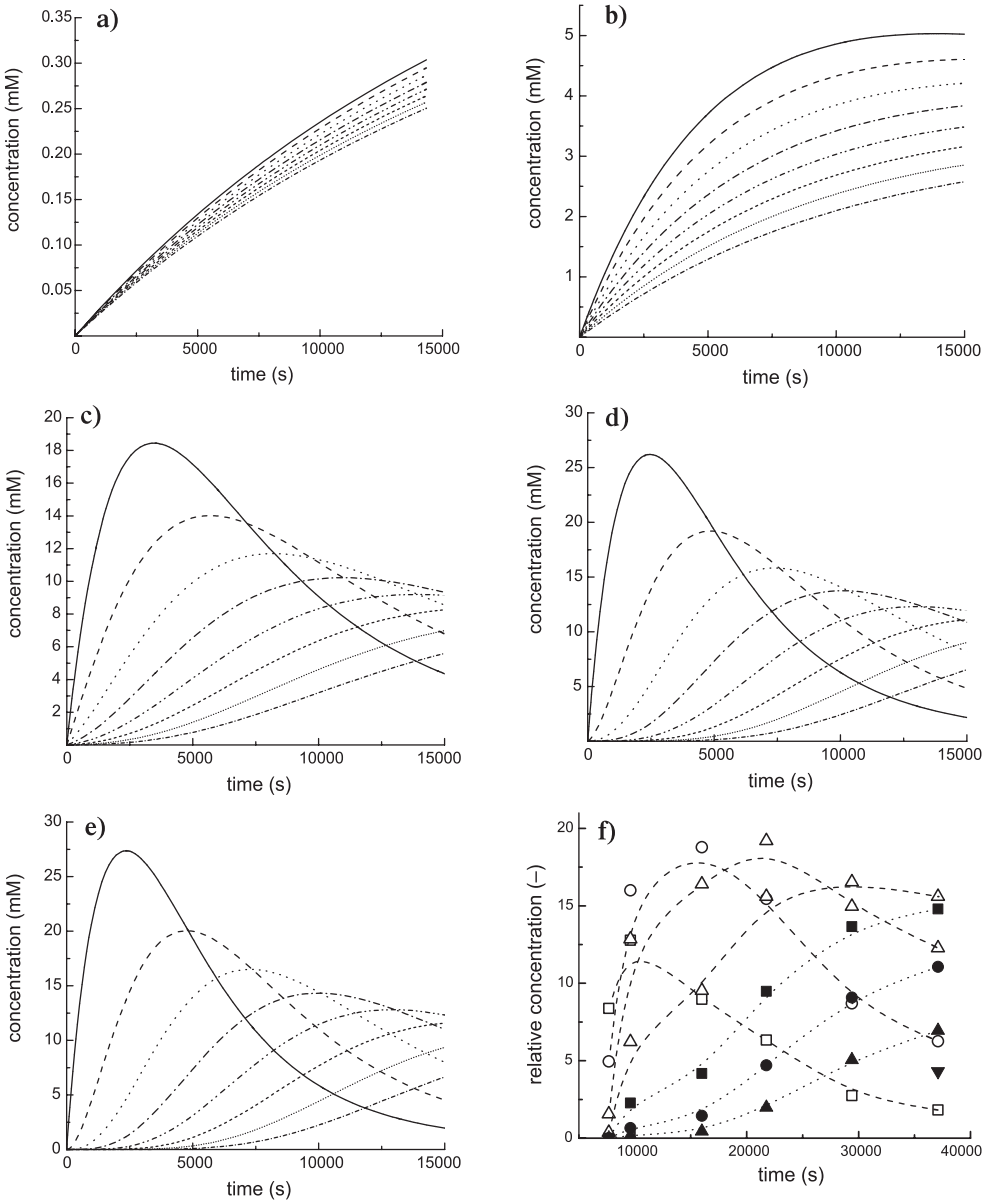

Figure 2.9. The effect of the transfer constant on the concentration profiles of eight oligomeric dormant species over time with one (—) to eight (·---) styrene units in their chains. The transfer constant, C_T, is 1 (**a**), 10 (**b**), 100 (**c**), 1,000 (**d**) and 10,000 (**e**). The experimental profiles, derived from the data in Figure 2.8, are given in **f**. Despite the discrepancy between the experimental and simulated time axis, the behavior qualitatively corresponds to the simulations with C_T in the order of magnitude of 1,000–10,000. Both the experimental plot and the simulated ones give information on oligomeric dormant species with degrees of polymerization (dp) of 1 to 8, in the expected order. dp = 1 (□), 2 (○), 3 (△), 4 (▽), 5 (■), 6 (●), 7 (▲) and 8 (▼). The B-spline fits in **f** serve solely as a guide to the eye.

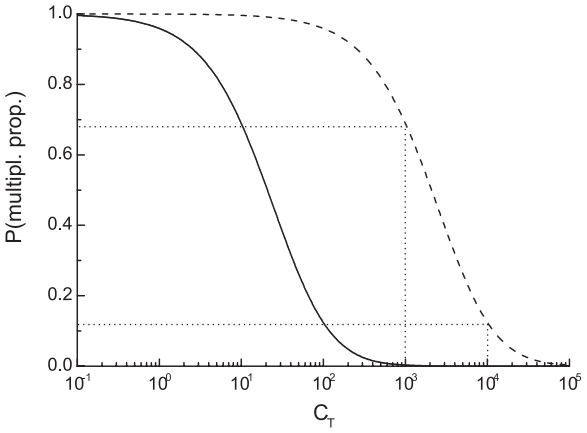

Figure 2.10. The probability that an active chain adds multiple monomer units, calculated using Eq. 2-9. Concentration monomer: 3.8 mol·dm^{-3}. Concentration RAFT: $7.5 \cdot 10^{-2}$(—) and $7.5 \cdot 10^{-4}$(---) mol·dm^{-3}. Note that for a living polymerization, this value need not be negligible, but that for the applicability of oligomer analysis by HPLC, C_T values are distinguished only when $P(prop)^2$ is different.

Obviously, $\overline{M}_n$ is not affected, when the initial RAFT agent is consumed. Differences between the profiles should be expressed in the polydispersity of the distribution, which in turn is related to the possibility that an active chain adds multiple monomer units. When this probability can be neglected, a further increase in C_T will not improve the polydispersity any more. The probability that an active chain adds two monomer units is given by Eq. 2-9, neglecting termination:

$$P(propagation)^2 = \left(\frac{[M]}{[M] + C_T \cdot [RAFT]} \right)^2 \qquad \textbf{(2-9)}$$

Figure 2.10 shows this probability as a function of C_T (—) for the aforementioned solution polymerization which is detailed in Table 2.1. The probability for the addition of multiple monomer units becomes negligible above $C_T = 1{,}000$. Only when the concentration of RAFT agent is lowered by two orders of magnitude (---), would the experiment produce a suitably different probability to be able to discriminate between $C_T = 1{,}000$ and *e.g.* 10,000 (····). This experiment was not conducted, however, as the timeframe useful for sampling would become considerably smaller. A degree of polymerization too high to be analyzed would quickly be reached in the polymerization and the contributions from termination reactions might have obscured the results.

This leaves us to conclude that for oligostyryl dithiobenzoates, and also for 2-(ethoxycarbonyl)prop-2-yl dithiobenzoate, the transfer constant in styrene polymerization has an extremely large value, in the range of 1,000 to 10,000. Using equations 2-3 and 2-6, a C_T of 10,000 leads to an addition rate constant (k_{add}) of $1.3 \cdot 10^7$ dm^3·mol^{-1}·s^{-1}. This value borders on that of a diffusion controlled reaction.

Considering that the reaction takes place between two macromolecular species, it will not be hard to imagine that at high conversions in highly viscous polymer systems, the transfer rate will be limited by diffusion.

2.3. Retardation in RAFT Polymerization

RAFT polymerizations conducted in a bulk or solution environment often show a marked retardation. Figure 2.11 shows the conversion–time profiles of three solution polymerizations conducted at different concentrations of RAFT agent, but otherwise identical. The retardation is unexpected, for the addition of a RAFT agent should not affect the concentration of propagating free radicals, which is dictated by the pseudo steady-state equilibrium between initiator decay and termination shown in Eq. 2-10, and therefore also the polymerization rate (R_p) should remain unchanged (Eq. 2-11):

$$[radicals] = \left(\frac{2 \cdot k_d \cdot f \cdot [I]}{k_t} \right)^{0.5} \qquad \textbf{(2-10)}$$

$$R_p = k_p \cdot M \cdot \left(\frac{2 \cdot k_d \cdot f \cdot [I]}{k_t} \right)^{0.5} \qquad \textbf{(2-11)}$$

where k_d is the dissociation rate constant of the initiator, f the initiator efficiency, $[I]$ the initiator concentration and k_t the termination rate constant. The presence of RAFT agent could result in a somewhat different termination rate constant, due to the difference in chain length of the propagating radicals. However, if this were the reason behind the retardation, the rate of a RAFT polymerization should increase with conversion as the chain length increases and the retardation should quickly diminish as the reaction proceeds. This is clearly not the case. Several other possible explanations have been proposed in the literature:[44]

I. a reduction of the Trommsdorff or gel effect.

II. slow fragmentation of adduct **2** (Scheme 2.8) formed from the initial RAFT agent.

III. slow fragmentation of adduct **4** (Scheme 2.8) formed from the polymeric RAFT agent.

IV. slow reinitiation by the expelled radical **R**.

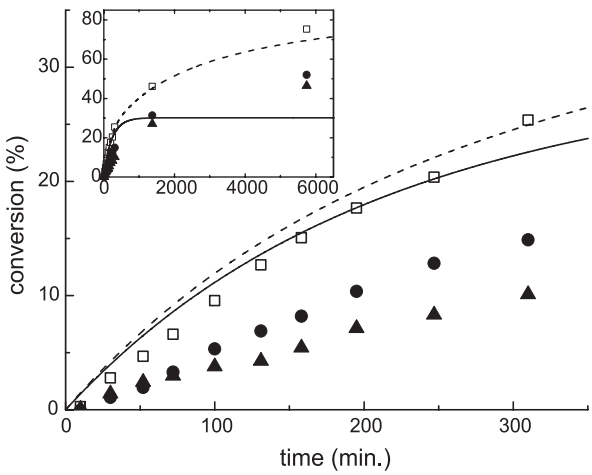

Figure 2.11. Conversion–time profiles of three styrene solution polymerizations in toluene, initiated by AIBN at 80 °C. Concentration styrene: 3.0 mol·dm^{-3}, AIBN: 4.4 mmol·dm^{-3}, RAFT: none (□), 40 mmol·dm^{-3} (●), 60 mmol·dm^{-3} (▲). The two curves are the result of simulations of the experiment without RAFT with (---) and without (—) accounting for the styrene thermal autoinitiation. The necessity of considering autoinitiation is demonstrated clearly in the inset, which shows the behavior at longer polymerization times.

V. specificity for the expelled radical **R** to add to the RAFT agent rather than to monomer.

VI. specificity for the propagating radical to add to the RAFT agent rather than to monomer.

The Trommsdorff effect, also known as autoacceleration or the gel effect, is a phenomenon that is commonly observed in free-radical polymerizations for polymers with high glass transition temperatures. At moderate to high conversion in bulk (and to a lesser extent in solution) polymerizations, high molar mass polymer that is formed causes a sharp increase in the viscosity thereby hindering the diffusion of growing polymeric species and effectively lowering the termination rate. This effect will surely be influenced by the large reduction in molar mass typically obtained in RAFT polymerizations. It plays a role, only at moderate to high conversions, and can be observed as a lack in acceleration. The effect should not be observable in dilute solutions at low conversion.

The remaining proposed explanations (II to VI) demand a more thorough investigation. In order to systematically test these assumptions, a model will be developed in the next section. First a *basic model* will be constructed that allows styrene solution polymerizations without RAFT agent to be simulated using accepted literature values and fair assumptions for the various rate constants. Then, the parameters within the model will be modified in order to test the proposed mechanisms for retardation. Finally, an additional reaction mechanism will be included to explain the observed retardation.

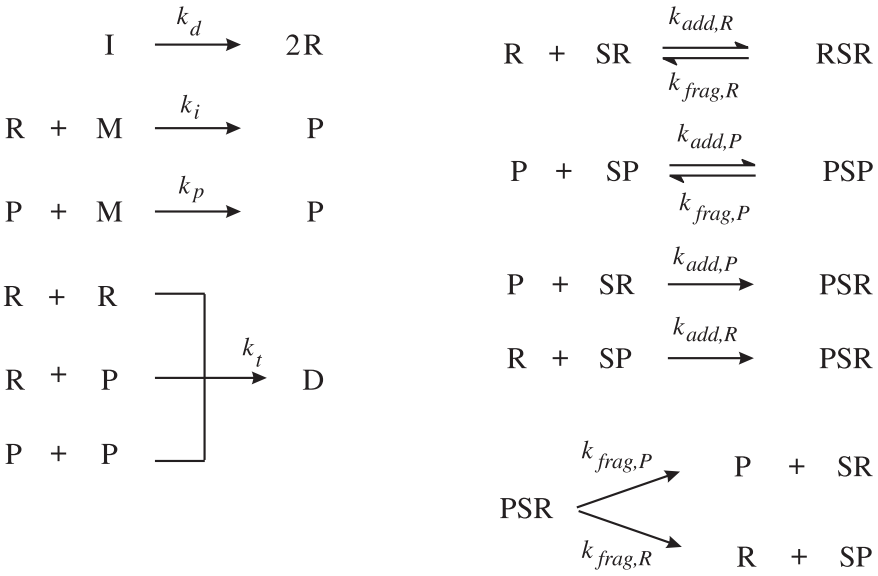

Scheme 2.11. Reaction scheme used in the numerical simulations. Initiator (**I**) dissociates to form initiating radicals (**R**), which add to monomer to form propagating radicals (**P**). Both types of radicals can add to the transfer agent (**SR**) and to a dormant chain (**SP**) to form various intermediate radicals (**RSR**, **PSR**, **PSP**) that do not undergo propagation but that fragment again.

2.3.1. Model Development

A model has been developed based on reactions that are expected to take place in RAFT polymerization. This set of reactions is given in Scheme 2.11. In this scheme, **I** and **M** represent the initiator and monomer, respectively. The other compounds are represented in a logical manner, considering that **R** is an initiating radical, **P** an oligomeric or polymeric radical and **S** is the dithiocarbonate moiety. This leads to the combinations **SR**, being the transfer agent, **SP**, a dormant species and **RSR**, **PSR** and **PSP** the intermediate radical structures with two species attached to the dithiocarbonate group.

Assumptions

One of the assumptions in the model is the similarity between initiator-derived radicals and RAFT-derived radicals (both **R**). Although systems can be designed in which these species are identical, this clearly need not be the case. In practice, however, the vast majority of these **R**-species are derived from the RAFT agent. Typical recipes apply a small amount of initiator compared to RAFT in order to

Table 2.2: Concentrations and parameters used in the *basic* simulation.

ingredient		concentration		rate constants			
concentration initiator	[I]	4.4	mmol·dm^{-3}	dissociation	k_d	1.35·10^{-4}	s^{-1}
concentration monomer	[M]	3.0	mol·dm^{-3}	initiation	k_i	660	dm^3·mol^{-1}·s^{-1}
concentration RAFT	[RAFT]	0	mmol·dm^{-3} (**exp. 1**)	propagation	k_p	660	dm^3·mol^{-1}·s^{-1}
		40	mmol·dm^{-3} (**exp. 2**)	addition	$k_{add,R}$	8·10^6	dm^3·mol^{-1}·s^{-1}
		60	mmol·dm^{-3} (**exp. 3**)		$k_{add,P}$	8·10^6	dm^3·mol^{-1}·s^{-1}
				fragmentation	$k_{frag,R}$	1·10^5	s^{-1}
					$k_{frag,P}$	1·10^5	s^{-1}
				termination	k_t	≤10^{9} a)	dm^3·mol^{-1}·s^{-1}
temperature		80	°C	thermal initiation	$k_{i,therm}$	4·10^{-9}	dm^6·mol^{-2}·s^{-1}

a) a chain length dependent coefficient is used. Reported is the maximum allowed value for termination between two monomeric radicals. This value is typically an order of magnitude lower for polymeric radicals.

preserve the living nature of the polymerization. When we wish to check assumptions IV and V, for instance, where the same constraints that are put on the RAFT-derived radicals will also apply for initiator derived radicals.

Furthermore, it is assumed that the addition rate constant of a radical to a dormant species or to a RAFT agent is not influenced by the leaving group that is already present in this species and, likewise, the fragmentation of a certain chain from an intermediate radical is not affected by the structure of the other branch present in this molecule, but solely by the leaving group character of the leaving chain. The model considers only concentrations and cannot predict molar mass distributions or molar mass averages.

Rate Constants

The **termination rate coefficient** is estimated using Eq. 2-12[50,51]

$$k_t^{ij} = 2\pi p_{ij}(D_i + D_j)rN_A \qquad \textbf{(2-12)}$$

where D_i and D_j are the diffusion coefficients of the two colliding radicals with chain lengths i and j, respectively. r is the maximum distance between the two radicals that allows them to react, approximated by the Van der Waals radius of a monomer unit and p_{ij} is the chance that the two spins will be anti-parallel so that

they can form a covalent bond. N_A is Avogadro's constant. The diffusion coefficient, D_i, can be calculated at varying weight fractions of polymer, w_p, according to the following relationship:[52]

$$D_i(w_p) = \frac{D_{mon}(w_p)}{i^{0.66 + 2w_p}} \qquad \textbf{(2-13)}$$

where D_{mon} is the diffusion coefficient for monomer. Termination for normal free-radical polymerizations is dominated by short–long termination, where the long chain is considered to be immobile and can only be terminated by a short mobile radical species. However, for the RAFT process, the chain length distribution of the radical species takes a completely different shape. Termination will be either between two equally sized polymeric radicals, or between one such radical and a short initiator-derived species. Both options are considered by the model. Although the model does not allow the chain length to be simulated, an estimate for the average degree of polymerization of a propagating radical species (i) is found using Eq. 2-14:[40]

$$i = \frac{x \cdot [M]}{[RAFT]} \qquad \textbf{(2-14)}$$

where x is the fractional conversion. This equation derives the degree of polymerization i by dividing the number of polymerized monomer units over a fixed number of chains, equal to the amount of RAFT agent. This ratio typically describes the chain length of the population of dormant chains, but the rapid equilibrium between these species and the propagating radicals will ensure that also their average chain length can be approximated by this size. When no RAFT agent is present, the model reverts to the kinetic chain length ($\bar{\nu}$), derived from the ratio of the propagation rate over the termination rate, and by substituting Eq. 2-10 is obtained:[53]

$$i = \bar{\nu} = \frac{k_p \cdot [M]}{2(f \cdot k_t \cdot k_d \cdot [I])^{1/2}} \qquad \textbf{(2-15)}$$

Although the model distinguishes initiating radicals (**R**) from propagating radicals (**P**), this division does not coincide with the one between short and long radicals, the combination of which dominates the termination event. A variety of

values can be found in the literature for the maximum length of a short radical, ranging from 5 to 85 monomer units.[51,52,54,55] The model treats the termination reaction between two propagating radicals **P** as a *short–long* event, with the appropriate rate constant. When the rate constant for *long–long* termination ($k_t^{i,i}$) was used, a considerable overestimation of the reaction rate occurred.

The **propagation rate coefficient** of styrene was taken from the work by Buback *et al.*[49] and the **decomposition rate constant** of AIBN from that of Moad *et al.*[56] The **addition rate constants** ($k_{add,R}$ and $k_{add,P}$) were assumed to be equal and their magnitude was calculated from the transfer constant determined by Goto *et al.*[45] for a polystyryl dithiobenzoate adduct, using Eq. 2-2. Under the assumption that k_β equals k_{-add}, the addition rate constant is twice as large as the transfer rate constant, which, in turn, was estimated to be 6000 times larger than the propagation rate constant (k_p).[45]

A value for the **fragmentation rate constant** was taken from preliminary experiments, using the nitroxide trapping technique.[57,58] In this work,[59] *tert*-butoxy radicals are generated in cyclohexane at 60 °C in the presence of 2-phenylprop-2-yl dithiobenzoate and a nitroxide trap (1,1,3,3-tetramethyl-1,3-dihydro-1*H*-isoindol-2-yloxyl). The *tert*-butoxy radicals add to the carbon–sulfur double bond to form a intermediate radical structure, comparable to **2** and **4** (Scheme 2.8). This radical either fragments or is directly trapped by the nitroxide. Upon fragmentation, the cumyl radical is trapped by the nitroxide. Comparing the various yields of trapped products, a fragmentation rate constant of $1 \cdot 10^6 s^{-1}$ was found. This value is, however, expected to be higher than that for the system that is simulated here, as the cumyl radical is a much better leaving group than either the ethyl methacrylate radical or the polystyryl chain that is attached to the dithiobenzoate moiety in these solution polymerizations. For this reason, simulations were carried out initially using a value of $1 \cdot 10^5 s^{-1}$ for both $k_{frag,R}$ and $k_{frag,P}$.

When the experiment without RAFT (see table 2.2) is simulated, good agreement with the experimental data is obtained for polymerization times below 350 min. (Figure 2.11), despite the rather simplified treatment of chain length dependent termination. After this time, a substantial amount of the initiator is

consumed and the polymerization essentially ceases (—, Figure 2.11). Therefore, **thermal styrene autoinitiation** needs to be taken into account. This was done in the form of an additional radical flux ($R_{i,\,therm}$) as shown in Eq. 2-16:

$$R_{i,\,therm} = k_{i,\,therm} \cdot [M]^3 \qquad \textbf{(2-16)}$$

in which a value of $4 \cdot 10^{-9}$ mol·dm^{-3} for $k_{i,\,therm}$ was found to yield the desired agreement with the experimental data (---, Figure 2.11). This value leads to a thermal polymerization rate of initially 3% per hour, which is close to the rate reported in the literature.[48]

Results of the basic model

Using this additional radical flux, the two experiments in the presence of RAFT agent were simulated. The results of these simulations are depicted in figures 2.12 and 2.13. As can be seen, the retardation caused by the addition of RAFT is not assessed correctly by the model. The presence of RAFT does not decrease the polymerization rate except for its effect on the chain length of the growing radicals and thereby on the termination rate coefficient. This causes the rate to be initially slightly lower, but the effect diminishes as the chains grow and has disappeared completely at high conversion.

These simulations form the *basic* simulations. They make use of the parameters given in table 2.2 and the reactions from Scheme 2.11 and result in the curves given in Figures 2.12 and 2.13. Systematic changes to these simulations will be made to investigate arguments II–VI (page 43) as well as the effect of the additional termination events depicted in Scheme 2.12.

2.3.2. Investigations of Proposed Explanations

In order to investigate the effect of slow fragmentation (**arguments II and III**), simulations were carried out in which the values for $k_{frag,\,R}$ and $k_{frag,\,P}$ were reduced step-wise from 10^5 to 1 s^{-1}. The data from experiment 2, together with the simulation results are given in Figures 2.14 and 2.15. When the fragmentation rate constant is reduced, the reaction rate is hardly affected. Only when an unrealistically low value of 1 s^{-1} is used, the rate drops during the initial stage of the polymerization. This is due to the large number of radicals that needs to be produced before the system reaches a pseudo steady-state. At longer polymerization times,

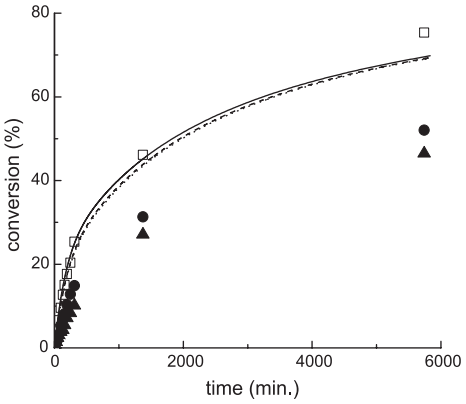

Figure 2.12. Simulations of the conversion–time plots, without the additional termination reactions of the intermediate species, for various RAFT concentrations. 0 mmol·dm^{-3} (–), 40 mmol·dm^{-3} (---), 60 mmol·dm^{-3} (····).

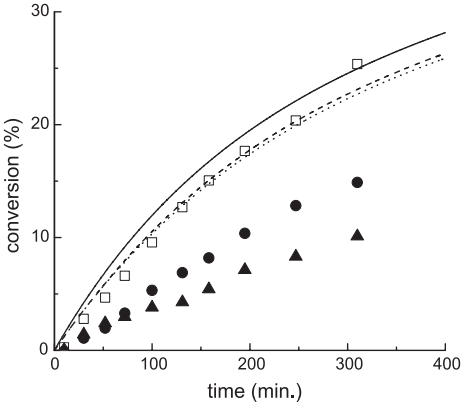

Figure 2.13. Detail of Figure 2.12. Focussing on the initial period of the polymerization.

the behavior is reversed and the simulations fail to predict conversion in this region. The same behavior is found for simulations of experiment 3, shown in Figures 2.16 and 2.17. The intermediate radical accumulates to reach excessively high values (Figure 2.18) that are completely out of line with the value of 0.8 μmol·dm^{-3} reported in the literature for a somewhat different styrene polymerization.[60] For this reason, slow fragmentation alone can be rejected as the reason behind the retardation.

Argument IV concerns slow reinitiation by the expelled radical **R**. The simulations make use of a value for k_i that is equal to k_p, which can already be considered low. The literature reports values that are much higher than k_p for the type of radical that is typically attached to the dithiobenzoate moiety.[61] Still, to illustrate the effect of slow reinitiation in a general sense, simulations were conducted using a initiation rate constant of 70 dm^3·mol^{-1}·s^{-1}; ten times lower than k_p. The results of these simulations are shown in Figures 2.19–2.21. In this case the initial rate of the polymerization is predicted rather accurately, but conversions at longer polymerization times, are too high. Physically, the RAFT agent can be viewed as a reservoir of 'slow' radicals. Once the transfer agent is converted into polymeric dormant species, the polymerization rate returns to its normal value. However, for such a low value for k_i, the conversion is slow and takes place during a large part of the polymerization (Figure 2.21). This would mean that the apparent transfer constant is low and that the polymer is of a broad molar mass distribution. This is in general not the case for RAFT polymerizations. The polydispersity of experiments

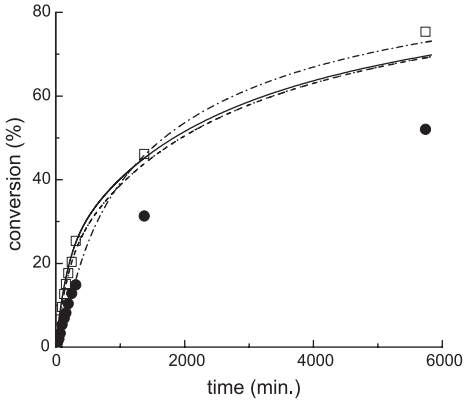

Figure 2.14. The effect of slow fragmentation. Blank experiment (□) and its basic fit (—). Simulations of the experiment with [RAFT]=40mmol·dm^{-3} (●), lowering $k_{frag,X}$ to 10^4s^{-1} (---), 100s^{-1} (·····), 1s^{-1} (·-·-·).

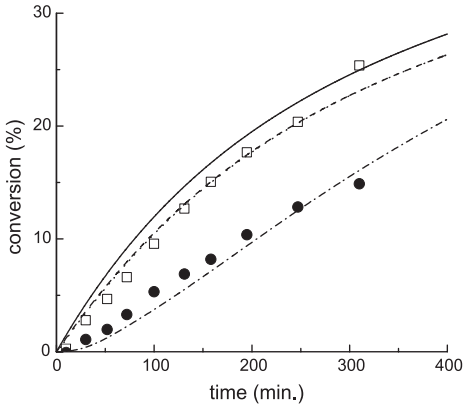

Figure 2.15. Detail of Figure 2.14. Only for extremely low values of $k_{frag,X}$ is there an effect on the rate. However, at long polymerization times, the effect is reversed (Figure 2.16).

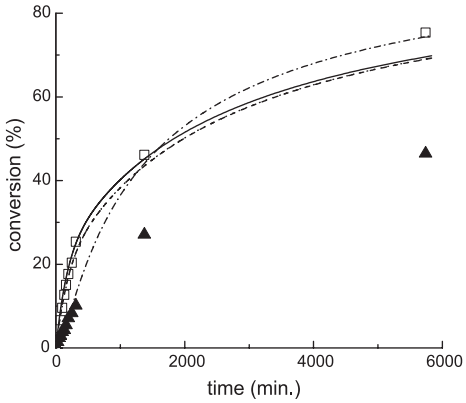

Figure 2.16. The effect of slow fragmentation. Blank experiment (□) and its basic fit (—). Simulations of the experiment with [RAFT]=60mmol·dm^{-3} (▲), lowering $k_{frag,X}$ to 10^4s^{-1} (---), 100s^{-1} (·····), 1s^{-1} (·-·-·).

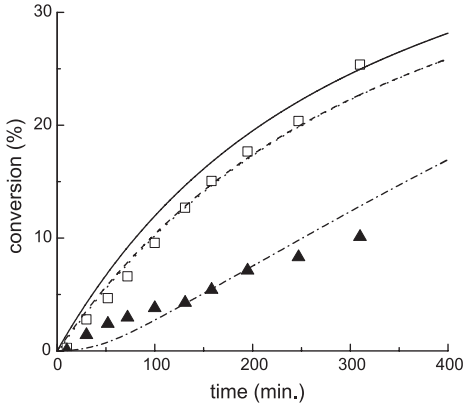

Figure 2.17. Detail of Figure 2.16. Only for extremely low values of $k_{frag,X}$ is there an effect on the rate. However, at long polymerization times, the effect is reversed (Figure 2.16).

2 and 3 was below 1.25. For this reason, also slow reinitiation should be rejected as the primary reason behind the retardation. Here it should be said that high RAFT concentrations in combination with slow reinitiation can cause a decreased rate or even an inhibition of the polymerization in its very early stages. This behavior has been observed in the literature[44] but is distinctly different from the effect described in this section where retardation is observed throughout the polymerization.

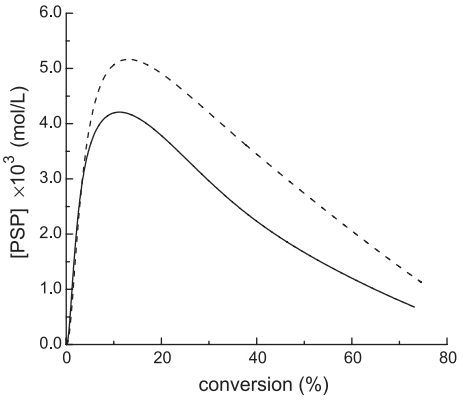

Figure 2.18. Concentration of the intermediate radical during a polymerization when $k_{frag,X}$ is lowered to $1\,s^{-1}$ in order to match the initial polymerization rate. Experiment 2 (—), experiment 3 (---).

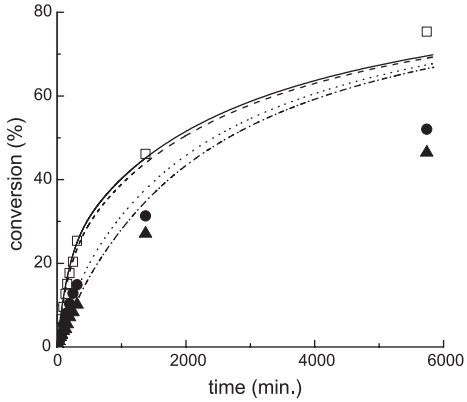

Figure 2.19. The effect of slow reinitiation by radical R. Contrasted with the 'basic' fit of the blank experiment (—) are the results from simulations with k_i equalling $70\,dm^3{\cdot}mol^{-1}{\cdot}s^{-1}$ and [RAFT] being zero (---), $40\,mmol{\cdot}dm^{-3}$ (····) and $60\,mmol{\cdot}dm^{-3}$ (·-·-·).

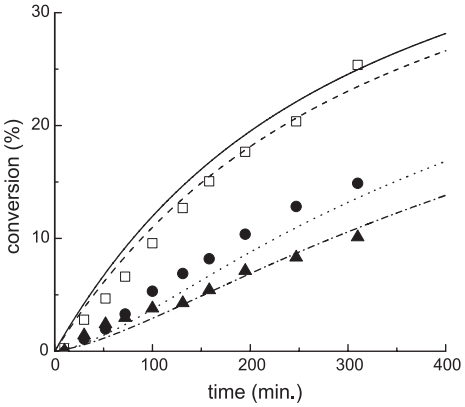

Figure 2.20. Detail from Figure 2.19, which focusses on the initial stage of the polymerization.

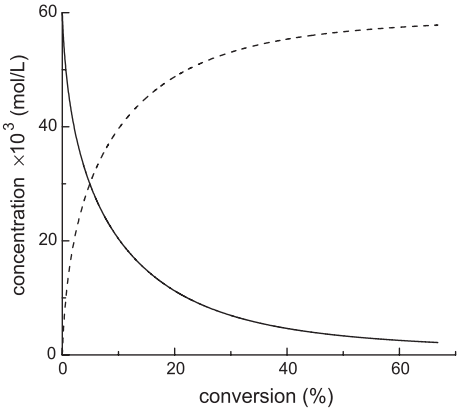

Figure 2.21. Concentration of RAFT agent (—) and dormant species (---) as a function of conversion when k_i is lowered from 660 to $70\,dm^3{\cdot}mol^{-1}{\cdot}s^{-1}$.

Argument V, specificity for the expelled radical **R** to add to the RAFT agent rather than to monomer, is more or less investigated already. Lowering k_i decreases the addition rate to monomer relative to the transfer rate and the termination rate of the radical, thereby increasing the specificity for **R** to add to RAFT. Additional simulations were carried out increasing the addition rate constants $k_{add,P}$ and $k_{add,R}$ by two orders of magnitude to investigate arguments V and VI. No significant effect on the polymerization rate could be observed (Figures 2.22 and 2.23).

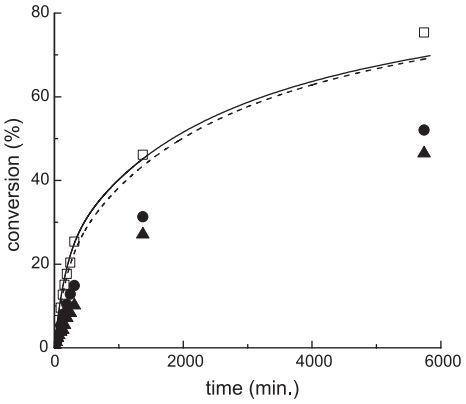

Figure 2.22. The effect of a high $k_{add,X}$. Comparison between the 'basic' fit to the blank experiment (—) with a simulation of experiment 3 using an addition rate constant of $7 \cdot 10^8 dm^3 \cdot mol^{-1} \cdot s^{-1}$ (---), two orders of magnitude larger than the *basic* simulation.

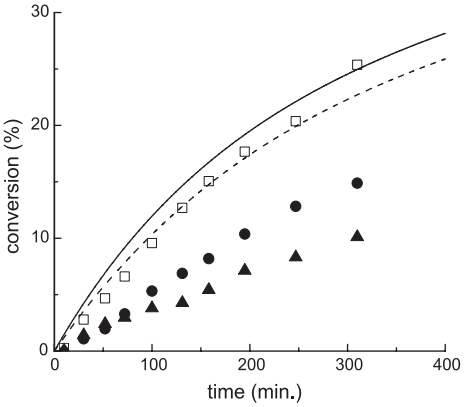

Figure 2.23. Detail of the simulation given in Figure 2.22 for short polymerization times.

Concluding this part of the simulations: the use of realistic simulation parameters results in a polymerization rate that is hardly influenced by the amount of RAFT agent. Pseudo steady-state radical concentrations are obtained that are not seriously affected by the RAFT agent. Only when very extreme values for either k_{frag} or k_i are used, the steady state is reached later in the polymerization and the rate at the beginning of the reaction is lower. The conversions at longer polymerization times, however, cannot be predicted using these values. Arguments relying on the **R** group (II, IV and V) do not seem realistic as the RAFT agent is transformed into dormant species during the first few percent of conversion, after which the **R** radical is no longer involved in any reactions.

Intermediate Radical Termination[62]

Clearly, another effect is at play. Although the concentration of the intermediate radical is low in an absolute sense, it surely cannot be neglected compared to the concentration of propagating radicals. These radicals are expected to be able to terminate with each other, resulting in an additional pathway that leads to a loss of radicals that lasts throughout the polymerization.

This argument to explain the observed retardation is investigated by invoking the termination reactions of **RSR**, **PSR** and **PSP** given in Scheme 2.12. Application of a chain-length dependent termination rate coefficient for these reactions gave the results shown in Figure 2.24. Despite the oversimplified treatment of the chain

Scheme 2.12. Intermediate radical termination as the mechanism to explain the observed retardation in RAFT polymerizations. Initiating (**R**) and propagating radicals (**P**) terminate intermediate radicals **RSR**, **RSP** (adduct **2**, Scheme 2.8) and **PSP** (adduct **4**, Scheme 2.8). These reactions are added to the simulation comprising the radicals shown in Scheme 2.11.

length dependence of the various termination events, the simulations closely follow the experimental values both in the initial phase of the polymerization and at longer reaction times. The simulations show that the model of Schemes 2.11 and 2.12, in combination with realistic values for the various rate constants, is able to describe these three experiments. These simulations further show that the RAFT agent is quickly transformed into dormant species (Figure 2.25), explaining the low polydispersities. Furthermore, it is shown that, despite the large effect on the polymerization rate, only ≈12 % of the dithiobenzoate moieties are destroyed during the 6000 min. polymerization time, making the effect on $\overline{M}_n$ difficult to detect by *e.g.* gel permeation chromatography. Faster recipes or monomers will result in an even smaller loss.

The model was validated further by simulating the literature recipe, used to detect the intermediate radical of a styrene polymerization by electron spin resonance spectroscopy.[60] This recipe consisted of 0.5 ml benzene, 0.5 ml styrene, $1.0 \cdot 10^{-4}$ mol 2-phenylprop-2-yl dithiobenzoate and $5.0 \cdot 10^{-5}$ mol 2,2'-azobisisobutyrate, and was reacted at 90 °C. The propagation rate constant of styrene was calculated to be 900 $dm^3 \cdot mol^{-1} \cdot s^{-1}$ [49] and the dissociation rate constant of the initiator was estimated at $4.5 \cdot 10^{-4}\ s^{-1}$.[63] The results (Figure 2.26) show a peak value for the concentration of PSP of approximately $5.0 \cdot 10^{-7}$ mol·dm^{-3}, in relatively good agreement with the experimental result in the aforementioned publication of $8.0 \cdot 10^{-7}$ mol·dm^{-3}.[60]

With these additional termination events, the key factor behind the retardation phenomenon in homogeneous RAFT polymerizations appears to be identified. This is based not only on the ability of the model to fit the available experimental data, but also on experimental evidence showing that such a termination reaction is definitely occurring. This evidence has, however, not been obtained under ordinary

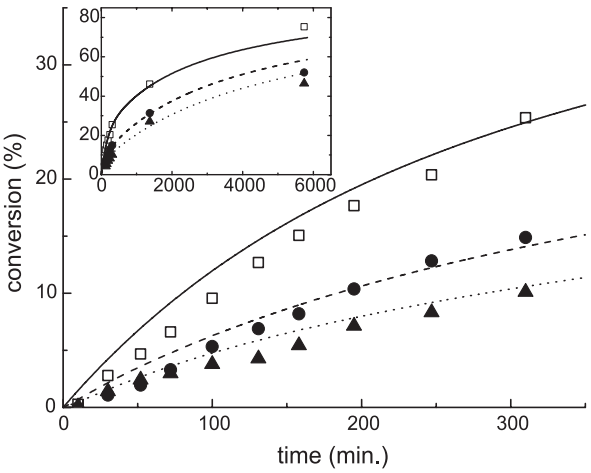

Figure 2.24. Conversion–time profiles of three styrene solution polymerizations in toluene, initiated by AIBN at 80°C. Concentration styrene: 3.0mol·dm^{-3}, AIBN: 4.4mmol·dm^{-3}, RAFT: none (□, –), 40mmol·dm^{-3} (●, ---), 60mmol·dm^{-3} (▲, ····). The three curves are the result of simulations, accounting for thermal styrene autoinitiation and termination of the intermediate radical species formed upon addition of a radical to a RAFT agent/ dormant species.

polymerization conditions. Figure 2.25 demonstrates that only a minor fraction of the dithiocarbonate groups is lost through termination. This material will be mixed with the dormant species and the other termination materials, making it difficult to detect, even more so because of its relatively broad molar mass distribution. Only under special circumstances will the product give a distinct peak, observable in the GPC trace. This situation is achieved in section 4.2.3, where a solution of a low polydispersity, macromolecular RAFT agent is irradiated by UV light, in the absence of monomer. Part of the RAFT agent dissociates to produce polymeric radicals. The intermediate species, which is formed by the addition of such a radical to a still intact dormant chain, is of double molar mass. Reaction of this intermediate radical with yet another polymeric radical produces the expected polymeric product with triple molar mass. As the polymeric radical has a well-defined length and cannot grow, the termination products have unique and detectable molar masses (Figure 4.5, page 96). Further evidence comes from the results from nitroxide trapping experiments, which showed that indeed the intermediate radical can combine with other radicals.[59]

Accepting these additional termination events, a new pseudo steady-state relationship can be derived to determine the effect of the various rate constants on the reaction kinetics. In Eq. 2-17 to 2-21, propagating species **P** will no longer be distinguished from the initiating radical **R**. The symbol **R** now represents the sum of

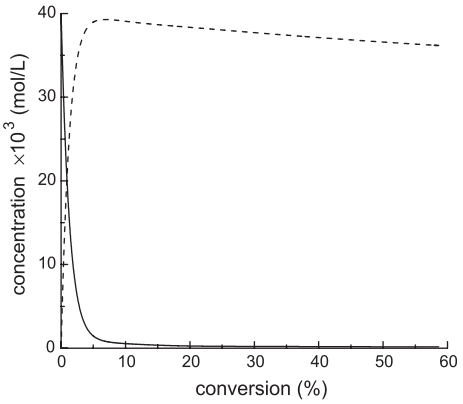

Figure 2.25. Concentration of the RAFT agent (SR, —) and of the dormant species (SP, ---) during the polymerization with the additional termination mechanism. Note that the sum of the two is not constant, but that RAFT moieties are destroyed during the reaction.

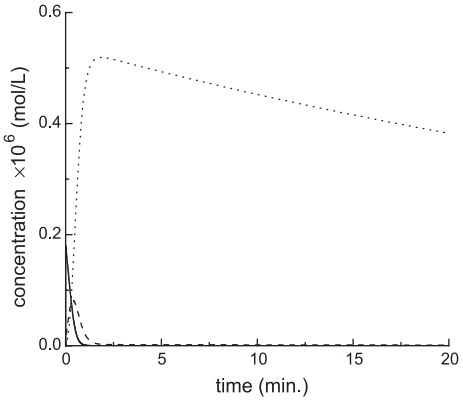

Figure 2.26. Simulation of a styrene polymerization found in the literature.[60] The concentration of the intermediate species PSP (·····) reaches a peak level of 0.5 μmol·dm^{-3}, while measurements indicate 0.8 μmol·dm^{-3}. The other intermediates have a much lower concentration and a shorter lifetime: RSR (—) and PSR (---).

both types of radicals. Likewise SR indicates the sum of RAFT agent and dormant species and RSR replaces all intermediate radicals. The steady-state expression for the intermediate radical concentration now becomes:

$$\frac{d[RSR]}{dt} = 0 = k_{add} \cdot [R] \cdot [SR] - k_{frag} \cdot [RSR] - k_t \cdot [R] \cdot [RSR] \qquad \textbf{(2-17)}$$

$$[RSR] = \frac{k_{add} \cdot [R] \cdot [SR]}{k_{frag} + k_t \cdot [R]} \qquad \textbf{(2-18)}$$

and the steady-state relationship for the propagating radicals is as follows:

$$\frac{d[R]}{dt} = 0 = 2 \cdot f \cdot k_d \cdot [I] - k_t \cdot [R]^2 - k_t \cdot [R] \cdot [RSR] \qquad \textbf{(2-19)}$$

The second term in the denominator of Eq. 2-18 can safely be neglected relative to k_{frag}. This equation is then substituted in Eq. 2-19 to yield expressions for the radical concentration (Eq. 2-20) and the polymerization rate R_p: (Eq. 2-21)

$$[R] = \left(\frac{2 \cdot f \cdot k_d \cdot k_{frag} \cdot [I]}{k_t \cdot (k_{frag} + k_{add} \cdot [SR])} \right)^{0.5} \qquad \textbf{(2-20)}$$

$$R_p = k_p \cdot M \cdot \left(\frac{2 \cdot f \cdot k_d \cdot k_{frag} \cdot [I]}{k_t \cdot (k_{frag} + k_{add} \cdot [SR])} \right)^{0.5} \quad \textbf{(2-21)}$$

These formulae show that the polymerization rate is very sensitive to the rate constants of the addition–fragmentation equilibrium, but only in an indirect way. When fragmentation is slow, the pseudo steady-state concentration of the intermediate radical will be high, which enhances the termination rate between this species and propagating radicals and, in this sense, the fragmentation rate is crucial. It is, however, not the underlying reason for retardation as was shown in Figures 2.14 to 2.17.

Some preliminary experiments were undertaken to investigate the effect of substituents on the phenyl ring of the RAFT agent (Figures 2.27 and 2.28). When Cyano-RAFT was substituted with a phenyl ring in the *para* position (species **27** on page 80), the polymerization rate in an MMA solution polymerization would be much lower than that of an unsubstituded Cyano-RAFT (species **26** on page 80). This is not unexpected as the intermediate radical formed from this species by the addition of a propagating radical has increased opertunity for radical delocalization, resulting in a more stable radical species with, it is assumed, a lower fragmentation rate constant. The reverse effect was observed when a methoxy group was attached at the *para* position of the Cyano-RAFT (species **28** on page 80). The polymerization rate with this agent would be the same as that of a polymerization without RAFT within experimental error. A similar effect could be observed when EMA-RAFT was substituted with methoxy groups in either the *ortho* (species **23** on page 78) or in both *ortho* and *para* positions (species **25** on page 78), the polymerization rate would fall in between that of a comparable uncontrolled polymerization and that with an unsubstituted EMA-RAFT. The effect of a methoxy group in the *meta* position could not be assessed (species **24** on page 78). This clearly illustrates the effect of reducing the stability of the intermediate radical. As it is likely to fragment faster, its steady state concentration will be reduced resulting in a slower rate of intermediate radical termination and a polymerization rate closer to that of a comparable polymerization without RAFT.

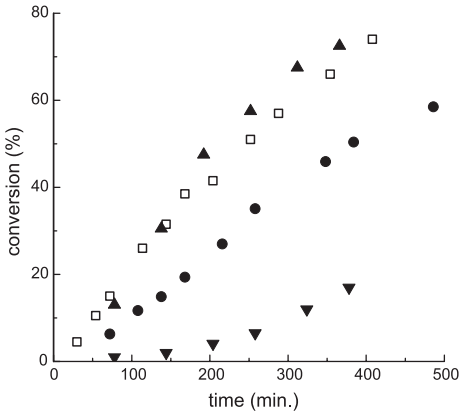

Figure 2.27. Solution polymerizations of methyl methacrylate (3 mol·dm^{-3}) in toluene using Cyano-RAFT derivatives. Control experiment without RAFT (□), Cyano-RAFT (●), *para*-phenyl derivative (▼) and *para*-methoxy derivative (▲). Polydispersities were below 1.2 for the polymerizations in the presence of RAFT agent.

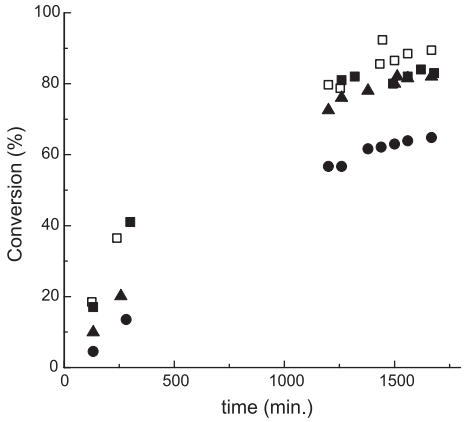

Figure 2.28. Solution polymerizations of styrene (3 mol·dm^{-3}) in toluene using EMA-RAFT derivatives. Control experiment without RAFT (□), EMA-RAFT (●), *ortho* & *para*-methoxy derivative (▼) and *para*-methoxy derivative (▲). Polydispersities were below 1.2 for the polymerizations in the presence of RAFT agent.

2.4. Conclusion

RAFT polymerization is one of the more versatile and robust techniques in the spectrum of 'living' radical polymerization. One of the reasons behind this, is its applicability to a broad range of monomers and the fact that polymerizations can be conducted under conventional conditions, using existing recipes and equipment to which the RAFT agent is added. The effect of the transfer constant on the polymerization outcome was investigated using simulations, in which it was shown that a value of approximately 10 is required to obtain low polydispersity material in batch polymerizations. Additionally, experiments were conducted in which the evolution of a number of oligomers was monitored, allowing a crude estimate to be obtained for the transfer constant of oligostyryl dithiobenzoate species in styrene polymerization. Their transfer constant was estimated to be in the range of 1,000 to 10,000, in agreement with values reported in the literature.

A different set of simulations was performed to investigate the retardation that is observed in RAFT polymerizations. It was found that existing hypotheses could not explain the particular behavior that is observed in a styrene solution polymerization. An additional and overriding mechanism was proposed to be termination of the intermediate radical that is formed in RAFT polymerization.

2.5. Experimental

Solution polymerizations: All solution polymerizations were carried out in a three-necked round bottom flask of an appropiate size. The reaction mixters were degassed by three consecutive freeze–pump–thaw cycles and submerged in an oil bath, which was at the reaction temperature. Monomers were purified by passing them through activated alumina. All other ingredients were used as received.

HPLC Analyses: Measurements were performed on a HP 1100 liquid chromatograph (Agilent Technologies, Waldbron, Germany), equipped with an autosampler, column oven and diode-array detector. The flow was set at 1 ml/min, detection was performed at 254 nm. A PC with HP Chemstation software was used for process control and data handling. The C18 column was a Zorbax Eclipse XDB-C18 (4.6×150 mm, dp=5 µm, pore size: 8 nm) from Hewlett-Packard (Agilent Technologies, Newport, Del, USA). Tetrahydrofuran (supra-gradient grade) was obtained from Biosolve (Bio-Lab, Jeruzalem, Israel) and was filtered prior to use. Water was prepared with a Milli-Q purification system (Millipore, Milford, MA, USA). Mixtures and gradients were made by volumetric mixing by the HPLC pump.

The THF–water gradient was started at the time of injection (40:60 → 70:30 THF:water in 15 min.). Before the first analysis of samples, a blank gradient was run. At the end of each gradient the eluent composition was gradually set back to the starting values and 20 column volumes were pumped through the column for equilibration prior to the next analysis. Samples were dissolved in THF and volumes of 30 µl were injected. Fractions were collected at the detector outlet. Their purity was checked by injecting 10 µl volumes without any preconcentration.

GPC Analysis: GPC analyses were performed on a Waters system equipped with two PLgel Mixed-C columns, a UV and an RI detector. Reported molar masses are apparent values expressed in polystyrene equivalents.

RAFT agents : The syntheses of the RAFT agents are described in chapter 3, and follow literature procedures.[32]

2.6. References

1. *Diesel guide for successful living*, www.diesel.com, **1999**
2. Szwarc, M. *Nature* **1956**, *178*, 1168
3. Szwarc, M.; Levy, M.; Milkovich, R. M. *J. Am. Chem. Soc.* **1956**, *78*, 2656
4. *J. Polym. Sci. Part A: Polym. Chem.* **2000**, *38 (10)*, Special Issue 'Living or Controlled'
5. Otsu, T.; Yoshida, M.; Tazaki, T. *Makromol. Chem., Rapid Commun.* **1982**, *3*, 133
6. Otsu, T.; Yoshida, M. *Makromol. Chem., Rapid Commun.* **1982**, *3*, 127
7. Otsu, T. *J. Polym. Sci., Part A Polym. Chem.* **2000**, *38*, 2121
8. Benoit, D.; Harth, E.; Fox, P.; Waymouth, R. M.; Hawker, C. J. *Macromolecules* **2000**, *33*, 363
9. Benoit, D.; Hawker, C. J.; Huang, E. E.;Lin, Z.; Russell, T. P. *Macromolecules* **2000**, *33*, 1505
10. Grimaldi, S.; Finet, J.-P.; Zeghdaoui, A.; Tordo, P.; Benoit, D.; Gnanou, Y.; Fontanille, M.; Nicol, P.; Pierson, J.-F. *ACS, Polym. Prepr.* **1997**, *38*, 651
11. Benoit, D.; Grimaldi, S.; Robin, S.; Finet, J.-P.; Tordo, P.; Gnanou, Y. *J. Am. Chem. Soc.* **2000**, *122*, 5929
12. Solomon, D. H.; Rizzardo, E.; Cacioli, P. European Patent 135280A2 (**1985**) U.S. Patent 4581429 (1985) [*Chem. Abstr.* **1985**, 102:221335q]
13. Rizzardo, E. *Chem. Aust.* **1987**, *54*, 32
14. Georges, M. K.; Veregin, R. P. N.; Kazmaier, P. M.; Hamer, G. K. *Macromolecules* **1993**, *26*, 2987
15. Veregin, R. P. N.; Georges, M. K.; Kazmaier, P. M.; Hamer, G. K. *Macromolecules* **1993**, *26*, 5316
16. Benoit, D. ;Grimaldi, S.; Finet, J.-P.; Tordo, P.; Fontanille, M. Gnanou, Y. *Polym. Prepr.* **1997**, *38*, 729
17. Goto, A.; Ohno, K.; Fukuda, T. *Macromolecules* **1998**, *31*, 2809
18. Fisher, H. *Macromolecules* **1997**, *30*, 5666
19. Souaille, M.; Fisher, H. *Macromolecules* **2000**, *33*, 7378
20. Kato, M.; Kamigaito, M.; Sawamoto, M.; Higashimura, T. *Macromolecules* **1995**, *28*, 1721
21. Wang, J. S.; Matyjaszewski, K. *Macromolecules* **1995**, *28*, 7901
22. Matyjaszewski, K.; Patten, T. E.; Xia, J. *J. Am. Chem. Soc.* **1997**, *119*, 674
23. Chambard, G. in *Control of Monomer Sequence distribution (Ph. D. thesis)*, Technische Universiteit Eindhoven, Eindhoven, **2000**, p. 88–89
24. Patten, T. E.; Matyjaszewski, K. *Adv. Mater.* **1998**, *10*, 901
25. Gaynor, S. G.; Matyjaszewski, K. in *Controlled Radical Polymerization*; Matyjaszewski, K., (Ed.); ACS Symposium Series No. 685; Washington DC, **1997**; p 396
26. Butté, A.; Storti, G.; Morbidelli, M. *Macromolecules* **2000**, *33*, 3485
27. Enikolopyan, N. S.; Smirnov, B.R.; Ponomarev, G.V.; Belgovskii, I.M. *J. Polym. Sci. Polym. Chem. Ed.* **1981**, *19*, 879
28. Cacioli, P.; Hawthorne, G.; Laslett, R. L.; Rizzardo, E.; Solomon, D. H. *J. Macromol. Sci.-Chem.* **1986**, *A23*, 839
29. Krstina, J.; Moad, G.; Rizzardo, E.; Winzor, C. L.; Berge, C. T.; Fryd, M. *Macromolecules* **1995**, *28*, 5381
30. Krstina, J.; Moad, C. L.; Moad, G.; Rizzardo, E.; Berge, C. T.; Fryd, M. *Macromol. Symp.* **1996**, *111*, 13
31. Moad, C. L.; Moad, G.; Rizzardo, E.; Thang, S. H. *Macromolecules* **1996**, *29*, 7717
32. Le, T. P.; Moad, G.; Rizzardo, E.; Thang, S. H. Patent WO 98/01478 (1998) [*Chem. Abstr.* **1998**, *128*:115390]
33. Chiefari, J.; Chong, Y. K.; Ercole, F.; Krstina, J.; Jeffery, J.; Le, T. P. T.; Mayadunne, R. T. A.; Meijs, G. F.; Moad, C. L.; Moad, G.; Thang, S. H. *Macromolecules* **1998**, *31*, 5559

34. Chiefari, J.; Mayadunne, R. T. A.; Moad, G.; Rizzardo, E.; Thang, S. H. Patent WO 99/31144 (1999)
35. Mayadunne, R. T. A.; Rizzardo, E.; Chiefari, J.; Chong, Y. K.; Moad, G.; Thang, S. H. *Macromolecules* **1999**, *32*, 6977
36. Mayadunne, R. T. A.; Rizzardo, E.; Chiefari, J.; Krstina, J.; Moad, G.; Postma, A.; Thang, S. H. *Macromolecules* **2000**, *33*, 243
37. Hagebols, E.; De Brouwer, H. *unpublished results*
38. Heuts, J. P. A.; Davis, T. P.; Russell, G. T. *Macromolecules* **1999**, *32*, 6019
39. *Polymer Handbook*, 4th ed.; Brandrup, J., Immergut, E. H., Grulke, E. A., (Eds.); John Wiley & Sons: New York, **1999**.
40. Müller, A. H. E.; Zhuang, R.; Yan, D.; Litvenko, G. *Macromolecules* **1995**, *28*, 4326
41. Mayo, F. R. *J. Am. Chem. Soc.* **1943**, *65*, 2324
42. Clay, P. A.; Gilbert, R. G. *Macromolecules* **1995**, *28*, 552
43. Moad, G.; Moad, C. L. *Macromolecules* **1996**, *29*, 7727
44. Moad, G.; Chiefari, J.; Chong, Y. K.; Krstina, J.; Mayadunne, R. T. A.; Postma, A.; Rizzardo, E.; Thang, S. H. *Polym. Int.* **2000**, *49*, 993
45. Goto, A.; Sato, K.; Fukuda, T.; Moad, G.; Rizzardo, E.; Thang, S. H. *Polymer Prep.* **1999**, *40*, 397
46. Goto, A.; Sato, K.; Tsujii, Y.; Fukuda, T.; Moad, G.; Rizzardo, E.; Thang, S. H. *Macromolecules* **2001**, *34*, 402
47. Chong, Y. K.; Le, T. P. T.; Moad, G.; Rizzardo, E.; Thang, S. H. *Macromolecules* **1999**, *32*, 2071
48. Moad, G.; Solomon, D. H. *The Chemistry of Free Radical Polymerization*, 1st ed.; Elsevier Science Ltd.: Oxford, **1995**
49. Buback, M.; Gilbert, R. G.; Hutchinson, R. A.; Klumperman, B.; Kuchta, F. D.; Manders, B. G.; O'Driscoll., K. F.; Russell, G. T.; Schweer, J. *Macromol. Chem. Phys.* **1995**, *196*, 3267
50. Russel, G.; Gilbert, R. G.; Napper, D. H. *Macromolecules* **1992**, *25*, 2459
51. Russel, G.; Gilbert, R. G.; Napper, D. H. *Macromolecules* **1993**, *26*, 3538
52. Griffiths, M. C.; Strauch, J.; Monteiro, M. J.; Gilbert, R. G. *Macromolecules* **1998**, *31*, 7835
53. Stevens, M. P. *Polymer Chemistry, an introduction* **1990**, 2nd ed., Oxford University Press, New York, p.204
54. Gilbert, R. G. *Emulsion Polymerization: A Mechanistic Approch*; Academic Press: London, **1995**
55. De Kock, J. in *Chain-length dependent bimolecular termination in free-radical polymerization (Ph. D. thesis)*; Technische Universiteit Eindhoven, Eindhoven, **1999**
56. Moad, G.; Rizzardo, E.; Solomon, D. H.; Johns, S. R.; Willing, R. I. *Makromol. Chem., Rapid Commun.* **1984**, *5*, 793
57. Nakamura, T.; Busfield, W. K.; Jenkins, I. D.;Rizzardo, E.; Thang, S. H.; Suyama, S. *J. Am. Chem. Soc.* **1997**, *119*, 10987
58. Nakamura, T.; Busfield, W. K.; Jenkins, I. D.;Rizzardo, E.; Thang, S. H.; Suyama, S. *Macromolecules* **1997**, *30*, 2843
59. Bussels, R.; Monteiro, M. J. *unpublished results*
60. Hawthorne, H. G.; Moad, G.; Rizzardo,E.; Thang, S. H. *Macromolecules* **1999**, *32*, 5457
61. Fischer, H. in *Free Radicals in Biology and Environment* **1997**, Minisci, F. (Ed.), Kluwer Academic Publishers, p. 63–78
62. Monteiro, M.; de Brouwer, H. *Macromolecules* **2001**, *34*, 349
63. Wako Chemicals GmbH, product brochure *Azo polymerization initiators*.

» Desire pulls stronger than experience «[1]

3. Experimental Procedures

Synthetic pathways *en route* towards desirable transfer agents

Synopsis: This chapter presents an overview of various possible routes that yield dithioesters, structures suitable as transfer agents for reversible addition–fragmentation reactions. Though not all of these routes were actively explored, they do provide a guideline for future syntheses, indicating specific advantages and drawbacks of the various approaches. Furthermore, the experimental part of this chapter details the synthesis of all transfer agents used in this thesis, thereby providing examples of several of the aforementioned synthetic pathways.

3.1. Introduction

In chapter 2 the general structure of the RAFT agents applied in this study was introduced along with several specific examples. Although numerous different structures may permit reversible addition–fragmentation chain transfer reactions, it was already pointed out that several classes of sulfur containing species are especially designed to be applied as such. Dithioesters are unsurpassed in activity by xanthates, trithiocarbonates and thiocarbamates which can be used as well. The work in this thesis makes use exclusively of aromatic dithioesters that contain a dithiobenzoate moiety. An overview will be presented to the reader detailing the most common known synthetic pathways to such dithioesters. Furthermore, the experimental details on the synthesis of several dithiobenzoate esters are provided. For clarity and consistency, general reaction schemes will make use of **Z** and **R** to

Scheme 3.1. Nucleophilic substitution of an alkyl halyde by a dithiocarboxylate salt forming a dithioester. The dithiocarboxylate can be an alkali(-earth) or ammonium salt.

indicate the activating group and the leaving group of the RAFT agent in the same way as in chapter 2 (see Scheme 2.8 on page 27). By doing so, one can quickly identify the starting materials needed to prepare a specific RAFT agent via the various pathways outlined in this chapter.

3.2. Synthetic Approaches to Dithioesters

3.2.1. Substitution Reactions with Dithiocarboxylate Salts.

The approach first requires the formation of a dithiocarboxylic acid salt which can be prepared in a number of different ways, which are outlined below. The dithiocarboxylate takes the role as nucleophile in substitution reactions with *e.g.* alkyl halides that are added directly to the reaction mixture or to the salts after isolation (Scheme 3.1). Most dithiocarbonate salts (alkali and alkali-earth) have a limited stability and should be used directly after preparation without isolation or extensive purification.[2,3] For conservation purposes, the conversion to an ammonium salt (in particular the piperidinium salt) appears to be the only acceptable option. These crystalline salts have been reported to be fairly stable. They allow facile generation of the free acid or can be used directly in substitution reactions.[4,5,6] Stable lead and zinc salts have been prepared as well for identification processes but these lack synthetic utility.[7,8,9] Both the ammonium and the alkali(-earth) salts can serve as nucleophiles in substitution reactions of alkyl halides, alkyl sulfates or alkyl sulfonates to produce the desired dithioesters.[6,10,11,12] When the substitution reaction is omitted, the dithioacid can be obtained by protonation of the salt with a strong acid. The dithioacid in turn can be converted to a dithioester by several other routes discussed in the sections 3.2.2, 3.2.3 and 3.2.7.

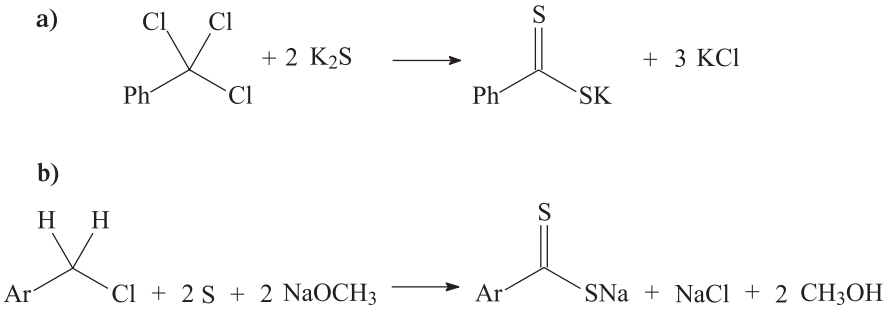

Scheme 3.2. **a**) Conversion of benzotrichloride to potassium dithiobenzoate. **b**) Conversion of aromatic monohalidemethylates to dithio carboxylates by the reaction with elemental sulfur and alkali alkoxylates. Both reactions take place in an alcoholic medium.

from Aromatic Mono-, Di- and Trihalidemethylates

The first syntesis of a dithiocarboxylate was reported by Fleischer[13] who prepared dithiobenzoic acid from benzalchloride ($C_6H_5CHCl_2$) and potassium sulfhydrate in ethanol and water, which yielded traces of the acid as a red oil upon the addition of hydrochloric acid. Wood *et al.*[14] later showed that the success of this synthesis was most likely due to impurities in the potassium sulfhydrate, most notably potassium sulfide. The latter reacts with benzal chloride to form thiobenzaldehyde as an unstable intermediate which, depending on the reaction conditions, can undergo the Cannizzaro reaction to yield potassium dithiobenzoate amongst other products.

Benzotrichloride can be converted to potassium dithiobenzoate by slow addition to a suspension of potassium sulfide in boiling methanol (Scheme 3.2, **a**).[15] The reaction is exothermic and needs to be cooled once it has started.

Another method to come to aromatic dithiocarboxylates is documented by Becke and Hagen.[16] Here, aromatic monohalidemethylates are treated with elemental sulfur and (earth) alkali alkoxydes (Scheme 3.2, **b**). The synthesis is compatible with a variety of substituents on the aromatic ring. Alkyl, alkoxy and halogen groups remain untouched while additional methylhalide groups will lead to multiple dithiocarboxylates moieties. This approach is taken in the synthesis of 2-phenylprop-2-yl dithiobenzoate (section 3.4.3, page 79). The methods outlined in Scheme 3.2 typically produce a variety of side products and salts and some degree of purification will be required before substitution reactions are performed.

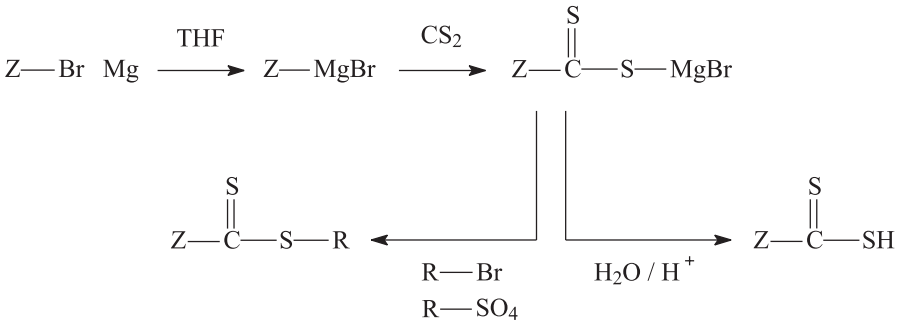

Scheme 3.3. The Grignard synthesis. The reaction between a Grignard reagent and carbon disulfide yields a reactive dithiocarboxilic acid salt which may be quenched and acidified to access the protonated acid or alternatively, an alkyl halide may be added to participate in a nucleophilic substitution.

from Grignard Reactions

Houben[7] was the first to report the use of Grignard salts in the synthesis of dithioacids. Arylmagnesiumhalides were allowed to react with carbon disulfide in dry ether, producing the magnesiumhalide salt of the corresponding dithioacid. These reactive species can be transformed directly into a dithioester by addition of a suitable alkyl halide or alkyl sulfate[17,7] to the reaction mixture. The literature reports reasonable yields for the coupling of especially aromatic but also of aliphatic intermediates with alkyl iodides and bromides.[12] RAFT agents, applicable to a wide range of monomers, generally require a tertiary halide (*e.g. tert*-butyl bromide) to be coupled to the active intermediate. The alkyl halide will form the **R**-group and needs to possess a good homolitic leaving-group character. Unsuprisingly, such groups are the most difficult to attach to the dithio carbonate moiety in the first place. This route was followed for the synthesis of 2-(ethoxycarbonyl)prop-2-yl dithiobenzoate which is detailed in section 3.4.2. According to Meijer *et al.*[18] the procedure can be optimized in several ways. First, the yield improved considerably when tetrahydrofuran was used as the reaction medium instead of ether. Second, the reaction rate of alkyl magnesium chlorides was found to be higher than that of the corresponding bromides in both the formation of the dithiocarbonate intermediate and that of the final ester, which could proove useful for the preparation of dithioesters with more sterically hindered **R**-groups. Third, it was found that reactions could be conducted at much lower temperatures when 10–20% hexamethylphosphoramide (HMPA, $[(CH_3)_2N]_3PO$) was added to the reaction. The alkylation of *e.g.* $C_2H_5C(S)SMgBr$ with CH_3I could be conducted at –35 °C whereas the same reaction without HMPA requires 30 to 40°C to proceed at an acceptable rate. Although they only showed the temperature effect for relatively

easy-coupling alkyl halides, the results could imply that also the yields for tertiary halides would benefit from the addition of HMPA. Westmijze *et al.*[19] found that the addition of catalytic amounts of copper(I)bromide to Grignard reaction significantly increased the yield of several dithioesters derived from rather unreactive starting materials. The more reactive organocopper intermediates allowed the preparation of dithioesters with sterically hindered and unsaturated **Z**-groups.

Beside the direct esterification of the dithiocarbonate magnesiumhalide, the Grignard may also be quenched at this point with water and a strong acid, to gain access to dithiocarboxylic acid. These acids are generally very unstable and should not be isolated as such.[12,15,20] They are readily oxidized by oxygen to bis(thioalkyl)disulfides and should be used directly in further reactions or be converted to more stable ammonium salts. The formation of the acid is performed in the synthesis of 2-cyanoprop-2-yl dithiobenzoate (section 3.4.4, page 80).

from Aromatic Aldehydes

Gonella *et al.*[21] reported a convenient route to come to aromatic dithioesters using benzaldehyde (**1**) as the starting material (Scheme 3.4). Reacting this compound with ethanedithiol (**2**) in the presence of a catalytic amount of *p*-toluenesulfonic acid affords a thioketal (**3**). When a solution of the thioketal in dimethylformamide (DMF) and hexamethylphosphoramide (HMPA) is treated with sodium hydride and an alkyl halide a dithioester is formed in varying yields (40–90%). The addition of the alkyl halide may also be ommited to gain access to the sodium salt of the aromatic dithioacid. The method has the advantage that it is tolerant to various functional groups on the aromatic ring.

Aromatic aldehydes can also serve as the starting material for the reaction with ammonium polysulfides. This approach was pioneered by Bost and Shealy[22] and later followed by Jensen and Pedersen.[23] The method is tolerant to various functional groups but gives only low to moderate yields (20–40%).

3.2.2. Addition of Dithio Acids to Olefins

The dithioacid in its protonated form can add to olefins to yield various dithioesters.[24] The ambivalent character of the dithioacid functionality allows addition to proceed by either a nucleophilic or electrophilic mechanism, depending on the nature of the olefin. Electrophilic olefins like acrylonitrile and vinylpyridine force the dithioacid to act as nucleophile. The reactions with (meth)acrylonitrile

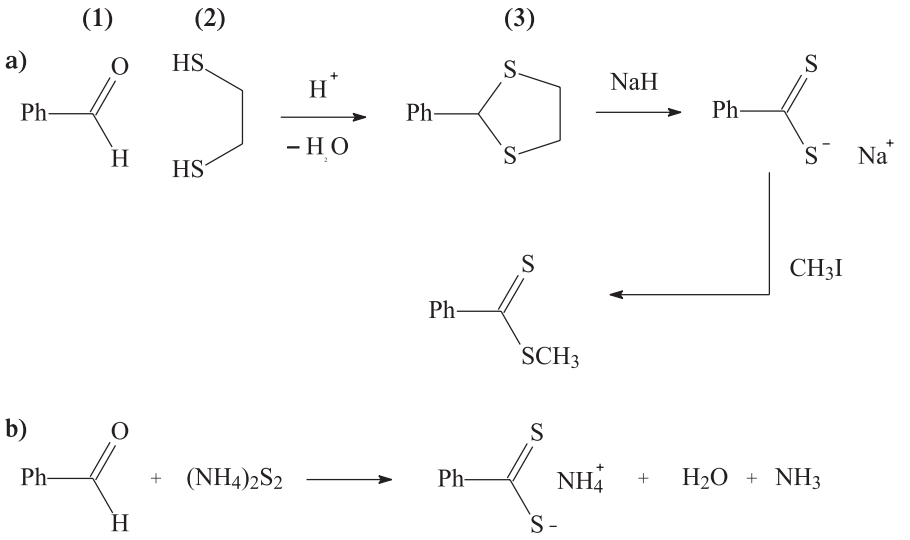

Scheme 3.4. a) The conversion of benzaldehyde to the sodium dithiobenzoate via a thioketal and subsequent esterification. **b**) Reaction between benzaldehyde and ammonium polysulfide of average composition $(NH_4)_2S_2$.[22]

and (meth)acrylic acid and their esters give dithioesters where the sulfur-containing group becomes attached to the least substituted side of the carbon-carbon double bond, making it inefficient raft agents (Scheme 3.5, **a**). Few electrophilic olefins exist that would result in good RAFT agents of which the addition to mesityl oxide (4-methyl-3-penten-2-one) is an example. This would give a dithioester possessing a good homolytic leaving group (Scheme 3.5, **b**).

The reaction with nuclephilic olefins obeys Markovnikov's rule. The olefin is protonated and the resulting carbocation combines with the negatively charged dithiocarboxylate group. The reaction with α-methylstyrene yields 2-phenyl-prop-2-yl dithiobenzoate (Scheme 3.5, **c**). Experimental details of this synthesis are found in section 3.4.3.

3.2.3. Thioalkylation of Thiols and Thiolates.

Thiols and alkali thiolates can be converted into dithioesters by thioacylation with *e.g.* bis(thioacyl) sulfides (**4**), thioacyl halides (**5**) and dithioesters (**6**, **7**, Scheme 3.6). These reactions typically proceed in good to excellent yields (70–95%) and the main advantage over the use of dithio acid salts lies in the increased reactivity of the thioacylating species. The reaction can be considered as a nucleophilic displacement at the thiocarbonyl carbon by a sulfur nucleophile.

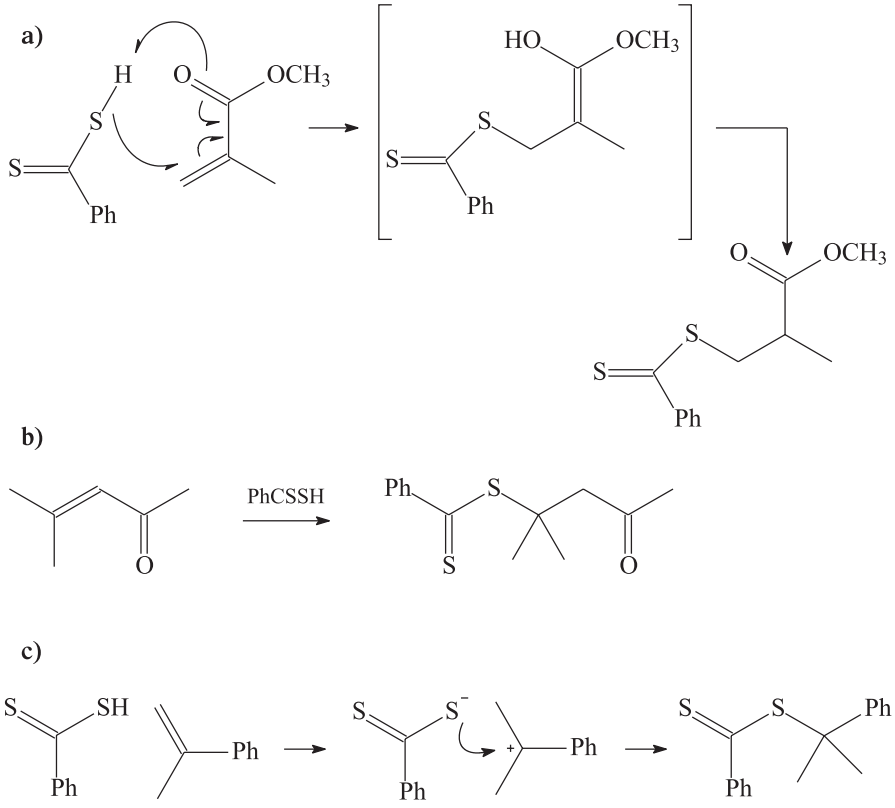

Scheme 3.5. **a**) Nucleophilic addition of dithiobenzoic acid to the carbon–carbon double bond of methyl methacrylate. The concerted mechanism of the addition is speculative.[24] The result is a RAFT agent with a poor homolytic leaving group. **b**) Nucleophilic addition of dithiobenzoic acid to mesityl oxide. The result is a RAFT agent with a good homolytic leaving group. **c**) Electrophilic addition of dithiobenzoic acid to α-methylstyrene. The nucleophilic olefin is protonated, followed by the electrophilic attack of the sulfur.

Bis(thioacyl) sulfides (**4**) are prepared by the reaction between dithio acids and 1,3-dicyclohexylcarbodiimide (DCC). The reaction between 4-methyl dithiobenzoic acid and half an equivalent of DCC in hexane at 0 °C gave bis(4-methylthiobenzoyl) sulfide in 80% yield.[25] Thioacyl halides (**5**) are prepared from dithioacids and thionyl chloride. In the case of dithiobenzoic acid, the reaction completes with 50 to 61% yield.[26,27]

Methyl dithiobenzoate (**6**) has been prepared in 50–90% yield by various methods oulined in section 3.2.1.[18,21] The transesterification of **6** and **7** can be considered as a special case of thioacylation of mercaptanes. The thioacylating agent is in this case a dithioester itself. The process can be used to convert dithioesters that are easily prepared (*e.g.* methyl dithiobenzoate, **6**) or commercially available (*e.g.*

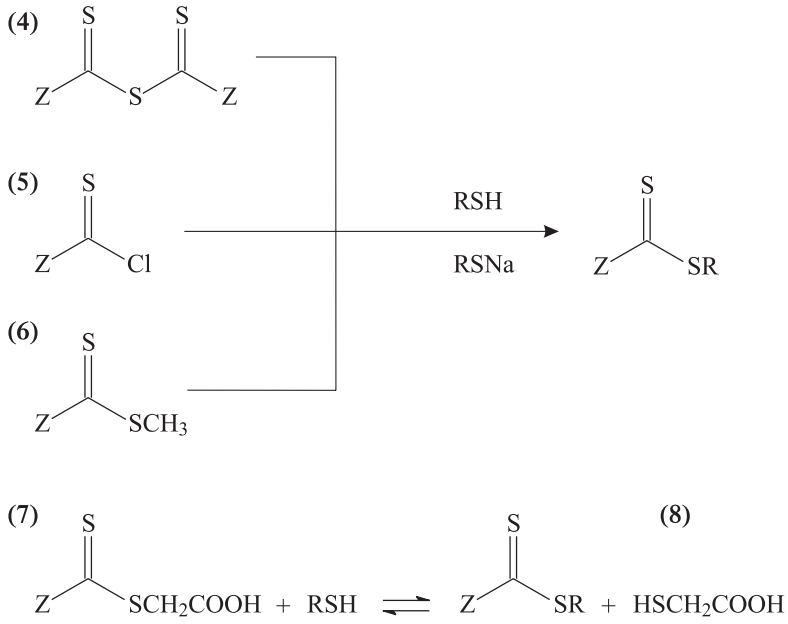

Scheme 3.6. Thioalkylation of thiolates. Thiols and alkali thiolates can be converted into dithioesters by thioacylation with bis(thioacyl) sulfides (**4**), thioacyl halides (**5**) and dithioesters(**6**, **7**).

S-(thiobenzoyl)thioglycollic acid, **7**, Scheme 3.6) to more suitable RAFT agents.[28] These reactions take place selectively in the presence of other functional groups like hydroxides.[29] An equilibrium is established but this can be shifted entirely to the product side by removal of the volatile methanethiol (b.p. 6 °C) in the case of **6**. The reaction of **7** can be conducted in aqueous solution from which the hydrophobic dithioester separates. If the mercaptane is insoluble in water, a suitable organic medium will have to be found and the equilibrium can be shifted to the product side by washing the organic phase with an alkaline solution to preferentially remove thioglycollic acid (**8**). The main disadvantage lies in the fact that besides a suitable thioacylating agent, the desired R group (Scheme 3.6) should be available in the form of a mercaptane. The supply of tertiary mercaptanes is limited to *e.g. tert*-butyl mercaptane and *tert*-dodecyl mercaptane, but nontheless, for these compounds, the routes presented in this section may be favoured to the substitution reactions of section 3.2.1, due to the higher yields.

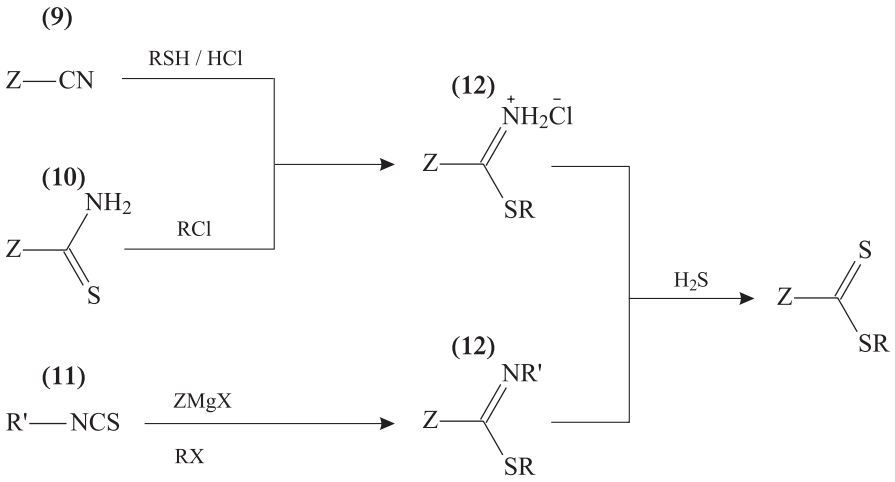

Scheme 3.7. Preparation of imidothioate esters and subsequent conversion to dithioesters with hydrogen sulfide.

3.2.4. via Imidothioate Intermediates

Treatment of imidothioates (**12**, Scheme 3.7) with hydrogen sulfide under acidic conditions is a widely used method to prepare dithioesters because of the broad range of available precursors. The imidothioate ester can be derived from a number of starting materials, *viz.* nitriles[30] (**9**), thioamides[31] (**10**) and isothiocyanates[32] (**11**). The yields of the process range from moderate to good (50–90%), but like in the majority of other routes, the **R** group should be available in the form of a halide or a mercaptane.

3.2.5. with Sulfur Organo-Phosphorus Reagents

Thiolesters (ZCOSR) are converted to dithioesters by the action of various sulfur organo-phosphorus reagents. When exposed to 2,4-bis(4-methoxyphenyl)-1,3-dithia-2,4-diphosphetane-2,4-disulfide (Lawesson's reagent, **13**, Scheme 3.8) dithioesters are obtained in high yields (≥90%).[33,34] The thiolesters themselves are obtained from the esterification reaction of thiols and carboxilic acids.[35,36,37] Unlike the esterification of carboxilic acids and alcohols, this reaction is not succesfully catalyzed by protons alone, but requires an activator like 1,3-dicyclohexylcarbodiimide to shift the equilibrium to a more favorable position.[38] Alternatively, thiols

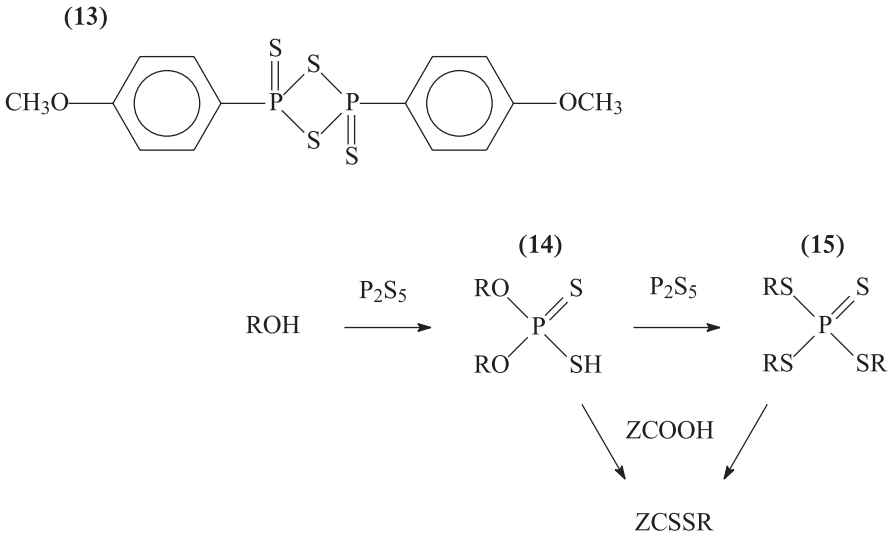

Scheme 3.8. Structure of Lawesson's reagent (**13**) and various intermediates (**14**, **15**) that are formed in the reaction between alcohols, diphosphorus pentasulfide and carboxylic acids.

can be reacted with acyl halides (ZCOCl) under mild conditions, catalyzed by tertiary amines,[39] or the thiolesters can be obtained from the reaction between carbonyl sulfide and Grignard salts.[40]

O,O-dialkyldithiophosphoric acids (**14**, Scheme 3.8) can be used to convert carboxylic acids directly to dithioesters in moderate yields.[41] The *O,O*-dialkyldithiophosphoric acids are prepared from alcohols and diphosphorus pentasulfide. If an excess of the latter is applied, the reaction proceeds to ultimately form trialkyl tetrathiophosphates (**15**),[42] which react with carboxylic acids in higher yields. Davy and Metzner[43] showed that the procedure can be simplified to a one pot synthesis, directly converting carboxylic acids and alcohols into dithioesters with diphosphorus pentasulfide in moderate to good yields (40–90%) for methyl and ethyl esters. Although the method uses convenient starting materials and allows for upscaling, the applicability to secondary and tertiary alcohols remains unexplored.

3.2.6. Friedel-Crafts Chemistry

An alternative route to (substituted) dithiobenzoate esters is reported by Viola *et al.*[44] In their approach, the dithiocarbonate group is first attached to the **R**-group to form a reactive chlorodithioformic acid ester (**17**), which, under Friedel-Crafts conditions, adds to activated arenes in high yields (Scheme 3.9, **b**). The chlo-

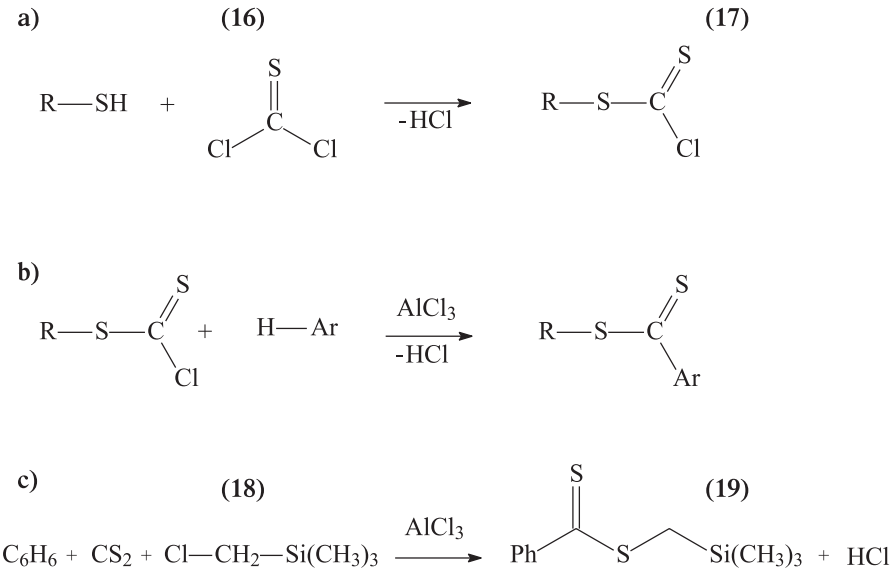

Scheme 3.9. Synthesis of dithioesters by Friedel-Crafts reactions. **a**) Preparation of chlorodithioformic acid ester. **b**) Coupling between the chlorodithioformic acid ester and a benzene ring. **c**) Participation of carbon disulfide in selective Friedel-Crafts reactions.

rodithioformic acid esters themselves are prepared from the reaction between thiophosgene (**16**) and mercaptanes[45] or from dithio acids and thionyl chloride.[46] The first process takes place with 80–90% yield in the case of methyl mercaptane.[45] For RAFT synthesis a tertiary mercaptane would be desired which is commercially available in *e.g. tert*-dodecylmercaptane. The branched alkyl would make a good leaving group and has the additional advantage that the behavior of the radical has been thoroughly investigated in both homogeneous and heterogeneous polymerization systems, as it is used as a chain transfer agent itself.[47] The coupling of the chlorodithioformic acid ester to an aromatic ring is unlikely to be influenced strongly by the **R**-group but largely depends on the substituents on the benzene ring. With methyl, methoxy, hydroxyl or halogen substituents, the dithioesters were obtained in 60–95% yield. The hydroxyl substituted aromatic ring is inaccessable by the Grignard method, besides, differently substituted benzenes are more easily available than their brominated analogues that are required in the Grignard synthesis.

Another report on the formation of dithioesters using Friedel-Crafts chemistry comes from George,[48] who described a one pot synthesis of trimethylsilylmethyl dithiobenzoate (**19**) from a mixture of benzene, carbon disulfide and (chloromethyl)methyldichlorosilane (**18**). The success of this method strongly depends on the

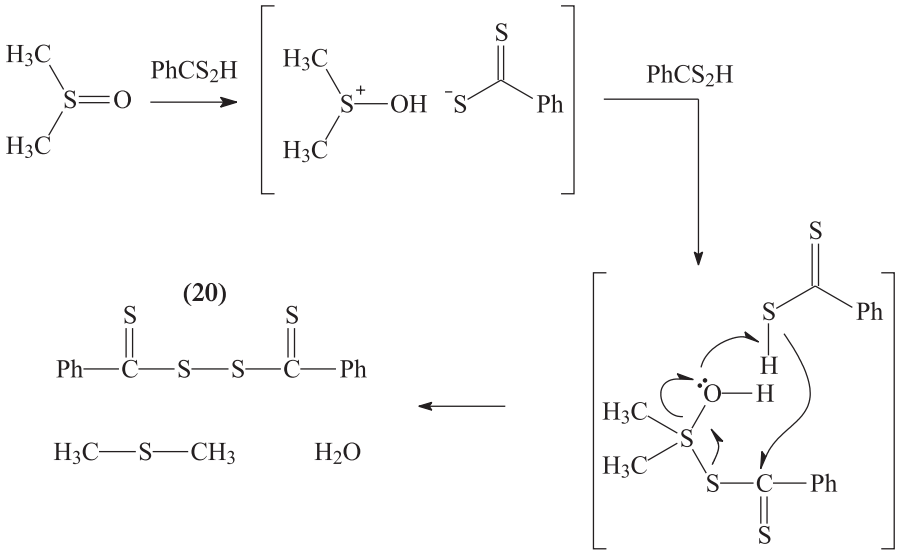

Scheme 3.10. Formation of bis(thiobenzoyl)disulfide (**20**) via the oxidative coupling of dithiobenzoic acid by dimethyl sulfoxide.

structure of the alkyl halogenide as in numerous other accounts, carbon disulfide is used as an inert solvent for the coupling between the alkyl halogenide and the aromatic ring. The details of the mechanism remain unclear, however, as the aluminium chloride appears to be a reactant rather than a catalyst.

3.2.7. via Bis(thioacyl)disulfides

A novel addition to the field of synthetic routes is that of the reaction between carbon-centered radicals and bis(thioacyl)disulfides.[49,50,51] The bis(thioacyl)disulfides (**20**) are prepared by oxidative coupling of dithioacids or their salts. Most dithioacids are oxidized by oxygen from the air, or in a more rapid and controlled manner by other mild oxidizing agents like iodine or hydrogen peroxide. Stronger oxidizers like potassium permanganate typically destroy the dithiocarbonate moiety. The coupling of dithiocarboxylates with iodine is an established process.[7,10] In the case of dithiobenzoate salts, the reaction is typically conducted in an aqueous medium from which the product precipitates. This procedure has been attempted initially in the synthesis of 2-cyanoprop-2-yl dithiobenzoate, which is described in section 3.4.4 on page 80. A very large amount of potassium iodide was needed to solubilize the required iodine in the water phase and the large reaction volume complicated upscaling. Besides, the product did not precipitate in crystals but separated out in the form of a sticky oil-like layer which was difficult to purify. The reaction

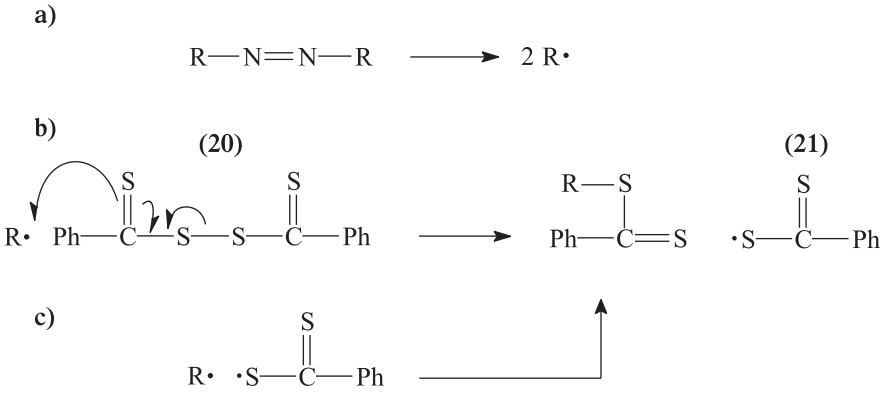

Scheme 3.11. Preparation of dithioesters by radical reactions. **a**) Radicals are generated by the dissociation of an initiator. **b**) Reaction between a radical and the bis(thioacyl)disulfide generates a dithioester molecule and a relatively stable dithiobenzoate radical (**21**). **c**) The dithiobenzoate radical (**21**) recombines with a initiator derived radical R, forming another instance of the dithioester.

can be conducted under more convenient conditions when dimethyl sulfoxide is used for the oxidation (Scheme 3.10).[24] The reaction could be performed in an open vessel at ambient conditions in bulk or in solution and produced bis(thiobenzoyl)disulfide in excellent yield (>90%, based on crude dithiobenzoic acid).

Carbon-centered radicals react with bis(thioacyl)disulfides (**20**) by the mechanism postulated in Scheme 3.11.[50] The radicals are generated by a conventional azo initiator (Scheme 3.11, **a**) in the first step and these react with a bis(thioacyl)disulfides, forming a dithioester together with a sulfur centered radical (**21**). This radical in turn can recombine with a carbon-centered radical to form the same dithioester species (Scheme 3.11, **c**). The advantage of this process is that functional and sterically hindered R groups can be introduced with great ease and without the formation of many side products. The only significant contamination is the product of the reaction between two carbon-centered radicals. The reaction between two sulfur-centered radicals regenerates the starting material (**20**), while the reaction between a carbon-centered radical and the dithioester is degenerate, *i.e.* the products are identical to the reactants. This route is followed in the synthesis of 2-cyanoprop-2-yl dithiobenzoate (section 3.4.4)

3.3. Conclusion

It is hard to recommend any of the aformentioned syntheses as *ideal* or *the best.* In terms of overall yield, values given in the literature for the various routes can hardly be compared because of the large discrepancies between primary, secondary and tertiary **R** groups. Within a certain route, the structure of the **R** group seems to be the 'yield-determining' factor. This is especially true for the most frequently applied substitution reactions discussed in section 3.2.1. The other chemistries intuitively do not seem to be affected so strongly by the structural details of the **R** group, but this hypothesis lacks experimental conformation. If this indeed proves to be the case, then tertiary thiols – commercially available in the form of *tert*-butyl mercaptane or *tert*-dodecyl mercaptane – will form interesting compounds for thioacylation (section 3.2.3) or a useful ingredient for the procedures outlined in the sections 3.2.4, 3.2.5 and 3.2.6. When it comes to functionalized R groups, the reaction of bis(thioacyl)disulfides with radicals derived from azo initiators remains the author's top-notch pick, because of the large variety of initiators available on the market nowadays. For a further overview of all the dithioesters that have been prepared by the various routes up to 1988 reference 52 can be consulted, while a larger overview of the synthetic pathways can be found in reference 53 as well.

3.4. Experimental Section

3.4.1. Synthesis of Benzyl Dithiobenzoate[54]

Phenylmagnesium bromide was prepared from bromobenzene and magnesium turnings. A three-necked 2L round bottom flask was fitted with two 500ml dropping funnels. All glassware was dried before use at 130°C overnight. Tetrahydrofurane (THF, Biosolve, PA [*109-99-9*]) was freshly distilled from lithium aluminium hydride (Aldrich, 95% [*16853-85-3*]). 100ml THF was put in the round bottom flask while 500ml was put in one of the dropping funnels. A few iodine crystals (Aldrich, 99+% [*7553-56-2*]) and 20g (0.82mol) of magnesium turnings (Aldrich, 98% [*7439-95-4*]) were added to the flask and the other dropping funnel was filled with 125.6g (0.80mol) bromobenzene (Aldrich, 99% [*108-86-1*]). Approximately 10% of the bromobenzene was allowed to flow into the magnesium/THF mixture, which was then carefully warmed with a powerful heat gun (Bosch PHG 630-2 LCE, 2000W) until the reaction started. This is indicated

by the sudden disappearance of the brownish iodine color. Both bromobenzene and THF were then added dropwise at such rates that the reaction kept on going and that the temperature remained between 30 and 35 °C. An ice bath was used to remove the heat of reaction. Upon completion of the addition, the mixture was left to stir until no energy was produced anymore. The mixture possessed the dark greenish translucent shade of black, typical for such Grignard compounds. The empty dropping funnels were recharged with 61 g (0.80 mol) of anhydrous carbon disulfide (Aldrich, 99+% [*75-15-0*]) and 154 g (0.90 mol) benzyl bromide (Aldrich, 98% [*100-39-0*]). The ice bath was reapplied to keep the temperature below 35 °C while carbon disulfide was added. Upon formation of the dithiobenzoate salt, the reaction mixture turned to a dark opaque brown. The reaction was allowed to reach completion and then the benzyl bromide was poured in. An oil bath was used to heat the mixture to 55 °C for two hours. Some water (approx. 20 ml) was added to neutralize remaining reactive Grignard compounds and part of the THF was removed under reduced pressure. The concentrated solution was taken up in 1 L water and extracted with three portions (250 ml each) of diethyl ether (Lamers-Pleu, [*60-29-7*]). The combined organic phase was washed with water and dried over anhydrous magnesium sulfate (Aldrich, 97+% [*7487-88-9*]). The solution was then filtered and the ether removed under reduced pressure. Vacuum distillation yielded 130 g benzyl dithiobenzoate (67%) as a red oil. The product was identified by ^{1}H NMR; δ(ppm): 4.57 (s, CH_2), 7.20–7.60 (m, 8H) and 7.95 (m, 2H ortho to the CS_2 group)

3.4.2. Synthesis of 2-(ethoxycarbonyl)prop-2-yl Dithiobenzoate[54]

EMA-RAFT will be used as a trivial name for 2-(ethoxycarbonyl)prop-2-yl dithiobenzoate (**22**) throughout this thesis, as the **R**-group is identical to the ethyl methacrylate monomeric radical (Scheme 3.12).

The procedure that is followed is identical to the synthesis of benzyl dithiobenzoate. Instead of benzyl bromide however, 140 g ethyl 2-bromoisobutyrate (Aldrich, 98% [*600-00-0*]) was added. When the addition was complete, the mixture was kept at 75 °C for two days. The reaction was then allowed to come to room temperature. A small amount of water was added and the mixture was concentrated under reduced pressure. The residue was taken up in water en extracted three times with diethyl ether. The combined organic phases where washed with water and dried over anhydrous magnesium sulfate. After removal of the ether under reduced pressure, the viscous red oil that resulted was subjected to column chromatography

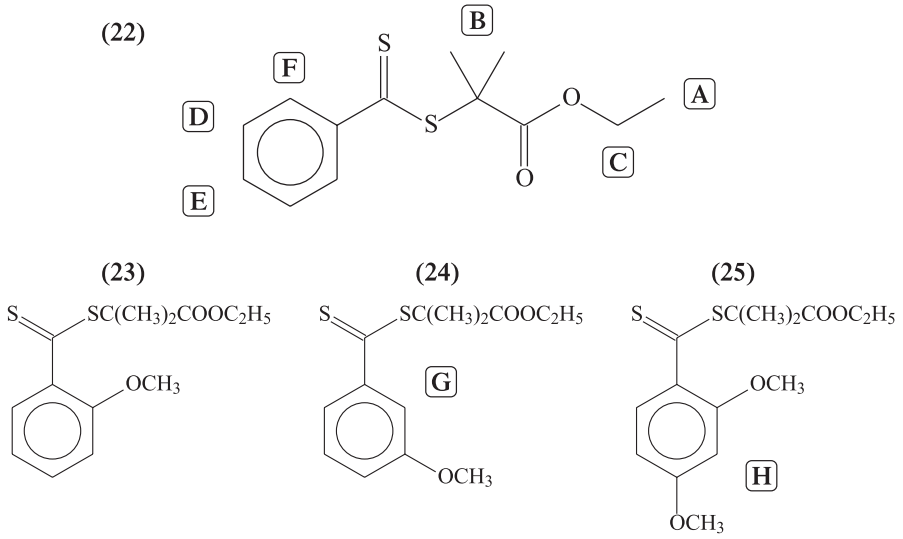

Scheme 3.12. 2-(ethoxycarbonyl)prop-2-yl dithiobenzoate (**22**) and three substituted derivatives.

on silica gel (Merck, 60 Å, 230–400 mesh [*112926-00-8*]) using pentane:heptane:diethyl ether (9:9:2) as the eluent. Starting from the same quantities as in the synthesis of benzyl dithiobenzoate, the yield was 69.6 g (32.5 %) of a red oily substance which was stored at –20 °C. At this temperature, the substance remained liquid. The product was identified by ^{1}H NMR; δ (ppm): 1.25 (t, 3H, **A**); 1.80 (s, 6H, **B**); 4.15 (q, 2H, **C**); 7.37 (t, 2H, **D**); 7.52 (t, 1H, **E**); 7.95 (d, 2H, **F**), see Scheme 3.12 for proton assignments.

Substituted derivatives of 2-(ethoxycarbonyl)prop-2-yl dithiobenzoate (**23**, **24**, **25**; Scheme 3.12) were prepared through the replacement of bromobenzene by 2-bromoanisole (Aldrich, 97 % [*578-57-4*]), 3-bromoanisole (Aldrich, 98+ % [*2398-37-0*]) and 1-bromo-2,4-dimethoxybenzene (Aldrich, 97 % [*17715-69-4*]) respectively. These syntheses typically produced a lot of (unidentified) side products, sometimes requiring multiple passes through a column, using the same conditions as for their unsubstituted counterparts. Yields ranged from 10 to 25 % and the products were identified by ^{1}H NMR. There was no significant change in the spectrum for the proton groups **A**, **B** and **C**. The methoxy protons on the aromatic ring gave a singlet signal at a chemical shift of 3.8 ppm corresponding to 3 protons for **23** and **24**, and to 6 protons for **25**. The four remaining protons in **23** produced multiplet signals centered around 6.9 and 7.4 ppm. In **24**, **G** gave a singlet at 7.5 ppm while the remaining 3 protons produced a multiplet ranging from 7.0 to 7.6 ppm. The aromatic protons in **25** produced signals at 6.4 and 7.6 ppm (**H**).

3.4.3. Synthesis of 2-phenylprop-2-yl Dithiobenzoate[54]

Cumyl-RAFT will be used as a trivial name for 2-phenylprop-2-yl dithiobenzoate throughout this thesis due to the cumyl radical that is expelled upon fragmentation.

sodium dithiobenzoate: 256 g of benzyl chloride (2.0 mol) was added dropwise to a stirred suspension of elemental sulfur (128 g, 4.0 mol, Merck, [*7704-34-9*]) and sodium methoxide (720 g of 30% solution, 4.0 mol, Merck [*124-41-4*]) in dry methanol (≈500 ml) at 70 °C. The methanol (Biosolve, abs. PA [*67-56-1*]) was dried over anhydrous molecular sieves (Merck, 4 Å) before use. Upon addition of the benzylchloride, a dark brown color appeared. The mixture was then stirred overnight. After cooling, the suspension was decanted and filtered over a Büchner funnel to remove the cooking salt (whitish yellow shade). Methanol was largely removed under reduced pressure and the oily brownish residue was taken up in water. The dispersion was refiltered over a glass filter, removing a second batch of the unidentified cooking salt after which a solution of sodium dithiobenzoate in water remained.

dithiobenzoic acid: Concentrated hydrochloric acid (Aldrich, 37 w% [*7647-01-0*]) was added until the brown color of the solution had disappeared completely and the dithiobenzoic acid had formed a separate layer below the waterphase. The organic layer was isolated and the waterphase was extracted twice with dichloromethane (Biosolve, PA [*75-09-2*]). The combined organic fractions were washed with a small portion of water, after which the dichloromethane was removed under reduced pressure (T<40 °C) to yield dithiobenzoic acid (208 g, 1.4 mol) as an intensely colored purple oil. Combined yield (steps a & b) is 68%.

2-phenylprop-2-yl dithiobenzoate: A mixture of dithiobenzoic acid (53 g, 0.35 mol), α-methylstyrene (50 g; 0.42 mol. Aldrich, 99% [*98-83-9*]) and carbon tetrachloride (40 ml. Aldrich, 99.9% [*56-23-5*]) was heated at 70 °C for 4 hours. The resulting mixture was reduced to a crude oil which was purified by column chromatography over aluminum oxide (Merck, standarized, Brockmann activity II–III, 60–200 mesh, 90 Å [1344-28-1]) using pentane:heptane (1:1, both Biosolve, PA [*109-66-0*] and [*142-82-2*]) as eluent to give 2-phenylprop-2-yl dithiobenzoate (27 g, 28% yield) as a dark purple oil. ^{1}HNMR ($CDCl_3$) δ (ppm): 2.03 (s, 6H); 7.20-7.60 (m, 8H) and 7.86 (m, 2H). Note that the use of activity I aluminium oxide resulted in impractically low R_f values. In repetitive experiments, attempts to

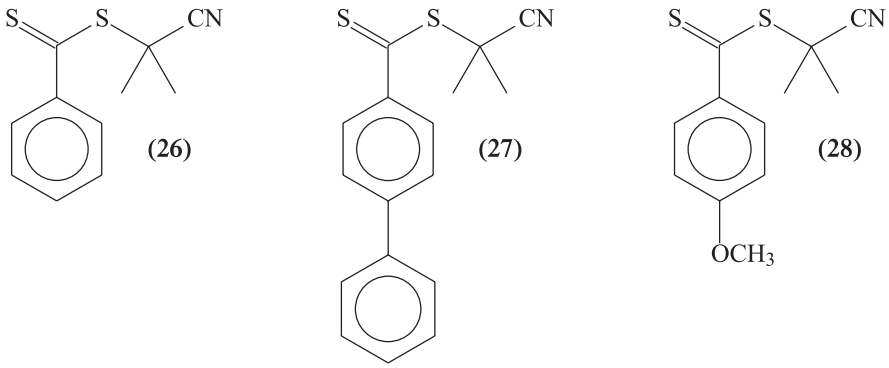

Scheme 3.13. 2-cyanoprop-2-yl dithiobenzoate (**26**) and two substituted derviatives that were synthesized.

increase the yield of the reaction with Brøndsted and Lewis acid catalysis, an inert atmosphere and even more delicate handling of the intermediate dithioacid (low T) did not result in any significant improvement of the yield.

3.4.4. Synthesis of 2-cyanoprop-2-yl Dithiobenzoate[50]

Cyano-RAFT will be used as a trivial name for 2-cyanoprop-2-yl dithiobenzoate, derived from the cyano functional **R** group.

dithiobenzoic acid: This compound was prepared in section 3.4.3, but an alternative route to this species is by the use of the Grignard reaction described in section 3.4.1. Once the reaction of phenyl magnesium bromide and carbon disulfide had completed, water (≈50 ml) was added slowly and carefully to the cooled reaction mixture with the aim of neutralizing the Gringnard coumpound. The mixture was then concentrated on a rotary evaporator and the resulting solution was diluted with water. The mixture was filtered to remove insoluble magnesium salts and subsequently treated with concentrated hydrochloric acid until the brown color had disappeared completely and pure dithiobenzoic acid separated from the resulting pink opaque liquid in the form of a purple oil. The pink liquid is extracted twice with dichloromethane and this organic phase was combined with the purple oil. Removal of the dichloromethane under reduced pressure yielded dithiobenzoic acid. This method was found to yield a considerably cleaner product than the dithiobenzoic acid obtained by the method described in section 3.4.3, which became obvious in the next step.

bis(thiobenzoyl) disulfide (20): 208 g of dithiobenzoic acid (1.36 mol) was mixed with 200 ml of ethyl acetate (Biosolve [*141-78-6*]). A few crystals of iodine (Aldrich, 99+% [7553-56-2]) were added to the solution and dimethylsulfoxide (53 g, 0.68 mol, Acros, [*67-68-5*]) was added dropwise. The mixture was kept in the dark overnight, though it was expected that the reaction had reached completion within an hour. Ethyl acetate was then removed under reduced pressure to yield the desired product in 90% yield (186 g, 0.61 mol). When the reaction was performed in a concentrated ethanol solution, the product crystallized upon formation in shiny red flakes. A second, considerably smaller batch was obtained by cooling the ethanol solution to –20 °C. The same procedure was also followed with a batch of dithiobenzoic acid generated by the reaction described in section 3.4.3. In this case the product failed to crystallize most likely due to large amounts of contaminants. Bis(thiobenzoyl) disulfide is characterized by the following signals in the ^{1}H NMR spectrum, δ(ppm): 7.45 (dd, 4H, meta position), 7.61 (m, 2H, para position), 8.09 (d, 4H, ortho position).

2-cyanoprop-2-yl dithiobenzoate (26): Bis(thiobenzoyl) disulfide (180 g, 0.59 mol) and 2,2'-azobis(isobutyronitril) (135 g, 0.83 mol, Wako Chemicals) are dissolved in ethyl acetate. The mixture is brought to reflux under an argon atmosphere for 30 minutes. Then the solution is then stirred overnight at 65 °C. Ethyl acetate is removed under reduced pressure to give a red oil which was subjected to flash chromatography using pentane:heptane:diethyl ether as eluent (9:9:2). The red product which was obtained in 59% yield (154 g, 0.69 mol), crystallized when stored at –20 °C and is a red oil at ambient temperature. The ^{1}H NMR spectrum showed the following peaks, δ(ppm): 1.93 (s, 6H, CH_3), 7.40 (m, 2H, meta), 7.55 (m, 1H, para), 7.90 (d, 2H, ortho). The major byproduct of this synthesis is the combination product of two AIBN derived radicals (2,3-dicyano-2,3-dimethyl-butane), which gives a singlet at 1.55 ppm.

Substituted derivatives of 2-cyanoprop-2-yl dithiobenzoate (**27**, **28**) were synthesized by a completely analoguous procedure, replacing the bromobenzene that is applied in the Grignard reaction by 4-bromobiphenyl (Aldrich, 98% [*92-66-0*]) and 4-bromoanisole (Aldrich, 99% [*104-92-7*]) respectively. Biphenyl derivative **27** is characterized by the following peaks in the ^{1}H NMR spectrum; δ(ppm): 1.95 (s, 6H), 7.4 (m, 6H), 7.6 (d, 1H), 8.0 (d, 2H) and methoxy derivative **28** gave 1.91 (s, 6H), 3.9 (s, 3H), 6.9 (d, 2H), 8.0 (d, 2H).

Ortho substituted derivatives similar to the ones discussed in 3.4.2 could not be prepared via this route. Starting from 2-bromoanisole (Aldrich, 97% [*578-57-4*]), 1-bromo-2,4-dimethoxybenzene (Aldrich, 97% [*17715-69-4*]) and 2-bromobiphenyl (Aldrich, 96% [*2052-07-5*]) the Grignard reaction proceeded smoothly, but the coupling of the protonated acid with dimethyl sulfoxide failed. Several alternative methods were attempted. The traditional approach applies a solution of iodine in water (with potassium iodine), to an aqeous solution of the potassium or sodium salt of the dithio acid.[7] Coupling of the magnesiumbromide salts of these ortho-substituted dithiobenzoic acids with iodine prooved ineffective. Also the oxidation with benzenesulfonyl cloride (Aldrich, 99% [*98-09-9*]) did not result in the desired bis(thioacyl) disulfides. Benzenesulfonyl chloride was reported to efficiently oxidize both the protonated form of dithioacids, as well as the magnesiumbromide derivative formed by a Grignard reaction.[8] Both variations on the process failed for ortho-substituted dithiobenzoic acids.

3.4.5. Synthesis of 4-cyano-4-((thiobenzoyl)sulfanyl)pentanoic Acid[50]

The preparation of 4-cyano-4-((thiobenzoyl)sulfanyl)pentanoic acid (**29**) closely follows the route to 2-cyanoprop-2-yl dithiobenzoate (section 3.4.4), except for the last step in which 4,4'-azobis(4-cyanopentanoic acid) substitutes 2,2'-azobis(isobutyronitril).

Bis(thiobenzoyl)disulfide (103 g, 0.34 mol) and 4,4'-azobis(4-cyanopentanoic acid) (132 g,* 0.47 mol, Aldrich, 75+% [*2638-94-0*]) are dissolved in ethyl acetate (Biosolve, [*141-78-6*]). The mixture is brought to reflux under an argon atmosphere for 30 minutes. The solution is then stirred overnight at 70 °C. Ethyl acetate was removed under reduced pressure. The resulting product was dissolved in a small amount of dichloromethane and subjected to column chromatography on silica gel, using pentane:heptane:ethyl acetate (1:1:2) as eluent. Removal of the eluent from the product yielded a red solid (123 g, 0.44 mol, 65% yield), m.p. 94 °C (lit.[50] 97–99 °C). ^{1}H NMR analysis revealed the following peaks (see Scheme 3.14 for assignments), δ (ppm): 1.93 (s, 3H, **A**), 2.4–2.8 (m, 4H, **B**), 7.42 (m, 2H, **C**), 7.58 (m, 1H, **D**), 7.93 (d, 2H, **E**).

* weighed quantities are 33% higer to correct for the low purity of the product (75%).

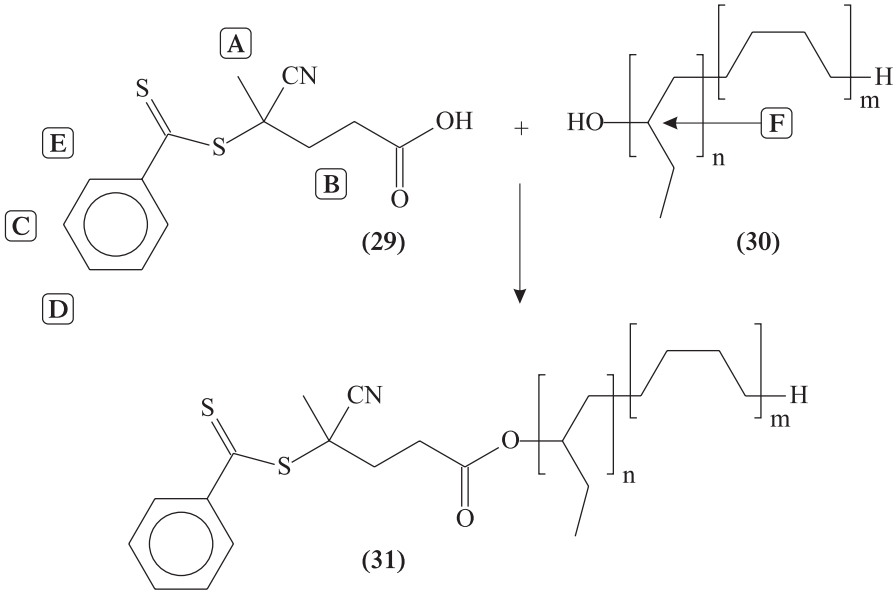

Scheme 3.14. Synthetic pathway to the Kraton-based macromolecular RAFT agent. The reaction proceeds in excellent yields and under mild conditions when 1,3-dicyclohexylcarbodiimide is used to activate the carboxilic acid group in **29**. Note that the representation of the polyolefin structure is simplified. Kraton is a more or less statistical sequence of ethylene and butylene units.

3.4.6. Synthesis of a Polyolefin Macromolecular Transfer Agent[55]

Kraton L-1203 (**30**) was obtained from Shell Chemicals ($\overline{M}_n \approx 3800\,g\cdot mol^{-1}$; $\overline{M}_w/\overline{M}_n \approx 1.04$) and dried under reduced pressure for several days before use. Anhydrous dichloromethane was prepared by distillation from lithium aluminum hydride, and stored over molecular sieves.

Kraton L-1203 (29.5 g, 8 mmol), *p*-toluenesulfonic acid (0.30 g, 1.6 mmol, Aldrich, 98.5% [*6192-52-5*]), 4-(dimethylamino)pyridine (0.29 g, 2.4 mmol, Aldrich, 99+% [*1122-58-3*]) and 1,3-dicyclohexylcarbodiimide (3.9 g, 19 mmol Aldrich, 99% [*538-75-0*]) were dissolved in anhydrous dichloromethane in a 1 L three necked round bottom flask equipped with a magnetic stirrer. 4-cyano-4-((thiobenzoyl)sulfanyl)pentanoic acid (2.5 g, 9 mmol) was dissolved in anhydrous dichloromethane and added dropwise to the reaction mixture at room temperature. Upon completion, the reaction mixture was heated to 30 °C and allowed to stir for 48 hours. A few milliliters of water was added to convert remaining 1,3-dicyclohexylcarbodiimide into the insoluble dicyclohexylurea. The mixture was then filtered and washed with water. The solution was dried with anhydrous magnesium sulfate,

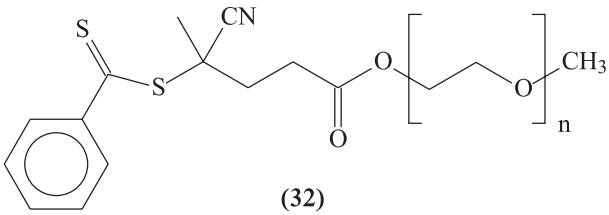

(32)

Scheme 3.15. A watersoluble macromolecular RAFT agent prepared from 4-cyano-4-((thiobenzoyl)sulfanyl)pentanoic acid and poly(ethylene glycol) methyl ether.

filtered and concentrated under reduced pressure. The crude product was purified by column chromatography over silica with heptane:ethyl acetate (9:1) as eluent. Removal of the solvent under high vacuum gave a purplish red viscous liquid (29.4 g, 92% yield, based on Kraton). The ^{1}H NMR spectrum indicated a quantitative yield based on the number of hydroxyl groups. The chemical shift of the set of protons in the Kraton situated next to the hydroxyl (**F**, Scheme 3.14) group changed from 3.6 to 4.2 ppm upon esterification.

3.4.7. Synthesis of a Poly(ethylene oxide)-based RAFT Agent

The synthesis of a water soluble poly(ethelene oxide)-based RAFT agent follows the same procedures as that of the polyolefin based RAFT agent discussed in section 3.4.6, but with the hydroxyl terminated poly(ethylene-*co*-butylene) replaced by a poly(ethylene glycol) methyl ether which is dried under vacuum before use for several days. A typical recipe consisted of *p*-toluenesulfonic acid (0.30 g; 1.6 mmol), 4-(dimethylamino)pyridine (0.18 g; 1.5 mmol) and 1,3-dicyclohexylcarbodiimide (5.0 g; 25 mmol) dissolved in anhydrous dichloromethane together with 9 mmol of the poly(ethylene glycol) methyl ether (Aldrich [*9004-74-4*]). The synthesis was conducted with material of different chain lengths, requiring 18 g of material with a molar mass of approx. 2000 g·mol^{-1} or 6.75 g with $\overline{M}_n \approx 750$ g·mol^{-1}. The reaction proceeds completely analogous to the synthesis in section 3.4.6. The product was not purified, but used as obtained after removal of the dichloromethane.

3.5. References

1. Gilroy et al. in *The haiku year*, Soft Skull Press, **1998**
2. Kato, S.; Itoh, K.; Hattori, R.; Mizuta, M.; Katada, T. *Z. Naturforsch.* **1978**, *B 33*, 976
3. Kato, S.; Yamada, S.; Goto, H.; Terashima, K.; Mizuta, M.; Katada, T. *Z. Naturforsch.* **1980**, *B 35*, 458

4. Kato, S.; Mitani, T.; Mizuta, M. *Int. J. Sulfur Chem.* **1973**, *8*, 359
5. Kato, S.; Mizuta, M. *Int. J. Sulfur Chem.* **1972**, *A 2*, 31
6. Kato, S.; Mizuta, M. *Bull. Chem. Soc. Jpn.* **1972**, *45*, 3492
7. Houben, J. *Ber.* **1906**, *39*, 3219
8. Kato, S.; Kato, T.; Kataoka, T.; Mizuta, M. *Int. J. Sulfur Chem.* **1973**, *8*, 437
9. Kato, S.; Mizuta, M.; Ishii, Y. *J. Organometal. Chem.* **1973**, *55*, 121 zink lood
10. Latif, K. A.; Ali, M. Y. *Tetrahedron* **1970**, *26*, 4247
11. Kato, S.; Goto, M.; Hattori, R.; Nishiwaki, K.; Ishida, M. *Chem. Ber.* **1985**, *118*, 1668
12. Bost, R. W.; Mattox, W. J. *J. Am. Chem. Soc.* **1930**, *52*, 332
13. Fleischer, M. *Liebigs Ann. Chem.* **1866**, *140*, 241
14. Wood, J. H.; Bost, R. W. *J. Am. Chem. Soc.* **1937**, *59*,1011
15. Cohen, I. A.; Basolo, F. *Inorg. Chem.* **1964**, *3*, 1641
16. Becke, F.; Hagen, H. (BASF AG) German patent 1 274 121 1968 [*Chem. Abstr.* **1969** 70:3573v]
17. Houben, J.; Schultze, K. M. L. *Ber.* **1910**, *43*, 2481
18. Meijer, J.; Vermeer, P.; Brandsma, L. *Recl. Trav. Chim. Pays-Bas* **1973**, *92*, 601
19. Westmijze, H.; Kleijn, H.; Meijer, J.; Vermeer, P. *Synthesis* **1979**, 432
20. Wheeler, A. S.; Thomas, C. L. *J. Am. Chem. Soc.* **1928**, *50*, 3106
21. Gonella, N. C.; Lakshmikanthan, M. V.; Cava, M. P. *Synth. Commun.* **1979**, *9*, 17
22. Bost, R. W.; Shealy, O. L. *J. Am. Chem. Soc.* **1951**, *73*, 25
23. Jensen, K. A.; Pedersen, C. *Acta Chem. Scand.* **1961**, *15*, 1087
24. Oae, S.; Yaghihara, T.; Okabe, T. *Tetrahedron* **1972**, *28*, 3203
25. Kato, S.; Shibahashi, H.; Katada, T.; Takagi, T.; Noda, I.; Mizuta, M.; Goto, M. *Liebigs Ann. Chem.* **1982**, *7*, 1229
26. Mayer, R.; Scheithauer, S. *J. Prakt. Chem.* **1963**, *21*, 214
27. Hedgley, E. J.; Fletcher, H. G. *J. Org. Chem.* **1965**, *30*, 1282
28. Leon, N. H.; Asquith, R. S. *Tetrahedron* **1970**, *26*, 1719
29. Hedgley, E. J.; Leon, N. H. *J. Chem. Soc. (C)* **1970**, 467
30. Hoffmann, R.; Hartke, K. *Liebigs Ann. Chem.* **1977**, 1743. Levesque, G.; Gressier, J.-C., Proust, M. *Synthesis* **1981**, 963
31. Hoffmann, R.; Hartke, K. *Chem. Ber.* **1980**, *113*, 919. Hartke,K.; Hoffmann, R. *Liebigs Ann. Chem.* **1980**, 483
32. Thuillier, A. *Phosphorus Sulfur* **1985**, *23*, 253
33. Pedersen, B. S.; Scheibye, S.; Clausen, K.; Lawesson, S.-O. *Bull. Soc. Chim. Belg.* **1978**, *87*, 293
34. Ghattas, A. B. A. G.; El-Khrisy, E. E. A. M.; Lawesson, S.-O. *Sulphur Letters* **1982**, *1*, 69
35. Kim, S.; Lee, J. I.; Ko, Y. K. *Tetrahedron Lett.* **1984**, *25*, 4943
36. Dellaria, J. F. Jr.; Nordeen, C.; Swett, L. R. *Synth. Commun.* **1986**, *16*, 1043
37. Ueda, M.; Mori, H. *Bull. Chem. Soc. Jpn.* **1992**, *65*, 1636
38. Grunwell, J. R.; Foerst, D. L. *Synth. Commun.* **1976**, *6*, 453
39. Bauer, W.; Kühlein, K. *Methoden Org. Chem. (Houben-Weyl)* **1985**, *E5*, 832
40. Katrizky, A. R.; Moutou, J.-L.; Yang, Z. *Organic Prep. Proc. Int.* **1995**, *27*, 361
41. Yousif, N. M.; Pedersen, U.; Yde, B.; Lawesson, S.-O. *Tetrahedron* **1984**, *14*, 2663
42. Blagoveshchenskii, V. S.; Vlasova, S. N. *Zhurnal Obshchei Khimii* **1971**, *41*, 1032
43. Davy, H.; Metzner, P. *Chemistry and Industry* **1985**, 824
44. Viola, H.; Scheithauer, S.; Mayer, R. *Chem. Ber.* **1968**, *101*, 3517
45. Arndt, F.; Milde, E.; Eckert, G. *Ber. dtsch. chem. Ges.* **1923**, *56*, 1976
46. Staudinger, H.; Siegward, J. *Helv. Chim. Acta* **1920**, *3*, 824
47. *e.g.* Manders, B. G.; Morrison, B. R.; Klostermann, R. *Macromol. Symp.* **2000**, *155*, 53. Ma, J. W.; Cunningham, M. F. *Macromol. Symp.* **2000**, *150*, 85. Mendoza, J. De la Cal, J. C.; Asua, J. M. *J. Polym. Sci., Part A: Polym. Chem.* **2000**, *38*, 4490
48. George, P. D. *J. Org. Chem.* **1961**, *26*, 4235
49. Bouhadir, G.; Legrand, N.; Quiclet-Sire, B.; Sard, S. Z. *Tetrahedron Lett.* **1999**, *40*, 277
50. Thang, S. H.; Chong, Y. K.; Mayadunne, R. T. A.; Moad, G.; Rizzardo, E. *Tetrahedron Lett.* **1999**, *40*, 2435
51. Moad, G.; Rizzardo, E.; Thang, S. H. PCT Int. Appl. PCT/AU98/00569. WO9905099A1
52. Kato, S.; Ishida, M. *Sulfur Reports* **1988**, *8*, 155

53. Ramadas, S. R.; Srinivasan, P. S.; Ramachandran, J.; Sastry, V. V. S. K. *Synthesis* **1983**, 605
54. Le, T. P.; Moad, G.; Rizzardo, E.; Thang, S. H.; Patent WO 98/01478 (1998) [*Chem. Abstr.* **1998**, *128*:115390]
55. De Brouwer, H.; Schellekens, M. A. J.; Klumperman, B.; Monteiro, M. J.; German, A. L. *J. Polym. Sci. Part A: Polym. Chem.* **2000**, *38*, 3596.

» Chosen are those artists who penetrate the region
of that secret place, where primeval power nurtures all evolution...
Who is the artist that would not dwell there?
In the womb of nature at the source of creation,
where the secret key to all lies guarded. «[1]

4. Living Radical Copolymerization of Styrene and Maleic Anhydride and the Synthesis of Novel Polyolefin-based Block Copolymers via RAFT Polymerization.[2]

Synopsis: This chapter describes the application of RAFT polymerization in the copolymerization of styrene and maleic anhydride. Novel well-defined polyolefin-based block copolymers are prepared using a macromolecular RAFT agent derived from a commercially available polyolefin (Kraton L-1203). The second block consisted of either polystyrene or poly(styrene-co-maleic anhydride). The product has a low polydispersity and is of predetermined molar mass. Furthermore, it is demonstrated that the colored labile dithioester moiety in the product of RAFT polymerizations can be removed from the polymer chain by UV photolysis.

4.1. Polyolefin-based Architectures

Polyolefins find application in a large number of areas ranging from cheap bulk commodity plastic to high added value engineering materials. One can think of packaging materials (plastic bags & bottles), rubbers and thermoplastic elastomers like EPDM and EPM (copolymers of ethylene, propylene, butadiene), superstrong fibres and coatings. The inert character of polyolefins is an advantageous property in many cases, *e.g.* contact with foods, tacking of dirt, resistance to solvents and other chemicals, but complicates efficient application as the adhesion of polyolefin coatings on substrates and the miscibility with other polymer materials is poor. The pure hydrocarbon polymer backbone with its low interfacial tension lacks the ability to form interactions with other materials by the formation of primary (covalent) or secondary bonds (acid–base or polar interactions). An established

technique for improving the interfacial tension between polymers and other materials is the use of block and graft copolymers as compatibilizers.[3,4,5] Small amounts of functional groups, concentrated in a few short segments dramatically increase the interaction between polyolefins and a broad range of materials containing polar groups with most of the original properties of the polyolefin retained. In principle, there are two ways to obtain functionalized polyolefins: ① chemical modification or free-radical grafting of preformed polyolefins; ② block copolymerizations and random copolymerizations of olefins with suitable polar monomers.[6]

The latter method gives direct access to the desired materials under mild and controlled conditions but suffers from the serious drawback of the limited compatibility between Ziegler-Natta and metallocene catalysts – both widely used to prepare polyolefins – and polar monomers. The first method is widely used, but requires aggressive reaction conditions. The polymer is activated by either exposure to high energy radiation or heating in the presence of a suitable free-radical initiator and followed by initiation of the second monomer.

In this chapter it will be shown how living radical polymerization techniques can be used to prepare macromolecular structures containing polyolefinic elements. Chapter 2 (*e.g.* Figure 2.2, page 32) showed that living radical polymerization is well suited for the preparation of block copolymers. This approach required the monomers for both blocks to be polymerized in a sequential manner, something which is bound to fail for olefins as free-radical techniques – living or not – are unable to polymerize these monomers. Several methods have been reported to overcome this problem allowing these techniques to be used for the preparation of polyolefin-based polymer architectures (block and graft copolymers).

It was shown that an alkene functionalized with an alkoxyamine moiety could be copolymerized with olefins like propene and 4-methylpentene using a cationic metallocene catalyst.[7] The resulting polyolefin with alkoxyamine groups scattered along its backbone was used as a macro-initiator in the nitroxide mediated polymerization of styrene to form polyolefin-*graft*-polystyrene with low polydispersity polystyrene grafts ($pd < 1.15$).

An alternative approach is the transformation of a ready-made polyolefin into a suitable dormant species by organic procedures. This requires a polyolefin starting material with some sort of functional group in the polymer chain that can be converted into the desired starting material for living radical polymerization.

Kraton L-1203, for example, is a commercial product prepared from butadiene. Low molar mass polybutadienes are end-capped and hydrogenated to form semi-random copolymers of ethylene and butylene with a terminal hydroxyl group. The hydroxyl group may be esterified with *e.g.* 2-bromo-2-methyl propionyl bromide to form a mono-bromide functionalized polyolefin which can be converted to a block copolymer by atom transfer radical polymerization (ATRP).[8,9,10]

Waterson and Haddleton[10] showed that this material could be used to prepare poly[(ethylene-*co*-butylene)-*block*-methyl methacrylate] and poly[(ethylene-*co*-butylene)-*block*-trimethylsilyl methacrylate] which in turn could be hydrolyzed to poly[(ethylene-*co*-butylene)-*block*-methacrylic acid]. Jancova *et al.*[9] used a similar Kraton derivative to prepare poly[(ethylene-*co*-butylene)-*block*-styrene] and poly[(ethylene-*co*-butylene)-*block*-(4-acetoxy styrene)]. Again this polymer was hydrolyzed forming poly[(ethylene-*co*-butylene)-*block*-(4-hydroxy styrene)]. Matyjaszewski *et al.*[11] transformed a commercial copolymer of ethylene and glycidyl methacrylate into a suitable initiator for ATRP, allowing the preparation of poly(ethylene-*graft*-styrene) and poly(ethylene-*graft*-methyl methacrylate).

The examples above show that an additional hydrolysis step is required to come to truly functional block copolymers. Although advances have been made in this field, the combination of ATRP and highly polar or functional monomers was found to be problematic. Direct polymerization of acidic monomers is not possible with the current generation of catalysts as the metals rapidly react with the acids to form metal carboxylates that are ineffective as deactivator and often insoluble in the reaction medium[12]. Polymerization of the sodium salts of methacrylic acid[13] and of 4-vinyl benzoic acid[14] has been reported but the required aqueous polymerization medium prevents the incorporation of these monomers in more complex polymer architectures together with most other (water insoluble) monomers.

For compatibilization purposes, maleic anhydride is often used as the grafting monomer as it introduces a highly polar group in the polyolefin, while the incorporation is regulated by its inability to form a homopolymer, restricting the addition to a single monomer unit per site.[15] Maleic anhydride has proved elusive so far in terms of controlled polymerization by living radical techniques. All attempts at the controlled copolymerization of styrene and maleic anhydride using ATRP, both in literature[16,17] and in our own laboratory, remained fruitless. Either polymerization

did not take place at all because of some deleterious interaction between the monomer and the ATRP catalyst,[17] or the molar mass developed in an unpredictable way.[16]

It has been shown that the copolymerization of styrene and maleic anhydride *can* proceed in a controlled fashion using nitroxide-mediated polymerization.[16] This required 2,2,5-trimethyl-4-phenyl-3-azahexane-3-nitroxide to be used at high temperatures (120 °C). Although this specially designed nitroxide is able to polymerize many different types of monomer,[18] its complicated synthesis[19] renders it unattractive. The more commonly applied and readily available 2,2,6,6-tetramethylpiperidinine-*N*-oxyl (TEMPO) was unable to control the polymerization.[16,20]

Reversible addition–fragmentation chain transfer (RAFT) polymerization is known to be compatible with acid- and amine-functional monomers,[21,22,23] and therefore appears to be the best choice for this type of work. It does not require more stringent polymerization conditions than conventional free-radical polymerization, and thereby allows the robustness of radical chemistry to be combined with a more sophisticated design of the polymer chain architecture. Especially in the context of block copolymers, the need for control on the polymer design cannot be overemphasized. The strong correlation between block lengths and block composition on the one hand and material properties on the other, requires careful tailoring of the polymer microstructure to arrive at materials with unique properties that are not solely of academic significance but are of commercial interest as well.[24,25,26] While random or statistical copolymers, in general, possess properties that appear to be an average of the properties found in the homopolymers of the constituent monomers, block copolymers retain many of the macroscopic characteristics of their homopolymers. Diblock copolymers can be used to prevent phase-compatibility problems in a variety of situations. Gaillard *et al.*[27] used poly(styrene-*b*-butadiene) as a compatibilizer for blends of polystyrene and polybutadiene. Duivenvoorde *et al.*[28] used block copolymers of ε-caprolactone and 2-vinyl pyridine as dispersants in powder coatings to stabilize pigment particles in polyester matrix materials. Amphiphilic diblock copolymers of styrene and styrene sulfonate have been used as surfactants in the emulsion polymerization of styrene.[29]

Scheme 4.1. Both 2-cyanoprop-2-yl dithiobenzoate **(1)** and macromolecular RAFT agent **(4)** were applied in the polymerization of this chapter. The latter was synthesized from a commercial hydroxyl terminated ethylene butylene copolymer (**3**, Kraton L-1203) and an acid functional dithioester **(2)**. The syntheses are described in chapter 2. Note that **3** consists of a more or less random sequence of ethylene and butylene units and that it is *not* a block copolymer as might be suggested by this simplified representation.

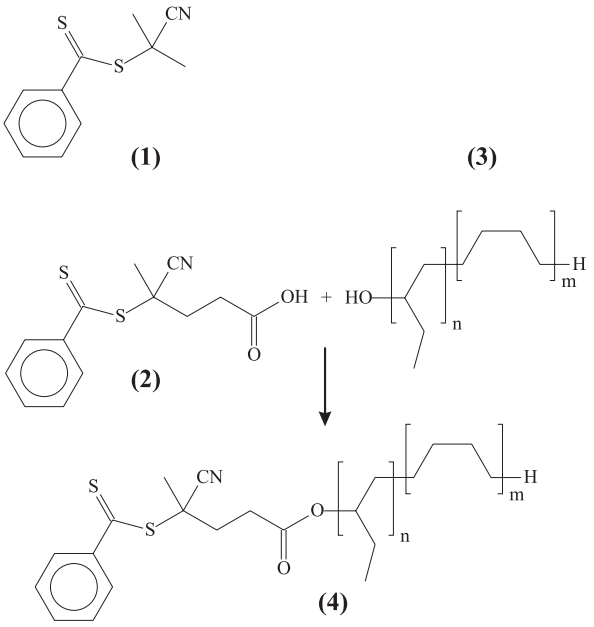

The aim of the work in this chapter is the preparation of low polidispersity block copolymers of predetermined molar mass, containing both a polyolefin block and a poly(styrene-*co*-maleic anhydride) block. This type of polymer may prove useful as blend compatibilizer or as adhesion promoter for polyolefin coatings on more polar substrates like metals.[30,31]

4.2. Results and Discussion

4.2.1. The Macromolecular RAFT Agent

The polyolefin block was introduced into the polymerization in the form of a macromolecular transfer agent. This was achieved by the modification of Kraton L-1203, a commercially available copolymer of ethylene and butylene (PEB) containing one hydroxyl end group and having a low polydispersity (≈1.04). The hydroxyl group was esterified with an acid-functional dithioester (Scheme 4.1) to yield a polyolefin-based RAFT agent **(4)**. Addition of this RAFT agent to a radical polymerization allows the PEB chain to be activated (reversibly), upon which it can incorporate monomer units and form a block copolymer. This course

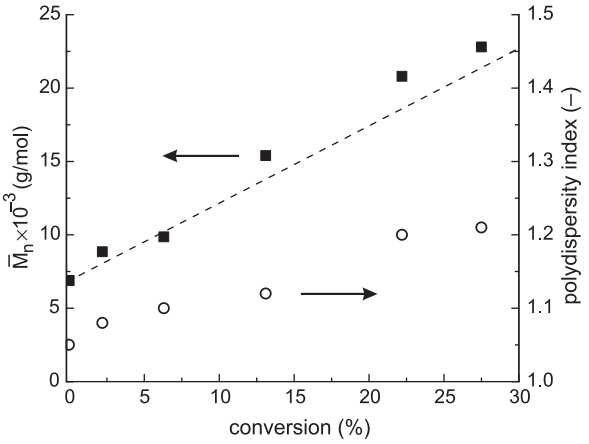

Figure 4.1. Experimentally determined number average molar mass (■, *left axis*) compared with theoretically expected values (---, *left axis*) and polydispersity indices (○, *right axis*) for several samples taken from experiment 2.

of reaction is studied first in several styrene polymerizations to develop and facilitate the analyses of the more complex anhydride containing block copolymers that will be prepared later (section 4.2.4).

4.2.2. Styrene Polymerizations

The polymerizations involving styrene and the macromolecular RAFT agent (**4**) (Table 4.1, page 99; experiments 1 and 2) allowed verification of the living character of the polymerization and confirmed that the polystyrene is indeed attached to the PEB chain. The number average molar mass is plotted against conversion in Figure 4.1. A linear relationship is found that corresponds closely to the theoretical values, which can be obtained using formula 4-1.

$$\overline{M}_{n,\,th} = \overline{M}_{n,\,raft} + \frac{FW_M \cdot x \cdot [M]_0}{[RAFT]_0} \qquad \textbf{(4-1)}$$

where $[M]_0$ and $[RAFT]_0$ are the starting concentrations of the monomer and the RAFT agent, respectively. x is the fractional conversion and FW_M is the molar mass of the monomer. $\overline{M}_{n,\,raft}$ is the number average molar mass of the RAFT agent as determined by GPC (in this case $6.5 \cdot 10^3 \text{g} \cdot \text{mol}^{-1}$). All molar masses are in polystyrene equivalents, as correction for the difference in hydrodynamic volume is inherently difficult when dealing with block copolymers of gradually changing composition. The molar mass distributions of samples taken at different conversions (Figure 4.2) clearly show the growth of the PS-*block*-PEB chains. In addition to these block copolymer chains, a small number of chains exist being derived from

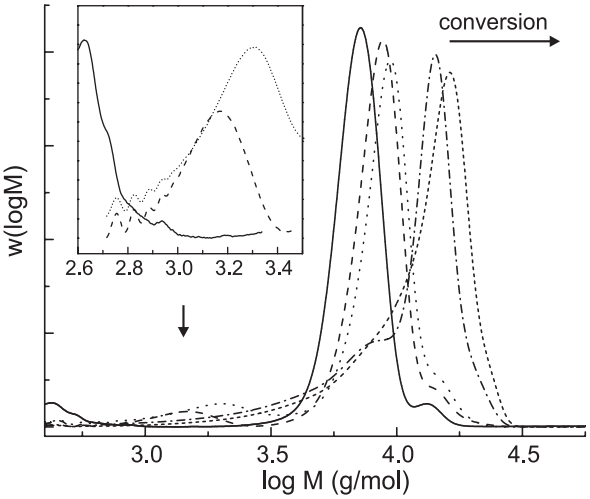

Figure 4.2. Normalized logarithmic molar mass distributions of samples taken from experiment 2. A gradually growing block copolymer can be observed while the inset shows the development of PS homopolymer (derived from initiator radicals) in the low molar mass region.

the azo initiator, rather than from the polymeric RAFT agent. These chains do not contain a PEB chain and are clearly visible in the first three samples as low molar mass polystyrene homopolymer (inset Figure 4.2). During the later stages of polymerization these homopolymer chains are no longer separated from the main peak, but remain visible as a low molar mass tail. All molar mass distributions have a shoulder at the high molar mass side, which is due to bimolecular termination. In this case, the block copolymer radicals recombine to form triblock copolymers, the middle block being polystyrene (reaction **b**, Scheme 4.2).

Both the high molar mass shoulder and the low molar mass homopolymer broaden the molar mass distribution and reduce the living character and the purity of the block copolymer. Although the effect on the polydispersity is not dramatic (table 4.1 & Figure 4.1), it should be noted that narrower molar mass distributions can be obtained with a careful choice of reaction conditions. Lowering the initiator concentration will reduce the amount of termination events relative to propagation. In addition, a reduction of the termination-derived shoulder will also eliminate most of the low molar mass tail of PS homopolymer. However, the trade-off in this case is a reduction of the polymerization rate as discussed in Chapter 2.

HPLC analyses of the same samples, using a triple detection setup, confirmed the GPC observations. This analysis allows the various components of the polymerizing system to be traced separately. The evaporative light scattering (ELSD) detector detects all polymeric compounds, while the diode array UV detector selectively observes the dithiobenzoate moiety at a wavelength of 320 nm and detects both the dithiobenzoate group and polystyrene at 254 nm.

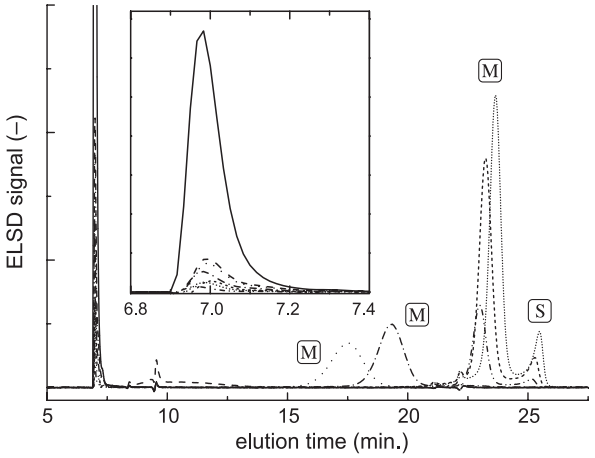

Figure 4.3. HPLC chromatograms of samples taken from experiment 2. The signal of the RAFT agent eluting at 7 min quickly disappears. The main peak (M) is the growing block copolymer. While the second peak (S) at higher elution volumes is expected to be the polystyrene homopolymer.

The signal of the macromolecular transfer agent, eluting at 7 minutes (Figure 4.3) diminishes rapidly during the initial phase of the polymerization. Although it disappears completely in the UV detection, a small ELSD signal, corresponding to a few percent of the starting material remains visible during the entire polymerization (The ELSD signal does not scale linearly with the amount of material.[32,33] This treatment indicates the *approximate* level of remaining material.). The signal is caused by unmodified PEB that is not coupled to the UV absorbing dithioester. This can be attributed to the fact that the starting material does not consist of purely monofunctional material. HPLC analyses of the original material (not shown) revealed that 2–3% of the chains is unfuctionalized. During these analyses no other irregularities (*e.g.* multifunctional material) were found. The disappearance of the corresponding UV signal indicates that the transformation of the RAFT agent into growing block copolymers is quantitative and rapid on the polymerization timescale. The main peak (**M**) which corresponds to the growing PS-*block*-PEB copolymer shifts towards longer elution times as the PS block increases in size. This peak precedes a secondary peak (**S**) that corresponds to the PS homopolymer material.

Figure 4.4 shows the ratio of the UV signal (λ=320nm) over the ELSD signal for both the main peak and the secondary peak. An increase in chain length is confirmed by the decrease in the end-group sensitive UV signal at 320nm relative to the two other signals. Furthermore, the signal ratio for the secondary peak is consistently higher, indicating the lower molar mass for the PS homopolymer. Again, no calibration was performed for the ELSD detector response to these materials, but the trends can be unmistakably observed.

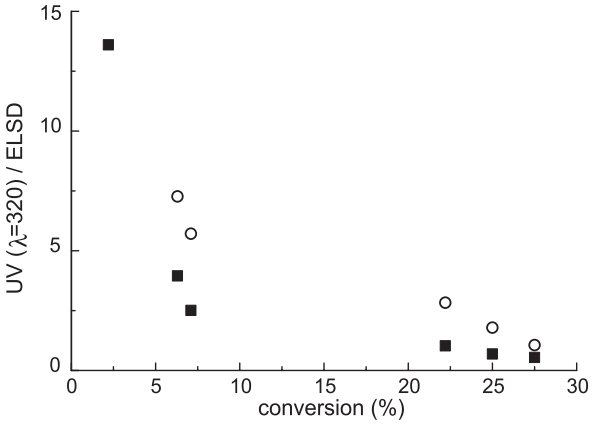

Figure 4.4. Evolution of the ratio of the end-group sensitive UV signal at a wavelength of 320nm and the ELSD signal for both the block copolymer (■) and the homopolymer (O).

The final product combined properties not found in the individual homopolymers that constitute the blocks. Upon precipitation in methanol a pink colored solid was isolated, whereas low molar mass ethylene–butylene copolymers have a sticky viscous liquid appearance. The polymer was fully soluble in heptane in contrast to polystyrene homopolymer of similar molar mass.

4.2.3. UV Irradiation

Low conversion samples of experiment 2, essentially block copolymers with a short PS block-length were dissolved in heptane and subjected to UV broadband irradiation for 5 hours. A part of the resulting product was passed through a short silica column using a mixture of heptane and dichloromethane (9:1) as the eluent. Both the crude product and the purified material were analyzed using GPC and their molar mass distributions were compared with those of the sample before irradiation. Although the UV irradiated product still had the same red color as the polymer before irradiation, the compound responsible for this color was no longer attached to the polymer chain. The polymer collected after passing through the column was colorless and the red color from the product had turned into a brown component with a very low R_f value. This color change is also observed when *e.g.* dithiobenzoic acid and its dimer, bis(thiobenzyl)disulfide, come into contact with silica and the brown color corresponds to that of dithiobenzoate salts. This led us to conclude that the dithioester group has been cleaved from the polymer chain and transformed into a more labile species. Examination of the molar mass distributions indicates that some of the material has been transformed into higher molar mass species of precisely twice and three times the original molar mass (as clearly visible in the second derivative in Figure 4.5). This is expected to be attributed to the reactions

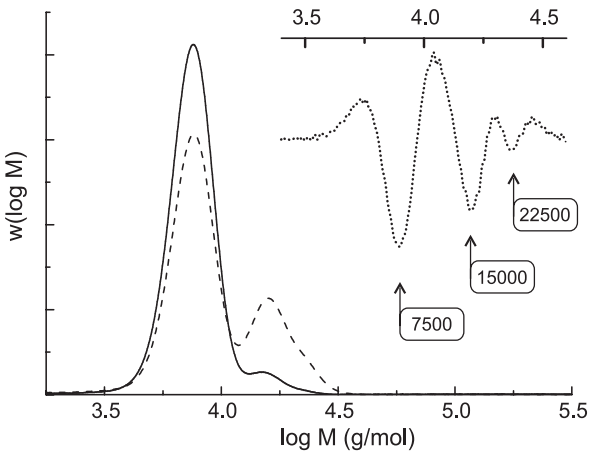

Figure 4.5. Normalized molar mass distributions of PEB-*block*-PS copolymers before (—) and after (---) UV irradiation. The second derivative of the distribution (····, *inset*) clearly shows the signal at twice and three times the original mass.

depicted in Scheme 4.2, which would mean that part of the diblock copolymer has been transformed into triblock material **(6)** free of the labile dithiogroup. The triple molar mass shoulder can be explained by combination of a block copolymer radical **(5)** with intermediate species **(7)** to yield a star shaped block copolymer with three arms **(8)**. Both termination reactions (**b** & **c**) take place during a common RAFT polymerization process as well. The occurrence of the additional termination reaction (**c**) forms the first experimental evidence for the postulate in section 2.3, explaining the retardation that is usually observed in RAFT homopolymerizations. Whereas this material will be difficult to detect under normal polymerization circumstances due to the minor fraction in which it is present combined with its relatively broad molar mass distribution (see section 2.3, page 43), the conditions in this experiment were such that the formation of the presumably star-shaped species yielded a material of a unique molar mass which could be identified by GPC analysis.

Although the colored dithiobenzoate group could be removed from the product by passing it over a short silica column, this process did not change the molar mass distribution. The process not only shows the facile removal of the labile colored end group, but also reveals the relative ease with which radicals are generated using UV irradiation. Such generation of radicals in a (post-)application phase forms an interesting potential for *e.g.* crosslinking reactions. In this respect one will have to solve the destination of the cleaved sulfur-containing moiety.

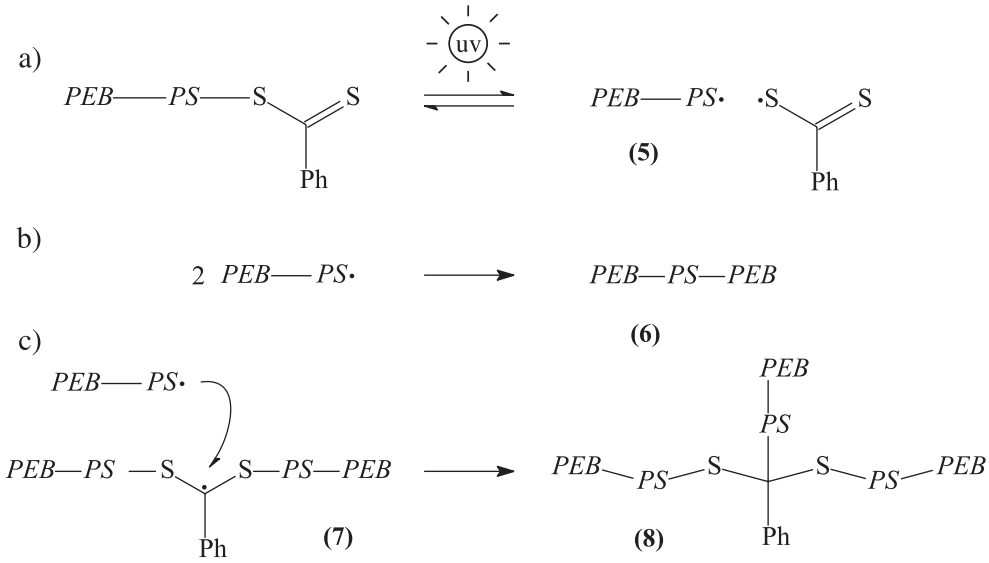

Scheme 4.2. Proposed reaction scheme. **a**) Under the influence of UV light the polymer dissociates and forms a dithiobenzoate radical and a block copolymer radical **(5)**. **b**) The polymer radicals can recombine to form triblock copolymers **(6)** or react with intact polymeric RAFT agent to form a intermediate radical **(7)** which can be terminated by a second block copolymer radical **(5)** to form a three-armed star **(8)**.

4.2.4. Styrene – Maleic Anhydride Copolymerizations

The free-radical copolymerization of styrene and maleic anhydride exhibits some interesting features. Maleic anhydride itself does not homopolymerize and its copolymerization with styrene has a strong tendency towards alternation, indicated by the reported reactivity ratios.[30] Convincing evidence was published a few years ago indicating that the STY/MAh copolymerization obeys the penultimate unit model.[34] On the basis of the copolymerization parameters it can easily be estimated that the vast majority of propagating radicals carries a terminal styrene unit. As the reaction between styrene-ended radicals and the RAFT agent proceeds rapidly, also the copolymerization of styrene with MAh is expected to proceed in a controlled fashion.

As can be seen in table 4.1 (experiments 3 to 5, page 99), three STY/MAh copolymerizations were carried out under similar conditions, but different with respect to the RAFT agent that was employed and the monomer concentrations used. The blank experiment without RAFT agent (experiment 3) became turbid after a few percent conversion. The heterogeneity was caused by precipitation due

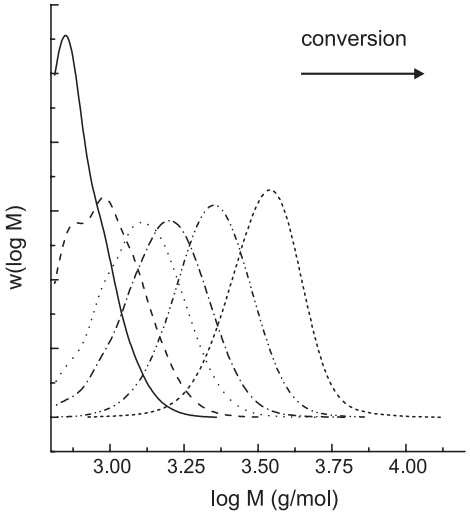

Figure 4.6. Normalized logarithmic molar mass distributions for samples taken during experiment 4, the controlled copolymerization of STY and MAh.

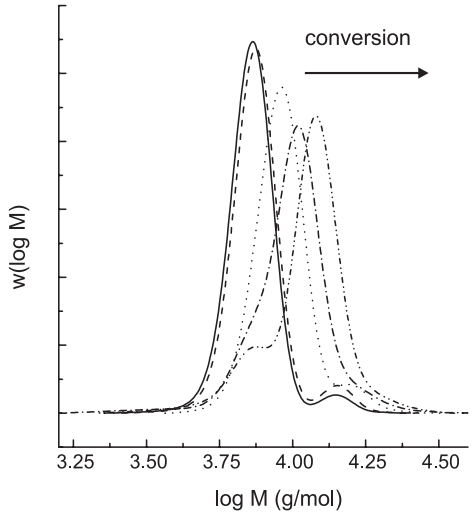

Figure 4.7. Normalized logarithmic molar mass distributions for samples taken during experiment 5, growing a STY/MAh block onto the PEB chain.

to the poor solvent properties of butyl acetate for high molar mass STY/MAh copolymer. The molar mass of the resulting polymer exceeded the exclusion limit of the applied columns ($M > 2 \cdot 10^6 g \cdot mol^{-1}$).

The experiment with RAFT agent **1** (experiment 4) remained homogeneous during the entire polymerization and GPC analysis of samples that were periodically drawn from the reaction mixture revealed a controlled growth (Figure 4.6). Due to the nonvolatile character of the MAh monomer, gravimetric conversion measurements are rather inaccurate but the molar mass of the final sample ($\overline{M}_n = 4.1 \cdot 10^3 g \cdot mol^{-1}$) is close to the expected theoretical value of $4.4 \cdot 10^3 g \cdot mol^{-1}$, obtained from equation 4-1. The polydispersity of the final product is 1.06.

Application of the macromolecular RAFT agent (**4**, experiment 5) allowed the preparation of low polydispersity poly[(ethylene-*co*-butylene)-*block*-(styrene-*co*-maleic anhydride)] polymers. Although the reaction mixture is heterogeneous at room temperature, it forms a clear, single-phase solution at the reaction temperature of 60°C. The first few samples at low conversion, phase separate when cooled to room temperature into a red PEB-rich phase and a colorless monomer rich phase. As conversion increases the STY/MAh block grows and solubilizes the PEB block to form a homogeneous solution at room temperature.

Table 4.1: Experimental Details of the RAFT Polymerizations

Exp.	Styrene concentration ($mol \cdot dm^{-3}$)	MAh concentration ($mol \cdot dm^{-3}$)	RAFT Agent [conc. $\times 10^2$ ($mol \cdot dm^{-3}$)]	Solvent	$\overline{M}_n \times 10^{-3}$ ($g \cdot mol^{-1}$)	$\overline{M}_w / \overline{M}_n$	Conversion (%)	Theoretical $\overline{M}_n$ [a] $\times 10^{-3}$ ($g \cdot mol^{-1}$)
1	2.0	—	**4** [1.0]	Xylene	10	1.18	21	10
2	4.8	—	**4** [1.0]	Xylene	23	1.20	28	20
3	1.0	1.0	None	BuAc	>2000	—[b]	—[b]	—[b]
4	1.0	1.0	**1** [2.6]	BuAc	4.1	1.06	57	4.4
5	0.50	0.50	**4** [1.3]	BuAc	11	1.12	62	12

a) calculated from formula 4-1.
b) polymerization turned heterogeneous at low conversion.

Low conversion samples exhibited a bimodal molar mass distribution (Figure 4.7). The first and large peak is the starting polyolefin-based RAFT agent (**4**), and the second is the block copolymer, which is of somewhat higher molar mass. The usual explanation for this type of behavior is a low transfer constant to the RAFT agent. It seems unlikely in this case, as this behavior was not observed in experiment 4 with RAFT agent **(1)**, since the electronic structure close to the reactive dithioester moiety of both RAFT agents is similar. A second reason to discount this explanation is the gradual growth of the remaining PEB somewhat later in the polymerization. This would be highly unlikely, for if the rate of the transfer reaction could not compete with the fast propagation, the polydispersity should increase further. It is therefore assumed that local inhomogeneities in the reaction mixture – aggregation of PEB molecules – cause propagating radicals to grow in a microenvironment that has a considerably lower concentration of dithioester groups than expected based on macroscopic calculations. As conversion increases, the production of more block copolymer acts as compatibilizer and makes the reaction mixture more homogeneous. The low molar mass found at higher conversion is presumably the starting polyolefin RAFT agent, suggesting that some of the transfer agent was not consumed.

The final product, a pink powder, has a molar mass close to the predicted value of $1.1 \cdot 10^4 g \cdot mol^{-1}$ and a polydispersity index of 1.12; only marginally increased from the starting value of the Kraton polymer (1.04).

4.3. Conclusions

It has been demonstrated that well-defined and low polydispersity polyolefin block copolymers can be prepared using a macromolecular RAFT agent. In addition to this it has been shown that the copolymerization of styrene and maleic anhydride can be performed under living conditions, something considered imposible until now. The combination of both achievements allowed the preparation of poly[(ethylene-*co*-butylene)-*block*-(styrene-*co*-maleic anhydride)], a polymer that is expected to be useful in coating applications. Furthermore, it was found that the highly colored and labile dithiobenzoate group could be removed from the polymer chain by UV irradiation facilitating a more extended range of polymer architectures, and perhaps future practical applications such as post grafting or crosslinking. Besides, experimental evidence was obtained of intermediate radical termination in support of the postulate describing retardation in section 2.3.

4.4. Experimental

General: The synthesis of 2-cyanoprop-2-yl dithiobenzoate (**1**) and 4-cyano-4-((thiobenzoyl)sulfanyl)pentanoic acid (**2**) are described in sections 3.4.4 (page 80) and 3.4.5 (page 82), respectively. The experimental conditions of the coupling of the latter to Kraton L-1203 (PEB, **3**), forming macromolecular transfer agent (**4**) are outlined in section 3.4.6 on page 83.

Polymerizations: The RAFT agent, monomer and solvent were added together with initiator (AIBN) in a 100 ml three-necked round bottom flask equipped with a magnetic stirrer. Copolymerizations contained an equal molar ratio of styrene and maleic anhydride. The initiator concentration was always one fifth of the RAFT agent concentration. The mixture was degassed using three freeze-evacuate-thaw cycles and polymerized under argon at 60 °C. Periodically samples were taken for analysis.

GPC analyses: GPC analyses of the styrene polymerizations were performed on a Waters system equipped with two PLgel Mixed-C columns, a UV and an RI detector. The analyses of the STY/MAh copolymers were carried out on a HP1090M1 with both UV-DAD and Viscotec RI/DV200 detectors. All molar masses reported in this chapter are polystyrene equivalents, except where stated otherwise.

HPLC analyses: The HPLC analyses were performed using an Alliance Waters 2690 Separation Module. Detection was done using a PL-EMD 960 ELSD detector (Polymer Laboratories) and using a 2487 Waters dual UV detector at wavelengths of 254 and 320nm. All samples were analyzed by injecting 10µl of a dichloromethane (DCM) solution of the dried polymer with a concentration of 5mg/ml. Columns were thermostated at 35°C. The PEB-*block*-PS copolymers were analyzed on a NovaPak® Silica column (Waters, 3.9×150mm) using a gradient going from pure heptane to pure THF in 50min. The system was step by step reset to initial conditions via MeOH, THF and then DCM, after which the column was re-equilibrated in 30 minutes with heptane. PEB-*block*-PS/MAh and PS/MAh copolymers were analyzed on a NovaPak® CN column (Waters, 3.9×150mm) by the application of the following gradient: (heptane:THF+5%v/v acetic acid:MeOH) (100:0:0) to (0:100:0) in 25 minutes, then to (0:0:100) from 25 to 35 minutes. After each run the system was stepwise reset to initial conditions via THF and then DCM, after which the column was re-equilibrated in 30 minutes with heptane. Data were acquired by Millennium 32 3.05 software.

UV irradiation: For UV irradiation of the concentrated block-copolymer solutions (in heptane), a broadband high pressure mercury lamp (Philips) was used with a maximum intensity at a wavelength of 360nm. The spectrum of the emitted light had a significant intensity as low as 290nm. These experiments were carried out at 25°C.

4.5. References

1. Paul Klee from *Paul Klee On Modern Art*, Faber & Faber, **1985** (original edition **1924**)
2. A slightly modified version of this chapter has been appeared elsewhere: De Brouwer, H.; Schellekens, M. A. J.; Klumperman, B.; Monteiro, M. J.; German, A. L. *J. Polym. Sci. Part A: Polym. Chem.* **2000**, *38*, 3596.
3. Riess, G.; Periard, J.; Bonderet, A. Colloidal and Morphological Behavior of Block and Graft Copolymers, Plenum Press, New York, 1971
4. Epstein, B. U.S. Patent 4,174,358 (**1979**) [*Chem. Abstr.* **1977** 86:107481k]
5. Lohse, D.; Datta, S.; Kresge, E.; *Macromolecules* **1991**, *24*, 561
6. Simonazzi, T.; De Nicola, A.; Aglietto, M.; Ruggeri, G. Comprehensive Polymer Science, Pergamon Press, New York, 1992, 1st suppl., chapter 7, p. 133
7. Stehling, U. M.; Malmström, E. E.; Waymouth, R. M.; Hawker, C. J. *Macromolecules* **1998**, *31*, 4396
8. Schellekens, M. A. J.; Klumperman, B. J. *Macromol. Sci. Rev. Macromol. Chem. Phys. C40(2&3)*, 167, **2000**
9. Jancova, K.; Kops, J.; Chen, X.; Batsberg, W. *Macromol. Rapid Commun.* **1999**, *20*, 219
10. Waterson, C.; Haddleton, D. M. *Polymer Preprints* **1999**, *40 (2),* 1045
11. Matyjaszewski, K.; Teodorescu, M.; Miller, P. J.; Peterson, M. L. *J. Polym. Sci. Part A: Polym. Chem.* **2000**, *38*, 2440

12. Patten, T. E.; Matyjaszewski, K. *Advanced Materials* **1998**, *10*, 901
13. Ashford, E. J.; Naldi, V.; O'Dell, R.; Billingham, N. C.; Armes, S. P. *Chem. Commun.* **1999**, 1285
14. Wang, X.-S.; Jackson, R. A.; Armes, S. P. *Macromolecules* **2000**, *33*, 255
15. Heinen, W.; Rosenmöller, C. H.; Wenzel, C. B.; De Groot, H. J. M.; Lugtenburg, J.; Van Duin, M. *Macromolecules* **1996**, *29*, 1151
16. Benoit, D.; Hawker, C. J.; Huang, E. E.;Lin, Z.; Russell, T. P. *Macromolecules* **2000**, *33*, 1505
17. Chen, G.-Q.; Wu, Z.-Q.; Wu, J.-R.; Li, Z.-C.; Li, F.-M. *Macromolecules* **2000**, *33*, 232
18. Benoit, D.; Harth, E.; Fox, P.; Waymouth, R. M.; Hawker, C. J. *Macromolecules* **2000**, *33*, 363
19. Benoit, D.; Chaplinski, V.; Braslau, R.; Hawker, C. J. *J. Am. Chem. Soc.* **1999**, *121*, 3904.
20. Park, E.-S.; Kim, M.-N.; Lee, I.-M.; Lee, H. S.; Yoon, J.-S. *J. Polym. Sci. Part A: Polym. Chem.* **2000**, *38*, 2239.
21. Le, T.; Moad, G.; Rizzardo, E.; Thang, S. H. Patent WO 98/01478 (1998) [*Chem. Abstr.* **1998**, *128*:115390]
22. Chiefari, J.; Chong, Y. K.; Ercole, F.; Krstina, J.; Jeffery, J.; Le, T. P. T.; Mayadunne, R. T. A.; Meijs, G. F.; Moad, C. L.; Moad, G.; Thang, S. H. *Macromolecules* **1998**, *31*, 5559
23. Chong, Y. K.; Le, T. P. T.; Moad, G.; Rizzardo, E.; Thang, S. H. *Macromolecules* **1999**, *32*, 2071
24. Hamley, I. W. The Physics of Block Copolymers, Oxford University Press, 1998, p.1-8
25. Goodman, I. *Developments in Block Copolymers – 2* Elsevier Applied Science Publishers Ltd., London, **1985**
26. Riess, G.; Hurtrez, G.; Bahadur, P. *Encyclopedia of Polymer Science and Engineering – 2*; Mark, H. F., Kroschwitz, J. I., Eds.; Wiley, New York, **1985**
27. Gaillard, P.; Ossenbach-Sauter, M., Riess, G. In *Polymer Compatibility and Incompatibility, Vol. 2*; Solc, K., Ed.; Harwood Academic Publishers: New York, **1982**, p 289
28. Duivenvoorde, F. L., Van Es, J. J. G. S., Van Nostrum, C. F., Van der Linde, R. *Macromol. Chem. Phys.* **2000**, *201*, 656
29. Bouix, M., Gouzi, J., Charleux, B.; Vairon, J.-P., Guinot, P. *Macromol. Rapid Commun.* **1998**, *19*, 209
30. Trivedi, B.C.; Culbertson, B.M. *Maleic anhydride*, Plenum Press, **1982**
31. Lin, C.-W.; Lee, W.-L. *J. Appl. Polym. Sci.* **1998**, *70*, 383
32. Stolyhwo, A.; Colin, H.; Guiochon, G. *J. Chromatogr.* **1983**, *265*, 1
33. Trathnigg, B., Kollroser, M., Berek, D., Nguyen, S. H., Hunkeler, D. *ACS Symp. Ser.* **1999**, *731*, 95
34. Sanayei, R. A.; O' Driscoll, K. F.; Klumperman, B. *Macromolecules* **1994**, *27*, 5577

» more and more of our experience...
becomes invention rather than discovery «[1]

5. Living Radical Polymerization in Emulsion using RAFT.

Synopsis: This chapter describes the application of Reversible Addition–Fragmentation Transfer (RAFT) in emulsion polymerization. A brief introduction to emulsion polymerization is given, followed by the application of living radical techniques in this heterogeneous medium, which is discussed on a theoretical level with references to the literature. Seeded emulsion polymerizations of styrene in the presence of two RAFT agents are then investigated. It is found that the polymerizations are significantly retarded by the presence of RAFT agent and it is proposed that exit from the particles after fragmentation was the main cause of retardation. The development of the molar mass distribution and the polydispersity deviate from the ideal 'living' behavior, found in homogeneous systems. Slow, continuous transportation of RAFT agent into the particles is postulated as a possible cause for this phenomenon. Besides, colloidal stability was found to be poor and irreproducable. The use of nonionic surfactants was found to improve the stability. Ab initio emulsion polymerizations are conducted as well, with the aim of exploring the effect of RAFT on the nucleation process. The reaction kinetics were distinctly different from those in conventional emulsion polymerization, indicated by the absence of an Interval II with constant polymerization rate.

5.1. Emulsion Polymerization

5.1.1. Introduction

A new challenge confronting living radical polymerization is its application in dispersed (*i.e.* heterogeneous) media. Water-borne polymerizations are an industrially preferred way to conduct radical polymerizations as they eliminate the need for organic solvents,[2] provide a good medium to remove the heat of reaction and guarantee a product (*i.e.* latex) that has a relatively low viscosity and is easy to

handle. Emulsion systems are relatively cheap and robust, with low sensitivity to impurities. The polymerization results in a relatively low viscosity latex that has a high solids content. Because of these advantages, emulsion polymerization has developed into an economically important process, responsible for effecting 40–50% of free-radical polymerizations. These, in turn, constitute approximately 30% of the total worldwide production of polymers. Some of the products made by emulsion polymerization are commodity materials such as artificial rubber and latex paints, while other products are high value-added, such as for diagnostic kits in biomedical applications. There are thus considerable incentives for the understanding of emulsion polymerization processes as well as the ability to control the micro- and macrostructure of polymers for the development of better products. If living radical polymerizations could be conducted in such systems, the range of possible industrial applications and products will be greatly enhanced through intelligent design of the polymer architecture.

The advances and developments made in the field of emulsion polymerization concerning kinetics and thermodynamics to derive the mechanism, have been documented by Gilbert.[2] The fundamental mechanisms of the polymerization process dictate what the properties of the polymer and latex will be, given particular operating conditions (*e.g.* choice of monomer, temperature, surfactant, transfer agent, feed profile). These properties of the polymer and of the latex govern the properties that are important to the customer, albeit frequently in a complex way.

5.1.2. A Qualitative Description

Without completely repeating here the classical descriptions of the emulsion polymerization mechanism that are available in numerous text books,[2,3] the key features that will be important in the discussion of living radical emulsion polymerization will be briefly reviewed. Traditionally, emulsion polymerizations are considered to be a three-stage process, as shown in Scheme 5.1.[4]

The reaction starts in *Interval I* from a mixture of water, monomer(s), surfactant and initiator. The water soluble initiator is dissolved in the continues water phase. The monomer is emulsified by agitation. A small quantity of monomer dissolves in the water phase, while most of it is present in the form of droplets ($d > 1\,\mu m$), stabilized by surfactant. The remainder of the surfactant is dissolved in the aqueous phase at a concentration above the critical micelle concentration (CMC) such that a large number of micellar aggregates ($d \approx 5\,nm$) is present. Hydro-

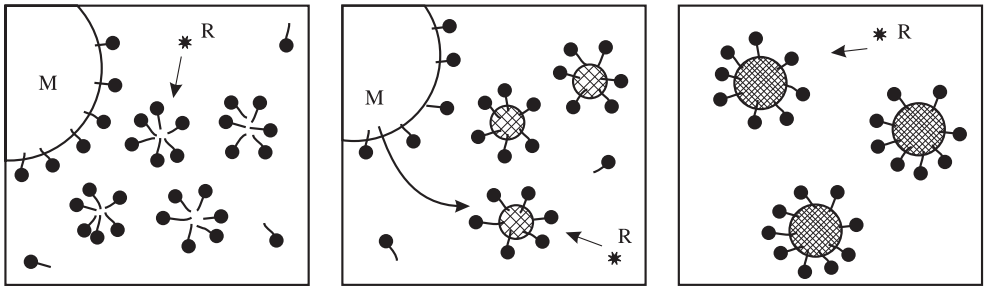

Interval I Interval II Interval III

Scheme 5.1. Classical three-stage concept for the emulsion polymerization process.[4] Interval I is characterized by the presence of large monomer droplets and small micelles. Radicals generated in the water phase enter the micelles and continue to polymerize, thereby attracting monomer from the droplets. Interval II: The particle formation is over and the micelles have disappeared either because they have been converted to polymer particles or because the surfactant has moved to the increasing particle–water interphase. Interval III: polymerization in the particles has proceeded to such an extent that all monomer droplets have vanished. The remaining monomer resides in the particles.

philic radicals, generated by dissociation of the initiator, are formed in the water phase. These radicals react with monomer dissolved in the water phase, so oligomers are formed. Provided that no termination takes place, monomer units are added until a critical chain length, z, is reached where the oligomer becomes surface active. At this point, the oligomeric radical will enter a micelle, swollen with monomer. Droplet entry can be neglected as the total surface area of the droplets phase is several orders of magnitude smaller than that of the micelles. The radical will continue to grow, thereby consuming monomer which is replenished by diffusion from the droplets, through the water, into the growing particle.

For small particles (<100 nm, depending on the monomer used), the zero–one assumption is used, meaning that any polymer particle contains either none or just a single growing radical. If a radical enters a particle that already contains another growing radical, instantanious termination will take place due to the extremely high, local concentration of radicals. This again reduces the number of radicals to zero, resulting in an *on–off* mechanism for any given polymer particle. Throughout Interval I, new particles are generated from micelles, increasing the number of polymerization *loci* and the polymerization rate. The polymer particles continue to grow and absorb an increasing amount of surfactant on their interface. This causes part of the micelles to dissolve. As this process proceeds, a point will be reached where all micelles have disappeared. Formation of new particles ceases. This point corresponds to the onset of Interval II and typically corresponds with a monomer conversion of 5–15 %, depending on the actual recipe.

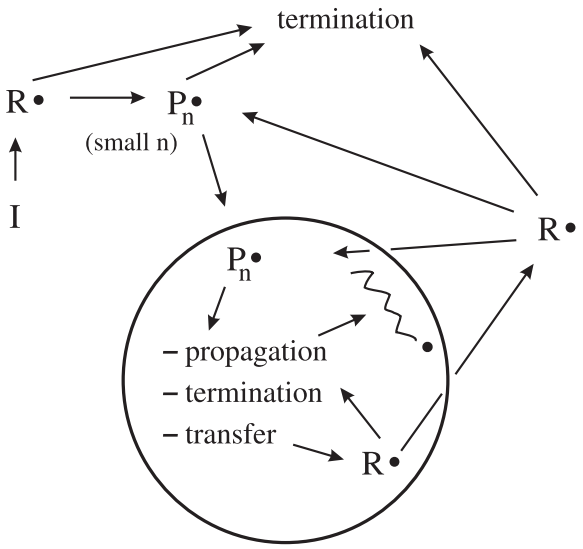

Scheme 5.2. Several kinetic events occurring during emulsion polymerization. Initiator derived radicals (R•) propagate in the water phase to form short oligomeric radicals (P_n•) that can undergo termination or enter a particle. Upon entry, the radical will either terminate an already existing radical or propagate until termination or transfer occurs. Short transfer derived radicals can propagate or exit the particle leading to a large variety of possible fates, among which propagation, re-entry and termination are the most prominent.

Interval II is characterized by a constant number of particles and the presence of monomer droplets. The concentration of monomer at the locus of polymerization, *i.e.* inside the particles, remains roughly constant as the monomer droplets are able to supply the particles with monomer at the same rate at which it is consumed. The constant number of particles together with the relatively constant monomer concentration inside them cause the polymerization rate to be constant as well.

Interval III starts when the monomer droplets have disappeared completely. This point corresponds to a monomer conversion of 50 to 80%, depending on the recipe. The remaining monomer resides in the particles and polymerization continues, but at an ever decreasing rate as the monomer concentration gradually decreases.

Scheme 5.2 illustrates the kinetic events occurring in an emulsion polymerization and shows how these events are associated with chain growth. Entry and exit, processes of phase transfer, strongly depend on the partitioning of the radicals. For a specific monomer, this is governed largely by their water solubility. A radical, generated in the water phase, will either propagate or terminate. If the radical reaches its critical chain length, z, it will become surface active and enter a particle. Droplet entry is unimportant due to the comparatively small surface area of this phase compared with that of the micelles (Interval I) and particles (Interval II). This critical chain length, z, depends on the type of monomer and the oligomer end-group, but is in the order of 2–5 for common monomers like styrene and methyl methacrylate in polymerizations using a persulfate initiator.[5] Once such a z-mer

radical has entered a particle it is assumed not to desorb anymore, but rather to react inside the entered particle. If another radical was already present within this particle, it will be terminated (assuming again zero–one kinetics). Otherwise, the incoming radical will continue growing until it is terminated by a second incoming radical or until transfer takes place to either the monomer or a transfer agent. The short radical that is formed can reinitiate polymerization or exit into the water phase where it can terminate, propagate or re-enter a particle. Its fate depends on its partitioning and the concentration of monomer and radicals in the water phase. In general, exit events reduce the polymerization rate. The large number of variables, conditions, concentrations and types of ingredients indicate that emulsion polymerization is a remarkably complex system based on a mechanism of interrelated kinetic and thermodynamic events.

5.1.3. Living Radical Polymerization in Emulsion

The desire to conduct living radical polymerizations in emulsion is not only based on the preferential use of existing processes and technology but there are advantages intrinsic to the heterogeneous system as well. From the outlook of living radical polymerization, a adventageous effect is to be expected from the reaction in a compartimentalized system. The quality of all living radical processes is influenced by the amount of bimolecular radical termination. In atom transfer radical polymerization (ATRP) and nitroxide mediated polymerization (NMP), equilibria are designed to yield a low radical concentration and in systems based on reversible transfer, initiator is used in a small amount to retain the living character of the polymerization. For this reason, application in bulk and solution is limited by the low rates of polymerization (see the remarks made at the end of section 2.1.2 on page 34).

Emulsion polymerization provides an ideal alternative to overcome this problem. High rates with little termination are found in emulsions due to the compartmentalization of the radicals in individual particles, in which radicals in one particle have no access or contact with radicals in another. High rates are achieved by controlling the number of particles by choice of surfactant and initiator concentrations. In conventional emulsion polymerization, very high molar masses are found,[6] showing that bimolecular termination is not prevalent and thus the main chain stopping events are primarily through transfer to monomer.

One of the key factors for a successful living radical emulsion polymerization is to get the deactivator at the locus of polymerization and to keep it there. Another qualifying factor is the undisturbed occurrence of Interval I, when particles are generated. During this stage, a relatively high radical production rate is desired in order to create a large number of particles, as growth of existing particles competes with the generation of new ones for the surfactant. This clearly conflicts with the desire for a low concentration of active species or radicals that prevails amongst the living polymerization techniques. Furthermore, chain growth in the water phase should not be hindered extensively, as this will prevent the growing radicals reaching their critical chain length required for entry. Despite their similarities in approach, some crucial differences exist between the application of living polymerizations based on reversible termination (section 2.1.1) and those based on reversible transfer (section 2.1.2).

Reversible Termination

The typical approach that is taken in the living radical schemes that rely on reversible termination (NMP and ATRP), is to start with a certain amount of low molar mass, dormant species from which radicals are generated (one starts on the left hand side of the equilibria in Schemes 2.4 and 2.5). In this case, the generation of active radicals and persistent radicals is balanced. The activation–deactivation equilibrium is however designed to yield a low concentration of radicals and therefore results in a slow nucleation process during Interval I, which is known to lead to a very broad particle size distribution in the final dispersion.[7] The initiator should generate radicals in the water phase in order to prevent droplet nucleation, which would cause the system to behave like a miniemulsion polymerization (see Scheme 6.1, page 140). The partitioning of the deactivator should find a suitable balance between the water and organic phases such that water phase radicals have a chance to grow and enter while still allowing rapid transportation of the deactivator from the droplets to the polymerization loci in order to prevent uncontrolled polymerization. Alternatively, one can start on the right hand side of these equilibria using a conventional initiator combined with nitroxide (Scheme 2.4, page 23) or the metal complex in its higher oxidation state (Scheme 2.5, page 24). This *reverse* approach has the advantage that the conventional initiator can provide the desired nucleation, but requires a carefully balanced quantity with respect to the deactivating species. Water phase propagation should not be hindered by reversible deactivation as in this case, entry will be postponed as the chains will not be able to reach their critical chain length for entry.

Notwithstanding these theoretical issues, conventional[8,9] and reverse[10,11] ATRP have been used to obtain polymer dispersions once practical problems, like the hydrolysis of initiator,[13] were overcome. The drastic change in kinetics interferes with the conventional nucleation mechanism causing a relatively broad particle size distribution with sometimes visually observable particles. The colloidal stability is difficult to reproduce, resulting in the appearance of a distinct organic phase[8] during the reaction, massive coagulation or sedimentation of polymer.[13] When all reaction components are designed to be located at the locus of polymerization, polymer of predetermined molar mass is obtained and polydispersities are fairly low. An unlucky choice of ligand or initiator will cause the polymerization to be inhibited or to proceed uncontrolled.[12,13]

Nitroxide mediated emulsion polymerizations have been restricted to styrene and confined to high temperatures (above the normal boiling point of water, under high pressure) calling for special equipment and causing coagulation during the reaction in both *ab initio*[14] and seeded[15] reactions. The polymerizations are extremely slow and polydispersities (1.4–2.0) cannot match the low values obtained in homogeneous systems.

Reversible Transfer

Living radical polymerizations based on reversible transfer are potentially more convenient because they, in principle, do not change the reaction rate. Additionally, once the initial transfer agent has been consumed, the transfer activity resides completely in polymeric species. The transfer event that occurs between active and dormant polymers (**b**, Scheme 2.8, page 27) will not give rise to small radicals that are subject to exit events. When this situation is attained, polymerization rate and phase transfer events in the polymerization will not be different from a conventional emulsion polymerization without transfer agent. Up to this point, the reaction will largely resemble an emulsion polymerization with a conventional transfer agent. Such systems are thoroughly investigated as in the majority of industrial emulsion polymerization recipes, chain transfer agents are used to limit the molar mass of the product. Three aspects are of importance when considering the use of large quantities of RAFT agent.

First, the concentration of transfer agent in the water phase should be relatively low. Deactivation of chains that propagate in this medium is undesired as it will give rise to large amounts of water soluble oligomers and, depending on the partitioning of the radical that is formed, preventing entry and thereby lowering the polymerization rate or hampering nucleation.

A second consideration concerns transport phenomena. An important prerequisite for living emulsion polymerization is that all chains grow for an equal period of time. This requires a rapid reaction of the transfer agent or dormant species at the locus of polymerization in the early stages of the reaction. This may prove to be a problem in RAFT polymerizations as transportation of highly reactive transfer agents with a poor water solubility is under diffusion limitation. This has, for instance, been documented for the seeded emulsion polymerization of styrene in the presence of *n*-dodecyl mercaptane,[16,17] as well as in *ab initio* reactions.[18] The transfer constant of the mercaptane is approximately 15 for similar reactions in homogeneous media.[19] When the seeded system contains a large number of small particles, the transfer agent is consumed at roughly 50% monomer conversion. This is virtually identical to a similar experiment conducted in bulk.[20] When the seed material consisted of a much smaller number of larger particles, the transfer agent was found to last longer, up to 80% conversion.[16] This is attributed to the change in surface area of the droplet and particle phases and not as much to the different kinetics of the two systems (zero–one *vs.* pseudo-bulk). The phase transfer events apparently form the rate determining step in the diffusion process. The most important transport barrier was found to be the phase transfer from the monomer droplets into the water phase.[16] The RAFT agents used in this work have even higher transfer constants.[21,22] In a homogeneous medium, they are typically consumed within the first 10% of conversion and thereby lay a serious demand on their transportation rate. Therefore, a well-dispersed system with a large droplet–water interface is essential.

A third important aspect of the RAFT process in emulsion that needs to be considered is the effect of exit of the transfer species **R** (Scheme 5.3) on the rate and control of molar mass. Whang *et al.*[23] found that the addition of the transfer agent, CBr_4, in seeded emulsion polymerization significantly retarded the rate of polymerization. In a more complete study of the kinetics[24] (using gamma relaxation) of transfer for CBr_4 and CCl_4 they found that exit of the incipient transferred radical from the particles was the main source of retardation. The fate of these radicals[25,26,27] depended on the radical concentration in the aqueous phase (Scheme

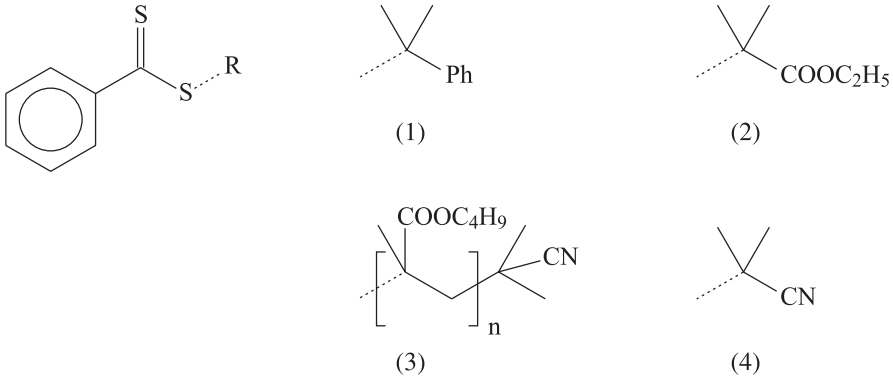

Scheme 5.3. RAFT agents applied in emulsion polymerizations. 2-phenylprop-2-yl dithiobenzoate or Cumyl-RAFT where **R** is **1**, 2-(ethoxycarbonyl)prop-2-yl dithiobenzoate or EMA-RAFT, in which **R** is **2** and 2-cyanoprop-2-yl dithiobenzoate or Cyano-RAFT with **R** equal to **3**, are all known to allow the living radical polymerization of styrene in homogeneous systems. For the application in heterogeneous systems, their partitioning and that of the expelled radicals, **R**, over the different phases is of importance as well. Radical **1** is the cumyl radical $\bullet C(CH_3)_2C_6H_5$ and **2** the ethyl methacrylate radical $\bullet C(CH_3)_2COOC_2H_5$. Refer to Scheme 2.8 on page 27 for the details of the addition–fragmentation equilibrium. RAFT agents in which **R** is**3** and **4** are used in ab initio polymerizations.

5.2). Cross-termination of the exited radical occurred primarily with ① radicals in the aqueous phase when the radical concentration was high and ② radicals in the particles via re-entry when the radical concentrationin the aqueous phase was low. The results also supported, that exit is diffusion controlled during Interval II. The size of the particles, the diffusion coefficient and the partition coefficient of the exited free radical in the water phase determine the value of the exit rate coefficient.[28]

The heterogeneity of emulsion polymerizations and the kinetic effects of transfer agents result in a mechanism of a complex network of fundamental reaction steps.[2] The work described so far in the literature with reversible transfer is largely focused at low reactivity reagents. Xanthates were used to prepare homopolymers,[29] block copolymer structures[30] and also to increase the number of particles.[31] When the monomer was fed slowly to the system and instantaneous conversions were high, a linear increase of the molar mass with conversion was observed.[29] In batch reactions, the xanthate system is similar to a reaction with a conventional transfer agent.[31] Experiments with seeded systems demonstrated that these agents strongly increase the exit rate and that, for an unclarified reason, the entry efficiency is reduced.[32] The combination of effects results in a much lower polymerization rate.

Reports on emulsion polymerizations with highly reactive RAFT agents are scarce. Butyl methacrylate has been polymerized in semi-batch emulsion polymerizations, using rather unusual feed conditions.[33] This is presumably to have all the RAFT agent reacted inside the particles at the beginning of the reaction. Beside homopolymers, block copolymers have been made consisting of a polystyrene part and a polymethyl or butyl methacrylate part.[34] Straightforward batch polymerizations have not been reported and, for unknown reasons, RAFT agents of moderate activity performed better than high reactivity reagents.[21] The emulsion stability was not addressed and particle sizes were not given. Uzulina *et al.*[35,36] found that living characteristics were observed but with up to 40% coagulation. They had more success with a hydrophilic transfer agent although only in combination with styrene. The use of methacrylates yielded high polydispersities.

5.1.4. Research Target

Obviously, the use of these reagents is not as straightforward as might be expected. It is the aim of this work to gain insights into the mechanisms operating for the RAFT process in the presence of droplets. Seeded systems are extremely useful for this purpose, since they eliminate many variables and can explore the effects of exit and droplets on the rate and control of molar mass in RAFT systems. Two RAFT agents with comparably high $C_{T,\,RAFT}$ were used in this study (see Scheme 5.3) each having a different leaving group **R**. *Ab initio* experiments were conducted to investigate the effect of RAFT agent on the nucleation process.

Table 5.1: Probability of escape, P(exit), Determined for RAFT agents with Cumyl and EMA Leaving groups.

	Cumyl	EMA
k_p^1 ($dm^3 \cdot mol^{-1} \cdot s^{-1}$) [a]	1705	9390
k_{dm} (s^{-1}) [b]	$3.98 \cdot 10^3$	$6.89 \cdot 10^4$
$P(exit)$	0.29	0.56

a) k_p^1 was determined for **1** by $\langle k_p \rangle_{STY}$ [37] by being multiplied by 5 (reasonable for small radical reactions); for **2**, $\langle k_p \rangle_{EMA}$ [38] was multiplied by 5 and also by 2 to compensate for the reactivity ratio of EMA to STY.[39]
b) The unswollen radius was 20 nm, which gave a swollen radius of 29.5 nm.

5.2. Seeded Emulsion Polymerizations[40]

5.2.1. Background Theory

Probability of Exit for R

Exit events can reduce the reaction rate significantly.[24] The more water soluble the leaving group (**R**) the greater the extent of exit.[41] The leaving radicals from Cumyl-RAFT and EMA-RAFT are the cumyl radical (**1**) and 2-(ethoxycarbonyl)prop-2-yl radical (**2**), respectively. The coefficient for desorption of a monomeric free radical (exit) from a particle with swollen radius r_s is given by Eq. 5-1:[28]

$$k_{dM} = \frac{3D_{R,w}}{r_s^2} \cdot \frac{[R]_w}{[R]_p} \qquad \textbf{(5-1)}$$

The probability of exit can then be determined by using Eq. 5-2:

$$P(exit) = \frac{k_{dM}}{k_{dM} + k_p^1 \cdot [R]_p} \qquad \textbf{(5-2)}$$

where $D_{R,w}$ is the diffusion coefficient of **R** in water, $[R]_p$ and $[R]_w$ are the concentrations of **R** in the aqueous phase and particle, respectively, and k_p^1 is the propagation rate coefficient for **R** to monomer. Using the approximation that $D_{R,w}$ is $1.6 \cdot 10^{-9}$ $m^2 \cdot s^{-1}$ for the two radicals and $[R]_w$ is similar to the monomer equivalent, $P(exit)$ was determined (see Table 5.1). It can be seen that **2** has a far greater probability of escape than **1**. This suggests that retardation should only be effective when RAFT agent is present in the system. Assuming a high value for $C_{T,RAFT}$ (found experimentally to be approximately 6000 for polymeric RAFT agents derived from the dithiobenzoate moiety[22]), all RAFT agent should be consumed in the first few percent of monomer conversion (see Eq. 5-5). After this transformation, exit should no longer be the dominant retardation mechanism.

Molar masses and Polydispersities in RAFT Systems

The equations used to predict the molar mass and polydispersity (PD) of polymer produced by the RAFT method in bulk or solution are those derived by Müller *et al.*[42] for living processes involving active and dormant species. The

equations are obtained via the method of moments.[43] For values of $C_{T,RAFT}$ much greater than one, the $\overline{M}_n$ and PD can be closely approximated by the following expressions:

$$\overline{M}_{n,th} = \gamma \cdot x \cdot FW_{mon} \qquad \textbf{(5-3)}$$

$$PD = \frac{1}{\gamma \cdot x} + \frac{1}{x}\left[2 + \frac{\beta - 1}{\alpha - \beta}(2 - x)\right] - \frac{2\alpha(1-\alpha)}{(\beta^2 - \alpha^2)x^2}[1 - (1-x)^{1+\beta/\alpha}] \qquad \textbf{(5-4)}$$

where γ is $[M]_0/[RAFT]_0$, FW_{mon} is molar mass of monomer, x is the fractional conversion, α is $[P_n]/[RAFT]$ and β is $C_{T,RAFT}$. The concentration of RAFT as a function of conversion is given by:

$$[RAFT]_x = (1-\alpha) \cdot [RAFT]_0 \cdot (1-x)^{\beta} \qquad \textbf{(5-5)}$$

The assumptions made in these expressions are that the steady-state radical concentration ($[P_n]$) is very low, the efficiency of the RAFT agent is 100% and bimolecular termination events are negligible. For equations 5-3 to 5-5 to be valid for a seeded emulsion polymerization, the RAFT agent must be transported from the droplets to the particles at the rate of transfer during Interval II.

5.2.2. Experimental Design

Design of the Seed Latex

The design of the seed is crucial for understanding the events that control the molar mass distribution. The size of the seed particles must be as small as possible to explore the effects of exit, since exit is inversely proportional to the particle radius squared (see Eq. 5-1).[41,44] However, the seed must have a minimum size, otherwise the concentration of monomer will change drastically during particle growth. This, to a good approximation, is determined by the Morton equation[45,46] and shows that for particles with unswollen radius greater than $\approx 20-30$ nm the monomer concentration inside the particle remains relatively constant during Interval II. Therefore, the unswollen seed radius for these styrene polymerizations was chosen to be approximately 20 nm.

In addition, a hetero-seed, consisting of polymethyl methacrylate (PMMA), was used so that the molar mass distribution (MMD) of polystyrene (PS) could be observed exclusively, by UV detection (λ=254 nm) since PMMA has no UV

absorption at this wavelength. For the purpose of these experiments, polymer immiscibility was neglected. This assumption seems valid due to the presence of monomer (which acts as a plasticizer), the very small size of the seed, and the low molar mass polymer being produced. Another important design parameter is the number of particles, which must be high in order to avoid secondary nucleation.[47] Therefore, N_c, the number of particles per unit volume of water, chosen for this work was approximately $4 \cdot 10^{17}\,\mathrm{dm}^{-3}$.

Polymerizations in Seeded Systems

The experimental conditions were chosen so that the changeover from Interval II to III occurred close to 10% conversion. This still gives us information on the influence of droplets, and its effect on the MMD. In addition, the effects of exit and transportation of RAFT on the rate up to the changeover can be studied.

Deviations from Zero–One Conditions

Zero–one conditions are obeyed when the size of the seed is sufficiently small such that entry of a z-mer[5] radical (*i.e.* $^{-}SO_4(STY)_z\cdot$) into a particle already containing a growing chain results in instantaneous termination. The criteria for zero–one conditions have been described by Maeder and Gilbert.[48] In simple terms, it depends upon the probability of termination upon entry of a small radical to that of propagation to form polymer.

Based on the mechanism of the RAFT process, the system may not obey the zero–one condition. For example, if entry of a z-mer should react first with a dormant species, then a long polymeric radical (active species) is formed. This can either react with monomer or terminate with the already growing chain. The chances of long–long chain termination are highly unlikely, and so the probability of bimolecular termination is reduced significantly. This means that two or more radicals can reside in the same particle. In the presence of RAFT, the probability of termination was calculated using Eq. 5-6, where the same values as Maeder and Gilbert[48] were used. The results that follow are based on the seeded system starting in Interval II:

$$P(termination)_z = \frac{k_t^{zL}/(N_A V_s)}{k_t^{zL}/(N_A V_s) + k_p C_p + k_{tr,RAFT}[RAFT]_P} \qquad \textbf{(5-6)}$$

In this formula, k_t^{zL} is the termination rate constant of a z-mer and a long chain radical, N_A is Avogadro's number, V_s is the particle volume, k_p the propagation rate coefficient and $k_{tr,\,RAFT}$ the transfer rate coefficient. The concentrations of dormant species inside the particles, $[RAFT]_P$, used were $1.5{\cdot}10^{-3}$ and $10.5{\cdot}10^{-3}$ mol·dm^{-3}, which are the lowest and highest RAFT agent concentrations applied in this study. The value $z = 3$ was used for styrene[2,44,5] and an unswollen radius of 20 nm.

The probability of termination without RAFT was found to be 0.82, but this probability will rapidly increase to unity as the chain grows. Addition of RAFT decreased the probability to 0.65 and 0.28 for $[RAFT]_P$ of $1.5{\cdot}10^{-3}$ and $10.5{\cdot}10^{-3}$ mol·dm^{-3}, respectively. The results clearly show that zero–one conditions may not hold when high concentrations of RAFT are used. However, it should be noted that the chain length of the dormant and active species is a function of both RAFT agent concentration and conversion according to Eq. 5-3. Consequently, the long–long termination assumption used may not be valid up to conversions of approximately 10%. Nevertheless, this shows that the RAFT system can deviate from zero–one conditions by simply increasing the amount of dormant species (or initial RAFT agent).

5.2.3. Results and Discussion

The concentration of monomer and RAFT agent in the separate monomer phase after creaming was determined by UV absorption spectroscopy. Table 5.2 shows the saturation concentration of monomer in the presence of the RAFT agents. The $[STY]_p^{sat}$ of styrene in the PMMA seed was 5.61 mol·dm^{-3}, which remained roughly constant when Cumyl-RAFT was added to the monomer but increased to 5.97 mol·dm^{-3} for EMA-RAFT. It can also be seen that the concentration of Cumyl-RAFT in the particles is much less than EMA-RAFT. Water solubilities, $[RAFT]_w^{sat}$, of both RAFT agents are in the region of 10^{-4} to 10^{-5} mol·dm^{-3}, which is much lower than $[STY]_w$ ($5{\cdot}10^{-3}$ mol·dm^{-3} at 50 °C).[49]

Seeded emulsion polymerizations of styrene were carried out at 60 °C in an argon atmosphere. The KPS and RAFT concentrations used are given in Tables 5.3 and 5.4 (pages 120 and 121). In all polymerizations, the appearance of the emulsion at the beginning of the reaction was a lighter shade of pink due to the red color of the RAFT agents. In the course of polymerization, a conspicuous red layer on top of the emulsion (when agitation was briefly ceased) was then observed. It was found

Table 5.2: Saturation Concentrations of Monomer in PMMA Seed at 60 °C in the Presence of RAFT Agent and the Concentration of RAFT Agent in the Monomer Layer and in the Particles.

	Control ($mol \cdot dm^{-3}$)	Cumyl-RAFT ($mol \cdot dm^{-3}$)	EMA-RAFT ($mol \cdot dm^{-3}$)
$[STY]_w^{sat}$	5.61	5.54	5.97
[RAFT] in styrene before swelling		$2.33 \cdot 10^{-2}$	$2.33 \cdot 10^{-2}$
[RAFT] in styrene after swelling		$2.74 \cdot 10^{-2}$	$3.01 \cdot 10^{-3}$
[RAFT] in the particle		$9.08 \cdot 10^{-4}$	$1.63 \cdot 10^{-3}$

that the appearance of the red layer occurred shortly after the commencement of polymerization. At conversions of approximately 10 %, which for these systems is the changeover from Interval II to III, a red coagulum was formed. NMR and GPC analysis of the red coagulum showed low molar mass polystyrene (M_p=2100 $g \cdot mol^{-1}$) without the presence of the initial RAFT agent.

The formation of this red layer is still unclear. One could be led to believe that transportation of the RAFT agents into the particle is slow on the polymerization time-scale. The rate of transportation can be calculated from Eq. 5-7, which is derived from Smoluchowski's equation:

$$\text{Rate of transportation} = 4\pi D_{RAFT,w} r N_A [RAFT]_w \qquad \textbf{(5-7)}$$

Using a diffusion coefficient, $D_{RAFT,w}$, similar to that of two styrene chain units,[2,50] the rate of transportation is approximately $10^6 s^{-1}$. This value is much larger than the rate of propagation, and on the time-scale of the reaction, diffusion should not be a factor. Therefore, the red layer seems to be more likely due to low molar mass dormant species swollen with monomer. The diffusion[16,17,51] of these species is extremely slow on the reaction time-scale, and therefore, transportation into the particles is slow. Once the changeover from Interval II to III has occurred, these dormant species coalesce to form the red coagulum, which is not in the emulsion samples analyzed with GPC.

The conversion profiles of these seeded experiments at different KPS and Cumyl-RAFT concentrations are given in Figures 5.1 and 5.2. The starting time was taken when KPS is added to the reaction mixture. At a high KPS concentration (Figure 5.1), the rate decreased as the RAFT concentration was increased. Similarly at low KPS (Figure 5.2) the trend is repeated but the retardation in rate is less drastic. In the case of EMA-RAFT, at a high KPS concentration (Figure 5.3) the

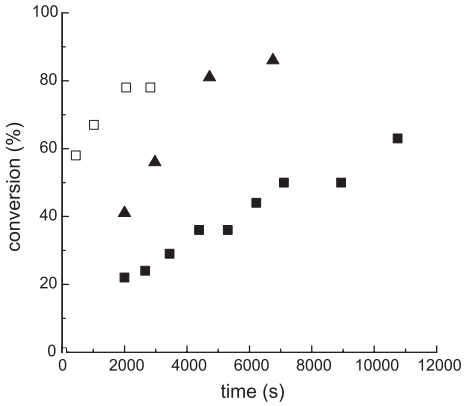

Figure 5.1. Conversion profiles of styrene in the presence of Cumyl-RAFT (**1**) at a high KPS concentration ($1{\cdot}10^{-3}$ mol·dm^{-3}) at 60°C. Control experiment (□); Low Cumyl (▲, exp. 2); High Cumyl (■, exp. 1).

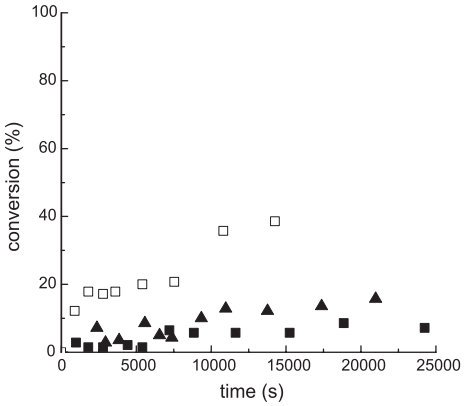

Figure 5.2. Conversion profiles of styrene in the presence of Cumyl-RAFT (**1**) at a low KPS concentration ($1{\cdot}10^{-4}$ mol·dm^{-3}) at 60°C. Control experiment (□); Low Cumyl (▲, exp. 4); High Cumyl (■, exp. 3).

rate also decreased as a function of EMA-RAFT concentration. Therefore, a very high KPS concentration (5 times higher) was required to gain similar rates to that of the control experiment (*i.e.* without RAFT agent). At low KPS concentration a conversion of about 20% was reached similar to the control experiment. A comparison of the conversion profiles between the Cumyl-RAFT and EMA-RAFT agents at high KPS concentration are given in Figure 5.4. It can clearly be seen that the retardation effect was more predominant for the EMA-RAFT compared to the Cumyl-RAFT polymerizations.

Retardation using RAFT agents has been observed in bulk and solution experiments (see *e.g.* section 2.3 and ref. 21). The possible explanations given (see page 43) do not explain the difference in rates between the Cumyl- and EMA-RAFT agents, since the free-radical chemistry will be identical, once the initial RAFT agent has been consumed. Therefore, it is believed that the main retardation effect for the two RAFT agents used in these emulsion systems is due to the higher exit rate of **2** compared to **1** from the particles (see section 5.2.1), in line with what Lichti *et al.*[24] found for normal transfer agents. This also suggests that the destabilization of the emulsion by the RAFT caused a slow rate of transportation of RAFT into the particles by possibly substantially decreasing the surface area of the droplets (producing an organic layer on top of the reaction mixture). At a high KPS

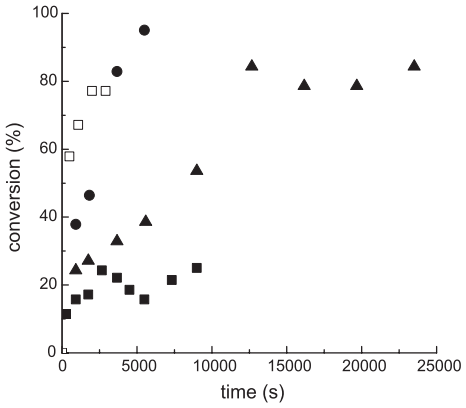

Figure 5.3. Conversion profiles of styrene in the presence of EMA-RAFT (**2**) at a high KPS concentration ($1{\cdot}10^{-3}$ mol·dm^{-3}) at 60°C. Control experiment (□); Low EMA (▲, exp. 7); High EMA (■, exp. 6); Very High KPS & High EMA (●, exp. 5).

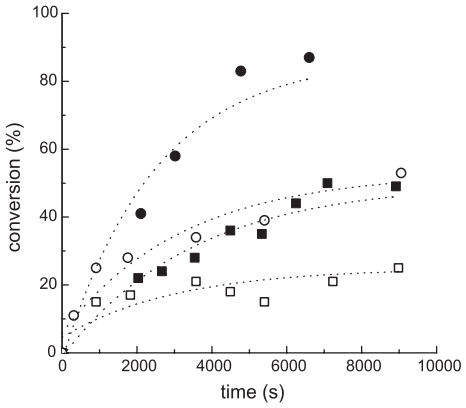

Figure 5.4. Comparison of conversion profiles between Cumyl-RAFT (**1**) and EMA-RAFT (**2**) agents at high KPS concentration ($1{\cdot}10^{-3}$ mol·dm^{-3}) at 60°C. The dashed lines are a guide for the eye. Low Cumyl (●, exp. 2); Low EMA (■, exp. 7); High Cumyl (○, exp. 1); High EMA (□, exp. 6).

concentration, the most probable cause of termination of **R** is with radicals in the aqueous phase. Whereas at low KPS concentrations, termination between re-entry of **R** into particle with a growing chain is the most probable process.

It should be noted, however, that retardation is effective during Interval II and III. A possible reason, despite the fact that droplets are no longer present in Interval III, is further transportation of RAFT agent into the particles from the water phase.

The influence of both Cumyl-RAFT and KPS on the evolution of $\overline{M}_n$ and polydispersity with fractional conversion is given in Table 5.3. At high RAFT and KPS concentrations (exp. 1), the $\overline{M}_n$ increased with conversion, but the PD remained in the range of 2.1 to 2.6. In addition, the $\overline{M}_{n,\,th}$ values calculated with Eq. 5-3 were far lower than experimental. When the RAFT concentration was lowered (exp. 2) only one $\overline{M}_n$ value could be obtained. Beside this, part of the MMD was beyond the exclusion limit of the SEC columns, and therefore only peak molar masses (M_p) are given. The $\overline{M}_n$ at 41% conversion was more than two times larger than $\overline{M}_{n,\,th}$, with a polydispersity of 2.33. In exp. 3 conversions of 14% were reached in 25 hours, and therefore only two $\overline{M}_n$ data points were taken, in which these values were again higher than $\overline{M}_{n,\,th}$. Experiment 4, at the lowest RAFT and KPS concentrations investigated, showed the closest correlation between $\overline{M}_n$ and $\overline{M}_{n,\,th}$. The polydispersities were high, however, in the range of 3.1 to 3.7. These results demonstrate that for all experiments the $\overline{M}_n$ increased with conversion and the polydis-

Table 5.3: $\overline{M}_n$ and Polydispersity of Styrene in PMMA Seed at 60 °C at Different Cumyl-RAFT and KPS Concentrations.

Experiment	[Cumyl-RAFT][a]	[KPS][a]	x [b]	$\overline{M}_n \times 10^{-4}$	PD	$M_p \times 10^{-4}$	$\overline{M}_{n,th}$ [c] $\times 10^{-4}$
	($mol \cdot dm^{-3}$)	($mol \cdot dm^{-3}$)		($g \cdot mol^{-1}$)		($g \cdot mol^{-1}$)	($g \cdot mol^{-1}$)
1	High	High	0.22	7.34	2.10		1.51
	$1.46 \cdot 10^{-2}$	$1.0 \cdot 10^{-3}$	0.29	7.44	2.40		1.96
			0.35	8.12	2.33		2.41
			0.50	8.65	2.28		3.40
			0.63	9.20	2.59		4.27
2	Low	High	0.41	39.61	2.33	106.3	15.40
	$2.65 \cdot 10^{-3}$	$1.0 \cdot 10^{-3}$	0.57[d]			109.2	21.57
			0.82[d]			106.1	31.10
			0.86[d]			103.9	32.65
3	High	Low	0.10	1.33	1.23		0.50
	$2.00 \cdot 10^{-2}$	$1.0 \cdot 10^{-4}$	0.14	0.88	1.61		0.69
4	Low	Low	0.04	3.37	1.03		—
	$5.58 \cdot 10^{-3}$	$1.0 \cdot 10^{-4}$	0.14	4.59	3.10		2.49
			0.17	4.33	3.67		3.12
			0.20	6.22	3.13		3.53
			0.33	5.84	3.28		5.98

a) The concentrations for RAFT and KPS were determined for the monomer volume and water plus the seed latex volume, respectively.
b) Conversion data are placed in the order of the polymerization time.
c) The theoretical number average molar mass was calculated using Eq. 5-1
d) The molar mass distribution exceeded the exclusion limits of the applied SEC columns, so the peak molar masses are given.

persities remained relatively constant. Furthermore, the $\overline{M}_{n,th}$ is always lower than $\overline{M}_n$ obtained experimentally. Still, the increase in $\overline{M}_n$ indicates the living character of the polymerization.

The influence of EMA-RAFT on the MWDs is collected in Table 5.4. In the case of high EMA-RAFT, the $\overline{M}_n$ values in exp. 5 (very high KPS) increased with conversion and are slightly larger than the $\overline{M}_{n,th}$, with polydispersities in the range of 2.1 to 3.4. Conversely, at a lower KPS concentration (exp. 6) the $\overline{M}_n$ values are far greater than theory with polydispersity indices as high as 6.4. In the cases where the RAFT concentration is low, the $\overline{M}_n$ values are in fact below that of theory, in which the polydispersities increased for exp. 7 but remained approximately constant for exp. 8. The results suggest that both the ratio of RAFT agent and KPS

Table 5.4: $\overline{M}_n$ and Polydispersity of Styrene in PMMA Seed at 60 °C at Different EMA-RAFT and KPS Concentrations.

Experiment	[EMA-RAFT] ($mol \cdot dm^{-3}$)	[KPS] ($mol \cdot dm^{-3}$)	x	$\overline{M}_n \times 10^{-4}$ ($g \cdot mol^{-1}$)	PD	$\overline{M}_{n,th} \times 10^{-4}$ ($g \cdot mol^{-1}$)
5	High	Very High	0.38	5.78	2.18	2.48
	$1.50 \cdot 10^{-2}$	$5.0 \cdot 10^{-3}$	0.46	5.93	2.25	3.03
			0.84	9.84	2.53	5.48
			0.95	6.99	3.36	6.22
6	High	High	0.11	9.89	8.68	0.78
	$1.40 \cdot 10^{-2}$	$1.0 \cdot 10^{-3}$	0.16	10.59	6.40	1.09
			0.22	15.67	6.42	1.56
7	Low	High	0.25	7.94	1.60	9.92
	$2.50 \cdot 10^{-3}$	$1.0 \cdot 10^{-3}$	0.28	8.09	2.51	11.19
			0.34	9.63	1.97	13.32
			0.39	9.55	2.56	15.51
			0.53	11.11	2.61	21.26
			0.87	8.40	4.68	34.23
			0.85	7.75	3.53	33.66
8	Low	Low	0.18	6.97	1.55	6.85
	$2.50 \cdot 10^{-3}$	$1.0 \cdot 10^{-4}$	0.21	6.24	2.32	8.00
			0.22	6.77	1.58	8.48
			0.20	5.64	1.60	7.84

concentrations had a more pronounced influence on the MWD for EMA-RAFT compared to Cumyl-RAFT experiments. This is presumably due to the different fates and reaction rates of the exited radicals.

The very broad molar mass distributions, even at low KPS concentrations, are a consequence of continuous transportation of RAFT into the particles during Interval II and a small amount during Interval III, where small chains are continually being formed. Therefore, it is not unexpected to find polydispersity indices much larger than one. The higher values of $\overline{M}_n$ observed experimentally suggest that there is a much lower than the expected amount of dormant species available for reaction inside the particles. This is also supported by the argument put forth for retardation (*i.e.* slow transportation of RAFT into the particles).

The deviation of $\overline{M}_n$ from theory is also caused by the concentration of KPS. The more KPS, the greater the deviation from theory. These results suggest that bimolecular termination due to entry is no longer negligible at high KPS concentra-

Table 5.5: The Effect of Variations in Experimental Conditions on the Inhibition Time in *Ab Initio* Emulsion Polymerizations.

Experiment[a)]	[EMA-RAFT] $\times 10^3$ (mol·dm^{-3})	Initiator concentration[b)] $\times 10^3$ (mol·dm^{-3})	Inhibition time (min.)
AI-1	—	2.1	—
AI-2	—	0.52	—
AI-3	4.5	2.2	540
AI-4	4.8	0.70	510
AI-5	0.78	2.4	90
AI-6 [c)]	2.7	2.4	210
AI-7 [c)]	2.7	2.1 [b)]	360
AI-8 [c,d)]	2.9	2.5	—

a) Recipes further consisted of 200 g water, 0.6 g SDS and 24 g styrene.
b) Potassium persulfate (KPS) is used as the initiator, except in AI-7 where 4,4'-azobis(4-cyanopentanoic acid) is used.
c) The mixture of monomer and RAFT was degassed using three freeze–evacuate–thaw cycles.
d) Methyl methacrylate was used as the monomer.

tions (exp. 1 and 7). So, over the time of the reactions, the amount of chains formed from initiator can be similar to those formed by the RAFT agents, consequently reducing the $\overline{M}_n$. Whereas at low KPS concentrations (exp. 4 and 8), the $\overline{M}_n$ values were closer to theory, suggesting only a small proportion of chains were formed from initiator. Therefore, the deviation from theory is proposed to be a combination of the lower than expected amount of RAFT agent available for reaction and the amount of initiator decomposed, which both act concomitantly to increase and decrease $\overline{M}_n$, respectively.

5.3. *Ab Initio* Emulsion polymerizations

A*b initio* emulsion polymerizations were conducted to investigate the effect of RAFT agents on particle nucleation. It was also hoped that the *ab initio* studies would reveal more mechanistic information about the emulsion polymerization of styrene in the presence of a RAFT agent, that could be viewed and interpreted in the light of the mechanistic information acquired from the seeded studies.

Two sets of experiments were performed. The first series was designed to determine the sensitivity of the RAFT emulsion on different reaction conditions while the second was designed to compare the effects of RAFT concentration and structure.

Table 5.6: Type and Concentration of RAFT Agents in the Second Series of Experiments.[a)]

	RAFT Concentration $\times 10^3$ (mol·dm^{-3})		
	Cumyl	EMA	PBMA
High	5.2	5.2	4.7
Medium	2.6	2.7	2.4
Low	1.1	1.0	0.87

a) [KPS] = 2.2×10^{-3} mol·dm^{-3}. For further details see the experimental section on page 131.

5.3.1. Variations in Reaction Conditions

Details of the first series are given in Table 5.5. In this series the sensitivity of the reaction towards three different aspects was investigated:

1. sensitivity towards oxygen.
2. sensitivity towards potassium persulfate and its derived radicals.
3. specific issues with styrene monomer.

Emulsion polymerizations are in general tolerant towards trace amounts of oxygen. It could be a possibility, however, that when RAFT is added to the system, it is oxidized to form strongly inhibiting or retarding compounds. Based on this hypothesis, experiments AI-6 to AI-8 were conducted using an organic phase that had been thoroughly deoxygenated before use. The water phase was deoxygenated in all cases (see 'Procedures for ab initio polymerizations' on page 131). Another possibility is that potassium persulfate reacts with the RAFT agent in an unknown way, causing retardation and possibly forming inhibiting or retarding side-products. Dithioesters are know to be susceptible to oxidation by strong oxidizing agents[52] and also in their specific identity as RAFT agent, mention has been made of this process.[36] Finally, styrene was replaced with methyl methacrylate to investigate the effect of monomer partitioning (AI-8). A higher concentration of monomer in the water phase will accelerate propagation and possibly promote entry.

5.3.2. Variations in RAFT Concentration and Structure

The experiments in this second series (Table 5.6) share the common characteristic that a red layer of organic material is formed at around 10% conversion. As the reaction proceeds, monomer is depleted from this phase and the red material coagulates on the stirrer bar in the form of a viscous oil.

Figure 5.5 shows the inhibition times for the various types and concentrations of RAFT. When RAFT agent is added to the polymerization, an inhibition period is observed. At low concentrations, the type of RAFT agent is unimportant, but when the concentration is increased, a distinct difference is found between Cumyl-RAFT on the one hand and both EMA-RAFT and PBMA-RAFT on the other. The inhibition times imposed by Cumyl-RAFT seem to level off, whereas those induced by both other RAFT agents increase when more RAFT is used.

When the inhibition times are neglected and the polymerization rate is plotted as a function of the conversion (Figures 5.6 to 5.8), it can be seen that the addition of RAFT causes a drop in the reaction rate. In a conventional emulsion polymerization, one would first expect an increase in the reaction rate during Interval I, when the number of particles increases. Then during Interval II, the reaction rate will be fairly constant as both the number of particles and the monomer concentration inside them remain the same. Finally, during Interval III, the rate should decrease as the monomer is consumed. In the control experiment (*i.e.* without RAFT), the two changeovers seem to fall around 10% and 60% conversion. In the experiments in the presence of RAFT, no plateau is reached in the reaction rate – in other words, Interval II does not seem to exist. This implies that either the number of particles or the monomer concentration within the particles is changing during the reaction. Particle size analysis using capillary hydrodynamic fractionation (CHDF) revealed that the weight-average particle size for *e.g.* the Cumyl-RAFT samples ranged from 26–32 nm throughout the reaction. For this reason, it is unlikely that nucleation takes place continuously. The small particle size, however, supports the other hypothesis of a changing monomer concentration. It is an established fact that the equilibrium monomer concentration is a marked function of the particle radius for particles with an unswollen radius below approximately 30 nm as predicted by the Morton equation.[45] As the particles grow, the monomer concentration inside will rise, thereby increasing the polymerization rate. A more noteworthy observation is the remarkably small particle size that is obtained in the presence of RAFT compared with that of the control experiment (≈95 nm). Apparently, the presence of a large quantity of active and dormant oligomeric species improves the nucleation process, resulting in a large number of small particles. In the light of these findings, the reaction rate in the presence of RAFT can be considered very low, for a much larger number of particles would in an equivalent system imply a much higher reaction rate. The experimentally determined rate is however much lower over the entire conversion trajectory (Figure 5.6).

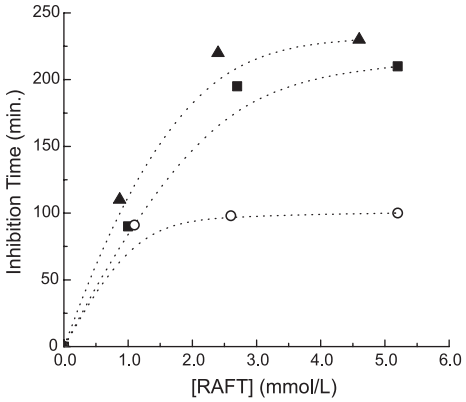

Figure 5.5. The effect of the concentration and structure of the RAFT agent on the inhibition period observed in *ab initio* emulsion polymerizations of styrene at 60°C and [KPS]≈$2\cdot10^{-3}$mol·dm^{-3}. Cumyl-RAFT (○), EMA-RAFT (■), PBMA-RAFT (▲).

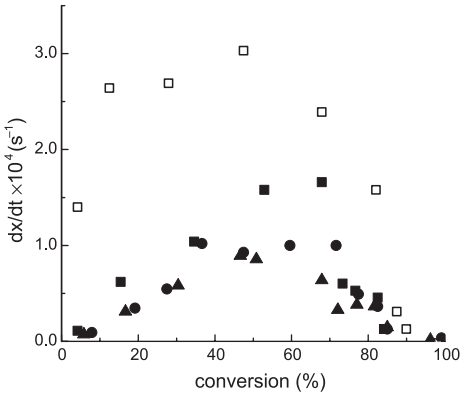

Figure 5.6. Reaction rate in *ab initio* emulsion polymerizations using Cumyl-RAFT. [RAFT]=0 (□); $1.1\cdot10^{-3}$ (■); $2.6\cdot10^{-3}$ (●); $5.2\cdot10^{-3}$ (▲) mol·dm^{-3}.

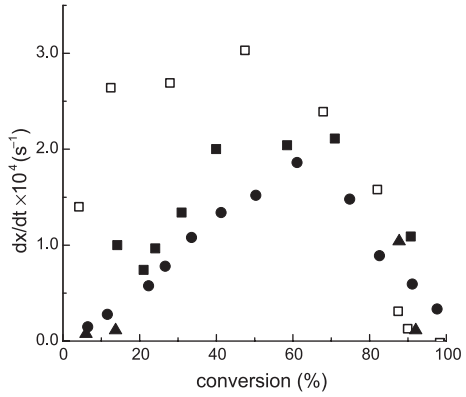

Figure 5.7. Reaction rate in *ab initio* emulsion polymerizations using EMA-RAFT. [RAFT]=0 (□); $1.0\cdot10^{-3}$ (■); $2.7\cdot10^{-3}$ (●); $5.2\cdot10^{-3}$ (▲) mol·dm^{-3}.

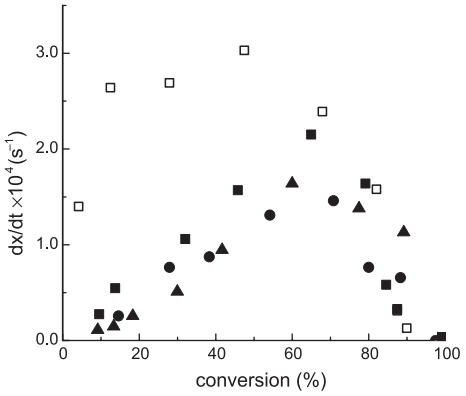

Figure 5.8. Reaction rate in *ab initio* emulsion polymerizations using PBMA-RAFT. [RAFT]=0 (□); $8.7\cdot10^{-4}$ (■); $2.4\cdot10^{-3}$ (●); $4.7\cdot10^{-3}$ (▲) mol·dm^{-3}.

Figure 5.9 gives an example of the development of the molar mass with conversion for the 'medium' RAFT concentrations. A linear relationship is apparent, but its slope is much larger than was to be expected, indicating that a living polymerization is taking place but with only a minor fraction of the RAFT agent in place. In the particular example given in Figure 5.9, the PBMA-RAFT performs slightly better than the other two compounds, but in the 'low' and 'high' concentration experiments, its behavior is very much the same as that of both EMA- and Cumyl-RAFT. The RAFT efficiency can be estimated from the molar mass and conversion

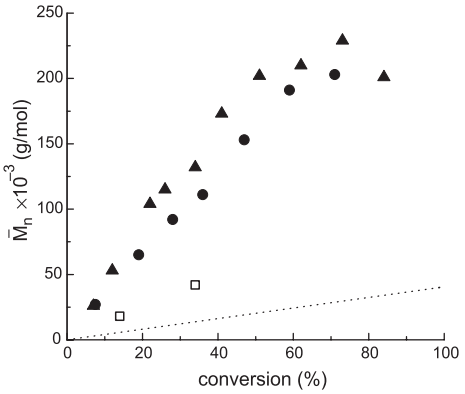

Figure 5.9. Evolution of the number-average molar mass during conversion in emulsion polymerizations with 'medium' concentrations of RAFT agent ($\approx 2.5 \cdot 10^{-3}$ mol·dm^{-3}). EMA-RAFT (▲); Cumyl-RAFT (●); PBMA-RAFT (□) are set off against the theoretically expected molar mass (·····).

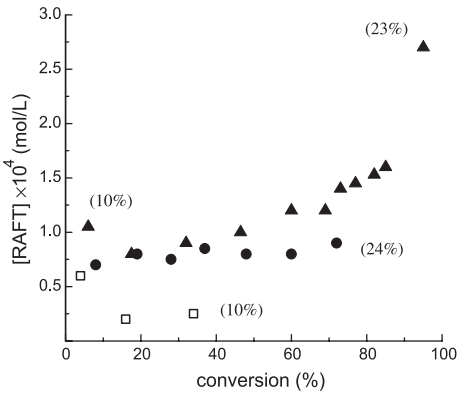

Figure 5.10. Concentration of Cumyl-RAFT agent, back-calculated from the molar mass and conversion for experiments conducted at low (□), medium (●) and high (▲) concentrations of RAFT agent (see Table 5.6 for details). RAFT efficiency between brackets.

data using Eq. 5-3. The results for the three Cumyl-RAFT experiments are depicted in Figure 5.10 and are qualitatively the same as those for the other RAFT agents. The concentration of RAFT actually participating in the reaction is only 10–20% of what was added to the reactor. From about 20% conversion onward the efficiency remains fairly constant or rises slightly. No specific trends on either the concentration or the type of RAFT agent could be found. The remainder of the RAFT agent obviously resides in the colored organic layer that is not sampled during the polymerization. The amount of RAFT that is lost in this manner depends on how large this phase grows and at what time during the reaction it starts to form. Poorly understood stability issues determine the RAFT efficiency in this case. Polydispersities in these polymerizations are generally high. Figure 5.11 gives the polydispersities for the polymerizations with Cumyl-RAFT. The results are again strongly affected by the stability issues. Results of the EMA-RAFT polymerizations are similar, with polydispersity ranging from 1.7 to 4.4. In the experiments with PBMA-RAFT, polydispersity went up to around 20, due to a multimodal molar mass distribution.

A last variation in RAFT structure that was tested comprises water soluble agents. Application of the sodium salt of 4-cyano-4-((thiobenzoyl)sulfanyl)pentanoic acid (compound **29** on page 83) and RAFT agents with poly(ethylene oxide) tails of various chain lengths (compound **32** on page 84) initially lead to solution

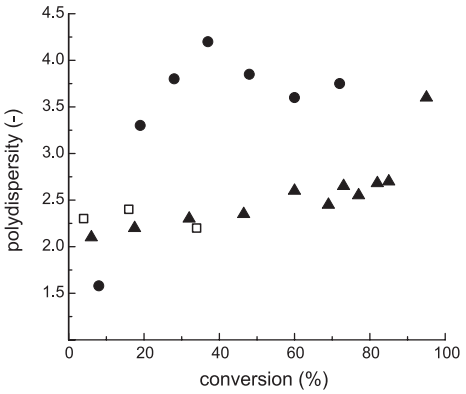

Figure 5.11. Polydispersities of polymerizations with Cumyl-RAFT at low (□), medium (●) and high (▲) concentrations of RAFT agent (see Table 5.6 for details).

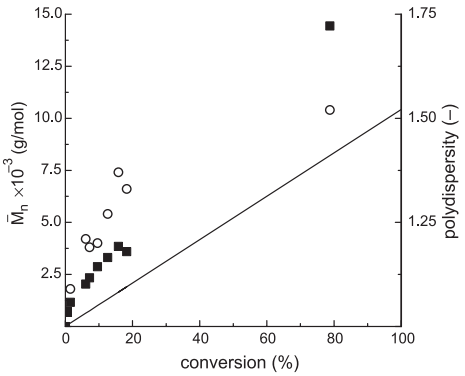

Figure 5.12. Development of molar mass (■, *left axis*) and polydispersity (○, *right axis*) during the seeded emulsion polymerization of styrene, stabilized by nonionic surfactant (NI-1). Theoretically expected molar mass (—, *left axis*)

polymerizations in the water phase, but upon reaching a certain critical chain length, full coagulation occured which prvented further investigations using this approach.

5.4. Emulsion Polymerizations with Nonionic Surfactants.

Evaluating the results reported in this chapter, living radical polymerization in emulsion polymerization appears to be possible. In both seeded and *ab initio* systems, a linear relationship between the number average molar mass and conversion was observed under certain circumstances. Transportation of the RAFT agent and emulsion stability are problematic. Only a small proportion of the RAFT agent is active at the locus of polymerization and a conspicuous red organic layer is formed. In order to avoid transportation problems, miniemulsion polymerization is a straightforward alternative. These experiments have been conducted and results of these miniemulsion reactions are reported in the next chapter. The reason why nonionic surfactants are investigated in this section is that also in miniemulsion polymerization, stability problems were encountered and it was found that these problems could be largely avoided by the use of nonionic surfactants. Table 5.7 gives the experimental details of several successful emulsion polymerizations stabilized by nonionic surfactants. In total, the series consisted of around 40 experiments with varying monomers, RAFT agents and initiators at a number of concentrations. The PMMA latices used for the seeded polymerizations had the anionic surfactant

Table 5.7: Emulsion Polymerizations in the presence of Nonionic Surfactants.[a)]

Experiment	Monomer		Surfactant		Initiator		RAFT agent	
	type	quantity[b)]	type	conc.[b)]	type	conc.[b)]	type	conc.[b)]
NI-1	STY	13.7	Igepal890	–[c)]	KPS	18.0	EMA	10
NI-2	MMA	26	Tween20	6.8	KPS	5.0	EMA	4.0
NI-3	MMA	30	Tween20	2.6	ACAP[d)]	1.7	Cyano	10
NI-4	BMA	30	Tween20	26	ACAP[d]	1.9	Cyano	12

a) *Ab initio* recipes (NI-1 to NI-3) are based on 160 g water, seeded recipe NI-4 is based on 100 g seed latex (8 % solids) and 10 g water. The anionic surfactant in this seed latex was replaced by Igepal890 before use.
b) Quantities in grams. Concentrations in mmol·dm^{-3}, based on the total emulsion volume.
c) Igepal890 was present in the PMMA seed latex.
d)4,4'-azobis(4-cyanopentanoic acid)

(Aerosol MA-80) removed by dialysis procedures after which Igepal890 was added to provide the required stabilization. The seed was swollen below saturation with monomer and RAFT agent. Polymerizations designed to start in Interval II, *i.e.* with monomer droplets present, had the remainder of monomer added before reaction to ensure that the RAFT agent was in the particles at the start of the reaction. Despite these precautions, a number of polymerizations starting in Interval II, but in Interval III as well, developed the same red organic layer as in the seeded polymerizations stabilized by SDS. In these cases, molar mass and polydispersity followed the same trends as those of the experiments with SDS shown in Tables 5.3 and 5.4 (pages 120–121). NI-1 is an example of a successful seeded emulsion polymerization. No signs of instability were observed. The efficiency of the transfer agent is around 50 % as the experimental molar mass is about a factor of two larger than the expected molar mass. Polydispersity remained below 1.50 (Figure 5.12).

Ab initio polymerizations conducted with a nonionic surfactant lead to highly variable results, without any apparent relationship to the type and concentration of the surfactant, initiator or RAFT agent. Three examples of successful emulsion polymerizations are described in Table 5.7 and in Figures 5.13 and 5.14. Experimental molar masses are higher than expected under all circumstances, but the RAFT efficiency has clearly improved, relative to the experiments with SDS, reaching values of 45 % (NI-2) to 85 % (NI-4). Polydispersities are also much better than in the experiments with anionic surfactants, ranging from 1.1 to 1.7. Particle size distributions were determined by dynamic light scattering. The distribution were generally broad and averages varied from 65 nm for NI-4 to 350 nm for NI-3.

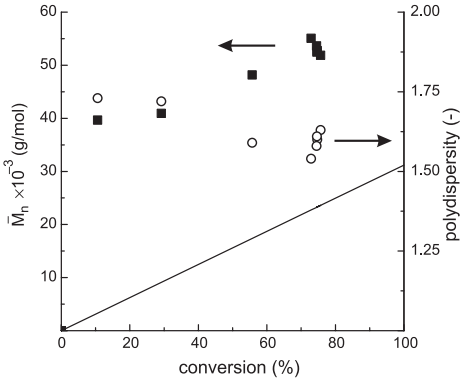

Figure 5.13. Development of molar mass (■, *left axis*) and polydispersity (O, *right axis*) during the ab initio emulsion polymerization of MMA, stabilized by nonionic surfactant (NI-2). Theoretically expected molar mass (—, *left axis*).

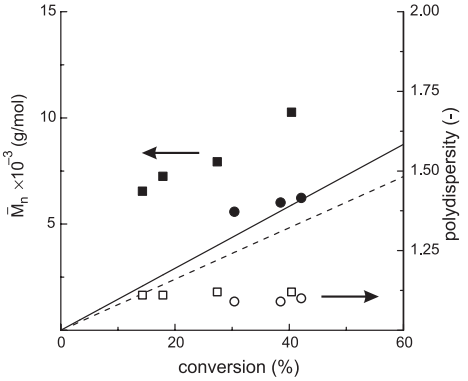

Figure 5.14. Development of molar mass and polydispersity during the *ab initio* emulsion polymerizations, stabilized by nonionic surfactant. Left axis: $\overline{M}_n$ (■ NI-3, ● NI-4); $\overline{M}_{n,\,th}$ (— NI-3, --- NI-4). Right axis: Polydispersity (□ NI-3, O NI-4).

The performance of nonionic surfactants in emulsion polymerizations is clearly better than that of SDS. Like in the miniemulsion polymerizations described in the next chapter, the reason is not fully understood.

5.5. Conclusion

The use of seeded experiments has allowed mechanisms affecting the RAFT process in emulsion to be studied. One of the important aspects of this study was retardation in rate, which was greater for the EMA-RAFT compared with the Cumyl-RAFT. This has been proposed to be due to greater exit of the radicals from the particles, formed after fragmentation of the EMA-RAFT agent. It was also found that the presence of monomer droplets resulted in polymers with high polydispersities. This is proposed to result from continuous transportation of RAFT agent into the particles primarily during Interval II and a small proportion during Interval III. The red layer was also a result of the presence of droplets. Once the switch from Interval II to III occurred, the low molar mass species coalesced to form the red coagulum. Deviation from theory of $\overline{M}_n$ was due to high amounts of chains formed by radical–radical termination and the lower than expected concentration of RAFT agent in the particles caused by trapped dormant species in the red coagulum. Therefore, the ideal system should contain large particles to reduce exit, and a stable system[53] should be sought to determine the effects of RAFT transportation into the particles.

From ab initio experiments it was learned that the RAFT agent causes severe inhibition and that it has a determental effect on the nucleation stage, which streches it to such an extent that no separate Interval II could be observed. RAFT efficiencies in these batch reactions are low, while polydispersities are high. The use of nonionic surfactants increased the stability of the emulsion and lead to improved RAFT efficiencies in several cases. The polydispersities are much lower (1.1–1.7) than in the anionically stabilized systems, but the system is labile as small variations in the recipe lead to highly different results.

5.6. Experimental

Materials: Styrene and methyl methacrylate (Aldrich) were purified of inhibitor by passing through an inhibitor-removal column (Aldrich). Sodium dodecylsulfate (SDS, Fluka) and sodium peroxidisulfate (SPS, Merck) were used as received.

RAFT agents : The syntheses of the RAFT agents, 2-phenylprop-2-yl dithiobenzoate, 2-(ethoxycarbonyl)propyl-2-yl dithiobenzoate and 2-cyanoprop-2-yl dithiobenzoate, denoted here as Cumyl-RAFT, EMA-RAFT and Cyano-RAFT (see Scheme 5.3), are described in chapter 3, and follows literature procedures.[34,54] PBMA-RAFT was prepared by a solution polymerization of butyl methacrylate (28 g) initiated by AIBN (7 g) and in the presence of bis(thiobenzoyl) disulfide (10 g) at 50 °C. The average degree of polymerization was 3 and GPC analysis revealed that within this mixture of oligomers no species were present with an polystyrene equivalent molar mass exceeding 600 $g \cdot mol^{-1}$.

Preparation of PMMA seed Latex: The recipe for the preparation of the PMMA seed latex is given in Table 5.8. The surfactant, buffer and most of the water was charged to a 1.3 L stainless steel reactor with baffles, and the reactor contents were allowed to reach 90 °C. The reactor contents were then degassed by bubbling argon through the mixture for 1 hr. with stirring. MMA monomer was then added to the reactor and the mixture was allowed to stir for 5 min. Initiator that had been dissolved in the remaining amount of water was then added to the reactor, after which the polymerization was allowed to proceed for 3 hr. The resulting latex was dialyzed for two weeks, with twice daily changes of deionized water to remove residual contaminants. The solids content after dialysis of 5.8 % was much lower than expected, which is due to coagulation.

Table 5.8: Recipe for the preparation of PMMA seed (with an unswollen radius of ≈20 nm) at 90 °C

	Amount (g)
Deionized water	821.0
Aerosol MA80 (surfactant)	14.11
$NaHCO_3$ (buffer)	1.074
Methyl methacrylate	130.0
KPS (initiator)	3.631

The number average diameter of the PMMA seed was determined to be 43.8 nm by Capillary Hydrodynamic Fractionation techniques (CHDF 2000 2.73, Matec Applied Sciences) and 39.4 nm with dynamic light scattering (Malvern 4700 multi-angle light scatterer with PCS for Windows). This strongly supports the production of a narrow particle size distribution. The PMMA seed was diluted in the seeded studies to give an N_c of $4.37 \cdot 10^{17}\,dm^{-3}$, which is above the critical particle number needed to avoid secondary nucleation.

Procedure for seeded polymerizations: 50 ml of the PMMA seed latex was measured into the dilatometer reactor and 78 ml of deionized water was added to the reactor to achieve a solids content of approximately 2.8 % and an N_c of $4.37 \cdot 10^{17}$. The stirred latex was then purged with argon at 60 °C for 30 minutes. A small portion of SDS (0.032 g) (well below its CMC) was then added to prevent coagulation during the reaction. Styrene and RAFT agent were then added to the dilatometer reactor and swelling was allowed to proceed overnight at 60 °C.

KPS was dissolved in deionized water, heated up to the reaction temperature and then added to the reactor through the septum. The volume of water used was added carefully so that the reaction mixture would be forced up slightly into the dilatometer bore. The start of the reaction was observed by monitoring the decrease in height of the reaction mixture in the capillary tube. Samples were drawn at regular Intervals for gravimetric determination of conversion. The dried samples were then dissolved in THF ($1\,mg \cdot ml^{-1}$) and filtered for Size Exclusion Chromatography (SEC) analysis. CHDF was used for particle size analysis of the emulsion samples to make sure that secondary nucleation was avoided.

Procedures for *ab initio* polymerizations: Deionized water was charged to a glass jacketed reactor and degassed for 1 hour at 60 °C by purging with argon gas while the reactor contents were being stirred. The surfactant was then added to the reactor and agitation was allowed to proceed for a further ½ hour at the reaction tempera-

ture. The RAFT agent (not present in AI-1 and AI-2) was then dissolved in the styrene. The monomer (and EMA-RAFT agent) was then added to the reactor and emulsification was allowed to proceed for 5 minutes before the addition of the pre-dissolved and pre-heated initiator.

Experiments AI-6 to AI-8 were carried out with rigorous degassing of the monomer and RAFT agent through three freeze–evacuate–thaw cycles and an increase in the emulsification period to 1 hour. Experiment AI-7 was carried out with 4,4'-azobis(4-cyanopentanoic acid) as the initiator, instead of KPS, under the same conditions as experiment AI-6.

SEC Analysis: SEC analysis was carried out using a WATERS Model 510 pump, WATERS Model WISP 712 autoinjector, Model 410 refractive index detector and Model 486 UV detector (at 254 nm). The columns used were a PLgel guard 5 mm 50×7.5 mm precolumn, followed by 2 PLgel mixed-C 10 mm 300×7.5 mm columns (40 °C) in series. THF was used as eluent (flow rate 1.0 mL·min^{-1}) and calibration was done using polystyrene standards (M = 580 – 7.1·10^6 g·mol^{-1}). Data acquisition was performed using WATERS Millennium 32 (v3.05) software and processed further using GeePeeSee (beta 2).

Determination of $[M]_p^{sat}$: The saturation monomer concentration within the seed latex particles, $[M]_p^{sat}$, was determined by creaming experiments according to the method used by Ballard *et al.*[55] The saturation concentrations of monomer were also determined in the presence of Cumyl-RAFT and EMA-RAFT agents. These were dissolved in the styrene monomer prior to the swelling of the seed. The concentration of the RAFT agent in the creamed monomer layer was then determined by UV absorption (in methanol) at a wavelength of 325 nm, which is above the styrene absorption range.

5.7. References

1. Boorstin, D.J. in *The image: a guide to pseudo-events in America*, **1962**, New York, Atheneum
2. Gilbert, R. G. *Emulsion Polymerization: A Mechanistic Approach*; Academic: London, **1995**.
3. *Emulsion polymerization and Emulsion Polymers*; Lovell, P. A.; El-Aasser, M. S. Eds.; John Wiley and Sons: Chichester, **1997**
4. Smith, W. V.; Ewart, R. H. *J. Chem. Phys.* **1948**, *16*, 592
5. Maxwell, I. A.; Morrison, B. R.; Napper, D. H.; Gilbert, R. G. *Macromolecules* **1991**, *24*, 1629
6. Gilbert, R. G. *Modelling rates, particle size distributions and molar mass distributions*; Lovell, P. A. and El-Aasser, M. S., Ed.; Wiley: London, **1997**, pp 165–204.
7. Kemmere, M. F.; Meuldijk, J.; Drinkenburg, A. A. H.; German, A. L. *J. Appl. Polym. Sci.* **1999**,

74, 3225
8. Matyjaszewski, K.; Shipp, D. A.; Qiu, J.; Gaynor, S. G. *Macromolecules* **2000**, *33*, 2296
9. Gaynor, S. G.; Qiu, J.; Matyjaszewski, K. *Macromolecules* **1998**, *31*, 5951
10. Qiu, J.; Gaynor, S. G.; Matyjaszewski, K. *Macromolecules* **1999**, *32*, 2872
11. Qiu, J.; Pintauer, T.; Gaynor, S. G.; Matyjaszewski, K.; Charleux, B.; Vairon, J.-P. *Macromolecules* **2000**, *33*, 7310
12. Chambard, G.; de Man, P.; Klumperman, B. *Macromol. Symp.* **2000**, *150*, 45
13. Matyjaszewski, K.; Qiu, J.; Shipp, D. A.; Gaynor, S. G. *Macromol. Symp.* **2000**, *155*, 15
14. Marestin, C.; Noël, C.; Guyot, A.; Claverie, J. *Macromolecules* **1998**, *31*, 4041
15. Bon, S. A. F.; Bosveld, M.; Klumperman, B.; German, A. L. *Macromolecules* **1997**, *30*, 324
16. Ma, J. W.; Cunningham, M. F. *Macromol. Symp.* **2000**, *150*, 85
17. Cunningham, M. F.; Ma, J. W. *J. Appl. Polym. Sci.* **2000**, *78*, 217
18. Mendoza, J.; De La, J. C.; Asua, J. M. *J. Polym. Sci., Part A: Polym. Chem.* **2000**, *38*, 4490
19. Hutchinson, R. A.; Paquet, D. A.; McMinn, J. H. *Macromolecules* **1995**, *28*, 5655
20. The behavior in bulk was compared by a numerical simulation using the parameters and concentrations mentioned in ref. 16 assuming an oil soluble initiator with the same activity as potassium persulfate.
21. Moad, G.; Chiefari, J.; Chong, Y. K.; Krstina, J.; Mayadunne, T. A.; Postma, A.; Rizzardo, E.; Thang, S. H. *Polymer Int.* **2000**, *49*, 993
22. Goto, A.; Sato, K.; Fukuda, T.; Moad, G.; Rizzardo, E.; Thang, S. H. *Polym. Prepr.* **1999**, *40*, 397
23. Whang, B. C. Y.; Lichti, G.; Gilbert, R. G.; Napper, D. H.; Sangster, D. F. *J. Polym. Sci. Polym. Letters Edn.* **1980**, *18*, 711
24. Lichti, G.; Sangster, D. F.; Whang, B. C. Y.; Napper, D. H.; Gilbert, R. G. *J. Chem. Soc. Faraday Trans. I* **1982**, *78*, 2129
25. Barandiaran, M. J.; Asua, J. M. *J. Polym. Sci. Part A Polym. Chem.* **1995**, *34*, 309
26. Asua, J. M.; Sudol, E. D.; El-Aasser, M. S. *J. Polym. Sci. Polym. Chem. Ed.* **1989**, *27*, 3903
27. Casey, B. S.; Morrison, B. R.; Maxwell, I. A.; Gilbert, R. G.; Napper, D. H. *J. Polym. Sci. A: Polym. Chem.* **1994**, *32*, 605
28. Ugelstad, J.; Hansen, F. K. *Rubber Chem. Technol.* **1976**, *49*, 536.
29. Charmot, D.; Corpart, P.; Adam, H.; Zard, S. Z.; Biadatti, T.; Bouhadir, G. *Macromol. Symp.* **2000**, *150*, 23
30. Monteiro, M. J.; Sjöberg, M.; Van der Vlist, J.; Göttgens, C. M. *J. Polym. Sci. Part A: Polym. Chem.* **2000**, *38*, 4206
31. Monteiro, M. J.; de Barbeyrac, J.; German, A. L. submitted to *Macromolecules*.
32. Smulders, W. W.; Monteiro, M. J.; Gilbert, R. G. publication in preparation
33. Chiefari, J.; Chong, Y. K.; Ercole, F.; Krstina, J.; Le, T. P. T.; Mayadunne, R. T. A.; Meijs, G. F.; Moad, G.; Moad, C. L.; Rizzardo, E.; Thang, S. H. *Macromolecules* **1998**, *31*, 5559
34. Le, T. P.; Moad, G.; Rizzardo, E.; Thang, S. H. Patent WO 98/01478 (**1998**) [*Chem. Abstr.* **1998**, *128*:115390]
35. Uzulina, I.; Kanagasabapathy, S.; Claverie, J. *Macromol. Symp.* **2000**, *150*, 33.
36. Kanagasabapathy, S.; Claverie, J.; Uzulina I. *Polym. Prepr.* **1999**, *218*, 422
37. Buback, M.; Gilbert, R. G.; Hutchinson, R. A.; Klumperman, B.; Kuchta, F.-D.; Manders, B. G.; O'Driscoll, K. F.; Russell, G. T.; Schweer, *J. Macromol. Chem. Phys.* **1995**, *196*, 3267
38. Hutchinson, R. A.; Paquet, D. A.; McMinn, J. H.; Fuller, R. E. *Macromolecules* **1995**, *28*, 4023
39. *Polymer Handbook*, 4th ed.; Brandrup, J., Immergut, E. H., Grulke, E. A., (Eds.); John Wiley & Sons: New York, **1999**.
40. Part of the work reported in this chapter was published elsewhere in a modified version: The Influence of RAFT on the Rates and Molecular Weight Distributions of Styrene in Seeded Emulsion Polymerizations. Monteiro, M. J.; Hodgson, M.; de Brouwer, H. *J. Polym. Sci., Part A: Polym. Chem.* **2000**, *38*, 3864
41. Morrison, B. R.; Casey, B. S.; Lacík, I.; Leslie, G. L.; Sangster, D. F.; Gilbert, R. G.; Napper, D. H. *J. Polym. Sci. A: Polym. Chem.* **1994**, *32*, 631
42. Müller, A. H. E.; Zhuang, R.; Yan, D.; Litvenko, G. *Macromolecules* **1995**, *28*, 4326.
43. The 'Method of Moments' is elucidated further in the appendix on page 191.
44. Gilbert, R. G. *Mechanisms for radical entry and exit: - Aqueous-phase influences on polymerization*; Asua, J. M., Ed.; Kluwer Academic: Dordrecht, **1997**; Vol. NATO Advanced

Studies Institute, p. 1–16
45. Morton, M.; Kaizerman, S.; Altier, M. W. *J. Colloid Sci.* **1954**, *9*, 300
46. Gardon, J. L. *J. Polym. Sci., Part A-1* **1968**, *11*, 2859
47. Morrison, B. R.; Gilbert, R. G. *Macromol. Symp.* **1995**, *92*, 13
48. Maeder, S.; Gilbert, R. G. *Macromolecules* **1998**, *31*, 4410
49. Lane, W. H. *Ind. Eng. Chem.* **1946**, *18*, 295
50. Wilke, C. R.; Chang, P. *AIChE J.* **1955**, 1, 264
51. Griffiths, M. C.; Strauch, J.; Monteiro, M. J.; Gilbert, R. G. *Macromolecules* **1998**, *31*, 7835
52. Kato, S.; Ishida, M. *Sulfur Reports* **1988**, *8*, 155
53. de Brouwer, H.; Monteiro, M. J.; Tsavalas, J. G.; Schork, F. J. *Macromolecules* **2000**, *33*, 9239. See also the next chapter of this thesis.
54. Thang, S. H.; Chong, Y. K.; Mayadunne, R. T. A.; Moad, G.; Rizzardo, E. *Tetrahedron Lett.* **1999**, *40*, 2435
55. Ballard, M. J.; Napper, D. H.; Gilbert, R. G. *J. Polym. Sci., Polym. Chem. Edn.* **1984**, *22*, 3225

» I've lost control again
And how I'll never know just why or understand, she said
I've lost control again
And she screamed out, kicking on her side and said
I've lost control again «[1]

6. Living Radical Polymerization in Miniemulsion using Reversible Addition–Fragmentation Chain Transfer.[2]

Synopsis: In theory, a miniemulsion comprises the ideal environment for 'living' radical polymerization by the RAFT process. Compartmentalization minimizes radical–radical termination events and droplet nucleation eliminates the mass transfer limitations found in conventional 'living' emulsion polymerizations as discussed in the previous chapter. In practice, however, several phenomena were observed when using the RAFT technique indicating a deviation from this idealized theory when the miniemulsion was stabilized by ionic surfactants. The appearance of a separate organic phase after initiation was an obvious indicator of droplet instability. The generation of oligomers in the early stages of the polymerization was postulated as the major culprit behind the destabilization. The application of nonionic surfactants allowed the controlled polymerization of methacrylates and styrene monomers, resulting in stable colloidal dispersions. The living character of this latex material was further exemplified by its transformation into block copolymers. The increased polymerization rate of the compartmentalized system allowed for improved block copolymer purity compared to homogeneous systems.

6.1. Miniemulsions

6.1.1. Introduction

Miniemulsions differ from emulsions solely in the 'mini' prefix. 'Mini' in this case refers to the monomer droplet size of the emulsion before polymerization and not to the particle size of the dispersion generated after polymerization. This

droplet size can be up to an order of magnitude smaller than in a macroemulsion or conventional emulsion.* In a typical macroemulsion polymerization, the diameter of the monomer droplets falls between one and ten micrometer at the start of the reaction,[3,4] while in a miniemulsion polymerization, the droplet size can range from an approximate 50 nm to around 500 nm.[5] Section 6.1.2 demonstrates how emulsions with such small droplets are prepared and how they are stabilized. Although mere size seems a rather arbitrary classification, the reduction in size together with the different method of preparation has some important consequences for the distribution of surfactant in the system, thereby impacting upon the nucleation mechanism (section 6.1.3, page 139).

This chapter describes the application of RAFT in miniemulsions with the aim to conduct a living polymerization. The highlight in sections 6.2 and 6.3 is on unforeseen phenomena observed involving destabilization of the miniemulsion due to the presence of the RAFT agent, when it was stabilized by either anionic or cationic surfactants. In section 6.4 these deleterious effects will be shown to be alleviated by substituting nonionic for ionic surfactants, thereby allowing the preparation of homopolymers and block copolymers with a 'livingness' unequalled by homogeneous systems.

6.1.2. Miniemulsion Preparation & Stability

The small droplets of a miniemulsion are actualized through ultra-high shear, usually by probe-sonication of the emulsion, and during this preparation a steady state droplet size is obtained after a certain minimum energy input. This equilibrium droplet size depends on the relative amounts of water, organic materials and surfactant. At this point, the rate of droplet fission by ultrasound balances the rate of droplet coalescence due to insufficient colloidal stability while thermodynamic aspects are of lesser importance during this stage.[6] When the energy input of the sonicator probe is stopped, the miniemulsion leaves its steady state situation and the droplets will slowly start growing as a result of insufficient thermodynamic and colloidal stability.

The colloidal stability is poor because of the incomplete surface coverage of the droplets with surfactant. Landfester *et al.* showed that the average droplet size of miniemulsions that are not polymerized, slowly increases to a certain plateau

* The remainder of this chapter will utilize the term 'macroemulsion' to refer to a conventional emulsion in order to emphasize the difference with miniemulsions.

value, the height of which is relatively independent of the initial droplet size.[6] In this final state the total interfacial area between the two phases has decreased to such a level that the available surfactant is able to provide the required colloidal stability. The addition of a small amount of surfactant right after the preparation of a miniemulsion effectively stops the tendency for the droplets to grow as the surface coverage with surfactant is completed. The addition of an excess surfactant, on the other hand, has an adverse effect. Free surfactant in the water phase increases the solubility of the organic material in the continuous phase which accelerates destabilization on thermodynamic grounds[7,8] and when polymerizing, free surfactant will promote secondary nucleation. The nucleation mechanism is discussed in section 6.1.3 on page 139.

Thermodynamically, the stability would be unsatisfactory if only a surfactant were applied to stabilize the droplets. This is caused by the Ostwald ripening process, which in general terms describes the effect that larger bodies tend to grow at the expense of smaller ones through diffussion of material. The effect is known to occur in aggregations of crystals for instance, but in the case of miniemulsions the bodies refer to the emulsion droplets. The effect is founded on the principle that the chemical potential of the material near an interface is higher than that of an imaginary interface-free bulk phase. The difference in chemical potential ($\Delta\mu$) between droplet material (μ_d) and bulk material (μ_b) is given by the Laplace pressure that takes the form of Eq. 6-1 for spherical liquid droplets:[9]

$$\Delta\mu = \mu_d - \mu_b = \frac{2 \cdot \sigma \cdot v_b}{r} \qquad \textbf{(6-1)}$$

where σ is the surface tension of the liquid–liquid interface, v_b is the volume of a single molecule and r the radius of the droplet. Considering the dependency of $\Delta\mu$ on r in Eq. 6-1, there will be a driving force for material to migrate from the smaller droplets to the larger droplets, attaining a state of lower energy until eventually $\Delta\mu$ is minimized. The smaller droplets will vanish as their contents diffuse to the larger ones finally resulting in the formation of a ‘single droplet’ or, in other words, complete phase separation. A somewhat lower surface energy introduced by the surfactant may reduce the rate of the process slightly but cannot prevent it.

Miniemulsions gain their stability from the addition of an extra component to the droplet phase.[7,10] Traditionally hexadecanol was used as a cosurfactant resulting in prolonged stability periods stretching from days to months. Its advantageous

effect was believed to originate from a rigid, structured complex formed by interaction of the hydrophobic tails of the surfactant (typically a long chain alkyl sulfate like dodecyl sulfate) with those of the cosurfactant, which would form an electrostatically charged barrier, decelerating monomer diffusion and, in addition, improving the colloidal stability. At present, completely hydrophobic materials like hexadecane,[10] dodecyl mercaptan[11] and stearyl methacrylate[12] often replace the cosurfactant as these were found to work even better. It is unlikely that these hydrophobic molecules will reside in the surfactant layer and the effectiveness of these costabilizers* is based on the osmotic pressure that they introduce to (partly) counterbalance the Laplace pressure, effectively minimizing the driving force for Ostwald ripening. This effect is quantified in Eq. 6-2 through the addition of an additional term on the right hand side:[9]

$$\Delta\mu = \mu_b - \mu_d = \frac{2 \cdot \sigma \cdot v_b}{r} - \frac{\eta \cdot k_B \cdot T \cdot v_b}{(4\pi/3) \cdot r^3} \qquad \textbf{(6-2)}$$

where η equals the number of hydrophobe molecules inside a particle, k_B is Boltzmann's constant and T is the absolute temperature. The total free energy of the system is found by integration of the chemical potential over all material, *i.e.* over all droplets of all volumes. The presence of the costabilizer molecules adds an important constraint on the minimization of the total free energy, namely that of a constant number of droplets. For if the costabilizer molecules are equally distributed over all droplets and approximately insoluble in the continuous phase, then the droplets initially formed cannot disappear completely by monomer depletion. In fact, should a number of large droplets expand at the expense of the smaller ones, then the osmotic pressure term for the small droplets rapidly becomes larger as r decreases, but due to the hydrophobe molecules, the system cannot be relieved of the small, high energy droplets. Strictly speaking, the Eq. 6-2 is no longer valid when the costabilizer molecules can no longer be considered 'dilute', but the formula reasonably indicates the trend in chemical potential when r decreases.

* In the current literature the term 'costabilizer' is used interchangably with 'hydrophobe' and sometimes 'cosurfactant' is still used. Though hydrophobicity is an important prerequisite for costabilizers, other aspects like solubility in the organic phase and molar masss have an important influence on their effectiveness as costabilizers. The term 'cosurfactant' is no longer indicative of the underlying mechanism of operation but seems to be adopted by some researchers and used for consistency with older literature.

Eq. 6-3 indicates that for a certain concentration of costabilizer, a droplet size exists that is thermodynamically stable. For this idealized picture to be realized in practice, it is of the utmost importance that the hydrophobe is completely insoluble in the water phase. If not, then η cannot be considered constant and the diffusion rate of the hydrophobe through the water phase is the rate determining step for the Ostwald ripening process. Since the *number* and not the *concentration* of hydrophobic species within each droplet determines its chemical potential, it is crucial that a (close to) monodisperse distribution of droplets is prepared from the homogeneous solution of costabilizer in monomer. A tailed particle size distribution containing a fraction of large droplets creates a complex situation with a similar distribution in η among the droplets, introducing a substantial driving force for interparticle monomer migration.

$$r = \left(\frac{3 \cdot \eta \cdot k_B \cdot T}{8\pi \cdot \sigma} \right)^{0.5} \qquad \textbf{(6-3)}$$

Larger hydrophobic species like polystyrene and poly(methyl methacrylate) have also been used to improve the particle stability causing higher reaction rates and a more robust nucleation process.[13,14,15] The mechanism behind their functioning is not clear, but in the light of the previous discussion it can be said that these polymers will not form very efficient costabilizers in the thermodynamic sense as their high molar mass results in a low number of molecules (η) per droplet when only a limited amount on a weight basis is used. Like their low molar mass counterparts, these polymers will fix the number of droplets as their presence prevents the disappearance of any droplets.

6.1.3. Nucleation Processes

In a macroemulsion, the surface area of the monomer phase is rather small because of the large droplet size and the consequently smaller number of droplets (typically $10^{13}\,dm^{-3}$). The surfactant micelles, small in size (5 to 10 nm) and large in number (typically $10^{20}\,dm^{-3}$), have a surface area that easily exceeds that of the monomer droplets.[4] For this reason, in a typical macroemulsion polymerization, micellar nucleation is the predominant mechanism for particle formation. Oligomer radicals – generated in the water phase – enter micelles and continue growing while

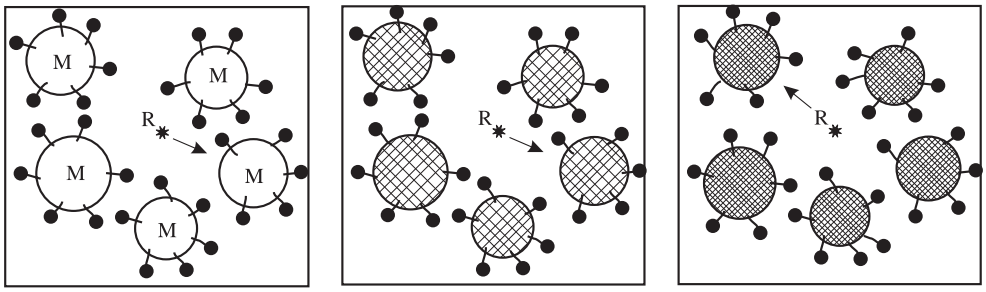

Scheme 6.1. Schematical progress of a miniemulsion polymerization. Compared with Scheme 5.3 on page 111, which represents a conventional emulsion polymerization, the starting situation of a miniemulsion polymerization is characterized by the absence of micelles in the continuous phase and by monomer droplets, that are typically larger in number and smaller in size. Particles are formed by polymerization taking place within these droplets eliminating the need for monomer migration through the continuous phase.

attracting monomer. As the micelles are converted into polymer particles, all of the reaction ingredients (*e.g.* monomer) have to migrate out of the droplets, through the water phase, into the growing particles.

In miniemulsions, the smaller droplet size has some important consequences for the course of the reaction. The smaller droplets share a much larger interphase with the continuous phase and absorb most of the surfactant in the recipe. This leaves little or no surfactant for the formation of micelles. Both the absence of micelles and the increased surface area of the droplet phase promote droplet nucleation and eliminate micellar nucleation. Oligomer radicals that are formed in the water phase enter droplets and start polymerization within them. Under these circumstances the droplets *themselves* are converted into polymer particles[16] and transport of monomer and other reaction components through the water phase is not necessary. In the ideal case, the droplets act completely independent and can be considered a collection of nanoscale bulk reactors. For this reason the resulting polymer dispersion is a copy of the initial emulsion in terms of particle size, number and identity (Scheme 6.1).[5]

Several factors may cause reality to deviate from this idealized situation. First, the presence of additional nucleation mechanisms cannot be ruled out completely. Although micellar nucleation is unlikely, due to the low free surfactant concentration, homogeneous nucleation has been shown to lead to the formation of new particles.[17,18] Homogeneous nucleation is a particle formation mechanism that takes place when an oligomeric radical in the water phase does not enter a droplet or micelle, but propagates till it reaches a critical chainlength (j_{crit}), upon which it is

no longer dissolved in the waterphase. Its coil collapses at this point, excluding water and attracting monomer thereby forming a new particle. The extent to which this occurs depends on numerous factors, the most important being the number of droplets, the amount of monomer in the water phase, the propagation rate constant in the waterphase and the type of initiator used.

Second, not all droplets may be converted into particles. It was shown in the previous section that a typical miniemulsion finds itself in a metastable situation. The chemical potential of the droplet material may be higher than that of a bulk phase but the difference is minimized through the addition of a costabilizer and all droplets share the same osmotic pressure. The difference in osmotic pressure among the droplets will be increased however, when in the course of the reaction some are nucleated while others are not. The droplets lacking polymer will eventually supply monomer to the reacting polymer particles and act as monomer reservoirs.

To fully enjoy the benefits of miniemulsion polymerization, *i.e.* completely eliminating mass transfer through the water phase, it is important to closely approach the situation of complete and exclusive droplet nucleation. This is of particular importance for living radical polymerizations as will be shown in the next section.

6.1.4. Living Radical Polymerization in Miniemulsions

In the previous chapter it was already mentioned that a major challenge confronting living radical polymerization is its application in dispersed media; most notably in water-borne systems. While macroemulsion polymerization is beyond any doubt the most straightforward approach to obtain water based polymeric dispersions, the previous chapter demonstrated that the application of RAFT in these systems resulted in unforeseen problems, even though a living mechanism based on reversible transfer was expected to be the most easily adaptable. In principle, the miniemulsion environment should allow the ideal conditions for living radical polymerization to be attained in a more straightforward manner. Similar to macroemulsion polymerization, irreversible radical–radical termination is minimized through compartmentalization, thereby allowing a higher polymerization rate compared to bulk or solution systems. The continuous water phase will dissipate the heat of reaction and produce a polymer dispersion which can easily be processed due to its low viscosity environment. Clearly distinct from macroemulsion polymerization is

the absence of complex particle formation and mass transfer events and in this respect every miniemulsion droplet can be considered the clichéd nanoscale bulk reactor, completely segregated from the other droplets. This bulk environment has been shown to be suitable for living radical polymerizations in previous chapters.

The literature reports several attempts to perform living radical polymerization in miniemulsion, applying techniques based on reversible termination (ATRP, nitroxides).[19,20,21] The disadvantage of these approaches is the troublesome partitioning of the small deactivating species over the two phases, which complicates the kinetics[22]. If the deactivating species moves into the water phase it will slow the growth of aqueous phase radicals, interfering with the process of radical entry and thereby decreasing the rate of polymerization. Control of molar mass at the main locus of polymerization (*i.e.* inside the particle) will suffer from the reduced concentration of deactivating species. Besides, it has been argued that the persistent radical effect, which adds to the control in bulk and solution polymerizations, will cause an exceedingly low polymerization rate in such compartmentalized systems[23]. Although living radical polymerizations were conducted, the theory was confirmed in that the molar mass distribution was broader than polymerizations in a homogeneous medium.[21]

Techniques based on degenerative transfer form a more likely candidate for this type of application since, in theory, the number of free propagating radicals remains unaffected. Another advantage is that the controlling species is (attached to) a dormant polymer chain and thus will not be able to diffuse out of the particle, negating the effect of exit and the corresponding lack of molar mass control. Several studies reported the successful application of such techniques in waterborne systems, but most of these studies use relatively inactive species to control the polymerization. The alkyl iodides used by several groups[23,24,25] have a transfer constant only slightly larger than unity. A similarly slow consumption of the compound can be expected for the RAFT agents applied by Kanagasabapathy *et al.*[26,27] and in our own group,[28] because of a poor homolytic leaving group and a rather unactivated carbon–sulfur double bond, respectively. Although these systems allow the preparation of complex architectures (*e.g.* block copolymers[25]), polydispersity is usually high (~2) since the conversion of transfer agent into polymer chains takes place during a prolonged interval of the polymerization and because the exchange reaction between growing radicals and dormant chains is slow in comparison with propagation.

The transition from transfer agents with low activity to those with a high activity appears to be straightforward, but in practice this turns out to be more complicated. The previous chapter discussed the application of several RAFT agents in conventional emulsion polymerizations, both seeded[29] and *ab initio*.[30] In contrast to low activity xanthates which could easily be used,[28] high reactivity agents based on the dithiobenzoate group invariably led to colloidal stability problems.[29,30] A large amount of the transfer agent was lost in the form of (oligomeric) coagulum resulting in a much higher molar mass than was to be expected for the emulsion material. The application of high reactivity agents in miniemulsions is only preceded by two examples in the first patent detailing the RAFT process[31] and this will be the starting point of the investigations in this chapter.

Special care should be taken in approaching the 'ideal' situation described in the previous section (6.1.3) as any aberration from 100% droplet nucleation will push the system in the direction of the mechanisms and kinetics that prevail in macroemulsion polymerization.

If, on the one hand, only a small part of the original population of droplets is nucleated, the remainder will eventually act as monomer reservoir. The RAFT agent contained within these reservoirs should then be transported to the reacting particles through the water phase. This may have two different, but both undesirable effects. First, the RAFT agent arriving later at the locus of polymerization, will start new chains later in the polymerization, and therefore broaden the molar mass distribution. Second, if the RAFT agent has already been converted into (oligomeric) dormant species in these droplets, transportation may no longer be possible because of their low water solubility. The most probable event is that these oligomers eventually precipitate as monomer is depleted from these droplets.

If on the other hand secondary nucleation takes place, particles will be created that do not contain any RAFT agent as the transfer active moiety is attached to polymer chains in the first generation of droplets/particles. For this reason, the polymerization in these particles will not be controlled.

6.2. Anionic Surfactants

The combination of SDS and either hexadecanol or hexadecane as the costabilizer is beyond any doubt the most commonly applied stabilizer system for miniemulsion polymerizations. The first patent on RAFT polymerization[31] mentions two

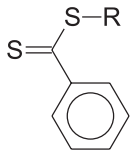

1. R = $C(CH_3)_2CN$
2. R = $C(CH_3)_2C_6H_5$
3. R = $C(CH_3)_2COOC_2H_5$
4. R = $C(CH_3)(CN)CH_2CH_2COO$-
-poly(ethylene-*co*-butylene)
5. R = poly(methyl methacrylate)

Scheme 6.2. RAFT agents applied in miniemulsion polymerizations. Their syntheses have been described in chapter 2.

examples of styrene miniemulsions using these components, and a similar system was taken as the starting point for our investigations. A series of preliminary experiments was conducted and this resulted in a remarkable observation.

Styrene miniemulsions, prepared using SDS as surfactant and hexadecane (with or without polystyrene) as the costabilizer, gave in most cases a visually stable miniemulsion. Miniemulsions are considered visually stable if they appear homogeneous to the eye, *i.e.* no separate organic or aqeous phase exists beside the emulsion phase. The droplet size was typically between 60 and 100 nm as measured by light scattering. When these miniemulsions were initiated with potassium persulfate (KPS), phase separation became apparent at the start of the reaction. A clear red monomer phase formed in the vortex of the stirred miniemulsion, and as the reaction proceeded this organic phase slowly increased in volume. The red color indicates the presence of species containing the dithiobenzoate group and GPC analyses revealed that the layer consisted of monomer swollen oligomers/polymers, usually of a considerably lower molar mass than the emulsion polymer and with a broader molar mass distribution (polydispersity typically between 3 to 5). This behavior is observed in all RAFT polymerizations stabilized with SDS, irrespective of the fact that in a variety of experiments the polymerization taking place in the emulsion phase below the organic layer exhibited living characteristics, *i.e.* a linear dependency of the number average molar mass on conversion.

Table 6.1: Overview of anionically stabilized miniemulsions[a)]

stabilization type	anionic
surfactant	SDS
monomer	styrene, BMA, EHMA
costabilizer	hexadecane, PS, Kraton
initiator	KPS, KPS/$Na_2S_2O_5$, AIBN, V-40, AIBN/V40
RAFT agent	**1**,**2**,**3**

a) These recipes typically apply 80 g water; 20 g monomer; 0.2 g surfactant; 0.2–0.5 g costabilizer; 0.2–0.6 g RAFT agent (2–4 g for **4** and **5**) and 0.1–0.2 g initiator.

Table 6.2: Anionically stabilized miniemulsions. Recipe details.

Experiment	AI-1	AI-2	AI-3	AI-4	AI-5	AI-6	AI-7
Monomer[a)] (g)	19.65	20.40	19.60	19.60	19.50	20.00[a)]	20.00[a)]
RAFT agent[b)] (g)	–	0.19	0.18	0.19	0.18	0.50	0.50
Water (g)	80.0	83.0	90.0	90.0	80.0	80.0	80.0
KPS (g)	0.12	0.11	0.14	0.25	0.14	0.20	0.20
SDS (g)	0.23	0.24	0.23	0.23	0.23	0.25	0.25
Hexadecane (g)	0.40	0.41	0.40	0.40	0.78	0.40	0.40
Fremy's Salt (g)	–	–	–	–	0.054	–	–
Sodium Bisulfite (g)	–	–	0.13	0.22	0.19	–	–

a) monomer is styrene except in AI-6 (EHMA) and AI-7 (BMA).
b) RAFT agent **2** was used.

Table 6.1 and Scheme 6.2 summarize the various monomers, RAFT agents and costabilizers that were used in combination with SDS in order to investigate this peculiar polymerization behavior.

6.2.1. Kinetics

To establish a basis for comparison of the accumulated data from RAFT experiments, a conventional styrene miniemulsion was performed in the absence of RAFT (AI-1). The recipe consisted of a typical miniemulsion concentration of SDS surfactant (0.01 mol·dm^{-3} H_2O) and a somewhat low concentration of KPS initiator (0.005 mol·dm^{-3} H_2O). This initiator concentration was chosen such that, when RAFT was added, transfer to RAFT agent or dormant RAFT polymer chains would dominate over bimolecular termination.[32] Table 6.1 provides a global overview of the ingredients used in the anionically stabilized miniemulsions while table 6.2 shows a more detailed description of the first series of miniemulsion polymerizations. A sample taken from AI-1 prior to initiation was monitored on shelf for several weeks with no visible monomer cream line, indicating a stable miniemulsion recipe. The miniemulsion recipe was then expanded to include RAFT agent **2** (see Scheme 6.2), with all other concentrations held constant (AI-2). In this manner, the effect of this RAFT agent on an otherwise stable system could be studied.

The conversion–time plots for the styrene polymerizations with and without **2** are given in Figure 6.1. A large drop in reaction rate is evident when comparing AI-1, (□, blank) to AI-2 (■, same recipe including **2**). In principle the nucleation of

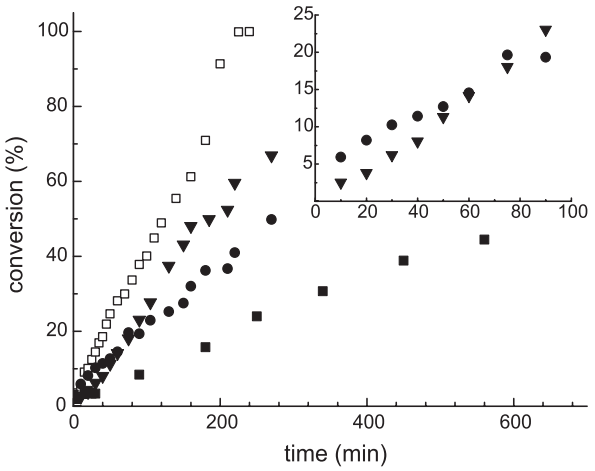

Figure 6.1. Conversion–time plots for miniemulsion polymerizations of styrene carried out at 75 °C, initiated by KPS. AI-1 (□), 'blank'. AI-2 (■), w/ RAFT. AI-3 (●), w/ RAFT & redox. AI-4 (▼), w/ RAFT & double redox.

the particles should be the same with and without RAFT agent. The decrease in rate can be attributed to two factors: ① exit of the transfer derived radical R (see Scheme 6.2) to terminate with radicals in the aqueous phase or termination by re-entry into a particle already containing a growing chain,[33,34] or ② termination of the entering propagating radical with the intermediate radical.[35] Based on the partitioning of radical R between the monomer and water phase, the large size of the droplets and the rate coefficient for re-initiation of radical R to monomer, the probability of exit is very low.[34,36] To further support this, the RAFT agent will be consumed within the first few percent of conversion (since $C_T \approx 6000$)[37]. Once the RAFT is consumed exit becomes even less probable due to the hydrophobicity and the low diffusion coefficient of the oligomeric chain, and should no longer affect the reaction rate. This suggests that retardation when **2** is added to the miniemulsion is due to termination of the intermediate radical, which has been shown to be the most likely mechanism at play in retarding the rate in bulk and solution experiments (page 43).[35]

A long polymerization time is not suprising, considering the relatively low propagation rate constant (k_p) for styrene[38] at 75 °C (563 $dm^{-3} \cdot mol^{-1} \cdot s^{-1}$), the low entry rate (ρ) of persulfate initiated chains in styrene macroemulsions[4] and the low initiator concentration. However, when this slow rate is exacerbated by the retardation mechanisms described above, KPS decomposition becomes an issue at relatively low conversions. This is seen more clearly in Figure 6.2 where the experimental molar mass of polymerization AI-2 (styrene/RAFT) is compared to theoretical calculations. The solid points are the experimental values for the

number-average molar mass ($\overline{M}_n$) corresponding to the appropriate monomer conversion. The solid line represents the theoretical molar mass as calculated using Eq. 6-4,

$$\overline{M}_{n,\,th} = FW_{RAFT} + \frac{x \cdot [M]_0 \cdot FW_M}{[RAFT]_0} \qquad \textbf{(6-4)}$$

in which FW_{RAFT} is the molar mass of the RAFT agent that constitutes the end groups of the polymer chain; FW_M is the molar mass of a single monomer unit; x equals the fractional conversion, $[M]_0$ and $[RAFT]_0$ are the initial concentrations of the monomer and the RAFT agent in the droplets. Eq. 6-4 only accounts for RAFT-derived chain growth and neglects any products from radical–radical termination.

The dashed curve in Figure 6.2, calculated with Eq. 6-5, also represents a theoretical molar mass but additionally accounts for termination products. Their contribution can be quantified by the amount of initiator decomposed over the reaction time corrected by two efficiency factors and assuming termination by combination. $[I]_0$ is the initial concentration of initiator.[39] f_I is the initiator efficiency for addition of initiator radicals to monomer and f_{entry} is the efficiency of entry, *i.e.* the probability for a chain to enter a particle before aqueous phase termination occurs. Furthermore Eq. 6.5 requires k_d, the decomposition rate coefficient for initiator in the aqueous phase, $[M]_w$ the monomer concentration in the aqueous phase,[39] $k_{t,\,aq}$ the termination rate coefficient in the aqueous phase, z is the lowest number of monomer units required for the oligomer to be surface active, t is time in seconds and $[I]_w$ the initial concentration of initiator in the aqueous phase.[39]

$$\overline{M}_{n,\,theory} = FW_{raft} + \frac{x \cdot [M]_0 \cdot FW_M}{[RAFT]_0 + 2 \cdot f_I \cdot f_{entry} \cdot [I]_0 \cdot (1 - e^{-k_d t})} \qquad \textbf{(6-5)}$$

with: $$f_{entry} = \left(\frac{\sqrt{k_d \cdot [I]_w \cdot k_{t,\,aq}}}{k_{p,\,aq} \cdot [M]_w} \right)^{1-z}$$

Note that both Eq. 6-4 and Eq. 6-5 assume rapid and complete conversion of the RAFT agent into dormant species, a condition that, under normal circumstances, will be obeyed after a few percents of monomer conversion for the RAFT agents applied in this study.

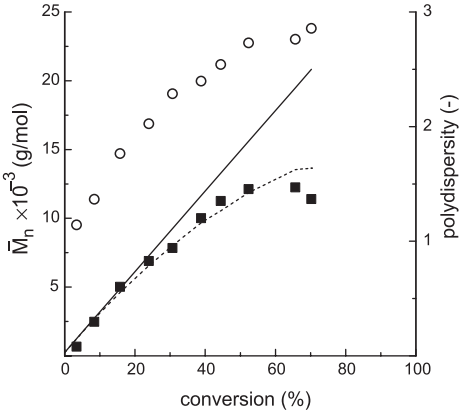

Figure 6.2. Number-average molar mass for miniemulsion polymerizations of styrene carried out at 75°C in the presence of SDS and RAFT, initiated by KPS (AI-2). Experimental $\overline{M}_n$ (■, *left axis*), Theoretical $\overline{M}_n$ accounting only for RAFT derived chains (—, *left axis*), Theoretical $\overline{M}_n$ accounting for RAFT derived chains and initiator derived chains (---, *left axis*). Polydispersity index (O, *right axis*)

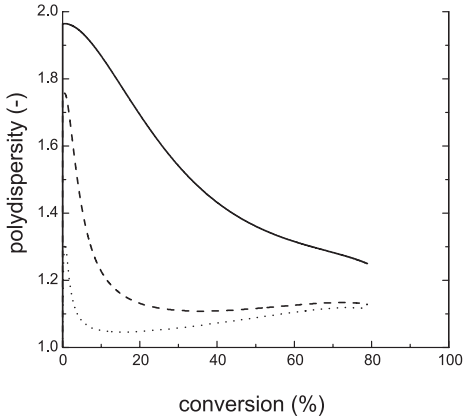

Figure 6.3. Simulations of the polydispersity index using Müller's equation.[40] Transfer constant (C_T) equals $6{\cdot}10^3$ (—), $6{\cdot}10^4$ (---) and $6{\cdot}10^6$ (·····).

Under most circumstances the second term of the denominator in Eq. 6.5 can be neglected relative to the concentration of RAFT agent since typical recipes apply a small amount of initiator compared to RAFT agent. The ratio of these two ingredients governs the amount of dead material as indicated by formula 6-6:

$$n_L = 1 - n_D = \frac{[RAFT]_0}{[RAFT]_0 + 2 \cdot f_I \cdot f_{entry} \cdot [I]_0 \cdot (1 - e^{-k_d t})} \qquad \textbf{(6-6)}$$

where n_L and n_D are the number fractions of living material and dead material, respectively. Terminated material not only excludes itself from further polymerization procedures (*e.g.* block copolymer preparation) but it also causes a broadening of the molar mass distribution. When the polymer molar mass and the maximum acceptable level of dead material are set, Eq. 6-5 and Eq. 6-6 give the ratio of monomer, RAFT agent and initiator. In solution and bulk polymerizations when a relatively pure or high molar mass material is desired this often leads to extremely low polymerization rates. With respect to the rate of polymerization, the situation is expected to be more favorable in dispersed systems where termination is reduced due to radical compartmentalization.

There are several points to be attention to with respect to Figure 6.2. Until roughly 25% monomer conversion, the theoretically derived molar mass relationship described by Eq. 6-4 is in good agreement with the experimentally observed molar mass. The linear relationship of $\overline{M}_n$ with conversion, matching theory, indicates living polymerization behavior. From roughly 25% conversion onward the experimentally determined $\overline{M}_n$ falls below the solid theoretically derived curve from Eq. 6-4. The data are now better approximated, however, by taking into account the presence of initiator-derived chains as described in Eq. 6-5. Due to the drastic retardation there is little conversion of monomer to polymer after approximately 70% but there is still an increase in the number of chains from initiator decomposition, thus the number average molar mass decreases.

More significant to note is the trend in the polydispersity index (○, *right axis*) which increased with conversion and reaction time. Figure 6.2 demonstrates that the polydispersity increases from a value of 1.1 (4% monomer conversion) to a final recorded value of 2.9 at 70% conversion. Theoretically,[40] in RAFT living systems, polydispersity should decrease with conversion ending close to unity upon full conversion if termination is negligible, *i.e.* if the number of initiator derived chains is small compared to the number of dormant chains. Using the method of moments derived by Müller *et al.*,[40] the theoretical profile of polydispersity is calculated in Figure 6.3 for the conditions of this run. The simulated polydispersity show that the system should in fact exhibit a decrease in polydispersity after the consumption of the RAFT agent. Also depicted in Figure 6.3 is the effect of the rate of consumption of the RAFT agent on the polydispersity. When C_T (= k_{tr}/k_p) is increased, the RAFT agent is consumed faster and the polydispersity is maintained at a lower value. The significance of this figure is that, in theory, the polydispersity of this system should be decreasing, in contrast to what is observed experimentally. The results given in Figures 6.2 and 6.3 reveal that initiation is a factor that cannot be ignored, and that it has a significant effect on the polydispersity.

A further observation from this data set that is not seen numerically, but that most definitely plays a role in the trends seen in Figure 6.2, is a distinct visual indication of an unstable miniemulsion, which has also been observed in macroemulsions[29,30] and in the preliminary experiments (page 144). The red organic phase slowly increases in volume making accurate sampling of the conversion impossible at longer reaction times. This stability issue will be discussed in more detail in section 6.2.2 and is stated at this point for the reader to better understand the phenomena that lead to the results presented in Figure 6.2.

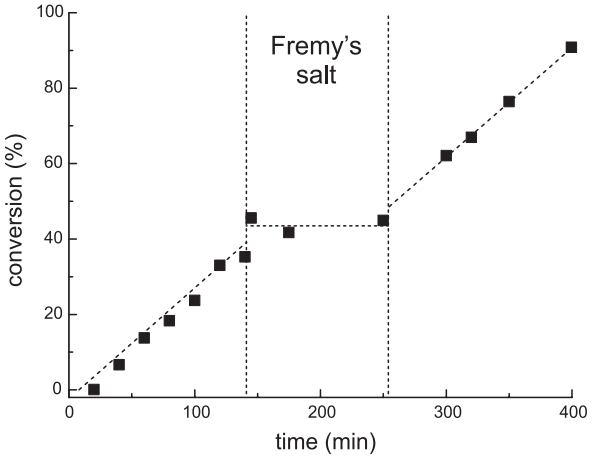

Figure 6.4. Conversion–time plot for AI-5 (■); miniemulsion polymerization of styrene using a redox system in the presence RAFT. Fremy's Salt was added at 45% conversion. (Note: the dotted line is a trend line, not a fit.)

The results from AI-2 suggest inefficient nucleation of the initial monomer droplet distribution due to the drastic retardation and the appearance of a red layer. To determine whether the red layer is caused by the low rate of polymerization a redox couple was added. Since a catalytic redox agent was not desired, but instead one that would merely aid in faster decomposition of KPS, sodium metabisulfite was chosen as the couple (AI-3). Its expediting action is confirmed by the addition of Fremy's Salt (potassium nitrosodisulfonate) at roughly 40% monomer conversion (AI-5, Figure 6.4). Potassium nitrosodisulfonate is a stable nitroxide radical that partitions strongly in the aqueous phase and will scavenge any carbon-centred radicals. It is modurately soluble in the droplets, so it may also terminate active chains in the particles. In Figure 6.4, monomer conversion is shown with the region of Fremy's Salt addition through to its consumption indicated. The Fremy's Salt did in fact stop the polymerization for roughly 100 min, *i.e.* the point at which it was fully consumed, after which polymerization continued at a similar rate to that prior to addition of Fremy's salt. This confirmed that the redox system is indeed an accelerator for initiator decomposition, and also allowed an approximate k_d value for the decomposition of initiator to be calculated, which is a required input parameter for the approximation of the number average molar mass by Eq. 6-5.

For the first 10% of monomer conversion (referring again to Figure 6.1), AI-3 (●, with RAFT and redox) showed no significant decrease in rate compared to AI-1 (□, no RAFT, no redox) of the same recipe and conditions. From 10% conversion onward, the rate of AI-3 (●, with RAFT and redox) was found to be less than that of the AI-1 (□, no RAFT, no redox), yet still markedly higher than that of AI-2 (■, RAFT system without redox). Assuming the same number of droplets initially

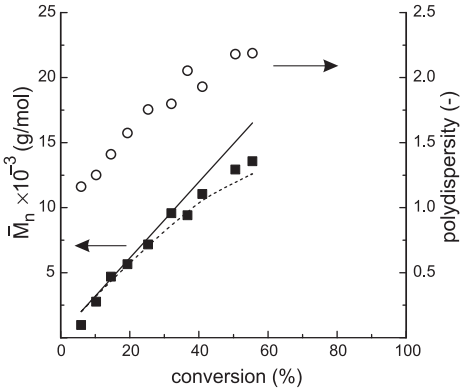

Figure 6.5. Number-average molar mass for miniemulsion polymerizations of styrene carried out at 75°C in the presence of SDS, RAFT agent **2** initiated by a redox couple (AI-3). Experimental $\bar{M}_n$ (■, *left axis*). Theoretical $\bar{M}_n$ accounting for RAFT derived chains only (—, *left axis*). Theoretical $\bar{M}_n$ accounting for RAFT derived chains and initiator derived chains (---, *left axis*). Polydispersity (O, *right axis*)

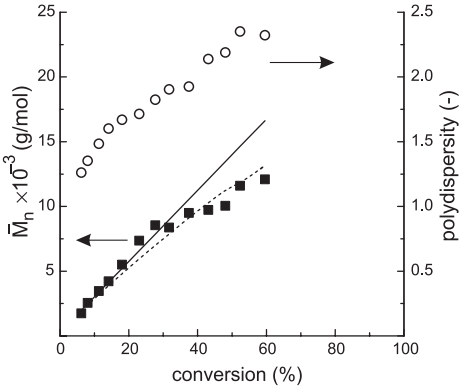

Figure 6.6. Number-average molar mass for miniemulsion polymerizations of styrene carried out at 75°C in the presence of SDS, RAFT agent **2** initiated by a redox couple (AI-4, [KPS] doubled from Figure 5). Experimental $\bar{M}_n$ (■, *left axis*). Theoretical $\bar{M}_n$ accounting for RAFT derived chains only (—, *left axis*). Theoretical $\bar{M}_n$ accounting for RAFT derived chains and initiator derived chains (---, l*eft axis*). Polydispersity (O, *right axis*)

present for both reactions, this indicated that a larger percentage of the initial droplet populatio was nucleated, effectively increasing the reaction rate. Figure 6.5 illustrates several beneficial effects of the redox agent on the evolution of the molar mass and polydispersity. Similar to the case without redox, the experimental molar mass agrees with the theoretically derived relations, yet with an increased reaction rate the disparity between the curve derived from Eq. 6-5 and the line described by Eq. 6-4 is less pronounced. Molar mass again showed contributions from initiator-derived chains and the polydispersity still has an upward trend. However, the polydispersity with redox initiation increased more slowly than that seen in Figure 6.2 (no redox, AI-1) and when it is compared at a monomer conversion of roughly 50% (2.18 in Figure 6.2 and 2.73 in Figure 6.5), the benefit of a greater number of droplets being nucleated is evident.

When the radical flux of the redox system was increased (by doubling both the concentrations of KPS and sodium metabisulfite), a further increase in polymerization rate was observed (AI-4, ▼, Figure 6.1). In fact, after the first 10% of conversion, the polymerization rate was comparable to that of the control experiment (AI-1). When the two redox systems are compared (inset, Figure 6.1) this becomes even clearer. The rate of the low radical flux recipe (AI-3, (●) is considerably higer

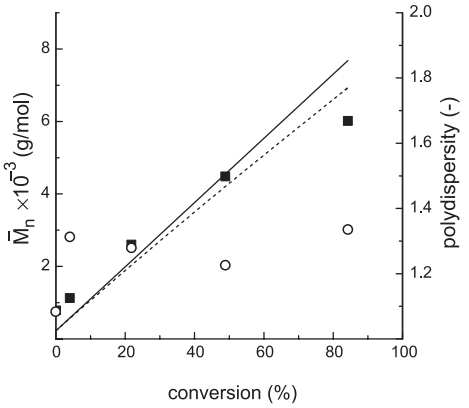

Figure 6.7. Number-average molar mass for mini-emulsion polymerizations of EHMA carried out at 75 °C in the presence of SDS, RAFT agent **1** initiated by KPS (experiment AI-6). Experimental $\bar{M}_n$ (■, *left axis*). Theoretical $\bar{M}_n$ accounting for RAFT derived chains only (—, *left axis*). Theoretical $\bar{M}_n$ accounting for RAFT derived chains and initiator derived chains (---, *left axis*). Polydispersity (O, *right axis*)

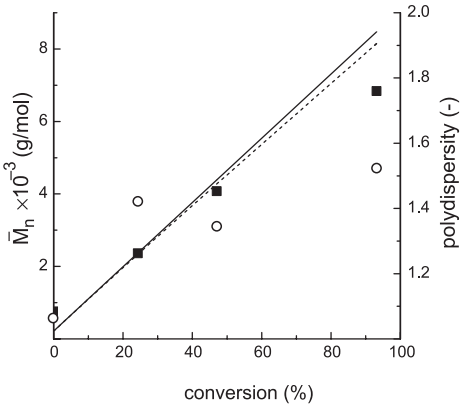

Figure 6.8. Number-average molar mass for mini-emulsion polymerizations of BMA carried out at 75 °C in the presence of SDS, RAFT agent **1** initiated by KPS (experiment AI-7). Experimental $\bar{M}_n$ (■, *left axis*). Theoretical $\bar{M}_n$ accounting for RAFT derived chains only (—, *left axis*). Theoretical $\bar{M}_n$ accounting for RAFT derived chains and initiator derived chains (---, *left axis*). Polydispersity (O, *right axis*)

than that of the recipe with the higher radical flux (AI-4, ▼) up to a conversion of roughly 14%, where the two profiles cross. The most probable explanation for the slower start of the higher radical flux run is a larger probability of termination in the aqueous phase, after which the rate is higher presumably due to a larger number of droplets nucleated. Conversion measurements after long reaction times in the redox reactions are not shown in Figure 6.1 as the formation of coagulum prevented accurate sampling.

A decrease of the ratio of [RAFT]/[KPS] will increase the amount of chains terminated by radical–radical reactions, and consequently produce a broader molar mass distribution as dictated by Eq. 6-6. This does not seem to be the case when the trends shown in Figure 6.6 are compared to those of Figure 6.5. The increase in radical flux of the system does not seem to have markedly affected the $\bar{M}_n$ or polydispersity. This is not unexpected since by increasing the number of particles, through a more efficient nucleation process, the entry rate (ρ) decreases and so does the amount of radical–radical termination[4].

In order to determine if the loss of colloidal stability is specific to styrene polymerizations, two experiments (AI-6 & AI-7) were performed keeping all other recipe concentrations constant while substituting methacrylic monomers for styrene

and substituting RAFT agent **1** for **2**. Methacrylates have higher propagation rate constants than styrene at 70 °C ($k_{p,styrene}$=440, $k_{p,BMA}$=1220 and $k_{p,EHMA}$=1470 $dm^{-3} \cdot mol^{-1} \cdot s^{-1}$).[41] The results indicated that macromolecular control with the methacrylates was much more easily achieved. Figure 6.7 and 6.8 both show the polydispersity to remain below 1.5, a dramatically lower value than that found in any of the styrenic systems, but regardless of better control the same miniemulsion destabilization phenomena were observed. With the higher reaction rate, the appearance of the red organic layer was much more immediate and up to 35 % of the organic material was lost to coagulation. This illustrates that the destabilization of the droplets is not related to the monomer type and seems to correlate to the reaction rate.

The next section attempts to investigate this behavior in anionically stabilized miniemulsions more thoroughly, while the use of other surfactants is discussed later in this chapter (starting on page 159).

6.2.2. Conductivity & pH Considerations

In an ideal stable miniemulsion, there should be no change in aqueous phase conductivity since there is negligible change in interfacial area, and consequently little rearrangement of surfactant[43,44]. Conversely, in a conventional (macro)emulsion the larger monomer droplets serve as reservoirs continually diffusing monomer across the continuous phase to the locus of polymerization in nucleated micelles. As these reservoirs are depleted, the total interfacial area in the system decreases and surfactant desorbs from the particle interface resulting in an increase in conductivity[44]. This is the theoretical foundation behind the conductivity experiments. Since a stable miniemulsion should exhibit a flat conductivity profile over conversion (all other factors constant, such as pH), an increase would indicate SDS being expelled from the particles into the aqueous phase. This may be the cause of the destabilization phenomena observed in the anionically stabilized systems.

Section 6.1.2 (page 136) made clear that the preparation of a miniemulsion typically leaves nothing more than a low equilibrium concentration (below the critical micelle concentration) of surfactant in the water phase and put the droplets in a critically stabilized situation. Coalescence slowly leads to a colloidally more stable situation without releasing surfactant to the continuous phase. With the

Table 6.3: Anionically stabilized miniemulsions. Recipe details.

Experiment	AI-8	AI-9	AI-10	AI-11	AI-12	AI-13	AI-14
Monomer[a)] (g)	14.83	14.83	14.83	14.83	22.26	14.66	14.66
RAFT agent (g)	–	–	0.14	0.14	0.21	0.14	1.37
Water (g)	60.0	60.0	60.0	60.0	90.0	60.0	60.0
KPS (g)	–	–	–	–	0.26	0.16	0.16
SDS (g)	0.17	0.17	0.17	0.17	0.27	0.17	0.17
Hexadecane (g)	0.30	0.30	0.30	0.30	0.53	0.30	0.30

a) monomer is styrene except in AI-9, AI-11 and AI-14 (EHMA).

excessive phase separation occurring in these miniemulsions it would be interesting to see how the conductivity evolves as this may yield information on the fate and the whereabouts of the surfactant during this process.

The first series of conductivity experiments (Table 6.3) compared the stability of miniemulsions on shelf to those of the same recipes when polymerized. The shelf experiments are miniemulsions without initiator that are stirred and kept at ambient temperature. Samples were taken over typical reaction times with further samples taken up to a time of three days. The shelf samples are all seen as a cluster of flat lines in the lower portion of Figure 6.9. These shelf experiments included 'blank' runs and those in the presence of RAFT for both styrene (experiments AI-8 and AI-10) and (2-ethyl)hexyl methacrylate (EHMA, experiments AI-9 and AI-11). Styrene was chosen due to the most pronounced level of instability observed in its miniemulsion RAFT systems, and EHMA was chosen for comparison purposes to see if instability was in any part a function of monomer characteristics. The flat profiles of all these shelf experiments suggest that the interaction of RAFT with other reagents is not a significant issue until polymerization is started. However, even in shelf samples, a small degree of instability was observed in the slow formation of a monomer cream line. The styrene shelf sample that included RAFT (Figure 6.9, □), showed a slight increase in conductivity but only after a shelf time of over 500 minutes. It should be noted that these shelf experiments were not under agitation.

Reacted samples, however, showed clear signs of an increase in surfactant concentration in the aqueous phase during polymerization, as evident in their increasing conductivity profiles in Figure 6.9. The styrene/RAFT miniemulsion polymerization at a reaction temperature of 75°C (AI-13, +) showed a more

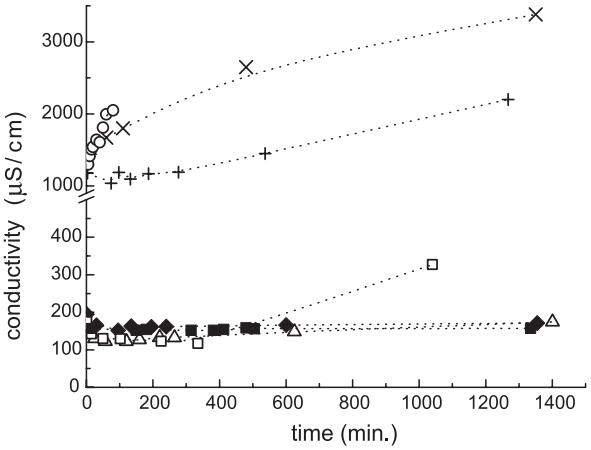

Figure 6.9. Conductivity of several styrene and EHMA miniemulsions 'on the shelf' (experiment AI-8, △; AI-9, ◆; AI-10, □; AI-11, ■) and during polymerization. (AI-12, ×; AI-13, +; AI-14, ○). See table 6.3 for experimental details.

dramatic increase in conductivity than that of the same reaction conducted at a reaction temperature of 45 °C (experiment AI-12, ×). The reaction involving EHMA and RAFT (experiment AI-14, ○) exhibited the fastest increasing conductivity. It seems that the conductivity increases in these reactions in a proportional manner to the rate of polymerization, similar to the correlation between the appearance of an organic phase and the polymerization rate.

The fact that the shelf experiments including RAFT did not show significant signs of increasing conductivity, while all reaction experiments did, leads to the conclusion that the destabilization is not only a matter of an incompatibility of the RAFT with typical emulsion components. Moreover, it suggests the key factor behind the observed destabilization has partially to do with oligomer formation which is the only distinction between the shelf and reaction experiments besides the temperature difference. The latter was found not to be important as tested by several verification experiments that were kept at higher temperatures.

An interesting point to note, however, is that when a styrene 'blank' polymerization (AI-8) was monitored for conductivity, the profile showed a downward trend over conversion eventually flattening out late in the reaction (not shown). This 'blank' was initiated by KPS, which is known to hydrolyze into sulfuric acid in an aqueous environment over time.[45] This effectively lowers the pH of the reaction medium with a profound effect on conductivity. In addition, the hydrolyzed form of KPS is no longer ionic – also affecting the conductivity towards lower values. For these reasons, sodium bicarbonate was added as a pH buffer and new reactions were again measured for conductivity, as shown in Table 6.4 and Figure 6.10.

Table 6.4: Anionically stabilized miniemulsions used for conductivity measurements.

Experiment	AI-15	AI-16	AI-17	AI-18	AI-19	AI-20	AI-21
Styrene (g)	21.91	14.12	17.11	20.00	19.80	19.65	19.35
RAFT agent (g)	–	0.13	0.16	–	0.20	0.35[a)]	0.65[a)]
Water (g)	90.0	60.0	70.0	80.0	80.0	80.0	80.0
Initiator[b)] (g)	0.24	0.16	0.56[b)]	–	–	–	–
SDS (g)	0.26	0.17	0.20	0.25	0.25	0.25	0.25
Hexadecane (g)	0.44	0.30	0.34	0.40	0.40	0.40	0.40
Sodium hydrogencarbonate (g)	0.09	0.06	0.07	–	–	–	–

a) These samples utilized an oligostyrene RAFT agent with degree of polymerization of 2 (AI-20) and 5 (AI-21).
b) Potassium persulfate is used as initiator except in AI-17, where AIBN was used.

In a buffered environment, after an initial increase in the first 25 minutes, the conductivity profile for the styrene 'blank' reaction (AI-15, □) in miniemulsion remained flat, as expected. The initial short lived rise in conductivity might be due to reactor contents coming to temperature. In a buffered environment the styrene RAFT miniemulsion polymerization, stabilized by SDS and initiated by KPS, showed no notable change in conductivity over the reaction timeframe (AI-16, ◆, Figure 10). Actually, the conductivity profile looked strikingly similar to the experiment without RAFT. This was a striking observation as the same recipe without buffer was found to be the most unstable. Even more significant is the appearance of the red organic phase in the vortex of the buffered styrene/RAFT miniemulsion polymerization although the conductivity was observed constant.

In attempt to rule out the sulfate group of the KPS initiator as a contributor to the RAFT destabilization phenomenon, a number of miniemulsion polymerizations were performed using 2,2'-azobisisobutyronitrile (AIBN) and 1,1'-azobis(1-cyclohexanecarbonitrile) (V-40) which are azo initiators that partition preferentially into the droplet phase. These miniemulsions differ from those initiated by KPS in several aspects. First of all, dissociation of these initiators does not change the pH. Second, the oligomers formed upon initiation are nonionic species so that there is no conflict between sulfate end-capped oligomers with the equally charged SDS surfactant. Third, oil phase initiation will suppress homogeneous nucleation if this would be present in the first place. Experiment AI-17 (●, Figure 6.10) is an example of such a polymerization. KPS was in fact proven not to be a large contrib-

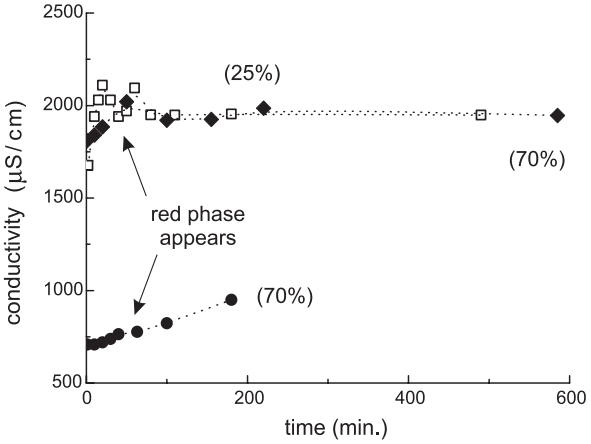

Figure 6.10. Conductivity of miniemulsion polymerizations of styrene under buffered conditions. 'blank' (AI-15, □), KPS w/ raft (AI-16, ◆), AIBN w/ raft (AI-17, ●). Conversion between brackets. See table 6.4 for experimental details.

utor (if at all) to the destabilization in these ionically stabilized systems. Even when initiated by AIBN, the same signs of destabilization and formation of the red organic layer were observed.

To achieve efficient nucleation of all particles, the radical flux was varied by changing the initiator from AIBN to V-40. While the stability remained poor it was found that the rate at which the organic layer was formed was (again) correlated to the speed of reaction; faster reactions exhibited faster formation of a separate organic phase.

It should also be noted here that the majority of radicals that partake in the polymerization are not derived from the initiator but originate from the applied RAFT agent. Its fast exchange reactions combined with its high concentration relative to that of the initiator causes the majority of both propagating and dormant species to have the R group, which was originally attached to the RAFT agent (Scheme 6.2), as end-group. Different RAFT agents (**1**, **2** and **3**) did not have any significant effect on the phase separation. Only when polymeric RAFT agents were used (**4** and **5**) some improvement could be observed. In these experiments the organic phase was much smaller in size and only slightly colored. The high weight fraction of polymeric species in the organic phase during the preparation of these miniemulsions disqualifies these experiments as suitable material to compare with the other polymerizations. This high weight fraction (up to 40%) is required to reach a comparable *molar* concentration of RAFT agent.

All the evidence presented points to the fact that phenomena occurring during the first few percents of conversion are the most pertinent to the destabilization of the miniemulsion. In this conversion period, small oligomers are created and exit into the aqueous phase is possible, thus forming the red organic layer. A distinct difference between these RAFT miniemulsion systems and traditional miniemulsion systems in the first few percent of monomer conversion is the chain length of polymer and the number of chains. In a traditional miniemulsion, much higher molar mass polymer would be formed when compared to that of a RAFT system at the same reaction time. If the particle interface were to undergo a great deal of traffic, as is the case with exit and re-entry of species at very low conversion, the presence of higher molar mass material would be expected to aid in the particle stability. However, when a small amount of polystyrene ($\overline{M}_w \approx 3\times10^5\,\mathrm{g\cdot mol^{-1}}$) is added to the organic phase no improvement in stability could be noted. The presence of oligomers therefore seems to be more disastrous than the lack of high molar mass material.

To test the conjecture that dormant oligomers are the key factors behind most of the discussed phenomena, the conductivity of miniemulsions in the presence of specially prepared oligomeric species was monitored in static experiments designed to mimic stages of a miniemulsion. Conditions of these runs were similar to the previously discussed shelf conductivity experiments, yet the contents were stirred under argon (without heating) and were monitored for over three weeks. The synthesized oligomers were prepared by solution polymerization from a reaction of 0.2 g of RAFT with styrene and AIBN. The isolated oligomers were dissolved in the usual organic medium of styrene and hexadecane while the amount of styrene was adjusted in such a way that the total mass of dormant species, RAFT and styrene was the same as would be in an actual polymerization. These miniemulsions however, were not polymerized, but the conductivity of these systems was monitored over time without reaction taking place. This data set consisted of a 'blank' (AI-18), a normal RAFT experiment (AI-19), a synthesized short dormant oligomer (AI-20, average of 2 monomer units), and a synthesized long dormant oligomer (AI-21, average of 5 to 6 monomer units).

Just from the conductivity data in Figure 6.11, it can be concluded that the RAFT agent does in fact play a role in destabilization and the longer it grows the smaller the effect. Apparently the length of oligo2 (the longer synthesized oligomer) is already such that the added stability through its contribution to the osmotic pressure is at least as large as its destabilization effect. That is, the oligo2

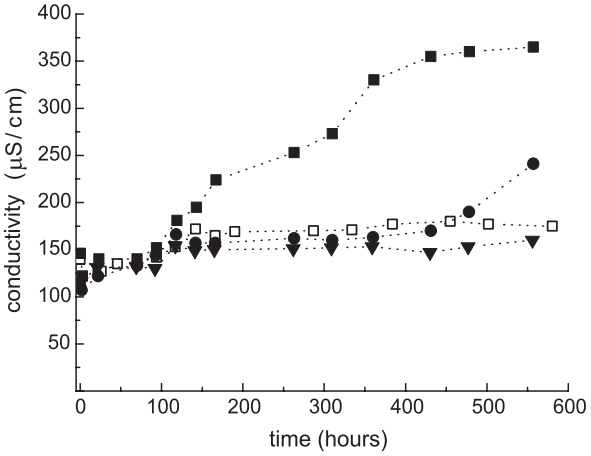

Figure 6.11. Conductivity of miniemulsion polymerizations of styrene carried out in the presence of different RAFT agents. AI-18 (□), no RAFT. AI-19 (■), raft. AI-20 (●), with short oligomers. AI-21 (▼), with longer oligomers. Experimental details are given in table 6.4

curve is remarkably similar to the 'blank' curve on Figure 6.11. However, conductivity does not divulge everything as the reactor contents showed clear signs of the red organic phase within a few hours while the conductivity of oligo1 (the short synthesized oligomer) does not show signs of instability until around 3 weeks after the inception of the experiment.

Possibly a more significant observation is that destabilization is observed at a maximum when RAFT miniemulsions are initiated. This destabilization effect is also observed much faster than seen in any of the 'static' experiments. This suggests that the destabilization is due to more than just the *presence* of oligomeric species because in the reaction experiments polymers grow to the 'stable' oligo2 chain length (roughly 5 monomer units) quite rapidly.

6.3. Cationic Surfactants

In an attempt to circumvent this stability issue, a different stabilization strategy was adopted from literature where it was shown that cetyl trimethyl ammonium bromide (CTAB), a cationic surfactant, could stabilize miniemulsions with an efficiency similar to that of SDS.[48] A series of miniemulsions was conducted employing this surfactant and 2,2'-azobis[2-methyl-N-(2-hydroxyethyl)propionamide] (VA-086) as initiator (Table 6.5). Again stable miniemulsions were obtained after sonication but phase separation was induced by the polymerization. Similar variations were made in the choice of hydrophobe and RAFT agent as in the series of SDS experiments, all with similar results in terms of stability. These systems typically react until the monomer is depleted from the 'emulsion phase'. In

Table 6.5: Cationically stabilized miniemulsions [a)]

stabilization type	cationic
surfactant	CTAB
monomer	styrene
costabilizer	hexadecane, PS, Kraton
initiator	VA-086, AIBN, V-40
RAFT agent	**2**,**3**,**4**,**5**

a) These recipes typically apply 80 g water; 20 g monomer; 0.2 g surfactant; 0.2–0.5 g costabilizer; 0.2–0.6 g RAFT agent (2–4 g for **4** and **5**) and 0.1–0.2 g initiator.

the end situation the organic layer would contain up to 40% of the total amount of monomer of which a substantial part had been polymerized. The emulsion material itself was of very low molar mass and had a multimodal distribution. In these experiments, polymeric RAFT agents (Scheme 6.2, agents **4** and **5**) were also investigated but these could not completely suppress the instability. Although the dithiobenzoate moiety was attached to a hydrophobic polymer chain, trapped in the droplet phase, a small organic phase with a light red color was formed.

6.4. Nonionic Surfactants

The third alternative way to stabilize miniemulsions comprises the use of nonionic surfactants. Recent literature reports the successful application of such surfactants in polymerizable miniemulsions.[48,49] A variety of nonionic surfactants was used in conjuction with hexadecane (alone or in combination with Kraton) as the hydrophobe. Application of surfactants with relatively high HLB values (15.3–17.8) in most cases led to stable miniemulsions. Samples taken from the unreacted emulsions were monitored for at least a week and during this period only a few cases showed some signs of creaming or destabilization after 4 to 5 days; the majority remained homogeneous to the eye. These miniemulsions typically reacted in the absence of an organic layer. Under some circumstances minor phase separation was observed 10 to 20 minutes after the start of polymerization, but quickly thereafter it would disappear without notable effect on the molar mass distribution and without the formation of any coagulum. The products from the polymerizations were stable for at least several months. The results of several such polymerizations are discussed in the sections ‘controlled polymerization’ (page 162) and ‘block copolymers’ (page 166).

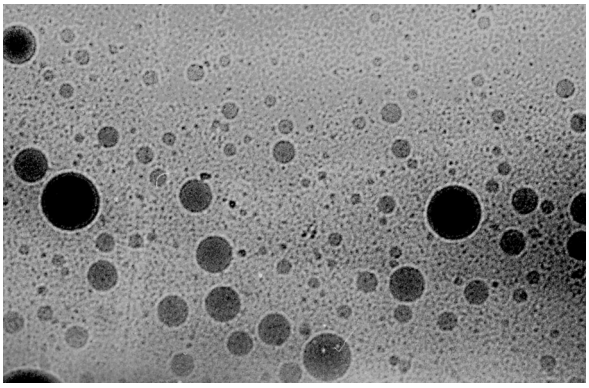

Figure 6.12. Cryo TEM image of a polymerized miniemulsion, stabilized by Igepal890, a nonionic surfactant (NI-2, see table 6.7). The number average particle size is 290 nm, but the distribution is of high polydispersity, possibly caused by monomer migration in the early stages of the polymerization.

The reason why nonionic surfactants are able to provide enough stability where the ionic surfactants fail is not clear. The investigations with the miniemulsions using SDS were particularly in depth, but using alternative ingredients for each and every one of the miniemulsion components could not reveal the particular perpetrator. Moreover, Matyjaszewski *et al.*[20] report strikingly similar observations of instability in studies of ATRP polymerizations in dispersed media and El-Aasser *et al.*[19] report data that imply similar instability phenomena are occurring in nitroxide mediated living miniemulsion polymerization, which indicates that the cause should not be sought in the specific RAFT chemistry. The only literature that does not indicate instability phenomena is that of RAFT agents (of the xanthate type)[28] or degenerative transfer agents (e.g. perfluorohexyl iodide),[24] however, polydispersity stays relatively high (1.5–3.2).[30,46] The distinction between the alkyl iodide system and the RAFT agents of this chapter is the activity of the chain transfer agent ($C_{T,styrene}$ = 1 to 1.4 for $C_6F_{13}I$)[23,47] which dictates that the molar mass at low conversions is close to the final $\overline{M}_n$ when using a RAFT agent with a very high C_T[40]. This further emphasizes the role of oligomers in the destabilization phenomena seen in (mini)emulsion polymerization with highly active chain transfer agents. When different stages occurring in such a polymerization were simulated by predissolving oligomers in the organic phase (AI-18 to AI-21) the stability was affected on the long run but appeared much better than in an actual polymerization. The only difference between a polymerization and the static experiments with oligomers is the distribution of these species over the droplets. By predissolving them, they are equally divided among the miniemulsion droplets while in a reaction they are generated in large amounts in individual droplets, namely those that are struck by a radical. Due to the high reactivity of the RAFT agent, a single radical can transform a lot of transfer agent molecules into dormant oligomers with a much lower water solubility adding considerably to the osmotic pressure in that particular

Table 6.6: Experimental details homopolymerizations with nonionic surfactants[a)]

ingredient	quantity (g)	quantity (mmol)	type
water	80		
monomer	20	100–200	see table 6.7
surfactant	4.0	2.0	Igepal 890
co-stabilizer	0.40	1.8	hexadecane
initiator	0.20	0.75	KPS
RAFT agent[b)]	0.60	2.5	**1**

a) NI-1 to NI-6
b) no RAFT agent was present in the control experiment NI-1

droplet. Although it is not necessary for a miniemulsion to be in a thermodynamically stable state, an important factor for metastability is an equal chemical potential in all droplets. This condition may be quickly lost as the polymerization commences. Based on all the experimental results gathered in this chapter, the dynamic 'dropwise' generation of oligomers seems to be the most likely cause of the destabilization. Apparently the nonionic surfactants impose better stability on the droplets but the same forces are present in these systems. Support for this hypothesis can be found from the particle size distributions which are broad for miniemulsions with RAFT as can be seen in Figure 6.12.

6.5. Controlled Polymerization

6.5.1. Homopolymerizations & Kinetics

Once stability was guaranteed, miniemulsions could be used as a tool in the preparation of sophisticated polymer architectures. Tables 6.6 and 6.7 provide details on a series of miniemulsions that was conducted in the presence of a nonionic surfactant.

Figure 6.13 shows conversion–time profiles for several miniemulsion polymerizations. When the rate of the experiment without RAFT (NI-1, table 6.7) is compared with that of the same experiment with RAFT (NI-2) it is shown that the addition of RAFT agent to the system causes a large decrease in the rate of polymerization. The reaction rates for the various methacrylates are roughly proportional to their propagation rate constants which have the same order of magnitude. Only the methyl methacrylate (MMA) polymerization showed deviating behavior.

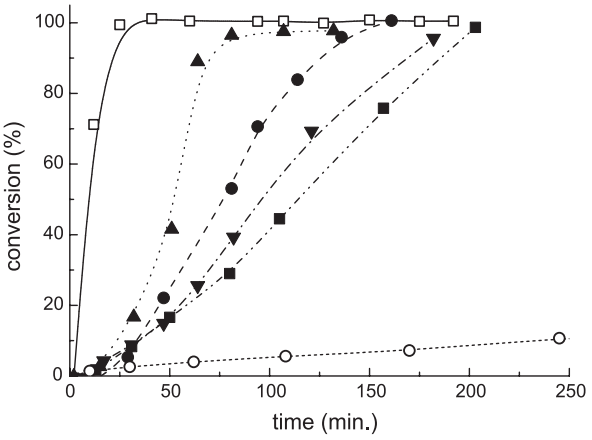

Figure 6.13. Conversion-time profiles for miniemulsion polymerizations: NI-1(□), NI-2(●), NI-3(▲), NI-4(▼), NI-5(■) and NI-6(○). See tables 6.6 and 6.7 for the experimental details of these polymerizations.

Due to its smaller particle size and consequently larger number of particles, it was expected to react faster. It initially, however, starts at a comparable polymerization rate but shows a notable acceleration during the first 40 minutes. It is unlikely that this can be attributed to the gel effect that is quite commonly observed in methyl methacrylate polymerization, since over this time interval the average polymer chain length does not exceed 30 repeat units. For a PMMA sample of such a chain length prepared in solution polymerization, the glass transition temperature (T_g) was found to be 85 °C, well below the literature value for high molar mass material of approximately 110 °C. As the droplets consist of only 20% of this polymeric material dissolved in about 80% of monomer at a reaction temperature of 70 °C, the gel effect is unlikely to occur. Another explanation is that additional particles are generated during this interval. The more hydrophilic MMA monomer and its oligomers may promote homogeneous nucleation and in this way increase the number of particles and thus the reaction rate. The newly formed particles would be deficient in RAFT agent resulting in uncontrolled polymerization. However, no evidence for such a process is found in the molar mass distributions.

The most likely explanation is the increased entry efficiency of MMA compared to *n*-BMA, *i*-BMA and EHMA. It has been calculated that the entry efficiency for MMA and BMA at 50 °C and at a KPS concentration of 0.01 mol·dm^{-3} were 94% and 15%, respectively,[4] and therefore MMA will have a higher average number of radicals per particle compared to BMA. The origin of this effect can be traced back to the greater water solubility of MMA.

Table 6.7: Experimental details for miniemulsions stabilized by nonionic surfactants

number	monomer	time (min.)	x (%)	$\overline{M}_{n,theory}$ ($\times 10^{-3}$ Da)	$\overline{M}_n$ [a)] ($\times 10^{-3}$ Da)	$\overline{M}_w/\overline{M}_n$ (–)	dp (nm)
NI-1	EHMA	25	100	–	>3000	–	–
NI-2	EHMA	29	5	–	–	–	–
		47	22	–	–	–	–
		81	53	4.1	5.4	1.07	–
		94	71	5.4	6.1	1.08	–
		114	84	6.4	6.7	1.08	–
		136	96	7.3	7.3	1.09	–
		161	100	7.6	7.6	1.09	290
NI-3	MMA	32	14	1.3	–	–	–
		51	38	3.2	5.3	1.07	–
		64	84	6.7	7.9	1.15	–
		81	95	7.4	8.3	1.17	160
NI-4	i-BMA	17	4	0.57	–	–	–
		31	9	0.90	2.0	1.10	–
		47	15	1.3	–	–	–
		64	26	2.1	4.9	1.07	–
		82	40	3.1	5.5	1.11	–
		121	70	5.3	6.8	1.19	–
		182	96	7.3	8.2	1.25	300
NI-5	n-BMA	31	8	0.93	–	–	–
		50	17	1.6	–	–	–
		80	29	2.6	4.9	1.06	–
		105	45	3.9	5.5	1.10	–
		157	76	6.5	7.0	1.17	–
		203	99	8.4	8.5	1.20	300
NI-6	STY	108	6	0.72	0.73	1.07	–
		170	7	0.86	0.78	1.06	–
		245	11	1.2	0.94	1.08	–
		348	14	1.4	1.3	1.13	–
		1280	42	4.0	4.3	1.12	221
NI-7	STY	66	5	8.0	8.0	1.12	–
		99	9	8.3	8.1	1.14	–
		180	16	8.8	8.4	1.17	–
		305	28	9.7	9.0	1.20	–
		2525	87	14	12	1.38	340
NI-8	MMA	32	41	9.3	9.1	1.23	–
		67	96	13	11	1.40	–
		140	100	13	11	1.40	240; 340
NI-9	EHMA	27	9	0.99	–	–	–
		42	29	2.6	3.5	1.09	–
		55	39	3.5	3.9	1.11	–
		67	56	4.8	4.6	1.13	–
		99	89	7.5	6.4	1.13	–
		125	99	8.4	7.1	1.10	–
	+ MMA/MA	165	–	–	7.9	1.11	–
		190	–	–	9.1	1.13	–
		215	–	–	1.0	1.16	230

a) Experimental molar masses are determined by GPC against polystyrene calibrants.

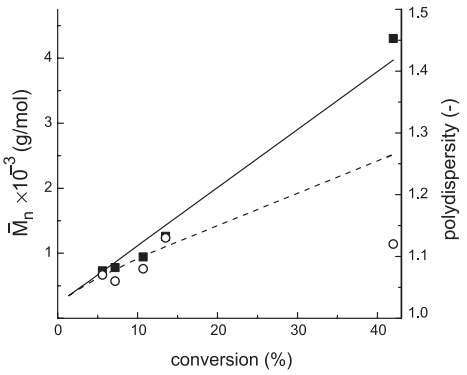

Figure 6.14. Results for the polymerization of styrene (NI-6). Number average molar mass: experimental values (■, in PS equivalents); theoretical values based on the dormant species (—); theoretical values corrected for initiator derived chains (---). Polydispersity index of the polymer (O, *right axis*).

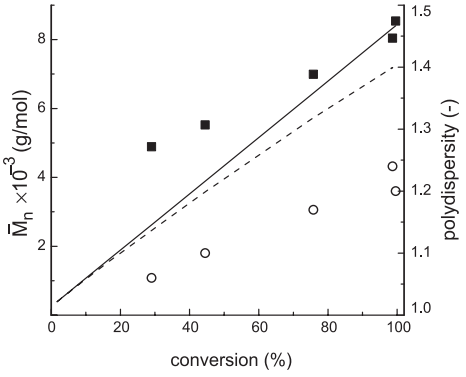

Figure 6.15. Results for the polymerization of *n*-BMA (NI-5). Number average molar mass: experimental values (■, in PS equivalents); theoretical values based on the dormant species (—); theoretical values corrected for initiator derived chains (---). Polydispersity index of the polymer (O, *right axis*).

The exceptionally low rate of the styrene polymerization can be explained by its lower propagation rate constant (k_p) combined with the fact that it has been shown to be stronger affected by the retardation inherent in RAFT polymerization.

Again Eq. 6-4 and Eq. 6-5 can be used to evaluate the evolution of the number-average molar mass with conversion and time. Figure 6.14 and Figure 6.15 show two predictions for molar mass. An overestimation is obtained when the initiator-derived chains are neglected (Eq. 6-4), denoted by the solid straight line. The dashed curve is an underestimation of the molar mass, and depicts the situation when $f_I \times f_{entry}$ equals 0.7, assuming that entry efficiency equals unity and initiator efficiency is 0.7 similar to solution experiments. As mentioned previously the difference between the two predictions often is negligible, but it becomes clear from Figure 6.14 that for slow polymerizations the time dependent term describing the initiator contribution plays a role. The styrene polymerization (Figure 6.14) closely follows the predicted values over the studied conversion range while the butyl methacrylate polymerization (Figure 6.15) seems to start above theory and slowly converges on the theoretical values. A reason for this behavior should not be sought in the miniemulsion kinetics as a similar trend was observed in solution polymerizations. The difference can be explained by the fact that the experimental molar mass has been determined by gel permeation chromatography (GPC) against polystyrene standards. Although Mark–Houwink parameters are available for the applied methacrylates such a correction procedure is known to yield unreliable

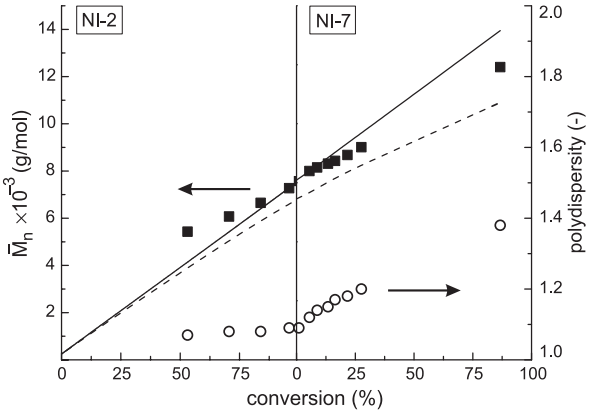

Figure 6.16. Molar mass data (*left axis*) for the preparation of the seed latex (NI-2) and the subsequent seeded polymerization of styrene (NI-7). Number average molar mass: experimental values (■, in PS equivalents); theoretical values based on the dormant species (—); theoretical values corrected for initiator derived chains (---). Polydispersity index of the polymer (○, *right axis*).

results for low molar mass polymer. The same drift is observed in the polymerization of EHMA, depicted on the left hand side of Figure 6.16. All of these polymerizations show living behavior with low polydispersities (<1.20).

6.5.2. Block copolymers

The living character of the miniemulsions was further instanced by their transformation into block copolymers. This was done either by two subsequent batch polymerizations where the initially prepared miniemulsion serves as a seed for the second polymerization or by a semi-continuous procedure where a second monomer was added to the polymerization reaction over a certain time interval, just after the first monomer had reached full conversion.

In the batch polymerizations the product of NI-2 was applied as the seed latex for experiments NI-7 and NI-8 (see Table 6.7, on page 164 for details). For each of these experiments the seed was swollen with an amount of monomer equal to the amount of polymer already present (on weight basis). A small amount of surfactant

Table 6.8: Block copolymers by batch reactions

ingredient	quantity (g)		
		7.0	PEHMA
latex NI-2	35	1.4	Igepal890
		0.04	KPS
monomer	7.0	STY (NI-7) / MMA (NI-8)	
surfactant	0.8	Igepal890	
initiator	0.04	KPS	

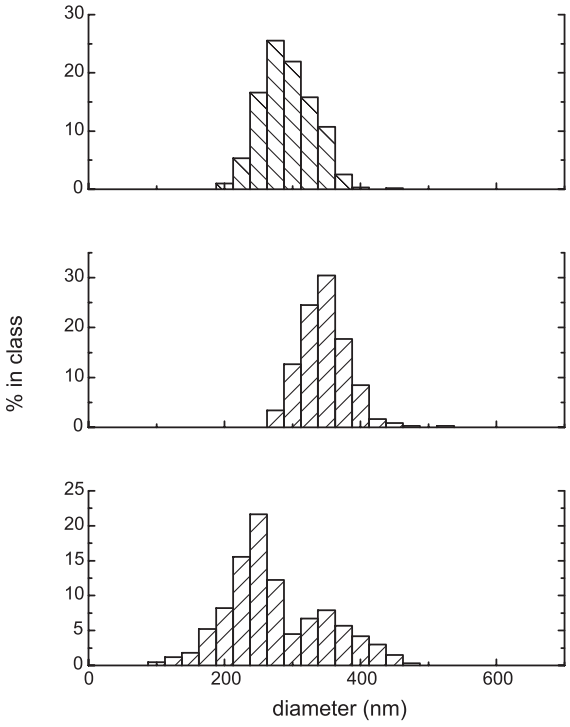

Figure 6.17. Particle size distributions for experiments NI-14 (*top*), NI-15 (*middle*) and NI-16 (*bottom*). In polymerization NI-15, the polymerization has taken place exclusively in the existing particles, therby enlarging them. In experiment NI-16, both the existing particles have grown while the material is transformed to diblock copolymer material while a new crop of particles is generated with a diameter of approx. 240nm. These patricles most likely consist of high molar mass PMMA homopolymer.

was added to stabilize the increased surface area of the particles. Assuming a constant number of particles, then doubling the volume will increase the total surface area with approximately 60%. The initiator concentration was brought back to the same level as at the start of the seed latex preparation NI-2. From the reaction time and the dissociation rate constant, KPS was assumed to be consumed for about 50%.

In polymerization NI-7, styrene is employed and due to its low k_p, the rate of polymerization is much lower than that of NI-2. Figure 6.16 shows the continued increase in molar mass of the seed latex material. Again the low polymerization rate suggests that Eq. 6-5 be implemented to account for chains started by initiator. The experimental values are between the theoretical line not taking into account initiator, and the curve using Eq. 6-5 with f equal to 0.7. Although the polydispersity increased during this second stage of the polymerization it remains low (1.38). The particle size (number-average) increased from 0.29μm for NI-2 to 0.34μm for NI-7. If a constant number of particles is assumed, then adding 87% to the volume of the particles (conversion of NI-7) should increase their diameter by approximately 23%, going up to 0.36μm. The difference between theory and measurement is small and no evidence for secondary particle formation could be found.

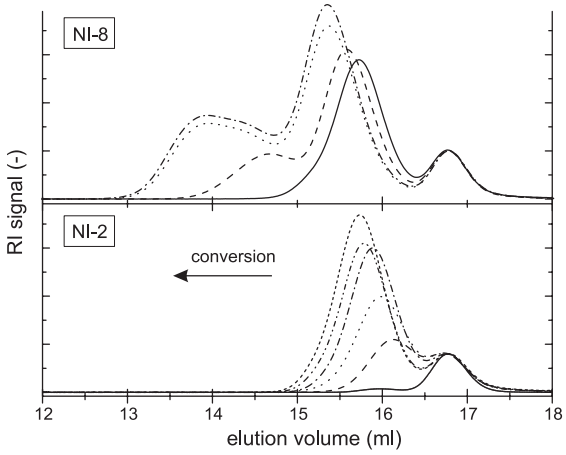

Figure 6.18. GPC traces (refractive index detector) for the preparation of the seed latex (NI-2, *bottom*) and the subsequent seeded polymerization of MMA (NI-8, *top*). The peak at 16.8 ml corresponds to the applied nonionic surfactant. This peak was used for normalization.

In polymerization NI-8, in which the seed latex is swollen with MMA, the reaction proceeds faster than the preparation of the seed (NI-2, same [KPS] and temperature), though the k_p of MMA is slightly lower than that of EHMA.[50] Again the high entry efficiency found for MMA polymerizations may play a role but a more important effect in this case is the generation of a new crop of particles. This process is confirmed by the particle size distribution as well as the evolution of the molar mass distribution. Doubling the volume of the original particles (MMA conversion is 100%) would increase their diameter from 0.29 µm to 0.37 µm. The particle size distribution (Figure 6.17) shows that the original population has grown only to 0.34 µm and that new particles are generated with a particle size of 0.25 µm. The newly formed particles will not contain any dithioester groups as these are securely attached to polymer chains in the original population of particles. For this reason polymerization in these particles will proceed in an uncontrolled manner and high molar mass PMMA homopolymer will be formed. This is confirmed by the GPC traces depicted in Figure 6.18.

The signal at an elution volume of 16.8 ml THF corresponds to the nonionic surfactant and has been used for normalization purposes. During the polymerization of EHMA (NI-2), low polydispersity material is formed with a number-average molar mass of $7.6 \cdot 10^3 \, g \cdot mol^{-1}$ (PS equivalents). During the seeded polymerization (NI-8), this material continues growing as it is being converted into poly(EHMA-*b*-MMA) and retains its narrow distribution. Simultaneously, material of high molar mass and higher polydispersity is formed which we expect to be PMMA homopolymer in the second crop of particles. It grows in a conventional uncontrolled fashion

Table 6.9: Block copolymer by a semi-continuous procedure (NI-9)

		quantity		
	ingredient	(g)	(mmol)	type
batch	water	80		
	monomer	20	100	EHMA
	surfactant	4.0	2.0	Brij98
	costabilizer	0.40	1.8	hexadecane
	costabilizer	trace		Kraton
	initiator	0.20	0.75	KPS
	RAFT agent	0.60	2.5	1
feed stream[a)]	monomer	9.2	92	MMA
	monomer	0.8	9	Methacrylic Acid

a) The monomer feed stream was started at a rate of 0.1 ml/min. two hours after the start of the reaction. At this point, the polymerization of EHMA was complete.

due to the absence of dithioester species, confirmed by the absence of the dithiobenzoate chromophore in the chromatogram generated by the UV detector at a wavelength of 320 nm (not shown).

Here we have prepared a latex, which may have very intriguing properties as it contains both high T_g particles of high molar mass and particles consisting of a low molar mass block copolymer that can act as *in situ* compatibilizer for the PMMA spheres and another material. Alternatively, the hard PMMA spheres may act as reinforcement filler for the block copolymer film cast from this latex. Indeed living radical polymerization in miniemulsion can open up the way to a whole new class of "designer-latices".

Experiment NI-9 differs from NI-2 in that it utilizes Brij98 as surfactant (table 6.9). In this polymerization block copolymer is prepared by a semi-batch procedure. First EHMA is polymerized to full conversion. The molar mass is again close to the theoretical value and polydispersity remained below 1.2 (Figure 6.19). A feed stream of a 10 g monomer mixture of MMA and methacrylic acid (12:1 on weight basis) was started at a rate of $0.1\,ml \cdot min^{-1}$. Samples taken during this part of the polymerization again exhibit controlled growth of the block copolymer. The GPC traces showed no evidence of non-block copolymers formed during this stage – in this case poly(MMA-*co*-methacrylic acid). Non-block copolymers are unavoidably formed to some extent and although their amount can be minimized, they are usually observable as low molar mass material in the GPC trace when block copolymers are prepared in bulk or solution.[51] The combination of high polymerization

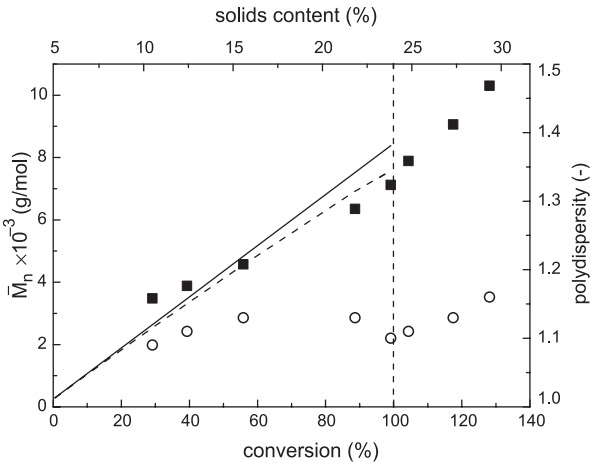

Figure 6.19. Molar mass data (*left axis*) for polymerization of EHMA (NI-9) and its transformation into poly(EHMA-*b*-[MMA-*co*-methacrylic acid]). Number average molar mass: experimental values (■, in PS equivalents); theoretical values based on the dormant species (—); theoretical values corrected for initiator derived chains (---). Polydispersity index of the polymer (O, *right axis*).

rate and low radical flux per particle – typical of compartmentalized systems – allows the preparation of block copolymers with a higher degree of purity than that is typically achieved in homogeneous media.

The high purity of block copolymers in compartmentalized systems is a function of the entry rate coefficient. This means that the polymerization rate can be increased by increasing the number of particles which in turn decreases the entry rate coefficient and thus improves the purity of the blocks produced.

To further establish the effectiveness of this procedure, the samples were precipitated in water/methanol (3:1) to remove the surfactant and analyzed by HPLC (Figure 6.20). Chromatograms were normalized on the Kraton (eluting around 3 min), a trace of which had been mixed in the organic phase as an internal standard. Several samples of different PEHMA chain lengths were injected and these gave two peaks between 6 and 8 min elution time. The three samples taken during the second stage of the polymerization (see table 6.7) had much higher elution volumes. The first has added an average number of only 7 monomer units per chain resulting in a very broad multimodal signal barely visible above the baseline between 9 and 32 ml elution volume. The exact elution volume is strongly dependent on the number of polar monomer units that has been added and especially on the incorporation of methacrylic acid. As the chains grow further and all start to contain methacrylic acid, the polymer elutes at 30 ml. The nonionic surfactant Brij98 eluted at 34 ml and was not present in the precipitated samples. Integration of the peaks revealed that less than 2% of the poly(EHMA) prepared in the first stage remained and the absence of its signal in the UV chromatogram (λ=320nm)

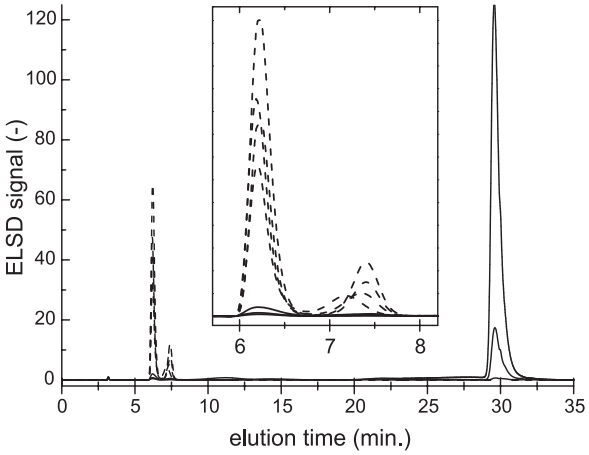

Figure 6.20. Gradient HPLC chromatograms of samples taken from miniemulsion NI-9. Samples taken during the polymerization of EHMA (---) and samples taken during the addition of the second monomer feed stream of MMA and methacrylic acid(—)

showed that these chains no longer have a dithiobenzoate end group. No peaks other than this one and the one attributed to the block copolymer were observed. This leads us to conclude that very narrow polydispersity poly(EHMA-*block*-[MMA-*co*-methacrylic acid]) was prepared with the surfactant as the single significant contaminant. The product was easily isolated by precipitation in water/ methanol.

6.6. Conclusions

The application of RAFT polymerizations in dispersed media is not as simple as might be expected from its straightforward free-radical chemistry. After previously reported difficulties using *ab initio* and seeded emulsion polymerizations it was expected that elimination of the need of the RAFT agent to be transported through the water phase would alleviate the encountered stability problems. This was found not to be the case in miniemulsion polymerizations using RAFT. Both anionic and cationic surfactants were found inadequate in maintaining the original droplet morphology upon the onset of reaction. A separated organic phase would appear, combined with a polymer product of relatively high polydispersity. Variations on the ingredients of the recipe did not result in identification of any particular deleterious component, although it must be said that there is only limited understanding of the interaction of the RAFT agent with other emulsion components at this point.

Quite remarkably, similar phenomena are reported in ATRP and nitroxide mediated polymerization which support the hypothesis that the cause of the destabilization should not be sought in specific chemical interactions or reactions of the RAFT system as these techniques apply completely different components to control the polymerization. One characteristic feature that they have in common and which distinguishes them from a conventional uncontrolled miniemulsion polymerization, is the existence of a time interval early in the reaction where oligomeric species dominate the molar mass distribution of both the inactive chains and the propagating radicals. Beyond any doubt, this will have a tremendous influence on kinetic issues like radical desorption, termination, and droplet nucleation.

The destabilization could not be simulated, however, by the deliberate addition of oligomers to the organic phase prior to the emulsification, which indicates that the dynamic formation of oligomers in the course of reaction is an important aspect. In this process droplets are generated with temporarily very different thermodynamic properties which may create substantial driving forces for monomer migration which are absent in an uncontrolled polymerization.

Only when nonionic surfactants were used, miniemulsions were obtained that were stable throughout the polymerization. A number of controlled polymerizations were performed where the advantages of compartmentalized systems were exploited. Their relatively low termination rate allowed for the controlled preparation of low polydispersity homopolymers having a predetermined molar mass. Moreover, several methacrylate and styrene block copolymers were prepared with a much higher level of block purity than obtainable in typical solution polymerizations. Finally, it was shown that living radical polymerization could be conducted simultaneously with conventional radical polymerization, leading to a blend of latex particles with completely different characteristics. This novel process allows sophisticated materials engineering by a careful choice of reaction conditions.

The application of living polymerization in a miniemulsion with RAFT is still a relatively unexplored field. An understanding of the interaction of oligomers in general and dormant RAFT chains in particular with other emulsion components has not fully developed yet, but with the increasing attention that living polymerization systems are acquiring (particularly in dispersed media), major developments can be expected in the near future.

6.7. Experimental

Reagents: Monomers were obtained from Aldrich Chemicals. Before use they were distilled (except for EHMA) and passed through an inhibitor removal column (Aldrich – specific to the inhibitor type). 2,2'-Azobis[2-methyl-N-(2-hydroxyethyl)propionamide] (VA-086) and 1,1'-Azobis(1-cyclohexanecarbonitrile) (V-40) were obtained from Wako Chemicals and used without purification. 2,2'-azobisisobutyronitrile (AIBN, 98%) was purchased from Merck and recrystallized from methanol before use. Potassium persulfate (KPS), hexadecane (HD), potassium nitrodisulfonate (Fremy's salt), and sodium hydrogen carbonate were obtained from Aldrich. Sodium metabisulfite ($Na_2S_2O_5$, used as redox couple with KPS) and sodium dodecyl sulfate (SDS) were obtained from Fluka. Hydroquinone, used to quench gravimetric samples, was obtained from Merck. All were used as received. Kraton L-1203 (a monohydroxyl functional copolymer of ethylene and butylene $M_n \approx 4 \cdot 10^3$ g/mol, polydispersity ≈ 1.05) was received from Shell Chemicals.

The synthesis of 2-cyanoprop-2-yl dithiobenzoate (**1**, Scheme 6.2), 2-phenylprop-2-yl dithiobenzoate (**2**, Scheme 6.2) and 2-(ethoxycarbonyl)prop-2-yl dithiobenzoate (**3**, Scheme 6.2) is described in chapter 3. Polymeric RAFT agents were prepared by either organic procedures (**4**, Scheme 6.2) or solution polymerization (**5**, Scheme 6.2) of methyl methacrylate in the presence of **1** (Scheme 6.2). The preparation and characterization of **4** is described in chapter 3 and in reference 51. RAFT agent **5** has an apparent number average molar mass of $3.5 \cdot 10^3$ g/mol and a polydispersity of 1.07, determined by GPC against polystyrene standards.

Miniemulsion Procedure: Monomer was mixed with RAFT agent, hydrophobe and oil soluble initiator (AIBN, V-40, if applicable), comprising the preliminary organic-phase. This organic phase was mixed well until all contents were dissolved. While stirring vigorously (magnetic stirrer), the organic phase was dropwise added to a solution of the surfactant in water. The flask was left stirring to homogenize for 60 minutes after which a sonicating probe (400W, Dr. Hielscher UP400S) was immersed into this pre-emulsion. Stirring continued for 12 minutes while sonicating (amplitude 30%, cycle 1.0). 10–12 minutes was found to be the optimum duration of sonication for these recipes, leading to almost immediate polymerization after injection of initiator. When the pre-mixed emulsion was sonicated for roughly 30 minutes, retardation in the early stages of polymerization was observed. During this process, the miniemulsion was cooled by a water bath to keep its temperature below 20°C. The miniemulsion was then transferred into a three-necked

250ml round bottom flask equipped with reflux cooler and containing water-soluble initiator (potassium persulfate or VA-086, when applicable). The round bottom flask was then immersed into an oil bath, that had been pre-heated to the reaction temperature (70 °C) and polymerization was carried out under an argon atmosphere. During regular time intervals, samples were taken for particle size analyses by light scattering, gravimetric conversion measurement and GPC analyses.

Kinetic Analysis: Conversion of monomer to polymer was followed through dry-solids (gravimetric analysis). Samples were taken regularly throughout the polymerization, quenched with a few crystals of hydroquinone, and pre-dried on a hotplate at 60 °C, followed by drying in a vacuum oven at slowely increasing temperatures up to 120 °C.

GPC Analysis: GPC analyses were performed on a Waters system equipped with two PLgel Mixed-C columns, a UV and an RI detector. Reported molar masses are apparent values expressed in polystyrene equivalents. Although Mark-Houwink parameters were available for the polymers studied, a correction procedure was not applied, as its validity is only established for molar masses exceeding approximately 2.0×10^4 g/mol.

Conductivity Analysis: Conductivity of the continuous phase was measured by sampling as on-line probe tips were suspect to accumulate polymer that would give anomalous readings. Samples were taken from the reactor and immediately measured using a Radiometer Copenhagen CDM 80 conductivity meter (20 µS/cm to 2000 mS/cm).

HPLC Analyses: The HPLC analyses were performed using an Alliance Waters 2690 Separation Module. Detection was done using a PL-EMD 960 ELSD detector (Polymer Laboratories) and using a 2487 Waters dual UV detector at wavelengths of 254 and 320 nm. All samples were analyzed by injecting 10 µl of a solution of the dried polymer in tetrahydrofuran at a concentration of 5 mg/ml. Columns were thermostated at 35 °C. Samples were analyzed on a NovaPak® CN column (Waters, 3.9×150 mm) by the application of a gradient from heptane to THF in 40 minutes. Data for both GPC and HPLC were acquired by Millennium 32 3.05 software.

Light Scattering: Particle diameters were determined by light scattering on a Malvern 4700. For this purpose, samples were diluted with water. Emulsion NI-6 was diluted with water saturated with styrene to preserve the original droplet size.

Electron Microscopy: A small film cast from the latex sample was vitrified by liquid ethane. Images were recorded on a Philips TEM (CM 12) at –120 °C. The advantage of cryogenic transmission electron microscopy is that staining of the latex is not nessecary and that the technique is readily applicable to polymers with a low glass transition temperature without changing the sample morphology.

6.8. References

1. taken from *She's lost control* by Joy Division on the album *Unknown Pleasures*, © Zomba Publishing / Fractured Music, **1979**
2. The work described in this chapter has been published elswhere in a slightly modified version. Miniemulsions stabilized by nonionic surfactants: De Brouwer, H.; Tsavalas, J. G.; Schork, F. J.; Monteiro, M. J. *Macromolecules* **2000**, *33*, 9239. Miniemulsions stabilized by ionic surfactants: Tsavalas, J. G.; Schork, F. J.; De Brouwer, H.; Monteiro, M. J. *Macromolecules* **2001**, in press.
3. Sudol, E. D.; El-Aasser, M. S. ; Lovell, P. A. and El-Aasser, M. S., Ed.: Chichester, 1997, p. 699
4. Gilbert, R. G. Emulsion Polymerization: A Mechanistic Approach; Academic: London, **1995**
5. Landfester, K.; Bechthold, N.; Forster, S.; Antonietti, M. *Macromol. Rapid Commun.* **1999**, *20*, 81
6. Landfester, K.; Bechthold, N.; Tiarks, F.; Antonietti, M. *Macromolecules* **1999**, *32*, 5222
7. Weiss, J.; McClements, D. J. *Langmuir* **2000**, *16*, 5879
8. Weiss, J.; Canceliere, C.; McClements, D, J. *Langmuir* **2000**, *16*, 6833
9. Webster, A. J.; Cates, M. E. *Langmuir* **1998**, *14*, 2068
10. Ugelstad, J.; Mørk, P. C.; Herder Kaggerud, K.; Ellingsen, T.; Berge, A. *Adv. Colloid Interface Sci.* **1980**, *13*, 101
11. Mouran, D.; Reimers, J.; Schork, F. J. *J. Polym. Sci. Part A: Polym. Chem.* **1996**, *34*, 1073
12. Chern, C. S.; Liou, Y. C.; Chen, T. J. *Macromol. Chem. Phys.* **1999**, *199*, 1315
13. Miller, C. M.; Blythe, P. J.; Sudol, E. D.; Silebi, C. A.; El-Aasser, M. S. *J. Polym. Sci. Part A: Polym. Chem.* **1994**, *32*, 2365
14. Blythe, P. J.; Morrison, B. R.; Mathauer, K. A.; Sudol, E. D.; El-Aasser, M. S. *Langmuir* **2000**, *16*, 898
15. Reimers, J.; Schork, F. J. *J. Appl. Polym. Sci.* **1996**, *59*, 1833
16. Reimers, J. L.; Schork, F. J. *J. Appl. Polym. Sci.* **1996**, *60*, 251
17. Choi, Y. T.; Sudol, E. D. Vanderhoff, J. W.; El-Aasser, M. S. *J. Polym. Sci. Polym. Chem. Ed.* **1985**, *23*, 2973
18. Reimers, J.; Schork, F. J. *J. Appl. Polym. Chem.* **1995**, *33*, 1391
19. Prodpran, T.; Dimonie, V. L.; Sudol, E. D.; El-Aasser, M. S. *Macromol. Symp.* **2000,** *155*, 1
20. Matyjaszewski, K.; Shipp, D. A.; Qiu, J.; Gaynor, S. G. *Macromolecules* **2000,** *33*, 2296
21. Farcet, C.; Lansalot, M.; Charleux, B.; Pirri, R.; Vairon, J. P. *Macromolecules* ASAP
22. Charleux, B. *Macromolecules* **2000**, *33*, 5358
23. Butté, A.; Storti, G.; Morbidelli, M. *Macromolecules* **2000**, *33*, 3485
24. Lansalot, M.; Farcet, C.; Charleux, B.; Vairon, J.-P.; Pirri,R. *Macromolecules* **1999**, *32,* 7354
25. Farcet, C.; Lansalot, M.; Pirri, R.; Vairon, J. P.; Charleux, B. *Macromol. Rapid Commun.* **2000**, *21*, 921
26. Kanagasabapathy, S.; Claverie, J.; Uzulina I. *Polym. Prepr.* **1999**, *218*, 422
27. Uzulina I.; Kanagasabapathy, S.; Claverie, J. *Macromol. Symp.* **2000**, *150*, 33
28. Monteiro, M. J.; Sjöberg, M.; Van der Vlist, J.; Göttgens, C. M. *J. Polym. Sci. Part A: Polym. Chem.* **2000**, *38*, 4206
29. Monteiro, M. J.; Hodgson, M.; De Brouwer, H. *J. Polym. Sci. Part A: Polym. Chem.* **2000**, *38*, 3864
30. Hodgson, M. *Masters thesis* **2000** University of Stellenbosch, South Africa
31. Le, T. P.; Moad, G.; Rizzardo, E.; Thang, S. H. Patent WO 98/01478 (1998) [*Chem. Abstr.* **1998**,

128:115390]
32. Moad, G.; Chiefari, J.; Chong, Y. K.; Krstina, J.; Mayadunne, R. T. A.; Postma, A.; Rizzardo, E.; Thang, S. H. *Polymer International* **2000**, *49*, 993
33. Lichti, G.; Sangster, D. F.; Whang, B. C. Y.; Napper, D. H.; Gilbert, R. G. *J. Chem. Soc. Faraday Trans. I* **1982**, *78*, 2129
34. Morrison, B. R.; Casey, B. S.; Lacík, I.; Leslie, G. L.; Sangster, D. F.; Gilbert, R. G.; Napper, D. H. *J. Polym. Sci. A: Polym. Chem.* **1994**, *32*, 631
35. Monteiro, M. J.; de Brouwer, H. *Macromol. Rapid Commun.* submitted.
36. Maeder, S.; Gilbert, R. G. *Macromolecules* **1998**, *31*, 4410
37. Goto, A.; Sato, K.; Fukuda, T.; Moad, G.; Rizzardo, E.; Thang, S. H. Polymer Preparations **1999**, *40*, 397
38. Buback, M.; Gilbert, R. G.; Hutchinson, R. A.; Klumperman, B.; Kuchta, F.-D.; Manders, B. G.; O'Driscoll, K. F.; Russell, G. T.; Schweer, *J. Macromol. Chem. Phys.* **1995**, *196*, 3267
39. Note that the initial concentration of initiator $[I]_0$ should be based on the same volume as $[M]_0$ and $[RAFT]_0$ and that the volume cancels out by the devision. Therefore these concentrations may be replaced by molar amounts. $[I]_w$ and $[M]_w$ are the actual concentrations of initiator and monomer in the water phase.
40. Müller, A. H. E.; Zhuang, R.; Yan, D.; Litvenko, G. *Macromolecules* **1995**, *28*, 4326
41. van Herk, A. M. *J. Macromol. Sci., Rev. Macromol. Chem. Phys.* **1997**, *C37*, 633
42. de Brouwer, H.; Tsavalas, J. G.; Schork, F. J.; Monteiro, M. J. *Macromolecules* in press
43. Fontenot, K.; Schork, F. J. *J. Appl. Polym. Sci.* **1993**, *49*, 633
44. Noël, L. F. J.; Janssen, R. Q. F.; van Well, W. J. M.; van Herk, A. M.; German, A. L. *J. Colloid & Interface Sci.* **1995**, *175*, 461
45. Blackley, D. C.; Haynes, A. C. J. Chem. Soc., *Faraday Trans. 1* **1979**, *75*, 935
46. Charmot, D.; Corpart, P.; Adam, H.; Zard, S. Z.; Biadatti, T.; Bouhadir, G. *Macromol. Symp.* **2000**, *150*, 23
47. Hoffman, B. Controlled radical polymerization using RAFT; Eindhoven University of Technology: Eindhoven, **2000**
48. Landfester, K.; Bechthold, N.; Tiarks, F.; Antonietti, M. *Macromolecules* **1999,** *32*, 2679
49. Chern, C.-S.; Liou, Y.-C. *Macromol. Chem. Phys.* **1998**, *199*, 2051
50. Van Herk, A in *Polymeric dispersions: principles and applications*, Asua, J. M. (Ed.) NATO ASI Series E, Applied Sciences **1997**, *335*, 17
51. De Brouwer, H.; Schellekens, M. A. J.; Klumperman, B.; Monteiro, M, J.; German, A. L. *J. Polym. Sci. Part A: Polym. Chem.* **2000**, *38*, 3596

» A year here and still he dreamed of cyberspace,
hope fading nightly. All the speed he took, all the turns he'd taken
and the corners he'd cut in Night City, and still he'd see the matrix in his sleep,
bright lattices of logic unfolding across that colorless void... «[1]

Appendix: Polymerization Models

Synopsis: This appendix discusses several approaches in the modeling of living radical polymerizations with their specific advantages and disadvantages.

A.1. Numerical Integration of Differential Equations

The reaction scheme of free radical polymerization, living or not, presented in chapter 2 shows that only a relatively small number of different species take part in these reactions: initiator, monomer, transfer agent, radicals, dormant polymer chains and dead polymer material. The latter three types, however, are polymeric species which means that they come in a variety of chainlengths. The way in which the chain length is dealt with constitutes the primary difference between the models described in this appendix. Three approaches can be distinguised.

First, the chainlengths can be completely ignored. Although simulations using such models will not yield any information on the polymer as such, they may be used to illustrate simple kinetic effects as in chapter 2, where it was shown that an additional reaction needs to be invoked to explain the retardation that is observed in RAFT polymerizations. The advantage of such a model is that it is both simple and executes very fast. The number of differential equations can range from about five to ten, depending on how detailed different termination and transfer events are treated. The most important disadvantage is of course that no information is gained on the polymer, other than its concentration (in moles per unit volume).

Second, all chainlengths can be considered individually. This means that for each of the polymeric species (radicals, dormant chains and dead polymer), a large number of differential equations needs to be solved. One for each individual chain-length that exists during the polymerization. The advantage is that the most complete picture of the resulting polymer is obtained. Full molar mass distributions

can be constructed from the data and within these it is possible to locate the dead and dormant materials. The disadvantage is that this approach may be applied only to a limited number of polymerizations. The number of differential equations is about three times larger than the number of chain lengths that is monitored during the polymerization. Uncontrolled free radical polymerizations grow chains of a few thousand repeat units from the start of the reaction resulting in simulations that require far more than 10,000 differential equations to be solved simultaniously. More often than not, these differential equations form a stiff system which rapidly becomes insolvable for any computer as the number of differential equations increases. Conventional free radical polymerizations therefore, cannot be simulated with such an approach on common computers. The situation is completely different for living free radical polymerizations. As outlined in chapter 2 the average chain length is a linear function of conversion and its distribution is of low polydispersity. This means if a reaction is set to produce material of say 150 monomer units, that during the entire reaction no material is formed which would significantly exceed this length. To accomodate material formed by combination – which may be slightly longer – and provide a bit of overhead for the non-monodispersity of the distribution, somewhat more than 450 differential equations are required and the simulation can be executed on a modern desktop computer in a timespan anywhere between a few minutes to a day. The simulations remain restricted however to living systems with a fast equilibrium between growing and dormant chains that aim at producing relatively low molar mass material. In this thesis, such a model is used to investigate the kinetics by matching simulations to molar mass distributions obtained by HPLC that show individual oligomers up to a chain length of about 15 monomer units.

A third method forms a compromise between the abovementioned simulations. It relies on the fact that any distribution can be characterized by a number of moments. The i^{th} moment of the distribution of X (μ_i^X) is defined as follows:

$$\mu_i^X = \sum_{j=0}^{\infty} j^i \cdot X_j \qquad \textbf{(7-1)}$$

in which X_j is the concentration of species X with degree of polymerization i.

The more moments are known, the more accurately a distribution can be reconstructed from these values. The zeroth moment corresponds to the total concentration of a certain species, covering all chain lengths. Higher moments take more

abstract forms but they do allow experimentally accessible and physically important polymer characteristics like number average molar mass, weight average molar mass and polydispersity index to be calculated. The number average molar mass ($\overline{M}_n$) is defined as follows:

$$\overline{M}_n = \sum x_i \cdot M_i = \frac{\sum n_i \cdot M_i}{\sum n_i} = \frac{FW_{mon} \cdot \mu_1^X}{\mu_0^X} \qquad \textbf{(7-2)}$$

where x_i is the mole fraction of molecules having degree of polymerization i. The equation can also be expressed in numbers of molecules n_i or alternatively in concentrations. The molar mass of a polymer chain can be replaced by the degree of polymerization (i) times the molar mass of the monomer which allows the number average molar mass to be expressed by the ratio of the first over the zeroth moment of the polymer chain distribution times the mass of a single monomer unit (FW_{mon}).

In an analogue derivation it can be shown that the weight average molar mass ($\overline{M}_w$) is equal to the ratio of the second moment over the first moment of the distribution, again multiplied by the mass of the repeat unit:

$$\overline{M}_w = \sum w_i \cdot M_i = \frac{\sum n_i \cdot M_i^2}{\sum n_i \cdot M_i} = \frac{FW_{mon} \cdot \mu_2^X}{\mu_1^X} \qquad \textbf{(7-3)}$$

The polydispersity index can then be calculated from the ratio of $\overline{M}_w$ over $\overline{M}_n$.

More complex molar mass averages as $\overline{M}_z$ and $\overline{M}_{z+1}$ are derived from the higher moments of a distribution in a similar way. For each of the moments of a distribution, a differential equation is required. The approach taken in this thesis is restricted to the first three moments. This results in a model with approximately fifteen differential equations which can readily be solved by ordinary desktop workstations. The derivation of the differential equations is however slightly more complicated then for the previous modelling approaches where, albeit the large number of differential equations, their structure was very straightforward.

The models result in a set of differential equations which is solved numerically using MATLAB, a widely used environment for scientfic computing.[2] MATLAB contains several different solvers for ordinary differential equations. For all models

derived in this appendix, `ode15s` was used, which is a quasi-constant step size integrator. It implements numerical differentiation formulas (NDFs) which can be considered an improvement over the more commonly used backward differentiation formulas (BDFs, also known as Gear's method) in terms of stability, speed and efficiency.[3] The transparent implementation adapts the stepsize of the integration (through time) and the order of the fit to remain within the error margins given by the user. The differential equations can either be hard-coded or constructed programatically.

A.2. Models

A.2.1. Model withouth Chain Lengths

Construction

A simple model that does not consider any chainlengths is easily derived from the reaction schemes in section 2.3 (Schemes 2.11 and 2.12) which shows how species are generated and how they are destroyed or transformed.

$$\frac{dI}{dt} = -k_d \cdot I \tag{7-4}$$

$$\frac{dM}{dt} = -k_p \cdot M \cdot P - k_i \cdot M \cdot R \tag{7-5}$$

$$\begin{aligned}\frac{dR}{dt} = {} & 2 f k_d \cdot I - k_i \cdot R \cdot M + k_{frag,\,R} \cdot (PSR + RSR) - k_{add,\,R} \cdot (SR + SP) \\ & - k_t \cdot R \cdot (R + P + RSR + PSR + PSP)\end{aligned} \tag{7-6}$$

$$\begin{aligned}\frac{dP}{dt} = {} & k_i \cdot R \cdot M - k_t \cdot P \cdot (R + P + RSR + PSR + PSP) \\ & - k_{add,\,P} \cdot P \cdot (SR + SP) + k_{frag,\,P} \cdot P \cdot (PSP + PSR)\end{aligned} \tag{7-7}$$

$$\frac{dSR}{dt} = k_{frag,\,P} \cdot PSR + k_{frag,\,R} \cdot RSR - k_{add,\,R} \cdot R \cdot SR - k_{add,\,P} \cdot P \cdot SR \tag{7-8}$$

$$\frac{dSP}{dt} = k_{frag,\,P} \cdot PSP + k_{frag,\,R} \cdot PSR - k_{add,\,R} \cdot R \cdot SP - k_{add,\,P} \cdot P \cdot SP \tag{7-9}$$

$$\frac{dD}{dt} = k_t \cdot R \cdot (R + P + PSP + PSR + RSR) + k_t \cdot P \cdot (P + RSR + PSR + PSP) \quad \textbf{(7-10)}$$

$$\frac{dRSR}{dt} = k_{add,R} \cdot R \cdot SR - k_{frag,R} \cdot RSR - k_t \cdot RSR \cdot (R + P) \quad \textbf{(7-11)}$$

$$\frac{dPSR}{dt} = k_{add,R} \cdot R \cdot SP + k_{add,P} \cdot P \cdot SR - k_{frag,R} \cdot PSR - k_{frag,P} \cdot PSR - k_t \cdot PSR \cdot (R + P) \quad \textbf{(7-12)}$$

$$\frac{dPSP}{dt} = k_{add,P} \cdot P \cdot SP - k_{frag,P} \cdot PSP - k_t \cdot PSP \cdot (R + P) \quad \textbf{(7-13)}$$

The model as presented here utilizes a single termination rate constant, but the actual computer files allow one to distinguish intermediate radical termination from the other termination events.

Implementation

Equations 7-4 to 7-13 can be rewritten in a form that is desired by the MATLAB solver. It can integrate ordinary differential equations if they are offered in the following form:

$$y' = F(t, y) \quad \textbf{(7-14)}$$

in which t is a scalar independent variable, in this case time; y is a vector of dependent variables; y' is a function of t and y returning a column vector the same length as y. In this case y could be the vector [I, M, P, T, S, D] and y' the vector containing the elements on the right hand side of the differential equations 7-4 to 7-13. Besides these two vectors a third one is required which indicates the starting conditions $y_0 = [I_0, M_0, 0, T_0, 0, 0]$ and last, the options for the integrator need to be set. These typically dictate the time interval for integration and the absolute and relative error margins. Furthermore, optionally user defined conditions may be constructed (so-called *events*) that prematurely stop the integration. In all the models in this chapter, events were created that stopped integration when either monomer or initiator had reached conversions higher than 99.999% and when the concentration of any species would drop below zero. Further integration beyond this point would

not result in additional meaningful results but stretched the required integration time considerably. Shown below are the contents of the two basic `.m` files required to run this simulation, stripped of all unnessecary functionality.

the file `startit.m`:

```
clear all;

name='noraftterm';
kd   = 1.35e-4;
ki   = 7e2;
kp   = 6.6e2;
kPaddSR  = 7e6;        %P adds
kPaddSP  = 7e6;
kRaddSP  = 7e6;        %R adds
kRaddSR  = 7e6;
kbetaPSP = 1.2e5;        %P fragments
kmaddPSR = 1.2e5;
kbetaRSR = 1.2e5;        %R fragments
kbetaPSR = 1.2e5;
ktbasis  = 2*pi*0.25*7e-9*6.02e23;
ktbI     = 1.5*pi*0.25*7e-9*6.02e23; %ktbasis; %set zero to eliminate intermediate
termination

kmatrix =[kd ki kp kPaddSR kbetaPSR kmaddPSR kRaddSR kbetaRSR kPaddSP kbetaPSP
kRaddSP ktbasis ktbI];

maxci = 0.9999;
maxcm = 0.9999;

mx = [maxci maxcm];

mmo=31;
msol=58;
mass=[mmo msol];

I   = 4.4e-3;  %initiator
M   = 3;       %monomer
R   = 0;       %ini- or raft-derived radicals
SR  = 0;       %raft
P   = 0;       %propagating radicals
SP  = 0;       %dormant species
D   = 0;       %dead chains
RSR = 0;       %intermediate
RSP = 0;       %intermediate
PSP = 0;       %intermediate
%-------------------------------------------------------------------------------------
y0=[I M R SR P SP D RSR RSP PSP];
tmax=[0 3.5e5];
options = odeset('AbsTol',1e-12,'RelTol',3e-
13,'BDF','off','Stats','on','Events','on');
%-------------------------------------------------------------------------------------
tic;
[t,x]=ode15s('simpleraft',tmax,y0,options,kmatrix,y0,mass,mx);
toc;
%-------------------------------------------------------------------------------------
fpm = fopen('overview.txt','a');
temp=[name '\r\n'];
fprintf(fpm,temp);
temp=['ini \t' num2str(I,'%.3g') '\r\n'];
fprintf(fpm,temp);
temp=['mono \t' num2str(M,'%.3g') '\r\n'];
fprintf(fpm,temp);
temp=['raft \t' num2str(SR,'%.3g') '\r\n'];
fprintf(fpm,temp);
temp=['kd \t' num2str(kd,'%.3g') '\r\n'];
fprintf(fpm,temp);
temp=['ki \t' num2str(ki,'%.3g') '\r\n'];
fprintf(fpm,temp);
temp=['kp \t' num2str(kp,'%.3g') '\r\n'];
fprintf(fpm,temp);
temp=['kRaddSR \t' num2str(kRaddSR,'%.3g') '\r\n'];
fprintf(fpm,temp);
```

```
temp=['kRaddSP \t' num2str(kRaddSP,'%.3g') '\r\n'];
fprintf(fpm,temp);
temp=['kPaddSR \t' num2str(kPaddSR,'%.3g') '\r\n'];
fprintf(fpm,temp);
temp=['kPaddSP \t' num2str(kPaddSP,'%.3g') '\r\n'];
fprintf(fpm,temp);
temp=['kbetaRSR \t' num2str(kbetaRSR,'%.3g') '\r\n'];
fprintf(fpm,temp);
temp=['kbetaPSP \t' num2str(kbetaPSP,'%.3g') '\r\n'];
fprintf(fpm,temp);
temp=['kbetaPSR \t' num2str(kbetaPSR,'%.3g') '\r\n'];
fprintf(fpm,temp);
temp=['kmaddPSR \t' num2str(kmaddPSR,'%.3g') '\r\n'];
fprintf(fpm,temp);
temp='\r\n\r\n';
fprintf(fpm,temp);
fclose(fpm);
%-------------------------------------------------------------------------------------
nm= [name '.dat']
fm  = fopen(nm,'w');
fprintf(fm,'t mc I M R SR P SP D RSR RSP PSP\n');
for i=1:max(size(t))
   mc=((M-x(i,2))/M)*100;
   fprintf(fm,'%.4e %.4e %.4e %.4e %.4e %.4e %.4e %.4e %.4e %.4e %.4e %.4e
%.4e\n',t(i),mc,x(i,1),x(i,2),x(i,3),x(i,4),x(i,5),x(i,6),x(i,7),x(i,8),x(i,9),x(i,10
));
end % for i
fclose(fm);
%-------------------------------------------------------------------------------------
clear all;
```

and the file `simpleraft.m`:

```
function varargout = simpleraft(t,y,flag,k,sv,m,mx)

switch flag
 case ''                       % Return dy/dt = f(t,y).
   varargout{1} = f(t,y,k,sv,m,mx);
 case 'events'                   % Return [value,isterminal,direction]
   [varargout{1:3}] = events(t,y,k,sv,m,mx);
 otherwise
   error(['Unknown flag ''' flag '''.']);
 end
% ------------------------------------------------------------
% 1  I       kd
% 2  M       ki
% 3  R       kp
% 4  SR      kPaddSR
% 5  P       kbetaPSR
% 6  SP      kmaddPSR
% 7  D       kRaddSR
% 8  RSR     kbetaRSR
% 9  PSR     kPaddSP
% 10 PSP     kbetaPSP
% 11         kRaddSP
% 12         ktbasis used for ordinary termination
% 13         ktbI    used for intermediate termination
% ------------------------------------------------------------
function dydt = f(t,y,k,sv,m,mx)

convM =(sv(2)-y(2))/sv(2);  % bereken conversie M
nc = (sv(4)-y(4))+2*(sv(1)-y(1));

if convM<1e-8
   convM=1e-8;
end

if nc<1e-8
   nc=1e-8;
end

if sv(4)>0
   length=round(convM*sv(2)/nc);   % radicaallengte=dormantlengte
else
   length=round((y(2)*k(3))/((2*(k(1)*y(1)*6e8)^0.5)+1e-3*y(2)));  %
radicaallengte=kinetische lengte
end
```

```
if length<3
   length=3;
end

wp=m(1)*convM/(m(1)+m(2)); % bereken wp

Dmon    = 9e-8;
Dshort  = Dmon;
Dlong   = Dmon/(length^min(2, 0.66+2*wp));
Ddouble = Dmon/((2*length)^min(2, 0.66+2*wp));

ktSS  = k(12)*(Dshort+Dshort);
ktISS  = k(13)*(Dshort+Dshort);
% ktLL  = k(12)*(Dlong+Dlong);
ktLS  = k(12)*(Dlong+Dshort);
ktILS  = k(13)*(Dlong+Dshort);
% ktLLL = k(13)*(Ddouble+Dlong);    %intermediate termination PSP P
ktLLS = k(13)*(Ddouble+Dshort);   %intermediate termination PSP R

eff=0.7;
Ithermal=4e-9*y(2)^3;
IT=Ithermal;

 dydt = zeros(10,1);
 dydt(1)=-k(1)*y(1);
 dydt(2)=-k(3)*y(2)*y(5)-k(2)*y(3)*y(2);
 dydt(3)=IT+k(1)*eff*2*y(1)+k(5)*y(9)+k(8)*y(8)-k(7)*y(3)*y(4)-k(11)*y(3)*y(6)-
ktLS*y(3)*y(5)-ktLLS*y(3)*y(10)-k(2)*y(3)*y(2)-ktSS*y(3)*y(3)-ktILS*y(3)*y(9)-
ktISS*y(3)*y(8);
 dydt(4)=k(6)*y(9)+k(8)*y(8)-k(4)*y(5)*y(4)-k(7)*y(3)*y(4);
 dydt(5)=k(2)*y(3)*y(2)+k(6)*y(9)+k(10)*y(10)-k(4)*y(4)*y(5)-k(9)*y(5)*y(6)-
ktLS*y(5)*y(5)-ktLLS*y(5)*y(10)-ktLS*y(3)*y(5)-ktLLS*y(5)*y(9)-ktILS*y(5)*y(8);
 dydt(6)=k(5)*y(9)+k(10)*y(10)-k(9)*y(5)*y(6)-k(11)*y(3)*y(6);

dydt(7)=ktLS*y(5)*y(5)+ktLS*y(5)*y(3)+ktLLS*y(5)*y(10)+ktLLS*y(3)*y(10)+ktISS*y(3)*y(
8)+ktILS*y(5)*y(8)+ktILS*y(3)*y(9);
 dydt(8)=k(7)*y(3)*y(4)-k(8)*y(8)-ktISS*y(3)*y(8)-ktILS*y(5)*y(8);
 dydt(9)=k(4)*y(4)*y(5)+k(11)*y(3)*y(6)-k(5)*y(9)-k(6)*y(9)-ktILS*y(3)*y(9)-
ktLLS*y(5)*y(9);
 dydt(10)=k(9)*y(5)*y(6)-k(10)*y(10)-ktLLS*y(5)*y(10)-ktLLS*y(3)*y(10);
 %-------------------------------------------------------------------------------
  function [value,isterminal,direction] = events(t,y,k,sv,m,mx)

 % sv(1)= concentration I at t=0,  sv(2)= concentration M at t=0
 % y(1) = concentration I at t=t,  y(2) = concentration M at t=t
 % mx(1)= maximum conversion of I, mx(2)= maximum conversion of M
 % abort integration when one of both components reaches max. conversion

 value = zeros(1,2);             % max conversion=zero crossing
 % value(1:2) = [((sv(1)-y(1))/sv(1))-mx(1), ((sv(2)-y(2))/sv(2))-mx(2)];
 value(1:2) = [1, ((sv(2)-y(2))/sv(2))-mx(2)];

 isterminal = zeros(1,2);
 isterminal(1:2) = [1,1];

 direction = zeros(1,2);         % direction unimportant
% ------------------------------------------------------------
```

when the `startit` command is given to MATLAB, the code in the first file is executed. The first section allows the user to set different rate constants and concentrations. The second section prepares the integration by constructing a vector of starting conditions and setting the options. The third section executes the integration using the `ode15s` solver and calling `simpleraft.m` for a description of the differential equations. When the integration is finished, the vector `t` contains the time points of the integration and the corresponding rows in matrix `x` contain the concentrations for each of the six different species. The fourth section creates a basic

output file containing all the data in ASCII format. Fully functional `.m` files can be obtained from the author upon request. They may also be downloaded from the author's website (currently www.xs4all.nl/~engel13).

A.2.2. Exact Model

Construction

The second approach mentioned in the introduction uses a differential equation for each individual chainlength for all species and several others for monomer, initiator, etc. The following reaction scheme allows the required set of differential equations to be derived.

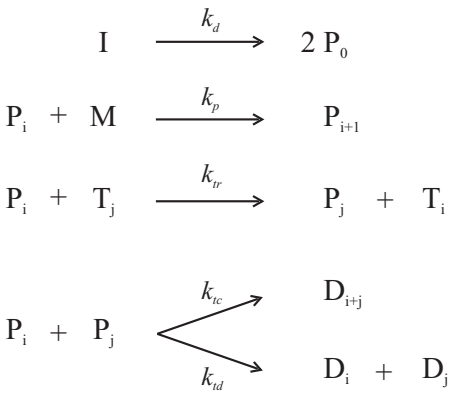

species	
initiator	I
monomer	M
radical	P
dormant chain	T
dead material	D

rate constants	
dissociation	k_d
propagation	k_p
combination	k_{tc}
disproportionation	k_{td}
transfer	k_{tr}
initiator effcicency	f

These then are as follows:

$$\frac{dI}{dt} = -k_d \cdot I \qquad \textbf{(7-15)}$$

$$\frac{dM}{dt} = -k_p \cdot M \cdot P \qquad \textbf{(7-16)}$$

$$\frac{dP_0}{dt} = 2 f k_d \cdot I - k_p \cdot P_0 \cdot M - k_{tr} \cdot P_0 \cdot \sum_{j=0}^{n} T_j + k_{tr} \cdot T_0 \cdot \sum_{j=0}^{n} P_j - k_{tc} \cdot P_0 \cdot \sum_{j=0}^{n} P_j - k_{td} \cdot P_0 \cdot \sum_{j=0}^{n} P_j \qquad \textbf{(7-17)}$$

$$\frac{dP_i}{dt} = k_p{\cdot}P_{i-1}{\cdot}M - k_p{\cdot}P_i{\cdot}M - k_{tr}{\cdot}P_i{\cdot}\sum_{j=0}^{n} T_j + k_{tr}{\cdot}T_i{\cdot}\sum_{j=0}^{n} P_j - k_{tc}{\cdot}P_i{\cdot}\sum_{j=0}^{n} P_j - k_{td}{\cdot}P_i{\cdot}\sum_{j=0}^{n} P_j \qquad \textbf{(7-18)}$$

$$\frac{dT_i}{dt} = k_{tr}{\cdot}P_i{\cdot}\sum_{j=0}^{n} T_j - k_{tr}{\cdot}T_i{\cdot}\sum_{j=0}^{n} P_j \qquad \textbf{(7-19)}$$

$$\frac{dD_i}{dt} = k_{tc}{\cdot}\sum_{j=0}^{i} P_j{\cdot}P_{i-j} + k_{td}{\cdot}P_i{\cdot}\sum_{j=0}^{n} P_j \qquad \textbf{(7-20)}$$

the subscript *i* in the disributed species denotes the number of monomer units. P_0 is therefore not a polymer radical, but a chemically different species derived from the initiator or transfer agent. T_0 – a dormant species without monomer units – is the initial transfer agent. When n different chainlengths are considered, the total number of differential equations equals 4n+1. Although the model is in principle ideal for most of the living polymerizations in this thesis, it does not allow for comparison of the results with those of (simulated) polymerizations applying less reactive transfer agents.

Besides, the transfer reaction cannot be unraveled further by the use of the full addition–fragmentation equilibrium. The intermediate species has two chains attached to the dithio moiety and the length of both needs to be remembered when it is formed which would result in ½n^2 extra differential equations. For the example given in the introduction this would result in an increase from 450 differential equations to 11,700!

Implementation

Luckily, not all differential equations need to be hardcoded. For each of the species, the differential equations for the various chain lengths are very similar and they can be constructed programatically using a loop to iterate through all chain lengths. Again two files are made:

the file `run.m`

```
clear all;       % clear all variables in the Matlab environment

n  = 80;         % number of identifiable species
nr = (4*n)+4;    % number of differential equations
```

```
ktr = 6.5e3;     % transfer rate constant
kp  = 6.5e2;     % propagation rate constant
kd  = 7.4e-5;    % dissociation rate constant
f   = 0.6;       % initiator efficiency

T = 5.9e-2;      % initial transfer agent concentration
I = 2e-2;        % initial initiator concentration
M = 3;           % initial monomer concentration

maxci=0.999999;  % stop integration at this conversion for initiator I
maxcm=0.999;     % stop integration at this conversion for monomer M
maxpc=0.01;      % max fraction of raft chains as undistinguishable species

tmax = 1e8;      % alternate time of integration
%---------section 2-------------------------------------------------------------
% gather the required parameters

kvalue=[kd ktr kp f];
conc=  [I M T];
maxc=  [maxci maxcm maxpc];
y0=zeros(1,nr);
y0(1:3)=conc;
%---------section 3-------------------------------------------------------------
% construct a matrix e containing the chain length dependend
% termination rate coefficients

TERM=zeros((n+1),(n+1));
for i=1:(n+1)
  for j=1:(n+1)
    if (i<=85)
      D1=3.1e-5/((i+1)^0.5);
    else
      D1=3.1e-5*(85^0.1)/((i+1)^0.6);
    end    % if i
    if (j<=85)
      D2=3.1e-5/((j+1)^0.5);
    else
      D2=3.1e-5*(85^0.1)/((j+1)^0.6);
    end    % if j
    TERM(i,j)=5.58e13*(D1+D2);
  end %for j
end %for i
%-----section 4--calculation--------------------------------------------------
[t,x]=ode15s('raft',[],y0,[],kvalue,conc,maxc,n,TERM);
%-----create output-----------------------------------------------------------
%-----section 5----open files-------------------------------------------------
fm = fopen('main.dat','w');
ft = fopen('raft.dat','w');
fp = fopen('rad.dat','w');
%-----section 6----create headers---------------------------------------------
fst='time mc';
fsp='time mc';

for j = 0:n
   fst=[fst ' t' num2str(j)];
   fsp=[fsp ' p' num2str(j)];
end

fst=[fst ' \n'];
fsp=[fsp ' \n'];

fprintf(fm,'time mc mono ini dead mnR mwR pdR mnD mwD pdD\n');
fprintf(ft,fst);
fprintf(fp,fsp);
%------section 7-----MW averages--raft-------------------------------------------

r=zeros(max(size(t)),6);
for i=1:max(size(t))
   for j=0:n
      r(i,1)=r(i,1)+x(i,3+j);                                    % SUM N
      r(i,2)=r(i,2)+(x(i,3+j)*(250+(j*104.15)));                 % SUM (N*M)
      r(i,3)=r(i,3)+(x(i,3+j)*(250+(j*104.15))*(250+(j*104.15))); % SUM (N*M^2)
   end
   r(i,4)=r(i,2)/r(i,1);   % number average molar mass   Mn= SUM(N*M)/SUM(N)
   r(i,5)=r(i,3)/r(i,2);   % weight average molar mass   Mw= SUM(N*M^2)/SUM(N*M)
   r(i,6)=r(i,5)/r(i,4);   % polydispersity index        PD= Mw/Mn
end
%------section 8----MW averages--dead--------------------------------------------
```

```
d=zeros(max(size(t)),6);
for i=1:max(size(t))
   for j=0:((2*n)-1)
      d(i,1)=d(i,1)+x(i,3+j);                                                    % SUM N
      d(i,2)=d(i,2)+(x(i,5+(2*n)+j)*(130+(j*104.15)));                           % SUM (N*M)
      d(i,3)=d(i,3)+(x(i,5+(2*n)+j)*(130+(j*104.15))*(130+(j*104.15)));  % SUM (N*M^2)
   end
   d(i,4)=d(i,2)/d(i,1);   % number average molar mass   Mn= SUM(N*M)/SUM(N)
   d(i,5)=d(i,3)/d(i,2);   % weight average molar mass   Mw= SUM(N*M^2)/SUM(N*M)
   d(i,6)=d(i,5)/d(i,4);   % polydispersity index        PD= Mw/Mn
end
%------section 9----output----main--raft--rad-------------------------------------

for i=1:max(size(t)),
   mc = ((M - x(i,2))/M)*100;
   fprintf(fm,'%.4e %.4e %.4e %.4e %.4e %.4e %.4e %.4e %.4e %.4e %.4e
%.4e\n',t(i),mc,x(i,2),x(i,1),x(i,(2*n+5)),r(i,4),r(i,5),r(i,6),d(i,4),d(i,5),d(i,6))
;
   fprintf(ft,'%.4e %.4e',t(i),mc);
   fprintf(fp,'%.4e %.4e',t(i),mc);

   for j = 0:(n-1)
      fprintf(ft,' %.3e',x(i,3+j));   % loop raft species
      fprintf(fp,' %.3e',x(i,4+n+j)); % loop radical species
   end
   fprintf(ft,' %.3e \n',x(i,3+n));   % add final species of each series and add
   fprintf(fp,' %.3e \n',x(i,4+n+n)); % an end-of-line character
end
%----section 10-- close files-----------------------------------------------------
fclose(fm);
fclose(ft);
fclose(fp);
%------section 11-----the-dead-files-------------------------------------------
aantal=(2*n)-1;           % aantal dode species
spf=200;                  % aantal species per file
bestand=fix(aantal/spf);  % aantal files (max 200 species per file) minus 1

for i = 0:bestand         % loop door veschillende bestanden (waarde nul is 1
bestand)
  naam=['dead' num2str(i) '.dat'];  %maak filenaam aan
  fd = fopen(naam,'w');             %open file

  if (i<bestand)
     sif=spf;             % sif is aantal bestanden in deze file alleen in de laatste
  else                    % file is het kleiner dan spf
     sif=aantal-(bestand*spf);
  end  %if

  fsd='time mc';          % header aanmaken
  for j = 0:(sif-1)
     fsd=[fsd ' d' num2str(j+(i*spf))];
  end      % for j
  fsd=[fsd ' \n'];
  fprintf(fd,fsd);

  for k=1:max(size(t)),          % tijden doorlopen
    mc = ((M - x(k,2))/M)*100;
    fprintf(fd,'%.4e %.4e',t(k),mc); % conversie & tijd printen

    for j = 0:(sif-2)            % species doorlopen op 1 na
      temp= x(k,5+(2*n)+j+(i*spf));
      if (temp<1e-120)           % prevent ultra-small numbers (unreadable by Origin)
          temp=0;
      end                        % if
      fprintf(fd,' %.3e',temp);  % loop dead species
    end                          %for j

    j=sif-1;                     % laatste species
    temp = x(k,5+(2*n)+j+(i*spf));
    if (temp<1e-120)
        temp=0;
    end                          % if
    fprintf(fd,' %.3e \n',temp);
  end                            % for k
  fclose(fd);
end                              %for i
%----section 12---MWDs-----------------------------------------------------------
```

```
conv=[1 2 5 10 15 20 25 30 40 50 60 70 80 90 95 96 97 98 99];
nummer=1;
wr=zeros(2,n);           % gewicht raft (1 kolom absoluut/2 geschaald)
wd=zeros(2,(2*n-1));     % gewicht dood (1 kolom absoluut/2 geschaald)

for k=1:max(size(t)),    % tijden doorlopen
   mc = ((M - x(k,2))/M)*100;

   if (nummer>max(size(conv))),break,end     % alle output files klaar

   if (mc>conv(nummer))
     nummer=nummer + 1;

     fn=['r' num2str(conv(nummer-1)) '.dat'];
     fm = fopen(fn,'w');

     for i = 0:(n-1)
       wr(1,(i+1))=(250+(i*104));             % mw as
       wr(2,(i+1))=x(k,3+i)*(250+(i*104));    % gewichts distributie
       fprintf(fm,'%.3e %.3e \n', wr(1,(i+1)), wr(2,(i+1)));
     end % for i

     fclose(fm);
     fn=['d' num2str(conv(nummer-1)) '.dat'];
     fm = fopen(fn,'w');

     for i = 0:(2*n-1)
       wd(1,(i+1))=(130+(i*104));                   % mw as
       wd(2,(i+1))=x(k,5+(2*n)+i)*(130+(i*104));    % gewichts distributie
       fprintf(fm,'%.3e %.3e \n', wd(1,(i+1)), wd(2,(i+1)));
     end % for i
       fclose(fm);
     end % if
end % for k
%-------------------------------------------------------------------------------
clear all;
```

and the file `raft.m`

```
function varargout = raft(t,y,flag,a,b,c,d,e)

 switch flag
 case ''                        % Return dy/dt = f(t,y)
   varargout{1} = f(t,y,a,b,c,d,e);
 case 'init'                    % Return default [tspan,y0,options]
   [varargout{1:3}] = init(a,b,c,d,e);
 case 'events'                  % Return [value,isterminal,direction]
   [varargout{1:3}] = events(t,y,a,b,c,d,e);
 otherwise
   error(['Unknown flag ''' flag '''.']);
 end

% ---------------+------------+----------+----------------------
% conc. in time  |k-values |conc. t=0 | max conversions
% ---------------+------------+----------+----------------------
%I   y(1)        kd   a(1)    I0  b(1)   max.conv. I     c(1)
%M   y(2)        ktr  a(2)    M0  b(2)   max.conv. M     c(2)
%T0  y(3)        kp   a(3)    T0  b(3)   max. long raft  c(3)
%Tn  y(3+d)      f    a(4)
%P0  y(4+d)
%Pn  y(4+2d)
%D0  y(5+2d)
%D2n y(4+4d)
% ---------------------------------------------------------------
%number of species d
%kt matrix         e
% ---------------------------------------------------------------
 function dydt = f(t,y,a,b,c,d,e)

 no = (4*d)+4;               % number of differential equations
 dydt=zeros(no,1);           % define output column vector
 rad=sum(y((4+d):(4+2*d)))   % total radical concentration
 raft=sum(y(3:(3+d)));       % total raft concentration
%---------------------------------------------------------------
% calculate the average radical chain length

 av=0;
```

```
 for i = 0:d              % for all chain lengths
    av=av+(y(4+d+i)*i);  % summarize concentration * length
 end

 if (rad<=0)              % avoid error right at the
    av=0;                 % start of integration
 else
    av=fix(av/rad)        %average radical chainlength
 end
%-------------------------------------------------------------
% construct differential equations

 dydt(1) = -a(1)*y(1);     % initiator decay
 dydt(2) = -a(3)*y(2)*rad; % monomer consumption

 for i = 0:d               % dormant species & radicals
   dydt(3+i)= a(2)*y(4+d+i)*raft-a(2)*y(3+i)*rad;
   dydt(4+d+i)=-a(3)*y(4+d+i)*y(2)-a(2)*y(4+d+i)*raft+a(2)*y(3+i)*rad
               -e((av+1),(i+1))*y(4+d+i)*rad;
 end

 for i = 1:(d)             % radicals
   dydt(4+d+i)=dydt(4+d+i)+(a(3)*y(2)*y(3+d+i));
 end
                           % initiator contribution to P0
 dydt(4+d)=dydt(4+d)+(2*a(1)*a(4)*y(1));

                           % cancel propagation for Pn
 dydt(4+2*d)=dydt(4+2*d)+(a(3)*y(4+2*d)*y(2));

                           % dead species-------------------------------------
 for i=0:(d-1)             % chain length dead material
   for j=0:i               % loop different combinations to form dead species
      r1=i-j;              % length radical 1
      r2=j;                % length radical 2
      dydt(5+(2*d)+i)=dydt(5+(2*d)+i)+e((r1+1),(r2+1))*y(4+d+r1)*y(4+d+r2);
   end
 end

  for i=d:(2*(d-1))        % chain length dead material
   for j=fix(i/2):-1:0     % loop different combinations to form dead species
      r1=i-j;              % length radical 1
      r2=j;                % length radical 2
      if (r1>(d-1))|(r2>(d-1)),break,end  % non existing radical length
      dydt(5+(2*d)+i)=dydt(5+(2*d)+i)+e((r1+1),(r2+1))*y(4+d+r1)*y(4+d+r2);
   end
 end

 dydt(4+4*d)=e(d,d)*y(4+2*d)*y(4+2*d);
%-------------------------------------------------------------------------------

 function [tspan,y0,options] = init(a,b,c,d,e)

 tspan = [0 1e8];    % default timespan
 nr = (4*d)+5;       % number of differential equations/compounds
 y0 = zeros(1,nr);   % starting concentrations
 y0(1:3) = b(1:3);
 options =odeset('AbsTol',1e-7,'RelTol',1e-7,'BDF','off','Stats','on','Events','on');
                     % error tolerances
%-------------------------------------------------------------------------------
 function [value,isterminal,direction] = events(t,y,a,b,c,d,e)

 % b(1)= concentration I at t=0,  b(2)= concentration M at t=0
 % y(1)= concentration I at t=t,  y(2)= concentration M at t=t
 % c(1)= maximum conversion of I, c(2)= maximum conversion of M
 % abort integration when one of both components reaches max. conversion

 % second criterium: integrating noise, [radicals]<0

 % third criterium: heap of non-distinguisable species > 1%

 value = zeros(1,d+4);             % max conversion=zero crossing
 value(1:2) = [((b(1)-y(1))/b(1))-c(1), ((b(2)-y(2))/b(2))-c(2)];

 for i =0:d
    value(i+3) = y(4+d(1)+i);      % [radical]<0
 end
```

```
 value(1,d+4)= (y(d+3)/b(3))-c(3); % third criterium

 isterminal = zeros(1,d+4);
 isterminal(1:2) = [1,1];
 isterminal(d+4) =[1];             % all are terminal events
 direction = zeros(1,d+4);         % direction unimportant
%-------------------------------------------------------------------------------
```

The files are for a large part self explanetory. Comments can be found inline with the code. The same general structure is applied as in the previous model. `run.m` collects and prepares the input parameters, calls the `ode15s` solver which uses the differential equations in `raft.m`, and produces several output files from the raw integration results. `raft.dat`, `rad.dat` and `deadX.dat` (`X` being an integer) contain the concentrations of each and every species in time. `Main.dat` contains the molar mass averages, polydispersities and conversion as a function of time. Section 12 generates a number of molar mass distributions at the conversions specified in the `conv` vector. For every point both an `rX.dat` and `dX.dat` (`X` being the conversion) file are created containing the molar mass distribution of the dormant chains and of the dead material respectively.

The `raft.m` file illustrates the use of events. As only a limited number of chain lengths is considered the model will need to check during the integration whether or not this number still suffices. If any material grows to larger chain lengths, the model needs to terminate. This can be achived by removal of the positive contribution of propagation from the largest radical species (in its differential equation). This prevents polymer 'growing out of the model'. The largest radical species P_n not only represents polymer radicals with length n, but cumilates all longer chains as well. In every iteration the model checks the concentration of P_n and as soon as it amounts to more then 1% of the total radical concentration, the integration is halted. Events are constructed in such a way that they represent a certain zero-crossing. The actual percentage of P_n is substracted from 1 so that the event-value evaluates to zero and is recognised by MATLAB. Reaching the maximum conversion for either initiator or monomer and negative radical concentrations also trigger events that halt the integration because they indicate that the polymerization is essentially finished and that further integration will yield meaningless results.

A.2.3. The Method of Moments

The third model discussed in the introduction aims to keep track of the molar mass averages of a distribution rather than the full distribution itself which, as shown in the previous section, is not possible for a lot of systems. The computa-

tional power released by this simplification can be employed to tackle more demanding polymerizations. The derivation of the differential equations from the reaction scheme is in this case slightly more complicated. The same reaction scheme is used as for the exact model to arrive at the following differential equations for the individual species:

$$\frac{dI}{dt} = -k_d \cdot I \qquad \textbf{(7-21)}$$

$$\frac{dM}{dt} = -k_p \cdot M \cdot P \qquad \textbf{(7-22)}$$

$$\frac{dP_0}{dt} = 2fk_d \cdot I - k_p \cdot P_0 \cdot M - k_{tr} \cdot P_0 \cdot \sum_{j=0}^{\infty} T_j + k_{tr} \cdot T_0 \cdot \sum_{j=0}^{\infty} P_j - k_{tc} \cdot P_0 \cdot \sum_{j=0}^{\infty} P_j - k_{td} \cdot P_0 \cdot \sum_{j=0}^{\infty} P_j \qquad \textbf{(7-23)}$$

$$\frac{dP_i}{dt} = k_p \cdot M \cdot (P_{i-1} - P_i) - k_{tr} \cdot P_i \cdot \sum_{j=0}^{\infty} T_j + k_{tr} \cdot T_i \cdot \sum_{j=0}^{\infty} P_j - k_{tc} \cdot P_i \cdot \sum_{j=0}^{\infty} P_j - k_{td} \cdot P_i \cdot \sum_{j=0}^{\infty} P_j \qquad \textbf{(7-24)}$$

$$\frac{dT_0}{dt} = k_{tr} \cdot P_0 \cdot \sum_{j=1}^{\infty} T_j - k_{tr} \cdot T_0 \cdot \sum_{j=1}^{\infty} P_j \qquad \textbf{(7-25)}$$

$$\frac{dT_i}{dt} = k_{tr} \cdot P_i \cdot \sum_{j=0}^{\infty} T_j - k_{tr} \cdot T_i \cdot \sum_{j=0}^{\infty} P_j \qquad \textbf{(7-26)}$$

$$\frac{dD_i}{dt} = k_{tc} \cdot \sum_{j=0}^{i} P_j \cdot P_{i-j} + k_{td} \cdot P_i \cdot \sum_{j=0}^{\infty} P_j \qquad \textbf{(7-27)}$$

The differential equations for the initiator and the monomer can be used directly in the model. Note that P_0 and T_0 are treated seperately and have been taken out of their distribution. This affects only the zeroth moment of the distribution as for the higher moments the contribution of the individual species is multi-

plied with its index (see formula 7-1) which cancels out the zero-length species. Before these equations can be put in the model they need to be rewritten so that they are expressed in moments:

$$\frac{dP_0}{dt} = 2fk_d \cdot I - k_p \cdot P_0 \cdot M - k_{tr} \cdot P_0 \cdot \mu_0^T + k_{tr} \cdot T_0 \cdot \mu_0^P - (k_{tc} + k_{td}) \cdot P_0 \cdot (P_0 + \mu_0^P) \quad \textbf{(7-28)}$$

$$\frac{dT_0}{dt} = k_{tr} \cdot P_0 \cdot \mu_0^T - k_{tr} \cdot T_0 \cdot \mu_0^P \quad \textbf{(7-29)}$$

The equations for P_i, T_i and D_i are used to derive the respective differential equations for the moments of these distributions. The differential equation for the zeroth moment of the radical distribution follows from summation over all i from 1 to infinity:

$$\frac{d\mu_0^P}{dt} = \frac{d\sum_{i=1}^{\infty} P_i}{dt} = k_p \cdot M \cdot \sum_{i=1}^{\infty} (P_{i-1} - P_i) - k_{tr} \cdot \left(T_0 + \sum_{j=1}^{\infty} T_j \right) \cdot \sum_{i=1}^{\infty} P_i + k_{tr} \cdot \left(P_0 + \sum_{j=1}^{\infty} P_j \right) \cdot \sum_{i=1}^{\infty} T_i - (k_{tc} + k_{td}) \cdot \left(P_0 + \sum_{j=1}^{\infty} P_j \right) \cdot \sum_{i=1}^{\infty} P_i \quad \textbf{(7-30)}$$

$$\frac{d\mu_0^P}{dt} = k_p \cdot M \cdot P_0 - k_{tr} \cdot \mu_0^P \cdot (T_0 + \mu_0^T) + k_{tr} \cdot \mu_0^T \cdot (P_0 + \mu_0^P) - (k_{tc} + k_{td}) \cdot (P_0 + \mu_0^P) \cdot \mu_0^P \quad \textbf{(7-31)}$$

$$\frac{d\mu_0^P}{dt} = k_p \cdot M \cdot P_0 + k_{tr} \cdot P_0 \cdot \mu_0^T - k_{tr} \cdot T_0 \cdot \mu_0^P - (k_{tc} + k_{td}) \cdot (P_0 + \mu_0^P) \cdot \mu_0^P \quad \textbf{(7-32)}$$

Keeping in mind that the zeroth moment is in fact the total concentration of polymeric radicals, the correctness of the obtained differential equation can easily be rationalized. There are positive contributions from initiator derived radicals that 'propagate into the distribution' as well as from dormant polymer chains that become activated by such a radical. Negative contributions result from both termination and the reaction between transfer agent and a propagating species which generates a P_0 instead of a P_i radical.

The same technique will be used to arrive at the differential equations for the first and the second moment although for these cases the result takes a more abstract form:

$$\frac{d\mu_1^P}{dt} = \frac{d\sum_{i=1}^{\infty} i \cdot P_i}{dt} = k_p \cdot M \cdot \sum_{i=1}^{\infty} i \cdot (P_{i-1} - P_i) - k_{tr} \cdot \left(T_0 + \sum_{j=1}^{\infty} T_j\right) \cdot \sum_{i=1}^{\infty} i \cdot P_i$$
$$+ k_{tr} \cdot \left(P_0 + \sum_{j=1}^{\infty} P_j\right) \cdot \sum_{i=1}^{\infty} i \cdot T_i - (k_{td} + k_{tc}) \cdot \left(P_0 + \sum_{j=1}^{\infty} P_j\right) \cdot \sum_{i=1}^{\infty} i \cdot P_i \qquad \textbf{(7-33)}$$

$$\frac{d\mu_1^P}{dt} = k_p \cdot M \cdot (P_0 + \mu_0^P) - k_{tr} \cdot (T_0 + \mu_0^T) \cdot \mu_1^P + k_{tr} \cdot (P_0 + \mu_0^P) \cdot \mu_1^T$$
$$- (k_{td} + k_{tc}) \cdot (P_0 + \mu_0^P) \cdot \mu_1^P \qquad \textbf{(7-34)}$$

and the second moment

$$\frac{d\mu_2^P}{dt} = \frac{d\sum_{i=1}^{\infty} i^2 \cdot P_i}{dt} = k_p \cdot M \cdot \sum_{i=1}^{\infty} i^2 \cdot (P_{i-1} - P_i) - k_{tr} \cdot \left(T_0 + \sum_{j=1}^{\infty} T_j\right) \cdot \sum_{i=1}^{\infty} i^2 \cdot P_i$$
$$+ k_{tr} \cdot \left(P_0 + \sum_{j=1}^{\infty} P_j\right) \cdot \sum_{i=1}^{\infty} i^2 \cdot T_i - (k_{td} + k_{tc}) \cdot \left(P_0 + \sum_{j=1}^{\infty} P_j\right) \cdot \sum_{i=1}^{\infty} i^2 \cdot P_i \qquad \textbf{(7-35)}$$

$$\frac{d\mu_2^P}{dt} = k_p \cdot M \cdot (P_0 + \mu_0^P + 2\mu_1^P) - k_{tr} \cdot (T_0 + \mu_0^T) \cdot \mu_2^P + k_{tr} \cdot (P_0 + \mu_0^P) \cdot \mu_2^T$$
$$- (k_{td} + k_{tc}) \cdot (P_0 + \mu_0^P) \cdot \mu_2^P \qquad \textbf{(7-36)}$$

The moments for the dormant species are derived as follows:

zeroth moment:

$$\frac{d\mu_0^T}{dt} = \frac{d\sum_{i=1}^{\infty} T_i}{dt} = k_{tr} \cdot \left(T_0 + \sum_{j=1}^{\infty} T_j \right) \cdot \sum_{i=1}^{\infty} P_i - k_{tr} \cdot \left(P_0 + \sum_{j=1}^{\infty} P_j \right) \cdot \sum_{i=1}^{\infty} T_i \quad \textbf{(7-37)}$$

$$\frac{d\mu_0^T}{dt} = k_{tr} \cdot (T_0 + \mu_0^T) \cdot \mu_0^P - k_{tr} \cdot (P_0 + \mu_0^P) \cdot \mu_0^T \quad \textbf{(7-38)}$$

first moment:

$$\frac{d\mu_1^T}{dt} = \frac{d\sum_{i=1}^{\infty} i \cdot T_i}{dt} = k_{tr} \cdot \left(T_0 + \sum_{j=1}^{\infty} T_j \right) \cdot \sum_{i=1}^{\infty} i \cdot P_i - k_{tr} \cdot \left(P_0 + \sum_{j=1}^{\infty} P_j \right) \cdot \sum_{i=1}^{\infty} i \cdot T_i \quad \textbf{(7-39)}$$

$$\frac{d\mu_1^T}{dt} = k_{tr} \cdot (T_0 + \mu_0^T) \cdot \mu_1^P - k_{tr} \cdot (P_0 + \mu_0^P) \cdot \mu_1^T \quad \textbf{(7-40)}$$

second moment:

$$\frac{d\mu_2^T}{dt} = \frac{d\sum_{i=1}^{\infty} i^2 \cdot T_i}{dt} = k_{tr} \cdot \left(T_0 + \sum_{j=1}^{\infty} T_j \right) \cdot \sum_{i=1}^{\infty} i^2 \cdot P_i - k_{tr} \cdot \left(P_0 + \sum_{j=1}^{\infty} P_j \right) \cdot \sum_{i=1}^{\infty} i^2 \cdot T_i \quad \textbf{(7-41)}$$

$$\frac{d\mu_2^T}{dt} = k_{tr} \cdot (T_0 + \mu_0^T) \cdot \mu_2^P - k_{tr} \cdot (P_0 + \mu_0^P) \cdot \mu_2^T \quad \textbf{(7-42)}$$

for the dead chains:

$$\frac{d\mu_0^D}{dt} = \frac{d\sum_{i=0}^{\infty} D_i}{dt} = k_{tc} \cdot \sum_{i=0}^{\infty} \sum_{j=0}^{i} P_j \cdot P_{i-j} + k_{td} \cdot \sum_{i=0}^{\infty} P_i \cdot \sum_{j=0}^{\infty} P_j \quad \textbf{(7-43)}$$

in which the contribution from disproportionation can readily be expressed in moments. Rewriting the contribution from combination requires the use of the following identity:

$$\sum_{n=0}^{\infty}\sum_{k=0}^{n} f(k,n) = \sum_{k=0}^{\infty}\sum_{n=k}^{\infty} f(k,n) = \sum_{n=0}^{\infty}\sum_{k=0}^{\infty} f(k,n+k) \qquad \textbf{(7-44)}$$

the first step can be visualized if we consider a three dimensional space:

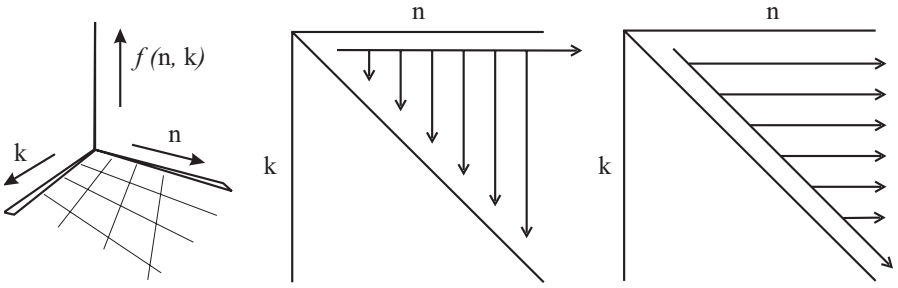

the middle illustration shows which area on the base, the *nk*-plane, is covered by the first summation. The same area is covered by the second summation. Here *k* runs from zero to infinity while *n* runs from the current *k* value to infinity. When in this summation, *n* is replaced by the new running variable *n+k*, the summation takes its final form. If this identity is applied to equation 7-43 , it can be expressed in the moments of the radical distribution.

$$\frac{d\mu_0^D}{dt} = k_{tc}\cdot\sum_{i=0}^{\infty}\sum_{j=0}^{\infty} P_j\cdot P_i + k_{td}\cdot\sum_{i=0}^{\infty} P_i\cdot\sum_{j=0}^{\infty} P_j \qquad \textbf{(7-45)}$$

$$\frac{d\mu_0^D}{dt} = (k_{tc}+k_{td})\cdot(P_0+\mu_0^P) \qquad \textbf{(7-46)}$$

the same identity is used in the derivation of the first and the second moment:

$$\frac{d\mu_1^D}{dt} = \frac{d\sum_{i=0}^{\infty} i\cdot D_i}{dt} = k_{tc}\cdot\sum_{i=0}^{\infty}\sum_{j=0}^{i} i\cdot P_j\cdot P_{i-j} + k_{td}\cdot\sum_{i=0}^{\infty} i\cdot P_i\cdot\sum_{j=0}^{\infty} P_j \qquad \textbf{(7-47)}$$

$$\frac{d\mu_1^D}{dt} = k_{tc} \cdot \sum_{i=0}^{\infty} \sum_{j=0}^{\infty} (i+j) \cdot P_j \cdot P_i + k_{td} \cdot \mu_1^P \cdot (P_0 + \mu_0^P) \quad \textbf{(7-48)}$$

$$\frac{d\mu_1^D}{dt} = (k_{td} + 2 \cdot k_{tc}) \cdot \mu_1^P \cdot (P_0 + \mu_0^P) \quad \textbf{(7-49)}$$

$$\frac{d\mu_2^D}{dt} = \frac{d\sum_{i=0}^{\infty} i^2 \cdot D_i}{dt} = k_{tc} \cdot \sum_{i=0}^{\infty} \sum_{j=0}^{i} i^2 \cdot P_j \cdot P_{i-j} + k_{td} \cdot \sum_{i=0}^{\infty} i^2 \cdot P_i \cdot \sum_{j=0}^{\infty} P_j \quad \textbf{(7-50)}$$

$$\frac{d\mu_2^D}{dt} = k_{tc} \cdot \sum_{i=0}^{\infty} \sum_{j=0}^{\infty} (i+j)^2 \cdot P_j \cdot P_i + k_{td} \cdot \mu_2^P \cdot (P_0 + \mu_0^P) \quad \textbf{(7-51)}$$

$$\frac{d\mu_2^D}{dt} = (k_{td} + 2 \cdot k_{td}) \cdot \mu_2^P \cdot (P_0 + \mu_0^P) + 2 \cdot k_{tc} \cdot (\mu_1^P)^2 \quad \textbf{(7-52)}$$

now that the appropiate differential equations have been derived, they can be put in a MATLAB .m file similar to the other models. The output matrix contains the evolution of the moments in time from which the molar mass averages and the polydispersity can be calculated according to equations 7-2 and 7-3.

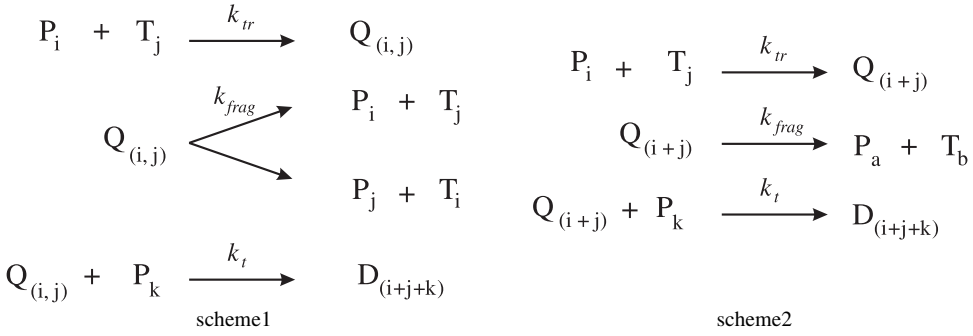

To develop the model further it would be desirable to use the full addition–fragmentation equilibrium and to investigate the intermediate radical as well. As mentioned in the previous model, the intermediate radical has a double distribution and the length of both chains attached to the dithiocarbonate moitey needs to be known (Scheme 1). Treatment of such a 'two dimensional' compound is impossible with the method of moments. When the intermediate is simplified to a one dimensional species, the length of the individual chains that are regenerated upon

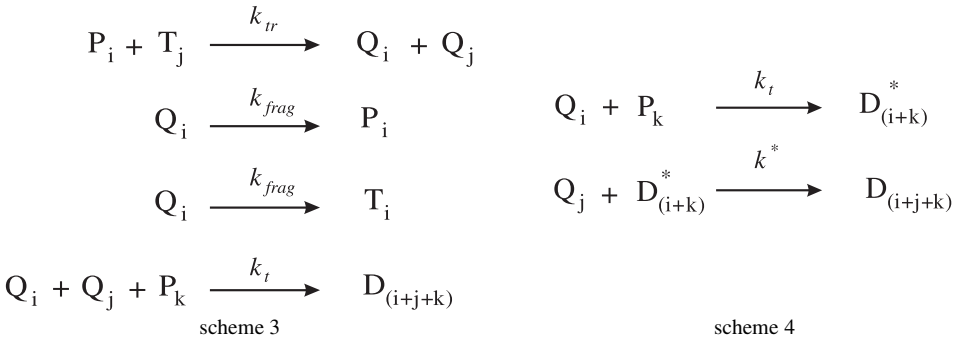

scheme 3 scheme 4

fragmentation is not known (Scheme 2). This approach is therefore rejected. A good alternative is the physically unrealisic scheme where the transfer reaction generates two polymer chains (Scheme 3). The reaction is mathematically identical to termination by disproportionation and can easily be described using the moments method. Fragmentation then can be described as a unimolecular transition to either a dormant or a radical species. The concentration dependencies of the rate (fragmentation being first order in the concentration of the intermediate) are maintained in the original state. The consequences of this unrealistic simulation are a faulty concentration of the intermediate species. This can be corrected as the difference is a factor of two. Calculating the average molar mass will also yield erroneous results, but these data are not of particular interest anyway. More important is the molar mass of the termination product formed in the reaction between the intermediate species and a propagating radical. To arrive at the correct molar mass, this will need to be a trimolecular reaction using two intermediate species and a radical.

When the model is transformed into differential equations, the correct rate structure will be lost. The rate of the last termination reaction, that of the intermediate radical will increase by a factor of four when the concentration of the intermediate radical doubles. The correct rate structure can be restored (first order in both intermediate and radical concentration) when substituting the last reaction in Scheme 3 with the two reactions in Scheme 4 allows the complete scheme to be expressed in differential equations, maintaining correct reaction rates and allowing the predication of all molar mass averages. However the prerequisite that the second reaction of Scheme 4 be much faster than the first (in other words, the first reaction is the rate determining step) makes the entire matrix of differential equations close to singular and leads to an extremely stiff system which cannot be solved anymore. The integrator will be required to make extremely small steps on the entire timescale solely because of this reaction. Up to now, no method was found to circumvent this problem.

A.3. Monte Carlo Simulations

Monte Carlo simulations are based on the element of chance. They do not require the chemical reactions to be transformed into a mathematical model of differential equations, but instead make use of probability functions and random numbers. The model used to investigate the effect of the transfer coefficient and the targeted degree of polymerization on the polydispersity of the final product requires four input parameters, in its current implementation: amount of monomer, amount of RAFT agent, the transfer rate coefficient and the propagation rate coefficient. Of the latter two, only their ratio is of importance, reducing the number of actual parameters to three. The simulation neglects termination events and physicalle corresponds to a polymerization with one single radical. One of the RAFT agents is randomly chosen to be the active species. Monomer species are added one by one to the active species. Before each addition occurs, the chance of transfer is calculated using Eq. 7-53:

$$P(transfer) = \frac{k_{tr} \cdot RAFT}{k_{tr} \cdot RAFT + k_p \cdot M} \qquad \textbf{(7-53)}$$

$P(transfer)$ is compared with a random value between 0 and 1 and if transfer occurs, a new, randomly chosen, species from the population is set to be active. The ratio of monomer to raft agent determines the target degree of polymerization, one of the experimental parameters, while the magnitude of the individual species determines the statistical variation. Larger populations of monomer and RAFT, but in the same ratio, will produce more consistent results.

A.4. References

1. From Neuromancer, William Gibson, 1984
2. www.mathworks.com
3. Shampine, L. F.; Reichelt, M. W. *SIAM J. Sci. Comput.* **1997**, *18*, 1.

» Orders came from downtown:
no more «[1]

Epilogue

An epilogue is here and now. It marks the turnover between the past and the future. In the preceding chapters, the work that has been performed over the past few years is described. The question remains, however, what the prospect is for RAFT in the future and in what way the work in this thesis can contribute to that.

One of the most prominent challenges that exist in the field of polymer chemistry nowadays is to gain control over the intramolecular polymer structure. If one thing has become apparent over the years, it is that *average* chain lengths, *average* compositions and *average* functionality numbers do not suffice to correlate macroscopic properties to molecular characteristics. Polymers with roughly the same *average* characteristics can exhibit totaly different material properties. One of the more familiar examples that can be mentioned in this respect is that of a block-copolymer and a statistical copolymer, constructed from the same monomers.

In the area of polymer characterisation tremendous progress has been made in the recent past so that complete molar mass distributions, chemical composition distributions and functionality type distributions have been made available. The increased knowledge that has been gained by these analyses on polymer structure–property relationships is now waiting to be applied. On the synthetic side, however, construction of polymers with predetermined and well defined intramolecular structures has been restricted to a small number of systems that are compatible with ionic polymerization techniques. Clearly the need exists for robust, versatile and generally applicable methods to prepare these materials.

Living radical polymerization can fill this gap that exists in our collection of synthetic tools. RAFT polymerization in particular appeared to be robust and versatile and therefore of general use, but when the investigations described in this thesis started, RAFT was documented exclusively in the patent literature.[2] From experience in the synthesis of non-reversible addition fragmentation chain transfer agents, it was decided to prepare several RAFT agents with the aim to study their

application in homogeneous and heterogeneous media. The results were encouraging. In fact, the level of control that was obtained was comparable to what colleagues in our department had achieved using atom transfer radical polymerization (ATRP). More amazing was the relative ease with which the molar mass distribution could be controlled. The quest for improved combinations of alkyl halides, ligands and metals to be used in ATRP seemed without end, whereas the RAFT agent was simply added to an existing recipe from an undergraduate practical course to yield similar results from the very first experiment. This immediately points out one of the major advantages of RAFT over other living radical polymerization techniques: the reaction conditions are identical to those of a conventional uncontrolled radical polymerization. The same temperature, solvent, monomer and initiator are used and the concentration of propagating radicals is hardly affected. As was shown in Chapter 2, the trade-off between polymerization rate and the level of 'livingness' is achieved by simply varying the concentrations of initiator and raft agent, rather than by a change of design of the ingredients as is the case in ATRP.

Another distinct advantage over ATRP is the absence of metal complexes in the product which have, up to the present day, prevented the industrial application of this technique. In this respect, however, polymer prepared via RAFT polymerization, has a comparable disadvantage. Well-controlled polymers are prepared by highly reactive RAFT agents that easily exchange the controlling moiety amongst the polymer chains during the process of preparation. These end-groups remain in the product as equally labile species, giving rise to an increased rate of degradation. In Chapter 4 it was shown that UV irradiation could cleave the dithiobenzoate moiety from its chain, thereby generating radicals. Thermogravimetric analysis revealed that poly(methyl methacrylate) samples started to degrade at around 120°C. The weight loss corresponded to that of the dithiobenzoate moiety, but once this had been removed, a further temperature increase revealed that the themal stability of the polymer was poorer than might be expected from poly(methyl methacrylate) samples. These issues may prevent the direct application of the product after its preparation, requiring a post-polymerization end-group modification. In a more positive sense, this feature could possibly be used to its benefit in *e.g.* a UV-curable coating. These types of coating usually require the deliberate addition or incorporation of photosensitive moieties that produce cations or radicals when irradiated, which would no longer be nessecary when using a RAFT polymer.

The problem is expected to disappear when low-reactivity RAFT agents are used. Such compounds cannot be used for preparing clean and pure polymer architectures in batch reactions, as the polymer end-group is less reactive during the reaction, but the end-group is quite likely also less labile in the product. For this reason, low reactivity reagents can be desirable for a number of reasons. They eliminate the need for post-polymerization modifications, they are usually more easily synthesized and can be readily applied in emulsion polymerization. For the application of high-reactivity RAFT agents in heterogeneous media like emulsion is characterized by a low efficiency and colloidal instability. This is postulated to be due to the drastic change in the distribution of both radical and polymer chain lengths which interferes with the nucleation process and results in unacceptable retardation througout the polymerization. Although these problems may partly be eliminated by using a semi–continuous procedure, one cannot expect to obtain a robust, reliable and reproducable sytem in this way. RAFT agents of lower reactivity will not have such a significant effect on the chain length distribution and can therefore be used with similar ease as conventional transfer agents.[3] Although it will not be possible to prepare latices consisting of pure block copolymers for instance, a certain fraction of these architectures could be incorporated in the latex particles in order to influence the particle morphology and the material properties in the resulting application.

This thesis has contributed to an understanding of the application of living radical polymerization in emulsion. Although RAFT is not without its problems, it is by far more easy to use than techniques based on reversible termination (like ATRP and nitroxide mediated polymerization). From a synthetic point of view, colorless, easily prepared, high reactivity RAFT agents would be desired, but more demanding at this point is research in the relatively unexplored area of polymer properties which was mentioned at the start of this epilogue. Most studies in living radical polymerization that have been published focus, like this thesis, on the polymer synthesis, but obviously the time has come to *apply* and to see what this tremendous progress that has been achieved over the past decade can bring in terms of smart materials, intellegent additives and products that we didn't even know we wanted to have before they existed...

References

1. Lt. Martin Castillio's typical way to end a Miami Vice episode, leaving the viewer with mixed feelings. For one knew that Crockett and Tubbs had given all that was in them, but that they had not been allowed to finish the job even though considerable progress was just around the corner. In fact, this is quite similar to the situation I experienced in september 2000, when I knew I had to stop the experimental work and start concentrating on this thesis, just a couple of weeks after we finally managed to produce pure block copolymers in miniemulsion. More advanced polymer architectures were/are in sight and the future is shining bright.
2. Le, T. P.; Moad, G.; Rizzardo, E.; Thang, S. H. Patent WO 98/01478 (**1998**) [*Chem. Abstr.* **1998**, 128:115390]
3. Monteiro, M. J.; Sjöberg, M.; Van der Vlist, J.; Göttgens, C. M. *J. Polym. Sci. Part A: Polym. Chem.* **2000**, *38*, 4206

Summary

Living radical polymerization represents a number of techniques which have drawn considerable scientific interest over the last few years, because they allow the preparation of complex polymer architectures in a relatively simple way and starting from a broad range of monomers. One of the latest of these techniques is RAFT polymerization (Reversible Addition–Fragmentation chain Transfer). Its reversibe deactivation mechanism is based upon a transfer reaction rather than a termination reaction which characterizes a number of other popular polymerization techniques. This has several important consequences for the polymerization kinetics and process. A conventional initiator can be used while the steady state concentration of radicals is determined by the equilibrium between initiation and termination, similar to a conventional free-radical polymerization. For this reason, a RAFT agent can be added to an existing recipe without any drastic changes in the polymerization procedure. The resulting polymer, however, will have a predetermined molar mass and monomer sequence distribution.

One of the most prominent kinetic parameters in RAFT polymerization is the transfer constant. Its effect on the molar mass distribution is illustrated by a number of computer simulations. These simulations indicate that a minimum transfer constant of ten is required to prepare low polydispersity material in a batch reaction. The evolution of the concentrations of a series of oligomers was analysed using high performance liquid chromatography. Comparison of these concentration profiles with computer simulations allowed an estimate to be obtained for the transfer rate coefficient of dormant polystyryl RAFT agents based on the dithiobenzoate moiety. Its value was found to be 1,000 to 10,000 times larger than the propagation rate coefficient, which ensures living characteristics under nearly all circumstances.

The radical concentration in RAFT polymerization should be the same as in a similar recipe without RAFT according to the mechanism, that is proposed in the literature. In practice, however, retardation is observed, which was investigated with the aid of computer simulations. This revealed that the explanations that are proposed in the literature are unrealistic. Termination of the intermediate radical, which is formed in the transfer reaction, is then proposed as an alternative explanation. Simulations demonstrate that this additional reaction pathway can explain the retardation without affecting the molar mass distribution, as is observed in practice.

Besides, accepted values can be used for the kinetic parameters in the polymerization scheme while the concentration of the intermediate radical agrees with experimental data reported in the literature.

The robustness and versatility of the RAFT process is further illustrated by the controlled copolymerization of styrene and maleic anhydride. The anhydryde monomer could not be polymerized in a controlled manner by other living radical techniques, but the application in RAFT polymerization allowed the preparation of low polydispersity copolymers of predetermined molar mass. A macromolecular polyolefin-based RAFT agent allowed the formation of poly(styrene-*block*-[ethylene-*co*-butylene]) and poly([styrene-*co*-maleic anhydride]-*block*-[ethylene-*co*-butylene]), polymers which are expected to show interesting properties, *e.g.* as compatibilizers.

It was shown that the labile colored dithiobenzoate group could be removed from the polymer chain quantitatively by photolysis. After this process, the molar mass distribution not only showed signs of the bimolecular combination product, but also of the terminated intermediate radical with a triple molar mass. The absence of monomer during photolysis allowed this species to be detected, thereby providing experimental evidence for the occurrence of this reaction.

The application of RAFT in emulsion polymerization is an important aspect when it comes to industrial acceptance. This application is also interesting from a scientific point of view as compartmentalization of the radicals leads to a reduction of termination, thereby improving the quality of the living process.

Both seeded as well as *ab initio* batch emulsion polymerizations are characterized by colloidal instability, a low RAFT efficiency, inhibition and retardation. These effects were first attributed to transport phenomena concerning the RAFT agent as the consumption rate of highly reactive transfer agents is known to be limited by the interphase transfer rate in many emulsion systems. Similar problems were observed, however, in miniemulsion polymerization in which phase transfer phenomena are essentially eliminated. A more thorough kinetic analysis of the emulsion polymerization demonstrated that the shift of the radical chain length distribution towards lower values increases the radical exit rate leading to a slower polymerization, while also particle formation is hindered. The key factor behind the instability in miniemulsion polymerization appears to be of a more thermodynamic nature. Droplet nucleation disturbs the metastable equilibrium between the droplets and causes a small number of droplets in which the RAFT agent has been trans-

formed into dormant oligomers to attract monmer from the unnucleated droplets. This hypothesis is, however, based upon elimination of alternative explanations and has not yet een verified experimentally.

When anionic surfactants were replaced by nonionics, the efficiency of the RAFT agent in miniemulsion polymerization was enhanced. Although stability problems could not be completely overcome, they were reduced to such an extent that they were no longer of importance on the polymerization timescale. This allowed living radical polymerizations to be conducted in a heterogeneous medium with the advantage of radical compartmentalization, leading to well-defined homopolymers (of methyl, butyl and 2-ethylhexyl methacrylate) but also allowed the preparation of 'designer-latices'. Depending on the process conditions (batch *vs.* semi-continuous), surfactant concentration and initiator, either exceptionally pure block copolymer latices could be synthesized (poly(2-ethylhexyl methacrylate-*block*-[methyl methacrylate-*co*-methacrylic acid])), or latices with an interesting bimodal particle size distribution could be obtained, consisting of a large number of small poly(methyl methacrylate) hard spheres and a smaller number of large poly(methyl methacrylate-*block*-2-ethylhexyl methacrylate) soft spheres of controlled molar mass.

All in all it may be concluded that the increased insight obtained in the mechanism of RAFT polymerization in (mini)emulsion has led to strongly improved microstructural control of the (co)polymers prepared.

Samenvatting

Levende radikaal polymerisatie (LRP) is een verzameling technieken die in het afgelopen decennium sterk in de belangstelling is komen te staan, omdat ze de mogelijkheid biedt om op een relatief eenvoudige wijze complexe polymeerarchitecturen te synthetiseren uitgaande van een breed scala aan monomeren. Een van de laatste technieken die in dit kader ontwikkeld is, is RAFT polymerisatie (*Eng.* Reversible Addition–Fragmentation chain Transfer). Het reversibele deactivatiemechanisme in RAFT polymerisatie berust op een ketenoverdrachtsreaktie in plaats van een terminatiereaktie, die een aantal andere populaire LRP technieken kenmerkt. Dit heeft een aantal belangrijke gevolgen voor de reaktiekinetiek en het polymerisatieproces. Een conventionele initiator kan gebruikt worden en de radikaalconcentratie wordt net als in een conventionele radikaalpolymerisatie bepaald door de balans tussen initiatie en terminatie. In principe kan het RAFT reagens daardoor aan een reeds bestaand recept worden toegevoegd zonder dat het proces daardoor ingrijpend verandert. Het resultaat van de polymerisatie is echter een polymeer waarvan de molmassaverdeling en samenstellingsverdeling een vooraf bepaalde vorm aannemen.

Een belangrijke kinetische parameter in RAFT polymerisaties is de ketenoverdrachtsconstante. Middels een aantal computersimulaties wordt de invloed van de ketenoverdrachtsconstante op de molmassaverdeling van het polymeer geïllustreerd. Deze simulaties laten zien dat in een batch reaktie, een minimum waarde voor de ketenoverdrachtsconstante van ongeveer tien gewenst is om tot lage polydisperiteiten te komen. Door middel van een gedetailleerde analyse van de evolutie van de concentratie van een serie oligomeren gedurende een solutiepolymerisatie, met behulp van hoge druk vloeistof chromatografie, wordt de grootte van de ketenoverdrachtsconstante experimenteel afgeschat voor RAFT reagentia met een dithiobenzoaat groep. Deze blijkt 1000 tot 10.000 keer groter te zijn dan de propagatiesnelheidsconstante in styreen polymerisaties, wat levende karakteristieken onder praktisch alle omstandigheden verzekert.

Het in de literatuur voorgestelde reactieschema voor RAFT polymerisaties resulteert in een onveranderd aantal radikalen ten opzichte van eenzelfde recept zonder RAFT. Desondanks wordt in de praktijk toch een lagere polymerisatiesnelheid waargenomen. Dit fenomeen is onderzocht met behulp van computersimulaties waaruit blijkt dat in de literatuur geponeerde verklaringen voor deze vertraging

onrealistisch zijn. Vervolgens wordt terminatie van het labiele intermediair, dat tijdens de transferreaktie gevormd wordt, naar voren geschoven als alternatieve verklaring voor het waargenomen gedrag. Simulaties van een aantal solutiepolymerisaties wijzen uit dat dit additionele reaktiepad de vertraging kan verklaren, zonder dat dit tot waarneembare effecten leidt op de molecuulgewichtsverdeling. Bovendien kunnen geaccepteerde literatuurwaarden voor de kinetische polymerisatieparameters gebruikt worden terwijl ook de concentratie van het labiele intermediair in overeenstemming is met experimenteel verkregen waarden gerapporteerd in de literatuur.

De robuustheid van RAFT polymerisaties wordt geillustreerd met de gecontroleerde copolymerisatie van styreen en maleinezuur anhydride. Het laatste monomeer blijkt erg moeilijk gecontroleerd te polymeriseren met andere LRP-technieken. Het gebruik van RAFT maakte het mogelijk om polymeren met een vooraf gedefinieerde lengte en smalle molecuulgewichtsverdeling te maken. Deze techniek werd vervolgens toegepast op een macromoleculair RAFT-reagens, dat was verkregen door modificatie van een commercieel verkrijgbaar copolymeer van etheen en buteen. Toepassing van deze verbinding als ketenoverdrachtsstof leidde onder andere tot poly(styreen-*blok*-[etheen-*co*-buteen]) en poly([styreen-*co*-maleinezuur anhydride]-*blok*-[etheen-*co*-buteen]). Vooral van dit laatste polymeer zijn interessante eigenschappen te verwachten, bijvoorbeeld als adhesiepromotor.

De gekleurde labiele dithiobenzoate eindgroep bleek door middel van fotolyse kwantitatief van het polymeer te verwijderen. Tijdens dit proces verandert de molmassaverdeling van het polymeer waarbij niet alleen het combinatieprodukt met een dubbele molmassa ontstaat, maar ook het getermineerde labiele RAFT intermediair met een drievoudige molmassa. De afwezigheid van monomeer tijdens de radicaalvorming zorgt ervoor dat het getermineerde intermediair afzonderlijk waarneembaar is in de molecuulmassaverdeling, waardoor experimentele verificatie van het optreden van deze reaktie mogelijk bleek.

De toepassing van RAFT in emulsiepolymerisatie is een belangrijk aspect wanneer het gaat om industriële acceptatie. Echter, ook vanuit wetenschappelijk standpunt is de toepassing van emulsiepolymerisatie in levende radicaalpolymerisatie interessant. Compartimentalisering van de radicalen in individuele latexdeeltjes hindert terminatie en leidt tot een intrinsiek andere verhouding tussen propagatie en terminatie, hetgeen de kwaliteit van het levende proces ten goede komt.

De toepassing in zowel *seeded* als *ab initio* emulsiepolymerisaties wordt gekenmerkt door colloidale instabiliteit, een lage efficientie van het RAFT reagens, inhibitie en retardatie. In eerste instantie werden deze effecten toegeschreven aan transportproblemen van de ketenoverdrachtsstof. De faseoverdrachtsnelheid van het RAFT reagens kan zijn hoge reaktiesnelheid niet bijbenen wat resulteert in brede molmassaverdelingen. Soortgelijke problemen doen zich echter ook voor bij polymerisaties in miniemulsie waarin faseoverdrachten in essentie geelimineerd zijn. Uit een meer gedegen kinetische analyse van de emulsiepolymerisaties kan geconcludeerd worden dat vooral de veranderde ketenlengteverdeling van de radikalen en het gevormde polymeer ten grondslag liggen aan de genoemde verschijnselen. Door de kortere ketens is de uittredesnelheid van de radicalen vergroot terwijl deeltjesvorming gehinderd wordt. De problemen in miniemulsiepolymerisatie lijken een meer thermodynamische grondslag te hebben. Door druppelnucleatie wordt het metastabiele evenwicht binnen de druppelpopulatie verstoord, waardoor een gering aantal druppels, waarin het RAFT reagens in oligomeren is omgezet, een enorme aantrekkingskracht uitoefent op het monomeer in de overige druppels. Deze verklaring is echter een hypothese die gevonden is door eliminatie van alternatieve verklaringen en berust niet op harde experimentele bewijzen.

Tijdens dit onderzoek aan miniemulsiepolymerisatie werd duidelijk dat het gebruik van niet-ionische surfactanten als alternatief voor anionische leidde tot een grotere efficiëntie van het RAFT reagens. Hoewel de stabiliteitsproblemen hiermee niet compleet verdwenen, werden ze gereduceerd waardoor ze op de tijdsschaal van de polymerisatiereactie niet langer van belang waren. Dit maakte het uiteindelijk mogelijk om levende radicaalpolymerisaties uit te voeren in een heterogene omgeving met het eerder genoemde voordeel van de gereduceerde terminatie ten opzichte van een homogeen reaktiemedium. Dit leidde niet alleen tot latices van nauwkeurig gedefinieerde homopolymeren (van methyl, butyl en 2-ethylhexyl methacrylaat) maar ook tot de vorming van 'designer-latices'. Afhankelijk van de procesvoering (batch versus semi-continu) en de hoeveelheid surfactant en initiator, konden ofwel latices van uitzonderlijk zuivere blokcopolymeren (poly[2-ethylhexyl methacrylaat-*blok*-(methyl methacrylaat-*co*-methacryl zuur)]) bereid worden, dan wel latices met een bimodale deeltjesgrootteverdeling bestaande uit een groot aantal kleine harde poly(methyl methacrylaat) bollen gecombineerd met een klein aantal grotere, zachte poly(methyl methacrylaat-*blok*-2-ethylhexyl methacrylaat) bollen van een gecontrolleerde molmassa.

Samenvattend kan worden geconcludeerd dat het verbeterde inzicht dat werd verkregen in het mechanisme van RAFT polymerisatie in (mini)emulsies heeft geleid tot sterk verbeterde microstructurele controle over de levende (co)polymeren.

Acknowledgements

Vele handen maken licht werk. Ook in de wetenschap geldt dat samenwerking de efficiëntste manier is om tot resultaat te komen en dikwijls ook nog de leukste. Daarom wil ik hier de mensen te noemen die me min of meer aktief geholpen hebben om tot de resulaten te komen die in dit boekje beschreven staan.

Een groot aantal studenten heeft zich aan mijn zijde geschaard omdat ze dit project net zo intrigerend vonden als ik zelf. Erik van Eert, Mieke Ogier en Maarten Seegers van de TU Eindhoven. Bedankt Maarten voor alle inspanningen die je in de chemie en de *programming* gestoken hebt. Gaby Simons, Erik Hagebols en Ben Hoffman van verschillende scholen voor Hoger Laboratorium Onderwijs voor hun zorgvuldige syntheses en schitterende labjournaals. James McLeary and Marcelle Hodgson from the University of Stellenbosch. Special thanks to you Marcelle for the unbelievably large number of emulsion polymerizations you performed and the nice report that formed such a convenient framework for chapter five. John Tsavalas from Georgia University of Technology for the nice teamwork, the lovely mini-emulsion experience and the quick questions.

Verder heb ik tijdens mijn AIOen drie begeleiders versleten die ik wil bedanken voor hun inbreng: Steven van Es, Bert Klumperman en Michael Monteiro. Thanks Michael for the scientific discussions and the wonderful *coaching*.

Wil Kortsmit, bedankt voor de nuttige aanwijzingen bij de ontwikkeling van GeePeeSee, de 32bits GPC data manipulator verantwoordelijk voor alle GPC resultaten in dit boekje, ook al verkeert hij nog steeds in een pre-beta fase. Jos Janssen, bedankt voor het dichten van de kloof tussen de wiskunde en de chemicus, een onontbeerlijk bruggetje bij de ontwikkeling van de modellen.

Wieb Kingma bedankt voor de betrouwbare metingen aan de talloze polymeermonsters op de GPC. Erik Vonk bedankt voor de HPLC analyses. Paul Cools, Joost van Dongen & Bastiaan Staal voor de diverse pogingen tot MALDI-TOF.

Verder gaat mijn dank uit aan SPC als entiteit die er voor heeft gezorgd dat het grootste deel van mijn tijd aldaar gespendeerd aangenaam was. Op het risico af, anderen tekort te doen door ze niet persoonlijk te noemen, wil ik toch meer in het bijzonder hiervoor Grégory, Mike, Robert en Frank bedanken voor onder meer en

onder andere de kopjes koffie. Greg en Mike ook bedankt voor het doorlezen van mijn proefschrift. Christianne, bedankt voor de 'just in time delivery' van de proefdrukken en natuurlijk voor het feit dat je het al die jaren hebt uitgehouden met mij.

Furthermore I would like to thank Akzo Nobel and Wako Chemicals for their donation of initiators, Shell Chemicals for the Kraton samples and all of the compagnies participating in the consortium for emulsion polymerization (SEP) for the funding of this research project.

Ton German bedankt voor de mogelijkheid die ik gekregen heb voor het zelfstandig verrichten van onderzoek en de grote mate van vrijheid.

Thanks to the people who roused my interest for polymer chemistry in the first place: Alex van Herk, Bart Manders and Bob Gilbert.

Uiteraard wil ik mijn ouders bedanken voor de jarenlange steun buiten kantooruren en last but not least mijn vriendin Marion, voor alle steun door de jaren heen en voor je wetenschappelijke inbreng bij de reconstructie van de figuren 2.27 en 2.28, zo net voor de deadline.

Curriculum Vitae

With irrefutable logic, Hans de Brouwer was born on labour day, May 1st 1973 in Goirle, The Netherlands. In 1991, he completed his secondary education at the Theresia Lyceum in Tilburg. That same year, he started his studies at the Faculty of Chemical Engineering at the Eindhoven University of Technology. In 1996 he graduated after which he started a Ph.D. project in the Department of Polymer Chemistry & Coatings Technology of prof.dr.ir. A. L. German. Since February 2001, he has been working as an R&D scientist for UCB Chemicals in Drogenbos, Belgium. RAFT memorabilia is his first book. His labtop computer suffers from a unique, reversible deactivated, ghost pixel at the position (1002, 1).

Publications

Pulsed Electron Beam Polymerization of Styrene in Latex Particles

van Herk, A. M.; de Brouwer, H.; Manders, B. G.; Luthjens, L. H.; Hom, M. L.; Hummel, A.

Macromolecules **1996**, *29*, 1027

Controlled Radical Copolymerization of Styrene and Maleic Anhydride and the Synthesis of Novel Polyolefin-Based Block Copolymers by Reversible Addition–Fragmentation Chain-Transfer (RAFT) Polymerization

de Brouwer, H.; Schellekens, M. A. J.; Klumperman, B.; Monteiro, M. J.; German, A. L.

J. Polym. Sci., Part A: Polym. Chem. **2000**, *38*, 3596

The Molar Mass Dependence of Latex Particle Deformation

de Brouwer, J. A. M.; van Es, J. J. G. S.; German, A. L.

Macromol. Symp. **2000**, *151*, 459

The Influence of RAFT on the Rates and Molecular Weight Distributions of Styrene in Seeded Emulsion Polymerizations

Monteiro, M. J.; Hodgson, M.; de Brouwer, H.

J. Polym. Sci., Part A: Polym. Chem. **2000**, *38*, 3864

Living Radical Polymerization in Miniemulsion using Reversible Addition-Fragmentation Chain Transfer (RAFT).

de Brouwer, H.; Tsavalas, J. G.; Schork, F. J.; Monteiro, M. J.

Macromolecules **2000**, *33*, 9239

Intermediate Radical Termination as the Mechanism for Retardation in RAFT Polymerization

Monteiro, M. J.; de Brouwer, H.

Macromolecules **2001**, *34*, 349

Living Radical Polymerization by Reversible Addition–Fragmentation Chain Transfer (RAFT) in Ionically Stabilized Miniemulsions

Tsavalas, J. G.; Schork, F. J. de Brouwer, H.; Monteiro, M. J.

Macromolecules **2001**, *34*, in press.

Stellingen
behorende bij het proefschrift

RAFT memorabilia
living radical polymerization in homogeneous and heterogeneous media

van

Hans de Brouwer

1. **Data storming:**
Het opsommen van een groot aantal mogelijke verklaringen voor de lagere reactiesnelheid van polymerisaties in de aanwezigheid van een RAFT reagens garandeert nog niet dat ook de hoofdoorzaak daarbij zit, maar duidt op de invoering van *combinatorial chemistry* binnen de theorievorming.

Moad, G.; Chiefari, J.; Chong, Y. K.; Krstina, J.; Mayadunne, R. T. A.; Postma, A.; Rizzardo, E.; Thang, S. H.
Polym. Int. **2000**, *49*, 993
Hoofdstuk 2 van dit proefschrift

2. De bewering dat de kinetiek van hoog reactieve RAFT reagentia in gedispergeerde systemen hetzelfde zou moeten zijn als die in homogene systemen, leunt erg sterk op *zou*.

Charleux, B. *Macromolecules* **2000**, *33*, 5358
Hoofdstukken 5 en 6 van dit proefschrift

3. Het gebruik van de fragmentatiesnelheidsconstante als '*fit parameter*' is alleen mogelijk wanneer een miniem gedeelte van de conversie–tijdcurve van een RAFT polymerisatie wordt gesimuleerd.

Barner-Kowollik, C.; Quinn, J. F.; Morsley, D. R.; Davis, T. P.
J. polym. Sci., Part A: polym. Chem. **2001**, *39*, 1353
Hoofdstuk 2 van dit proefschrift

4. **Spelregels:**
Ondanks de gedistribueerde COM technologie, kunstmatige intelligentie, fuzzy logic en morfologische taalkennis die in de huidige generatie spellingscontroleroutines is ingebouwd, bestaat nog steeds de kans dat in dit proefschrift gesproken wordt in magische termen als *dematerialized water* of *ironically stabilized particles* op die plaatsen waar de auteur op een verkeerde *button* drukte.

5. **Oogkleppen:**
De breedte van een onderzoek is omgekeerd evenredig met de wijdte van het blikveld van de onderzoeker.

6. **Neologisme:**

placebokoe (de (v.); -ien; -tje), een alleszins gezond stuk rundvee dat afgemaakt wordt, louter met als doel het consumentenvertrouwen in biefstuk te herstellen, vgl. *offerrund*.

7. **Internal affairs:**

Hoewel het verkrijgen van hoofdpijn vaak wordt gerelateerd aan externe oorzaken, zit het fenomeen opmerkelijk genoeg altijd tussen de oren.

8. **Archivering:**

Niettegenstaande de persistente meerwaarde die een labjournaal geeft aan experimentele resultaten, pleegt het bijhouden ervan een zware aanslag op de flexibiliteit en de wetenschappelijke intuïtiviteit van de experimentator.

9. **Samplingfrequentie:**

Het is frappant dat in het huidige tijdsgewricht waarin alles groter, beter en sneller moet, er in de interpersoonlijke communicatie wel sprake kan zijn van te snel praten, doch nooit van te langzaam luisteren.

10. De hals over kop toegenomen regelgeving met betrekking tot de uitvoering van experimenten alsmede de daarmee samenhangende administratieve rompslomp maken computersimulatie veelal de enige werkbare overgebleven techniek om tot *experimentele* resultaten te komen.

Paul Weijmans — private communications, **1996**–**2000**
intranet.chem.tue.nl/ArboMilieu/

11. *Beige* is niet meer dan een sjiek woord voor pastelbruin.

12. Het gebruik van de term *'uitworp'* met betrekking tot het vrijkomen van organische stoffen met een hoge dampspanning bij de bereiding en verwerking van verf, doet geen recht aan het luchtige en spontane karakter van het verdampingsproces en de vluchtige aard van deze stoffen, maar suggereert een actieve rol van de werpende partij die de verbeelding prikkelt aangaande de industriële uitvoering van dit proces.

Staatsblad **1999** *529*

13. Boeren dierenliefde reikt net zo ver als de portemonnee breed is.

14. Een *lits-jumeaux* verenigt de negatieve aspecten van een tweepersoonsbed met de nadelen van twee eenpersoonsbedden.

15. Wanneer men van een chemische reactie meer analyseert dan alleen het eindproduct, bedrijft men nog geen kinetiek.